



**EFFECT OF SURFACE-MODIFIED CALCIUM CARBONATE
NANO-PARTICLES ON PROPERTIES OF BIOCOMPOSITES**

**By
Bawornkit Nekhamanurak**

**A Thesis Submitted in Partial Fulfillment of the Requirements for the Degree
DOCTOR OF PHILOSOPHY
Program of Polymer Science and Engineering
(International Program)
Graduate School
SILPAKORN UNIVERSITY
2011**

**EFFECT OF SURFACE-MODIFIED CALCIUM CARBONATE
NANO-PARTICLES ON PROPERTIES OF BIOCOMPOSITES**

**By
Bawornkit Nekhamanurak**

**A Thesis Submitted in Partial Fulfillment of the Requirements for the Degree
DOCTOR OF PHILOSOPHY
Program of Polymer Science and Engineering
(International Program)
Graduate School
SILPAKORN UNIVERSITY
2011**

The Graduate School, Silpakorn University has approved and accredited the Thesis title of “Effect of surface-modified calcium carbonate nano-particles on properties of biocomposites” submitted by Bawornkit Nekhamanurak as a partial fulfillment of the requirement for the degree of Doctor of Philosophy, Program of Polymer Science and Engineering.

.....
(Assistant Professor Panjai Tantatsanawong, Ph.D.)
Dean of Graduate School
...../...../.....

The Thesis Advisors

1. Asst. Prof. Pajaera Patanathabutr, Ph.D.
2. Asst. Prof. Nattakarn Hongsriphan, D.Eng.

The Thesis Examination Committee

..... Chairman
(Asst. Prof. Chanchai Thongpin, Ph.D.)
...../...../.....

..... Member
(Assoc.Prof. Duangdao Aht-Ong, Ph.D.)
...../...../.....

..... Member
(Asst. Prof. Pajaera Patanathabutr, Ph.D.)
...../...../.....

..... Member
(Asst. Prof. Nattakarn Hongsriphan, D.Eng.)
...../...../.....

51402801 : MAJOR : POLYMER SCIENCE AND ENGINEERING

KEYWORDS : CALCIUM CARBONATE NANO-PARTICLES / SiO₂-CaCO₃ NANO-PARTICLES / BIOPLASTICS / POLY(LACTIC ACID)/ BIOCOMPOSITES

BAWORNKIT NEKHAMANURAK : EFFECT OF SURFACE - MODIFIED CALCIUM CARBONATE NANO-PARTICLES ON PROPERTIES OF BIOCOMPOSITES.

THESIS ADVISORS : ASST. PROF. DR. PAJAERA PATANATHABUTR, Ph.D.,
ASST. PROF. DR. NATTAKARN HONGSRIPHAN, D.Eng. 192 PP.

There is an increasing demand on the use of biodegradable plastic, which can be renewable. A five-year Roadmap (2008-2012) for bioplastic development in Thailand was approved. Currently, biodegradable poly(lactic acid) (PLA) is offering a potential alternative to petrochemical plastics in food packaging applications. However, it is comparatively brittle and stiff at room temperature, so modification is needed for PLA in order to apply with flexible-desired applications with breathability and gas barrier properties. This research aims to investigate the effect of CaCO₃ nano-particles and plasticizers on mechanical, physical, thermal properties and rheology of PLA nanocomposite, and to improve its breathability and gas barrier properties by adding SiO₂-CaCO₃ nano-particles at different mole ratio of Si:Ca. This research found that adding of nano-sized CaCO₃ into PLA could improve processability of this commercialized biopolymer by lowering T_{cc} to around 105 °C, resulting in maintaining melt strength of the nanocomposites throughout the casting rolls. Polyethylene glycols (PEGs) and tributyl citrate (TbC) plasticizers could improve flexibility of CaCO₃-PLA nanocomposites as well as caused good dispersion of nano-sized CaCO₃ in plasticized PLA matrix. The research found the synergism of fatty acid coating on CaCO₃ and transesterification of PEG/TbC plasticizers on thermal degradation of PLA, caused the dramatically decrease in mechanical properties of PLA. However, TbC plasticizer could improve flexibility as well as maintain processability of CaCO₃-PLA nanocomposites, especially handling in casting rolls. The successful preparation of high porosity and hydrophilic modified SiO₂-CaCO₃ nano-particles by sol-gel process using TEOS as precursor was performed in this research. Adding of SiO₂-CaCO₃ nano-particles had positive effect on mechanical properties, thermal properties and thermal stability of PLA. TbC plasticized [SiO₂-CaCO₃]-PLA nanocomposites sheet showed ability to be innovated as active food packaging materials because it gave higher O₂ and CO₂ permeability but slight increase of water vapor permeability, compared to neat PLA. These properties were desirable for keeping fresh fruit and vegetable and extending the shelf life of the products.

Department of Materials Science and Engineering Graduate School, Silpakorn University
Academic Year 2011

Student's signature

Thesis Advisors' signature 1. 2.

Acknowledgments

I would like to express my eternal gratitude to my Ph.D. dissertation advisor, Asst. Prof. Dr. Pajaera Patanathabutr for her constant advice and inspiration to conducting this research as well as to my co-advisor, Asst. Prof. Dr. Nattakarn Hongsriphan for her consulting on results and discussion. My sincerely thanks also to the examination committee, Asst. Prof. Dr. Chanchai Thongpin and Assoc. Prof. Dr. Duangdao Aht-Ong, for their invaluable time and comments on the research.

I would like to express my gratefulness to Department of Materials Sciences and Engineering, Silpakorn University for research funding, traveling funding for presentation abroad, and providing research facilities. Moreover, I would like to express my thank to Center of Excellence for Petroleum, Petrochemicals, and Advanced Materials, Chulalongkorn University for Ph.D. scholarship and travelling funds supported for presentation abroad. I would like to thank National Metal and Materials Technology Center (MTEC) for supporting partial budget for material testing in the their laboratory as; scanning electron microscope (SEM), capillary rheometer, rotational rheometer, plunger impact tester, gel permeation chromatography (GPC), particle size analysis, dynamic light scattering and X-ray fluorescence (XRF).

I am gratefully appreciated for Dr. Supakit Suttiruengwong who kindly provides the use of BET surface area testing instrument, and Mr. Pathompong Puathawee, who facilitated and operated this instrument. I would like to thank Faculty of Science, Silpakorn University for conducting X-ray diffraction (XRD) analysis. Moreover, I would like to thank Dr. Amporn Sane for facilitating the extrusion sheet process by sheet chill roll line at Department of Packaging and Materials Technology, Faculty of Agro-Industry, Kasetsart University, Bang Khen Campus. Furthermore, I would like to thank Central laboratory and Greenhouse complex of Kasetsart University, Kamphaengsaen Campus for supporting the transmission electron microscope (TEM) of the nanoparticles. My special thanks to Miss Voraluck Pongsorrarith for her kindness and conducting the scanning electron microscope (SEM) at National Nanotechnology Center (NANOTEC). I would like to thank Department of Science Service, Ministry of Science and Technology for supporting the carbon dioxide transmission rate (CO₂TR) and water vapor transmission rate (WVTR) test. In addition, I would like to thank Department of Packaging and Materials Technology, Faculty of Agro-Industry Kasetsart University, Bang Khen Campus for supporting the oxygen transmission rate (O₂TR) test.

A special acknowledgement is extended to all my friends for their profound sympathy, encouragement and supports during my study at Silpakorn University. In particular, my best friend, Miss. Nicha Jamrerckjang for her patience and helping me get through the difficult times, especially throughout my dissertation writing. Finally, I am indebted to my family, especially my beloved passing mother. Thank you for your love and inspiration, and for always being here for me.

Table of Contents

	Page
Abstract	c
Acknowledgments.....	d
List of Tables	g
List of Figures	h
Chapter	
1 Introduction.....	1
Petroleum base plastics and problems	1
Bioplastics and situation	4
The research concept.....	7
Objectives and scope	9
2 Literature review	12
Properties of poly(lactic acid).....	12
Processing of poly(lactic acid)	21
Poly(lactic acid) composites	23
Blending of PLA and other polymers	24
Compounding PLA with plasticizers	25
Compounding of PLA with fillers	33
PLA/clay nanocomposites.....	33
Blending of PLA with calcium carbonate.....	37
Blending of PLA with silicon dioxide	44
3 Research Methodology	50
Phase I: The effect of particle size and particle loading on the mechanical, physical and thermal properties of CaCO ₃ -PLA biocomposites	50
Materials	50
Specimen preparation	50
Experiments	51
Thermal stability studies	51
Thermal properties studies	51
Mechanical properties studies.....	51
Dynamic mechanical properties studies.....	51
Morphology studies.....	51
Rheology studies	52
Phase II: The effect of plasticizers on the CaCO ₃ -PLA nanocomposites	52
Materials	52
Specimen preparation	53
Experiments	53
Thermal stability studies	53
Thermal properties studies	54
Mechanical properties studies.....	54
Dynamic mechanical properties studies.....	54
Morphology studies.....	54
Rheology studies	54

Chapter	Page
Phase III: The effect of SiO ₂ surface treatment on CaCO ₃ nano-particles on PLA nanocomposite.....	55
Materials	55
Preparation of silica coated calcium carbonate composite particles.....	55
Particle characterization.....	55
Specimen preparation	55
Experiments	57
Thermal stability studies	57
Thermal properties studies	57
Mechanical properties studies	57
Dynamic mechanical properties studies.....	57
Morphology studies.....	57
Rheology studies	58
Permeability studies	58
4 Results and discussion	59
Phase I: The effect of particle size and particle loading on the mechanical, physical and thermal properties of CaCO ₃ -PLA biocomposites.....	59
Materials characterization.....	59
Thermal stability studies	63
Thermal properties studies	65
Mechanical properties studies.....	67
Dynamic mechanical properties studies	69
Morphology studies	70
Rheology studies.....	73
Phase II: The effect of plasticizers on the CaCO ₃ -PLA nanocomposites	78
Thermal stability studies.....	78
Thermal properties studies.....	81
Mechanical properties studies.....	84
Dynamic mechanical properties studies	87
Morphology studies	89
Rheology studies.....	92
Phase III: The effect of SiO ₂ surface treatment on CaCO ₃ nano-particles on PLA nanocomposite.....	94
SiO ₂ -CaCO ₃ nano-particle characterization.....	95
Thermal stability studies	100
Thermal properties studies.....	102
Mechanical properties studies.....	105
Dynamic mechanical properties studies	109
Morphology studies	112
Rheology studies.....	115
Permeability studies	117

Chapter	Page
5 Conclusions and suggestion.....	122
Conclusions.....	122
Suggestion for future study.....	125
References.....	127
Appendices.....	137
Appendix A. Research data.....	138
Appendix B. Publication and Presentation	158
Biography.....	192

List of Tables

Table		Page
1	List of company that relate to bioplastics in Thailand.....	5
2	The overall method in the research.....	10
3	Classification of biodegradable polyesters	14
4	The world bioplastic consumption in 2010 and projected consumption for 2015 (type classification).....	15
5	General physical properties of PLA	16
6	The Engineering properties of Ingeo™ Biopolymer	17
7	CO ₂ , O ₂ and N ₂ gas permeation value of PLA	18
8	Solubility test results for Ingeo™ biopolymer	18
9	Properties of PEG 400	27
10	The commercial esters and their compatible used materials	30
11	Properties of tributyl citrate (TbC)	31
12	Typical percent oxide composition of commercial calcium carbonate	38
13	Physical and thermal properties of calcium carbonate	38
14	Typical percent oxide composition of ground silica.....	44
15	Definition of silica structure level	45
16	Physical and thermal properties of natural silica.....	46
17	Physical properties of synthetic silica.....	47
18	Some properties of polyethylene glycol and tributyl citrate plasticizer ...	52
19	Designations of materials and their compositions used in phase II.....	53
20	Designations of materials and their compositions used in phase III	56
21	Single particle and agglomeration size of CaCO ₃	61
22	Thermal stability analysis of the unfilled and filled PLA biocomposites with various loading of CaCO ₃	63
23	Thermal properties of CaCO ₃ -PLA biocomposite extrusion sheet.....	67
24	Thermal stability analysis of the unfilled and filled PLA nanocomposite without and with PEG/TbC plasticizers	80
25	Molecular weight determination of PLA and plasticized PLA	81
26	Thermal properties of plasticized CaCO ₃ -PLA nanocomposites	84
27	Solubility parameters (δ) for PLA and PEG/TbC plasticizers.....	86
28	The elemental analysis of SiO ₂ -CaCO ₃ nano-particles.	99
29	The Si : Ca mole ratio in synthesized SiO ₂ -CaCO ₃ nano-particles	99
30	Thermal stability analysis of PLA, CaCO ₃ -PLA nanocomposite and [SiO ₂ -CaCO ₃]-PLA nanocomposite with and without PEG/TbC plasticizer	102
31	Thermal properties of [SiO ₂ -CaCO ₃]-PLA nanocomposites without and with PEG/TbC plasticizer of 10 phr	104

List of Figures

Figure		Page
1	The growth of plastic production in 1970 to 2003	1
2	Categories of plastics product factories in Thailand.....	2
3	The growth of plastic production and exported market value of plastic pellet in Thailand from 1996 to 2003.....	2
4	The amount of plastics waste recycle and energy recovery in Western Europe in 2002	3
5	Bioplastics life cycle.....	4
6	The U.S. biopolymers market based on specific raw materials in 2003...	7
7	Calcium carbonate (CaCO_3)	8
8	The life cycle model of bioplastics	13
9	Polymerization process of PLA	16
10	L-lactic acid and D-lactic acid structure	19
11	L-lactide, D-lactide and meso-lactide structure.....	20
12	Poly(L-lactic acid) and poly(D-lactic acid) structure	20
13	Application of biodegradable polymers.....	20
14	Typical geometries of a screw for single-screw extruder.....	21
15	The chemical structure of tributyl citrate (TbC).....	31
16	Molecular structure of SiO_2	46
17	Chemical structure of plasticizers; (a) polyethylene glycol and (b) tributyl citrate	52
18	DSC thermograms of PLA pellet (Natureworks®2002D)	60
19	SEM micrographs of Micro- CaCO_3 -1740, Nano- CaCO_3 -1041 and Nano- CaCO_3 -280 particles	60
20	XRD patterns of (a) Micro- CaCO_3 -1740, (b) Nano- CaCO_3 -1041 and (c) Nano- CaCO_3 -280 particles.....	61
21	FT-IR spectra of (a) Micro- CaCO_3 -1760, (b) Nano- CaCO_3 -1041 and (c) Nano- CaCO_3 -280 particles.....	62
22	TGA curves of CaCO_3 used in this research; Micro- CaCO_3 -1740, Nano- CaCO_3 -1041 and Nano- CaCO_3 -280 particles.....	62
23	TGA curves of the CaCO_3 -PLA biocomposites with various loading of CaCO_3 ; a) Micro- CaCO_3 -1740, b) Nano- CaCO_3 -1041 and c) Nano- CaCO_3 -280.....	62
24	DSC thermograms of CaCO_3 -PLA biocomposite extrusion sheet	66
25	Mechanical properties of PLA and CaCO_3 -PLA biocomposite; a) Young's modulus, b) Percentage of strain and c) High-speed tensile strength	68
26	Storage modulus of extruded PLA and CaCO_3 -PLA biocomposite sheet.....	69
27	Tan δ of extruded PLA and CaCO_3 -PLA biocomposite sheet.....	70
28	XRD patterns of (a) extruded sheet PLA, (b) 5 wt% Micro- CaCO_3 -1740-PLA sheet, (c) 20 wt% Micro- CaCO_3 -1740-PLA sheet and (d) melt-pressed PLA sheet	71

List of Figures

Figure		Page
29	XRD patterns of (a) extruded sheet PLA, (b) 5 wt% Nano-CaCO ₃ -1041-PLA sheet, (c) 20 wt% Nano-CaCO ₃ -1041-PLA sheet and (d) melt-pressed PLA sheet	71
30	XRD patterns of (a) extruded sheet PLA, (b) 5 wt% Nano-CaCO ₃ -280-PLA sheet, (c) 20 wt% Nano-CaCO ₃ -280-PLA sheet and (d) melt-pressed PLA sheet	71
31	The distribution of CaCO ₃ particles in the PLA matrix; Micro-CaCO ₃ -1740 (10,000X) and Nano-CaCO ₃ -1041 (50,000X) and Nano-CaCO ₃ -280 (50,000X)	72
32	The melt flow index of pure PLA after extrusion process and those of micro- and nano-sized CaCO ₃ -PLAbiocomposite sheet at 5-20 wt% loading of CaCO ₃	74
33	The melt flow index variation with filler loading fraction of micro- and nano-sized CaCO ₃ -PLAbiocomposite sheet (170°C and 2.16 kg test load condition)	74
34	Viscosity properties of CaCO ₃ -PLA biocomposite at low shear rate; a) Micro-CaCO ₃ -1740-PLA biocomposite, b) Nano-CaCO ₃ -1041-PLA biocomposite and c) Nano-CaCO ₃ -280-PLA biocomposite.....	75
35	Viscosity properties of CaCO ₃ -PLA biocomposite at high shear rate; a) Micro-CaCO ₃ -1740-PLAbiocomposite, b) Nano-CaCO ₃ -1041-PLA biocomposite and c) Nano-CaCO ₃ -280-PLA biocomposite.....	77
36	TGA curves of a) Neat PLA, 5 wt% CaCO ₃ -PLA nanocomposite and plasticized CaCO ₃ -PLA nanocomposite, b) PEG plasticized PLA and plasticized CaCO ₃ -PLA nanocomposite, c) TbC plasticized PLA and plasticized CaCO ₃ -PLA nanocomposite	79
37	TGA curve of CaCO ₃ nano-particles (Nano-CaCO ₃ -280).....	81
38	DSC thermograms of plasticized CaCO ₃ -PLA nanocomposites	83
39	Mechanical properties of PLA, PLA nanocomposite and plasticized PLA nanocomposite; a) Young's modulus, b) Percentage of strain and c) Impact Strength.....	85
40	Dynamic mechanical properties of PLA, PLA nanocomposite and plasticized PLA nanocomposite; a) Storage modulus, b) tan δ of PLA, CaCO ₃ -PLA nanocomposite and plasticized PLA and c) tan δ of plasticized PLA nanocomposite	88
41	X-Ray diffraction pattern of PLA, CaCO ₃ -PLA nanocomposite and plasticized CaCO ₃ -PLA nanocomposite	90
42	SEM micrographs of fractured surface of CaCO ₃ -PLA nanocomposites without and with plasticizer; (a) PLA/CaCO ₃ , (b) PLA/CaCO ₃ /20PEG and (c) PLA/CaCO ₃ /20TbC	91
43	SEM micrographs of impact fractured specimen of PLA/CaCO ₃ /plasticizers nanocomposites. The white arrow indicates stress direction in the impact test	92

List of Figures

Figure		Page
44	Viscosity properties at low shear rate range of a) Neat PLA, 5 wt% CaCO ₃ -PLA nanocomposite and plasticized CaCO ₃ -PLA nanocomposite, b) PEG plasticized PLA and plasticized CaCO ₃ -PLA nanocomposite, c) TbC plasticized PLA and plasticized CaCO ₃ -PLA nanocomposite.....	93
45	FT-IR spectra of (a) CaCO ₃ nano-particle and (b) SiO ₂ -CaCO ₃ nano-particles.....	96
46	Morphologies of (a) CaCO ₃ nano-particles and (b-d) SiO ₂ -CaCO ₃ nano-particles.....	96
47	XRD pattern of CaCO ₃ nano-particles	97
48	XRD pattern of synthesized SiO ₂ particles	97
49	XRD pattern of amorphous SiO ₂ -CaCO ₃ nano-particles.....	97
50	Z-average diameter of CaCO ₃ and SiO ₂ -CaCO ₃ nano-particles.....	98
51	Surface areas, pore volume and pore size of CaCO ₃ and SiO ₂ -CaCO ₃ nano-particles	100
52	TGA curves of a) Neat PLA, 5 wt% [SiO ₂ -CaCO ₃]-PLA nanocomposite and plasticized [SiO ₂ -CaCO ₃]-PLA nanocomposite, b) PEG plasticized PLA and plasticized [SiO ₂ -CaCO ₃]-PLA nanocomposite at various Si : Ca mole ratio, c) TbC plasticized PLA and plasticized [SiO ₂ -CaCO ₃]-PLA nanocomposite at various Si : Ca mole ratio	101
53	DSC thermograms of [SiO ₂ -CaCO ₃]-PLA nanocomposites without and with PEG/TbC plasticizer of 10 phr	103
54	Young's modulus of PLA, plasticized PLA, plasticized CaCO ₃ -PLA and [SiO ₂ -CaCO ₃]-PLA nanocomposites at various Si : Ca mole ratio ...	106
55	Percentage of strain at break of PLA, plasticized PLA, plasticized CaCO ₃ -PLA and [SiO ₂ -CaCO ₃]-PLA nanocomposites at various Si : Ca mole ratio	107
56	Impact strength of PLA, plasticized PLA, plasticized CaCO ₃ -PLA and [SiO ₂ -CaCO ₃]-PLA nanocomposites at various Si : Ca mole ratio	108
57	Storage modulus of PLA, plasticized PLA, plasticized CaCO ₃ -PLA and [SiO ₂ -CaCO ₃]-PLA nanocomposites at various Si : Ca mole ratio.....	110
58	Tan δ of PLA, plasticized PLA, plasticized CaCO ₃ -PLA and [SiO ₂ -CaCO ₃]-PLA nanocomposites at various Si : Ca mole ratio.....	111
59	X-Ray diffraction patterns of PLA, plasticized PLA, plasticized CaCO ₃ -PLA and [SiO ₂ -CaCO ₃]-PLA nanocomposites at various Si : Ca mole ratio	113
60	SEM micrographs of fractured surface of PLA, plasticized PLA, plasticized CaCO ₃ -PLA and [SiO ₂ -CaCO ₃]-PLA nanocomposites at various Si : Ca mole ratio	114
61	SEM micrographs of fractured surface of [SiO ₂ -CaCO ₃]-PLA nanocomposites without and with plasticizer; (a) PLA/SiO ₂ -CaCO ₃ , (b) PLA/SiO ₂ -CaCO ₃ /10PEG and (c) PLA/SiO ₂ -CaCO ₃ /10TbC.....	115

List of Figures

Figure		Page
62	Viscosity of plasticized PLA nanocomposite at various shear rate range	116
63	Extrusion sheet process and PLA, CaCO ₃ -PLA nanocomposite and plasticized [SiO ₂ -CaCO ₃]-PLA nanocomposite sheets	118
64	Gas permeability of PLA, CaCO ₃ -PLA nanocomposite and plasticized [SiO ₂ -CaCO ₃]-PLA nanocomposite sheets; a) O ₂ TR, b) CO ₂ TR and c) WVTR.....	120

CHAPTER 1

INTRODUCTION

1. Petroleum base plastics and problems

Nowadays, more than 200 million tons of the plastics are produced worldwide a year [1]. Plastics become important candidates in various fields of applications due to their low price, light weight, water resistance and rust-free of the materials. Moreover, their mechanical and thermal properties along with their stability and durability are attractive to be selected to produce products in many applications. In Figure1, National Bioplastic Roadmap present that the world plastics production in 2003 estimated to 169 million tons and over 200 million tons in the recent. The growth of production approximates to 5% per year from 1985-2000 and tends to increase in the future [2].

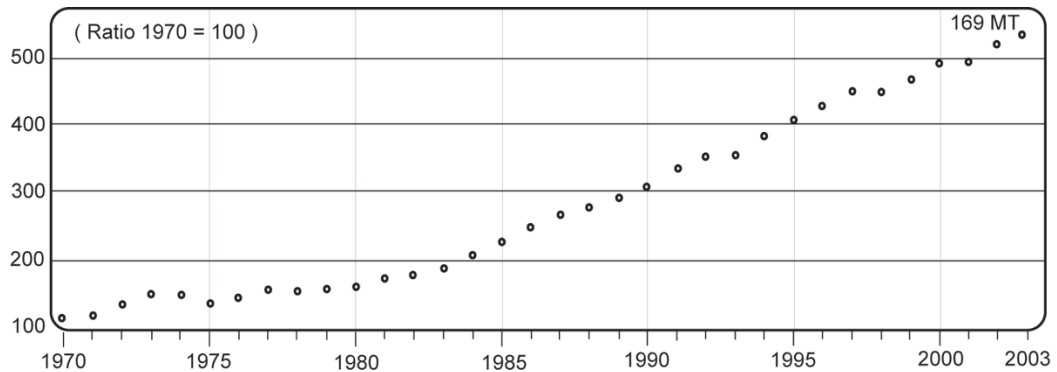


Figure 1. The growth of plastic production in 1970 to 2003 [3].

Recently, plastics are processed to be variety products, Packaging as Bottles and film are the majority of plastic consumption in the United States [4] as well as the amount of plastics product factories in Thailand as shown in Figure 2 [2]. There are a variety of methods used to process plastic. Each method has its advantages and disadvantages and is well suited for specific applications. These methods include: injection molding, blow molding, thermoforming, transfer molding, reaction injection molding, compression molding, and extrusion [5].

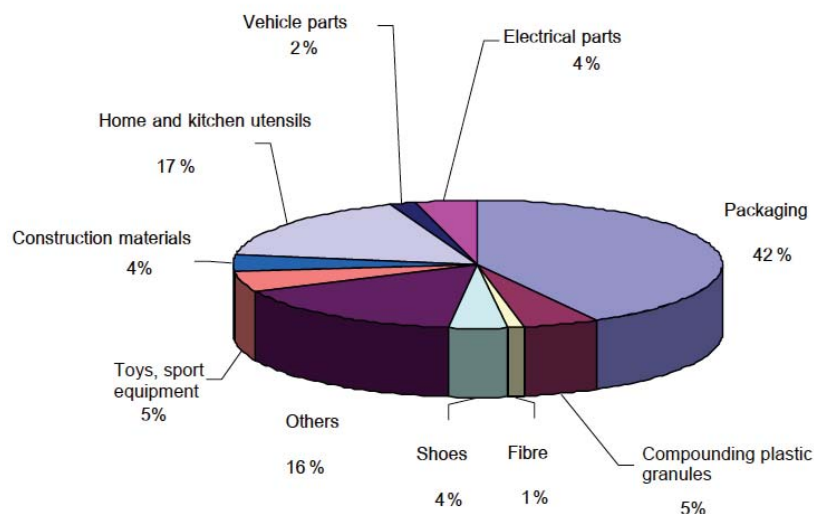


Figure 2. Categories of plastics product factories in Thailand [2].

Thai Bioplastics Industry Association (TBIA) reports the growth of plastic production in Thailand and the aspect trend as shown in Figure 3, the quantity of production and value of export market of plastic industry in Thailand have grown up continuously and there are over 100,000 million baht of values in the present. Thailand is the leader of plastic products exporter in South-East Asia and the 8th in worldwide. As shown in Figure 3, the growth of exported market value from 1996 to 2003 is over 40% and the total exported value of plastic pellet and product are equivalent to 140,000 million baht [2].

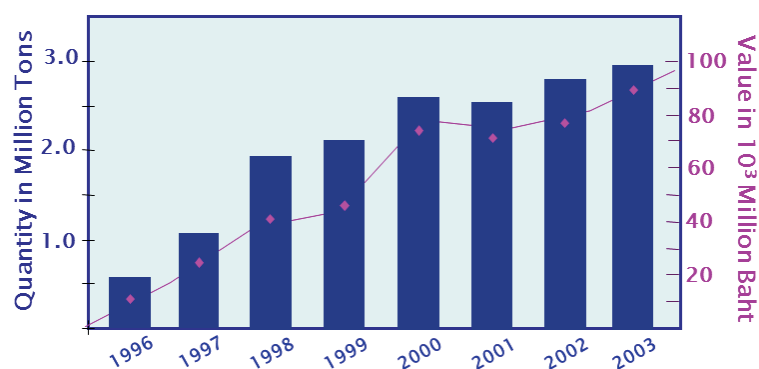


Figure 3. The growth of plastic production and exported market value of plastic pellet in Thailand from 1996 to 2003 [2].

Plastics are generally developed to provide resistance to various forms of degradation causing a lot of plastic waste and environmental pollution. They do not only take many decades to be decomposed in nature, but also produce toxins during the process of degradation [1]. So there are large amounts of non-degradable plastic wastes have been accumulated in the world. The presence of the plastic wastes is affecting the potential survival of many species including deleterious effects on wildlife and on the aesthetic qualities of cities and forest.

There are two approaches that can be used for keeping the environment free from these plastic wastes: First one is the storage of wastes at landfill sites. But because of very fast development of society, satisfactory landfill sites are also limited. Another approach is the utilization. This approach can be divided into two steps: incineration and recycling.

Incineration and recycle are ways to solve this problem. However, incineration of the plastic wastes always produces a large amount of carbon dioxide, which is a greenhouse gas causing global warming. Also, many plastic wastes produce other toxic gases, which contribute to global pollution for human and animals. For recycle, it requires considerable expenses of labor and energy; removal of plastics wastes, sorting and separation due to different types of plastics being mixed, washing, drying, grinding, and reprocessing to final products. Therefore, the recycle process would make plastic packaging to be more expensive and the quality of the recycled plastics is also lower than that of the virgin materials.

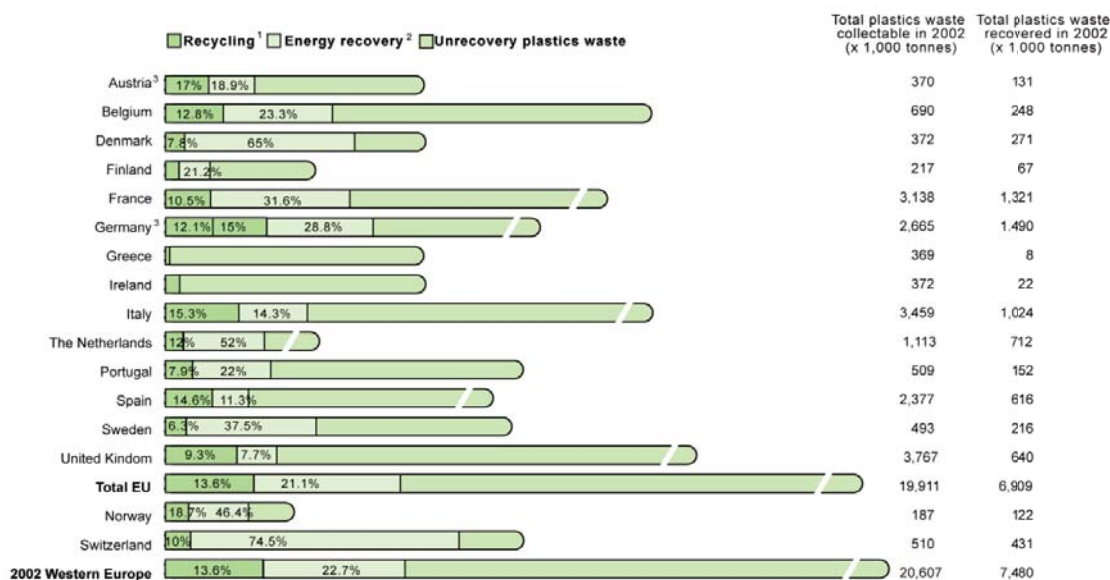


Figure 4. The amount of plastics waste recycle and energy recovery in Western Europe in 2002 [2].

The information in Figure 4 shows that there are large amount of plastic waste, which are not recovered when compare with the recycle and energy recovery or incineration of waste plastics. This reveals that the capability of the recovery plastic in EU, countries that are aware in environment and have high technology, is just 30% of plastics waste. That is not enough for the growth of plastic waste, thus there are an accumulation of plastics waste and environmental problem [2].

From reasons that have been stated above, there is an urgent need for the development of green polymeric materials without using toxic or noxious components in their manufacture and can be degraded in the natural environment. Research in biodegradable and bio-based polymers has received increasing attention in recent years [6-8].

2. Bioplastics and situation

Biodegradable plastics are plastics that will decompose in natural aerobic (composting) and anaerobic (landfill) environments. Biodegradation of plastics can be achieved by enabling microorganisms in the environment to metabolize the molecular structure of plastic films to produce an inert humus-like material that is less harmful to the environment. They may be composed of either bioplastics, which are plastics whose components are derived from renewable raw materials, or petroleum-based plastics, which utilize an additive. The use of bio-active compounds compounded with swelling agents ensures that, when combined with heat and moisture, they expand the plastic's molecular structure and allow the bio-active compounds to metabolize and neutralize the plastic. Furthermore, biodegradable polymers can be derived from the petroleum sources or may be obtained from mixed sources of biomass and petroleum. The best known petroleum source-derived biodegradable polymers are aliphatic polyesters or aliphatic-aromatic copolyesters such as poly(butylene succinate) (PBS) and poly(butylene adipate-co-butylene terephthalate) (PBAT). However, biodegradable polymers made from renewable resources like poly(lactic acid) (PLA) are attracting much more attention because of more eco-friendliness from their origin as contrast to the fully petrochemical biodegradable polymers and control of carbon dioxide (CO₂) balance after their composting [6,9,10].

Bioplastics are a new generation of biodegradable and compostable plastics. They are derived from renewable raw materials like starch (e.g. corn, potato, tapioca, etc), cellulose, soy protein and lactic acid or can also be synthesized by bacteria from small molecules like butyric acid or valeric acid that gives polyhydroxybutyrate (PHB) or polyhydroxyvalerate (PHV), respectively. Corn starch is currently the main raw material being used in the manufacture of bioplastic resins in USA. Bioplastics are environmentally friendly, compared with petrochemical plastics, because their production results in the emission of less CO₂, which is thought to cause global warming, and decompose back into CO₂, water and biomass when discarded [11,12]. Bioplastics life cycle is shown in Figure 5.

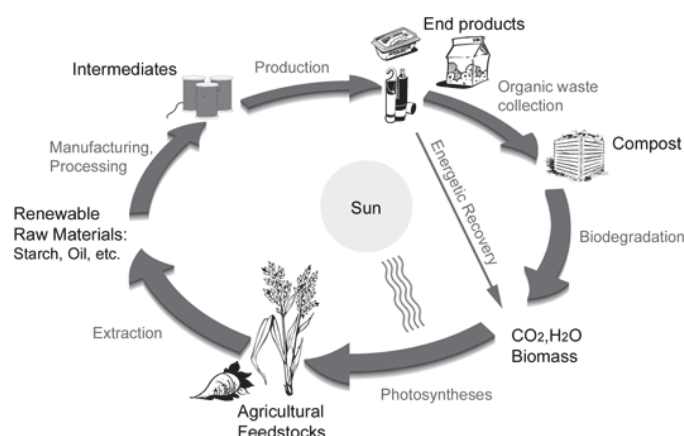


Figure 5. Bioplastics life cycle [13].

Many company in Thailand trade and produce some plastic products from bioplastic. In addition, these companies try to develop their own technology and

collaboration with some abroad company, government research center, and university to find and developed new product to the market. This showed that plastic industry in Thailand are interested in bioplastic and the bioplastics industry can grow up and sustainable in this country. Table 1 shows the list of company that relate to bioplastics in Thailand.

Table 1. List of company that relate to bioplastics in Thailand [2,14-18].

Company	Product	Technology/Activity
1. Advance Packing Co.,Ltd. (Special Tech Group)	Plastic bag for plant	- Develop the product from corn - Import the bioplastics pellet from the US and process
2. M.S.V. Trading Ltd.	Food container and related such as plate, dish, spoon and fork	- Import the bioplastics pellet from the US and process products
3. Bio Green World Co., Ltd. (BGW)	Food container and related such as plate, dish, spoon and fork	- Import the bioplastics pellet from Taiwan - Compounding PLA with starch and process products
4. BIOFOAM Jazzy Creation Co., Ltd	Compostable containers	- Hot compression process of tapioca flour
5. Biodegradable Packaging for Environment Co.,Ltd. (BPE)	Compostable containers	- Produce products by using bagasse as raw materials
6. KU-GREEN: Biodegradable Package	Compostable containers	- Hot compression process of tapioca flour

Company	Product	Technology/Activity
7. Thantawan Industry Public Co.,Ltd.	Bags and film	<ul style="list-style-type: none"> - Import the bioplastics pellet from the US and compounding pellet from Japan - Develop compounding bioplastic - Develop business partner with Novamont, Italian leading starch-bio plastic producer
9. PTT Chemical Public Co.,Ltd.	Trading and develop bioplastics pellet and chemicals	<ul style="list-style-type: none"> - Joint-venture with NatureWorks LLC, the world's leading bioplastics manufacturer as PLA - Joint-venture with Myriant Technologies, Inc. (Myriant), a privately-held, biotech developer and manufacturer of renewable bio-based chemicals as succinic acid.
10. IRPC Public Co.,Ltd.	Green Acrylonitrile-Butadiene-Styrene (ABS)	Value addition to ABS by mixing replace synthesis rubber with natural rubber and modified natural rubber
11. SCG Chemicals Co., Ltd.	Compostable compounds	<ul style="list-style-type: none"> - Compounding bioplastics and biochemicals - Joint-venture with Mitsui Chemicals, Inc., developer and manufacturer of renewable bio-based chemicals in Japan
12. PURAC (Thailand) Ltd.	Lactic acid	Produce lactic acid, PLA precursor.

Furthermore, the big user organisation as Thai Airways International PCL is now interested and paying attention in the environmental issue and the bioplastics products. Thai Airways International PCL order eco-friendly bioplastic bags to use in 30 branches of the Puff & Pie Shop and serve the bioplastic cups on the green flight as biofuels flight [19,20].

Among all bioplastics, polylactide or poly(lactic acid) (PLA) is the majority of the market as shown in Figure 6, which is mainly used to produce plastic packaging as film. In 2003, the U.S. biopolymers market revenues were approximately at \$27 million, corresponding to 22.9 million pounds of unit shipment. The market for biopolymers may grow by 30% per year over the decade. By 2010, market for biopolymers is expected to grow to 1.5-4.8% of the total plastics market, with the forecasted market revenue of \$67.8 million. Currently, various biopolymers are commercially available in the market. Based on specific raw materials, revenue share of biopolymers market in 2003 was the greatest for lactic acid-based biopolymers, followed by co-polyester-based, starch-based, polycaprolactone-based and other-based biopolymers [1].

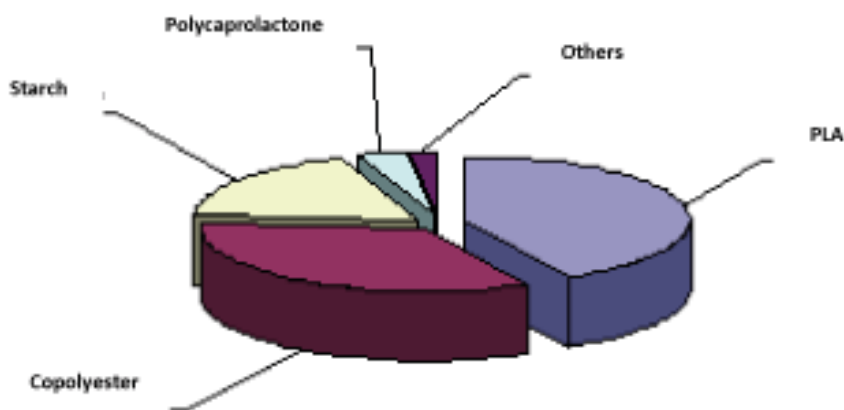


Figure 6. The U.S. biopolymers market based on specific raw materials in 2003 [1].

PLA still has some difficulty in melt film process due to its inherent brittleness. One important requirement for packaging materials is high flexibility at room temperature during storage time. Other requirements include transparency and high crystallinity to tolerance film tearing and cracking when subjected to loads during package manufacturing. Moreover, good breathability and gas absorbability of food packaging materials are highly considerate. PLA, however, is comparatively brittle and stiff at room temperature due to its glass transition temperature (T_g) is higher than room temperature [8,12], so modification is needed for PLA in order to apply with flexible-desired applications as food packaging.

3. The research concept

The concept of this research is to develop PLA compounding for food packaging application. This packaging has some good properties such as mechanical

properties and thermal properties. Permeability is also study because this property is necessary for fruit and vegetable containers. The optimum permeability can prevent these products from ripening and spoilage. It can extend the shelf life of these products before customers select them.

Adding fillers into plastics is usually implemented to improve their mechanical properties. Recently, there are widely attempts to improve polymeric materials' properties with nano-size inorganic fillers such as ZnO, SiO₂, clay, precipitated calcium carbonate (PCC) surface modified with rare earth elements, and noble metals [6,21-28]. Properties of filler-filled composites are closely related to the dispersion of the particles in polymer matrix.



Figure 7. Calcium carbonate (CaCO₃) [29].

As shown in Figure 7, calcium carbonate (CaCO₃) is a common substance found in rocks in all parts of the world, and is the main component of shells of marine organisms, snails, pearls, and eggshells. CaCO₃ is widely used as filler in plastics, rubbers, paper, paints and other fields. Polypropylene compounds are often filled with CaCO₃ to increase rigidity, which is needed more at high temperature applications. Fine ground CaCO₃ is an essential ingredient in the micro-porous film used in babies diapers and some building films as the pores are nucleated around the CaCO₃ particles during the manufacture of the film by biaxial stretching [22,27,30,31].

Nano-sized CaCO₃, having a particle size between 1–100 nm, is an important engineering material that has been developed in the 1980s. The super fine nano-CaCO₃ particles have large surface areas compared to the volume of the crystals resulting in a “small size effect” and a “surface effect” that ordinary CaCO₃ does not have [32]. Furthermore, the composite strength could be reduced with increasing loading of particles at and larger than 80 nm [33]. Since PLA is well known for its difficulty to crystallize, adding of CaCO₃ could have an impact on its properties as well as potential applications replacing petrochemical based plastics [21,22].

Plasticizers are an important class of low molecular weight non-volatile compounds that are widely used in polymer industries as additives. The primary role of such substances is to improve the flexibility and processability of polymers by lowering the second order transition temperature, the glass transition temperature (T_g). The council of the IUPAC (International Union of Pure and Applied Chemistry)

defined a plasticizer as a substance or material incorporated in a material (usually a plastic or elastomer) to increase its flexibility and workability. These substances reduce the tension of deformation, hardness, density, viscosity and electrostatic charge of a polymer, at the same time as increasing the polymer chain flexibility, resistance to fracture and dielectric constant. Plasticizers are widely used to improve processability, flexibility and ductility of polymers. In the case of semicrystalline polymers like PLA, an efficient plasticizer has to reduce the glass transition temperature but also to depress the melting point and the crystallinity. Lactide monomer, for instance, is a good candidate to plasticizing PLA but it tends to migrate to the material's surface causing a stiffening of the films in time. The most common plasticizers used for PLA are polyethylene glycols and citrates [34].

When incorporating plasticizer into PLA, Pillin et al. [34] reported that the polyethylene glycols (PEGs) were the most efficient for the T_g reduction and it clearly appeared when the compositions of plasticizer were higher than 20 wt%, all the blends presented a limit of miscibility and the glass transition temperature reached a plateau value. Mechanical characteristics of these materials showed a decrease in modulus and stress at break. Ljungberg et al. [35] proved that tributyl citrate oligomeric plasticizers drastically lowered the glass transition temperature of PLA, thus creating homogeneous and flexible materials. The plasticization effect was larger with low molecular weight tributyl citrate plasticizers as same as PEGs case.

Filler as CaCO_3 and modified CaCO_3 , and plasticizers as polyethylene glycols (PEGs) and tributyl citrate (TbC) can affect on PLA properties in the difference and variety aspects. The incorporation of these additives have potential to give the appreciate properties for PLA. Some requirement properties of PLA can be adjusted for suitable application by control the type and content of these additives.

4. Objectives and scope

The research aims to investigate the effect of particle size and particle loading on the mechanical, physical and thermal properties of CaCO_3 -PLA nanocomposites. In the experiment, CaCO_3 nano-particles are treated by SiO_2 via sol-gel process of tetraethylorthosilicate (TEOS) at which the ratio of CaCO_3 nano-particles to TEOS is varied to study the influence of SiO_2 content on SiO_2 - CaCO_3 nano-particles morphology and its absorbability. The research also determines the effect of plasticizers on the biocomposite cast sheets for potential use in food packaging applications. In addition, the effect of SiO_2 surface treatment on CaCO_3 nano-particles on breathability of the biocomposite cast sheets is investigated.

The study on the effect of surface-modified CaCO_3 nano-particles on properties of biocomposites is divided the study into 3 phases:

Phase I is to study the effect of particle size and particle loading on the mechanical, physical and thermal properties of CaCO_3 -PLA biocomposites.

Phase II is to study the effect of plasticizers on the mechanical, melt, thermal properties of the CaCO_3 -PLA nanocomposites.

Phase III is to study the effect of SiO_2 surface treatment on CaCO_3 nano-particles on properties and breathability of the nanocomposite and plasticized nanocomposite.

The overall methods in the research are summarized in Table 2. The biocomposites were compounded and fabricated to be sheet in phase I by a twin-screw extruder. However, the limitation of low melt strength plasticized nanocomposites caused the specimens in phase II to have to be prepared by compression molding. Finally, SiO₂ coated CaCO₃ particles were developed in phase III and the properties of the nanocomposites were studied. Furthermore, the breathability properties and the gas absorption ability of nanocomposite are discussed in this final phase.

Table 2. The overall method in the research.

Research	Outcome
Phase I. The effect of particle size and particle loading on the mechanical, physical and thermal properties of CaCO ₃ -PLA biocomposites.	<p>To prepare melt cast sheets of CaCO₃-PLA biocomposites by a co-rotating twin screw extruder.</p> <hr/> <p>To investigate the effect of CaCO₃ particle size (micro- and nano-size) and CaCO₃ particle loading on the followings properties;</p> <ul style="list-style-type: none"> - thermal stability - thermal properties - tensile and impact properties - dynamic mechanical properties - SEM of fractured surface - crystallinity - rheology behavior
Phase II. The effect of plasticizers on the CaCO ₃ -PLA nanocomposites.	<p>To prepare melt of CaCO₃-PLA nanocomposites with and without plasticizers as polyethylene glycol (PEG) and tributyl citrate (TbC) by a compression molding.</p> <hr/> <p>To investigate the effect of plasticizer type and plasticizer loading on the followings properties;</p> <ul style="list-style-type: none"> - thermal stability - thermal properties - tensile and impact properties - dynamic mechanical properties - SEM of fractured surface - crystallinity - rheology behavior

Research	Outcome
Phase III. The effect of SiO ₂ surface treatment on CaCO ₃ nano-particles on properties and breathability of nanocomposites and plasticized nanocomposites.	To prepare SiO ₂ -CaCO ₃ nano-particles at different ratio of SiO ₂ :CaCO ₃ .
	To determine surface and porosity of SiO ₂ -CaCO ₃ nano-particles.
	To prepare melt cast sheets of [SiO ₂ -CaCO ₃]-PLA nanocomposites with and without plasticizers as polyethylene glycol (PEG) and Tributyl citrate (TbC).
	To investigate the effect of SiO ₂ surface treatment and plasticizer on the followings; <ul style="list-style-type: none">- thermal stability- thermal properties- tensile and impact properties- dynamic mechanical properties- crystallinity- SEM of fractured surface- rheology behavior- O₂ and CO₂ and water vapor permeability

CHAPTER 2

LITERATURE REVIEW

Because polymers present several desired features like softness, lightness and transparency, they have supplied most of common packaging materials as films. However, increased use of synthetic polymer packaging films has led to serious ecological problems due to their non-biodegradability. The use of long-lasting polymers as packaging materials for short application is not justified because physical recycling of these materials is often impractical due to food contamination. So there is an increasing demand on the use of biodegradable polymer which could be easily renewable [36,37]. The aim of this review was to offer view related to most commercialized biopolymer poly(lactic acid) (PLA) which exhibits high tensile strength and modulus but very low strain-at-break and toughness. Thus, many current researches aim to improve its properties by blending with other polymeric materials and nano-sized fillers.

1. Properties of poly(lactic acid)

In 2008, the global consumption of plastics is more than 200 million tones, with an annual grow of approximately 5% [2,38]. Petrochemical-based plastics such as polyethylene terephthalate (PET), polyvinylchloride (PVC), polyethylene (PE), polypropylene (PP), polystyrene (PS) and polyamide (PA) have been increasingly used as packaging materials because their large availability at relatively low cost and because their good mechanical performance such as tensile and tear strength, good barrier to oxygen, carbon dioxide, anhydride and aroma compound, and heat sealability. However, nowadays their use has to be restricted because they are not non-totally recyclable and/or biodegradable so they pose serious ecological problems [3,23]. Plastic packaging materials are also often contaminated by foodstuff and biological substance, so recycling these material is impracticable and most of the times economically not convenient. Polymers from renewable resources have been attracting increasing attention over the past two decades, predominantly for two reasons: the first being environmental concerns and the second being the realization that our petroleum resources are finite [39]. Biopolymers are now playing significance; it can be viewed as sustainable in term of variables such as raw materials supply, water and energy use and waste product generation. Since most biopolymers are biodegradable or compostable, they can become ‘food’ for the next generation of materials as shown in the bioplastic life cycle in Figure 8 [38].

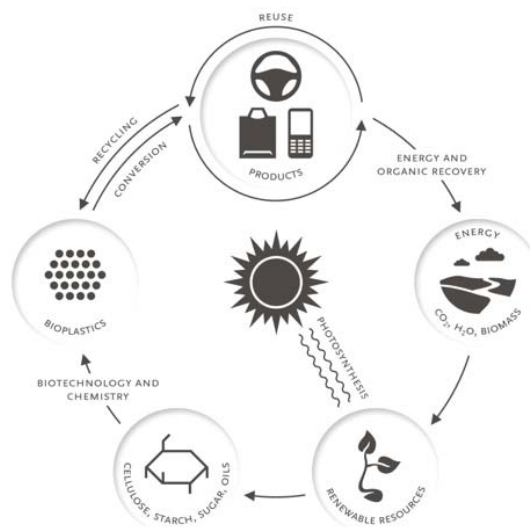


Figure 8. The life cycle model of bioplastics [40].

It is not easy to decide how to classify biodegradable polymer. They can be sorted according to their chemical composition synthesis method, processing method, economic importance, application, etc. Each of these classifications provides different and useful information. In the present review, the biodegradable polymers are classified according to their origin into two groups: natural polymers, polymers coming from natural resources and from mineral origins, most of which are synthesized from crude oil.

Biopolymers from natural origins include, from a chemical point of view, six sub-groups as:

1. Polysaccharides (e.g., starch, cellulose, lignin, chitin)
2. Protein (e.g., gelatin, casein, wheat gluten, silk and wool)
3. Lipids (e.g., plant oil including castor oil and animal fat)
4. Polyesters produced by micro-organism or by plants (e.g., polyhydroxy alkanates, poly-3-hydroxybutyrate)
5. Polyesters synthesized from bio-derived monomer (polylactic acid)
6. Miscellaneous polymer (natural rubber, composites)

Biopolymers from mineral origins include four sub-groups as:

1. Aliphatic polyesters (e.g., polyglycolic acid, polybutylene succinate, polycaprolactone)
2. Aromatic polyesters or blends of two types (e.g., polybutylene succinate terephthalate)
3. Polyvinyl alcohols
4. Modified polyolefins (polyethylene or polypropylene with specific agents sensitive to temperature or light)

Poly(lactic acid) (PLA) is in the category of biopolymers from natural origins because its monomer (lactic acid) is today largely produced by fermentation of corn. It is also mention in the category of the synthetic aliphatic polyesters because it can be synthesized from oil. Polyesters can be classified following the composition of

their main chain. There are aliphatic and aromatic polyesters as shown in Table 3. PHA, PHB, PHV and PHH are found as aliphatic polyesters from natural origins. PBS, PBSA and PCL are listed in the mineral origins. PLA and PGA are originated from both origins. In the family of aromatic polyesters, those coming from PET or from PBT (PBST, PBAT, PRMAT) and copolymer are separately classified.

Table 3. Classification of biodegradable polyesters [41].

Groups		Type	Derivate	Origin	Production
Polyesters	Aliphatic	PHA	PHB	Natural	Natural
			PHV	Natural	Natural
			PHH	Natural	Natural
		PGA		Double	Synthetic
		PLA		Double	Synthetic
		PBS	PBSA	Mineral	Synthetic
		PCL		Mineral	Synthetic
	Aromatic	PBT	PBAT	Mineral	Synthetic
			PBST	Mineral	Synthetic
			PTMAT	Mineral	Synthetic

The bioplastic consumption tends to increase gradually. European bioplastic association reports the world bioplastic consumption in 2010 and its projected consumption for 2015 is shown in Table 4.

Poly(lactic acid) (PLA) or Polylactide is a biocompatible and biodegradable polymer, belongs to the family of aliphatic polyester synthesized from bio-derived monomers lactic acid, and now commercially available [39,41]. The difference in terminology indicates simply the synthesis method chosen to produce the polymer. The interest in this material started in the 1930s with the work of Carothers but the molecular weight and the mechanical properties were weak [41]. In 1954, DuPont patented a PLA presenting higher molecular weight and in 1972, the first co-polymers allowed the production of medical resorbable sutures. PLA was synthesized from the esterification of lactic acid produced by fermentation. The micro-organism can be Lactobacilli, Pediococci or certain fungi such as *Rhizopus Oryzae*. Nowadays, the PLA cost decrease is due mainly to the improvement of the bacterial yield [41].

From lactic acid, there are two pathways to produce PLA as shown in Figure 9. The first one has been developed through step-growth polymerization technique relies on the condensation of hydroxy-acids or of mixtures of diacids and diols. The major drawbacks of this polycondensation mechanism are the high temperatures and long reaction times generally required that favor the side reactions, together with the deleterious effect on the molecular weight of any short deviation from the reaction stoichiometry. Such reaction is also limited to equilibrium. Water must thus be removed from the polymerization medium to increase the conversion and the molecular weight [42].

Table 4. The world bioplastic consumption in 2010 and projected consumption for 2015 (type classification) [43].

Type	Year 2010 tonnes (%)	Year 2015 tonnes (%)
Bio-PE	200,000 (28%)	450,000 (26%)
Biodegradable starch blends	117,800 (16%)	124,800 (7%)
PLA	112,500 (15%)	216,000 (13%)
PHA	88,100 (12%)	147,100 (9%)
Biodegradable polyester	56,500 (8%)	143,500 (8%)
Bio-PET	50,000 (7%)	290,000 (17%)
Regenerated cellulose ¹	36,000 (5%)	36,000 (2%)
Bio-PVC	-	120,000 (7%)
Bio-PA	35,000 (5%)	75,000 (5%)
Cellulose derivatives ²	8,000 (1%)	-
PLA-blends	5,100 (1%)	35,000 (2%)
Bio-PP	-	30,000 (1%)
Bio-PC	-	20,000 (1%)
Other	7,500 (1%)	22,300 (1%)
Total	724,500 (100%)	1,709,700 (100%)

¹only hydrated cellulose foil, ²only cellulose ester

This can be achieved by azeotropic distillation of high boiling point solvents as used for the industrial synthesis of high molecular weight poly(lactic acid) (PLA) by Mitsui in Japan [44]. First of all, the aqueous lactic acid solution is purified and concentrated. Then, the direct condensation and cyclisation reactions are performed at elevated temperatures in the presence of a catalyst. The condensate is removed by distillation. This process produces a poly(lactic acid) of high molecular weight presenting a broad distribution [41]. However, the use of high boiling organic solvents, difficult to remove by evaporation, is poorly compatible with production of solvent free PLA [42].

The second process is indirect called ring-opening polymerization. A lactide is produced from two lactic acid molecules by cyclisation and dimerisation. Lactide oligomers can then be polymerized in polylactide. The dimerisation step is a critical and more expensive pathway. Cargill Dow uses the second process: ring-opening polymerization of lactic acid through the lactide intermediate. In the first step of the process water is removed carrier to concentrate lactic acid followed by polymerization to a low molecular weight prepolymer. This prepolymer is then fed to a reactor in which a catalyst is added to facilitate generation of lactide, the depolymerization product of poly(lactic acid). The lactide generated is continuously fed to distillation system as a liquid or vapor wherein water and other impurities are removed. The resultant purified liquid lactide is fed directly to a polymerization

process [45,46]. The purified lactide is polymerized in a solvent free ring-opening polymerization and processed into polylactide pellets. The melt-stable lactide polymer comprises a plurality of polylactide polymer chains, residual lactide in concentration of less than 2 percent and water in concentration of less than 1,000 parts-per-million. By controlling the purity of the lactide it is possible to produce a wide range of molecular weights. A process for manufacture of a melt-stable lactide polymer composition includes polymerizing of a lactide mixture and adding stabilizing agents sufficient to reduce depolymerization of the polylactide during melt-processing, followed by devolatilizing the polylactide to remove monomer and water [47,48].

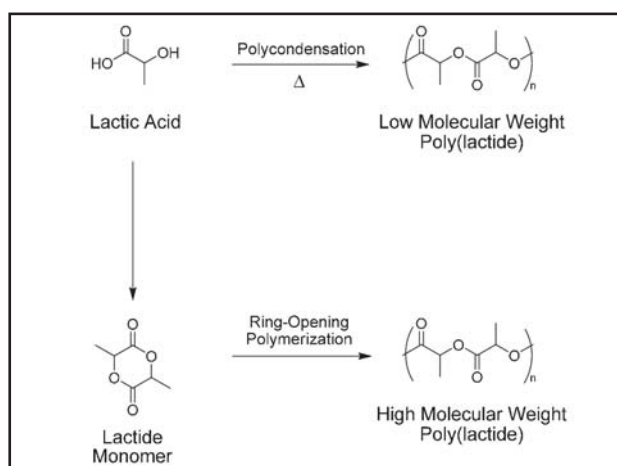


Figure 9. Polymerization process of PLA [49]

PLA is commercially and largely available (large-scale production) in a wide range of grades. It has a reasonable price and some remarkable properties to fulfill different applications. Table 5 shows various properties of PLA up to grade and their applications. The properties of PLA change from one producer to another but general properties are resistance to fat, food oil, humidity, solvent and smells. Biodegradation occurs by composting (in 3-4 weeks). Some grades are really bright and transparent but are also more brittle [41].

Table 5. General physical properties of PLA [50].

Properties	Unit	Value
Density	g/cm ³	1.23 to 1.25
Melt Mass Flow Rate	g/10 min	0.20 to 37
Flexural Modulus	MPa	598 to 9,500
Tensile Strength	MPa	13.0 to 72.3
Tensile Elongation	%	1.0 to 10
Rockwell Hardness		84 to 115
Notched Izod Impact	J/m	13 to 33
DTUL @ 66 psi (0.45 MPa)	°C	46.8 to 121
DTUL @ 264 psi (1.8 MPa)	°C	48.0 to 50.1

The PLA production capacity of Cargill (USA) or NatureWorks in 2007 was 140 kT per year at 2–5 Euros per kg. Other companies, such as Mitsui Chemical (Lacea-Japan), Treofan (Netherland), Galactic (Belgium), Shimadzu Corporation (Japan), produce smaller quantities [51]. The engineering properties of PLA from NatureWorks (IngeoTM) are shown in Table 6.

Table 6. The Engineering properties of IngeoTM biopolymer [52].

Property	Value	
Thermal conductivity (amorphous sheet)	- 8 °C	0.127 J/m -°K-s
	25 °C	0.130 J/m -°K-s
	58 °C	0.131 J/m -°K-s
	124 °C	0.126 J/m -°K-s
	190 °C	0.121 J/m -°K-s
Thermal conductivity	25 °C	0.160 J/m-°K-s
specific heat, Cp (amorphous sheet)	25 °C	1.20 J/g °C
	60 °C	2.14 J/g °C
	90 °C	2.16 J/g °C
Glass Transition Temperature, T _g	55–60 °C	
Peak Melt Temperature, T _m	145-170 °C	
Specific Gravity, ρ	1.24-1.25 g/cc	
Melt Density (200°C), ρ melt	1.12 g/cc	
Pellet Bulk Density, ρ bulk	0.79-0.85 kg/liter	
Typical Flake Bulk Density, ρ flake	0.593 kg/liter	

For food packaging, gas and water vapor permeability is an important property. As many of biobased materials are hydrophilic, the gas permeability of hydrophilic biobased materials may increase manifold when humidity increases. Notably, this is a phenomenon also seen with conventional polymers. The gas permeability of high gas barrier materials, such as nylon and ethylvinyl alcohol, is likewise affected by increasing humidity. Gas barriers based on PLA and PHA is not expected to be dependent on humidity [36,37]. There are some reports on gas permeability of PLA. Rhim et. al. reported the water vapor permeability (WVP) of control PLA solvent casting film is 1.8×10^{-11} g m/(m² s Pa) [53] and the website name biodeg also reported this properties at 172 g/m²/day at 25 °C [54].

Bao et.al. reported the permeation of nitrogen, oxygen, carbon dioxide, and methane in amorphous films of PLA cast from solution. At 30°C, N₂ permeation in PLA is 0.05 (10⁻¹⁰ cm³ (STP) cm/cm² s cmHg), oxygen permeation in PLA is 0.26 (10⁻¹⁰ cm³ (STP) cm/cm² s cm Hg) and its carbon dioxide permeation is 1.1 (10⁻¹⁰ cm³ (STP) cm/cm² s cmHg) [55]. The details of PLA gas permeation are shown in Table 7.

Table 7. CO₂, O₂ and N₂ gas permeation value of PLA [55].

Gas	L:D content	Permeability (Barrer*)
Carbon dioxide (CO ₂)	98.7 : 1.3	1.1
	80 : 20	0.51
	50 : 50	0.71
Oxygen (O ₂)	98.7 : 1.3	0.26
	80 : 20	0.18
	50 : 50	0.17
Nitrogen (N ₂)	98.7 : 1.3	0.05
	80 : 20	0.02
	50 : 50	0.03

*A Barrer is a non-SI unit of gas permeability (specifically, oxygen permeability) used in the contact lens industry. It is a bulk property. It is named after Richard Barrer, 1 Barrer = 846 millilitre . mm/(cm² . day. bar(a)) = 3.348 x 10⁻¹⁹ kmol.m/(m² s Pa) [56].

Sometime PLA was contacted to the chemical solvent that may effect to the solubility of PLA. NatureWorks Company has concluded the PLA solubility test results in some grade and solvent as shown in Table 8.

Table 8. Solubility test results for Ingeo™ biopolymer [52].

Solvent	Ingeo 4060D* % Soluble (std dev)	Ingeo 4032D** % Soluble (std dev)
1,2 Dichloroethane	99.8 (+0)	99.9 (+0)
DMF	99.8 (+0.1)	67.5 (+5.2)
Heptane	8.6 (+3.9)	27.5 (+12.3)
Isopropyl alcohol	0 (+0.2)	0 (+1.8)
MIBK	20.6 (+1.7)	0 (+0.4)
Octanol	1.3 (+3.8)	5.2 (+0.5)
THF	99.8 (+0)	99.9 (+0)
Toluene	99.8 (+0.1)	0.4 (+1.6)

* Ingeo™ Biopolymer 4060D For Heat Seal Layer in Coextruded Oriented Film

**Ingeo™ Biopolymer 4032D Biaxially Oriented Films – High Heat

Due to the chiral nature of lactic acid, several distinct forms of polylactide exist. Poly-L-lactide (PLLA) is the product resulting from polymerization of L,L-lactide (also known as L-lactide). PLLA has a crystallinity of around 37%, a glass transition temperature between 60-65 °C, a melting temperature between 173-178 °C and a tensile modulus between 2.7-16 GPa. However, heat resistant PLA can withstand temperatures of 110 °C (230 °F). PLA has similar mechanical properties to PETE polymer, but has a significantly lower maximum continuous use temperature. PLA can be processed like most thermoplastics into fiber (for example using conventional melt spinning processes) and film. The melting temperature of PLLA can be increased 40-50 °C and its heat deflection temperature can be increased from approximately 60 °C to up to 190 °C by physically blending the polymer with PDLA (poly-D-lactide). PDLA and PLLA form a highly regular stereocomplex with increased crystallinity. The temperature stability is maximized when a 50:50 blend is used, but even at lower concentrations of 3-10% of PDLA, there is still a substantial improvement. In the latter case, PDLA acts as a nucleating agent, thereby increasing the crystallization rate. Biodegradation of PDLA is slower than for PLA due to the higher crystallinity of PDLA. However, PDLA has the useful property of being optically transparent [57].

Because there are four unique groups attached to the central carbon atom, lactic acid is a chiral molecule. Chiral molecule exists as ‘mirror images’ or stereoisomers. The optically active lactic acid has an ‘l’ and ‘d’ stereoisomer as shown in Figure 10. ‘l’ and ‘d’ are also referred to as R and S (d = R = right handed and l = S = left handed). Chemically synthesized lactic acid gives the racemic mixture (50% d and 50% l). Fermentation-derived lactic acid typically consists of 99.5% of the l-isomer and 0.5% of the d-isomer. Production of the cyclic lactide dimer results in three potential forms; the d, d-lactide (called d-lactide), l, l-lactide (called l-lactide) and l, d or d, l-lactide called meso lactide as shown in Figure 11. Meso lactide has different properties from d- and l-lactide. The d- and l-lactide are optically active, but the meso is not. Before polymerization the lactide stream is split into a low d-lactide stream and a high d/meso lactide stream. Ring- opening polymerization of the optically active types of lactide can yield a ‘family’ of polymers characterized by the molecular weight distribution and by the amount and the sequence of d-lactide in the polymer backbone. Polymers with high l-lactide levels can be used to produce crystalline polymers while the higher d-lactide materials are more amorphous [58]. Poly(L-lactic acid) and poly(D-lactic acid) structure are shown in Figure 12.

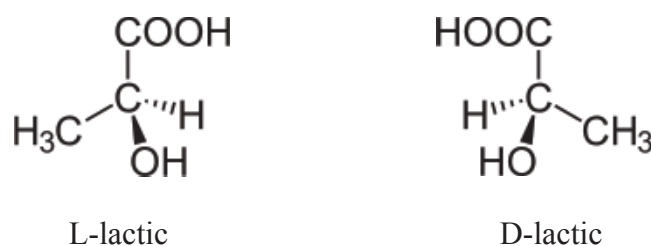


Figure 10. L-lactic acid and D-lactic acid structure [59].

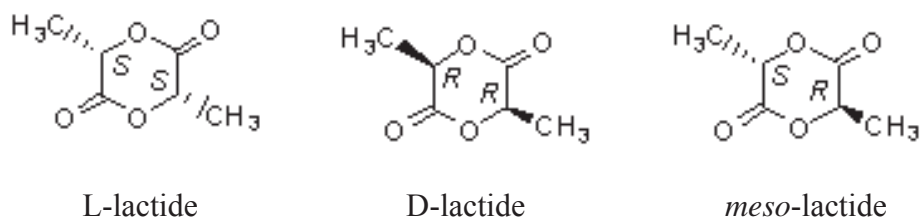


Figure 11. L-lactide, D-lactide and meso-lactide structure [60].

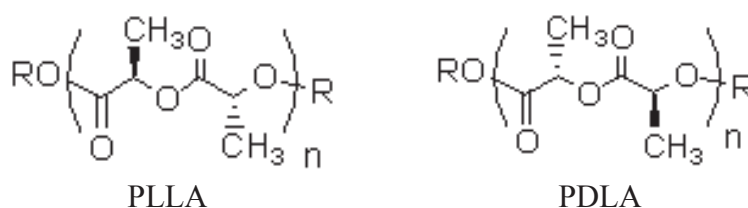


Figure 12. Poly(L-lactic acid) and poly(D-lactic acid) structure [60].

Biodegradable polymers have currently two major applications; one is as biomedical polymers that contribute to the medical care of patients such as PAA: Poly(acid anhydride); PCA: Poly(α -cyanoacrylate); PDLA: Poly(DL-lactide) or Poly(DL-lactic acid); PGA: Poly(glycolide) or Poly(glycolic acid); PGALA: Poly(glycolide-co-lactide) or Poly(glycolic acid-co-lactic acid); POE: Poly(orthoester). The other is as ecological polymers that keep the earth environments clean such as PBS: Poly(butylene succinate); PEA: Poly(ester amide); PEC: Poly(ester carbonate); PES: Poly(ethylene succinate); PHA: Poly(hydroxyalkanoate); PHB: Poly(3-hydroxybutyrate). Most of the currently available biodegradable polymers are used for either of medical and ecological applications, but some of them are applicable for both such as PCL: Poly(ϵ -caprolactone); PLLA: Poly(L-lactide) or Poly(L-lactic acid), as illustrated in Figure 13 [61].

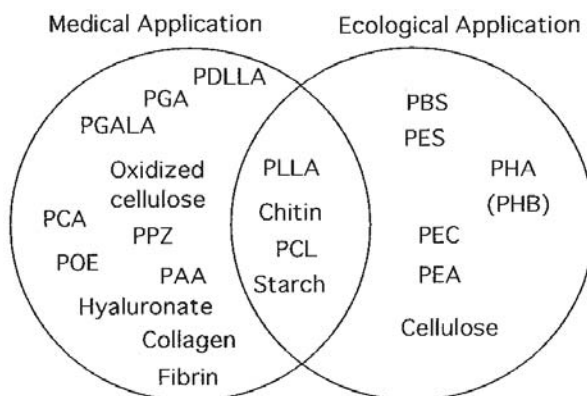


Figure 13. Applications of biodegradable polymers [61].

2. Processing of poly(lactic acid)

PLA can be processed by extrusion, thermoforming, injection, blow molding, fiber spinning or stretching. It is printable and heat sealable. The actual or potential applications are found in the crop and food sectors (films, food packaging and soft drinks) and for non-woven materials in hygienic products. Alternatively, PLA has attractive for biomedical and medical application [62]. The properties of biocompatibility and of bioresorption of PLA permit the development of suture threads and clips, orthopaedic fixations (screws, pins) and of resorbable implants. Section, molding of foam products, blow molding, thermoforming, extrusion and fiber spinning [41]. In addition, some studies and researches about the improving, adjusting properties and processing of PLA to be used in the required applications.

Lim et al. [63] reviewed the processing technologies for PLA by extrusion, injection molding, injection stretch blow molding, casting, blown film, thermoforming, foaming, blending, fiber spinning, and compounding. They reported that PLA can be processed on standard converting equipment with minimal modifications, its unique material properties must be taken into consideration in order to optimize the conversion of PLA to molded parts, films, foams, and fibers. Prior to melting processing of PLA, the polymer must be dried sufficiently to prevent excessive hydrolysis (molecular weight drop) which can compromise the physical properties of the polymer. Typically the polymer is dried to less than 100ppm (0.01%, w/w). Drying of PLA takes place in the temperature range of 80–100°C. Commercial grade PLA resin pellets are usually crystallized, which permits drying at higher temperatures to reduce the required drying time. In contrast, amorphous pellets must be dried below the T_g (~60°C) to prevent the resin pellets from sticking together, which can bridge and plug the dryer. It is noteworthy that because PLA degrades at elevated temperatures and high relative humidity, the resins should be protected from hot and humid environments. Drying of PLA is commonly achieved using a closed loop dual-bed regenerative desiccant-type dryer. In this type of dryer, the resin pellets are contained in a hopper that is purged with dry air at elevated temperature. The hot air from the process stream removes the moisture from the resin in the hopper.

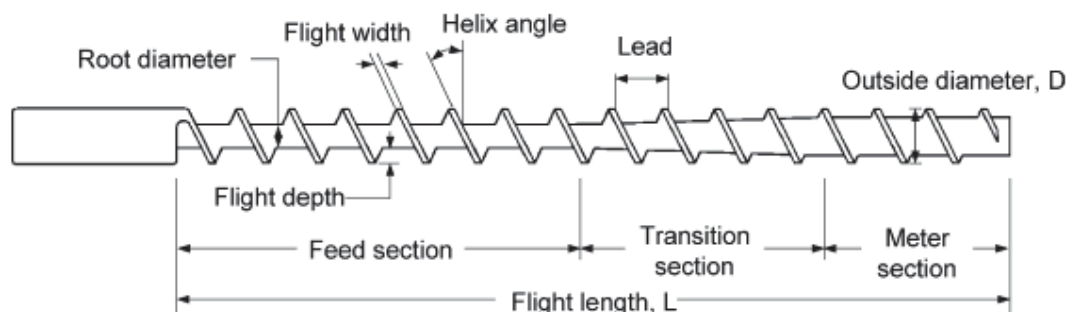


Figure 14. Typical geometries of a screw for single-screw extruder [63].

Extrusion is the most important technique for continuously melt processing of PLA. The plasticizing extruder can be part of the forming machine systems for

injection molding, blow molding, film blowing and melt spinning. Figure 14 shows a schematic representation of the major components of an extruder for an injection molding machine. A typical screw consists of three sections: (1) feed section – acts as an auger which receives the polymer pellets and conveys the polymer into the screw; (2) transition section (also known as compression or melting sections) – flight depth decreases gradually, which compresses the pellets to enhance the friction and contact with the barrel. In order to segregate the molten polymer pool from the pellet unmelted pellets, various barrier flight designs have been adopted; (3) metering section – characterized by a constant and shallow flight depth, which acts as a pump to meter accurately the required quantity of molten polymer. The l/d ratio, which is the ratio of flight length of the screw to its outer diameter, determines the shear and residence time of the melt. Screws with large l/d ratio provide greater shear heating, better mixing, and longer melt residence time in the extruder. Commercial grade PLA resins can typically be processed using a conventional extruder equipped with a general purpose screw of l/d ratio of 24–30. Extruder screws for processing PET, which are typically low-shear for gentle mixing to minimize resin degradation and acetaldehyde generation, are also suitable for processing PLA resin. Another important screw parameter is the compression ratio, which is the ratio of the flight depth in the feed section to the flight depth in the metering section. The greater the compression ratio a screw possesses, the greater the shear heating it provides. The recommended compression ratio for PLA processing is in the range of 2-3.

During the plasticizing process, PLA resin pellets are fed from a hopper near the end of a barrel. The screw, driven by an electric or hydraulic motor, rotates and transports the material towards the other end of the barrel. The heat required for melting is provided by the heater bands wrapped around the barrel. As the screw rotates, the flights shear and push the polymer against the wall of the barrel which also provides frictional heat for melting the polymer. The combined thermal energy from the heater and frictional heat due to friction between the plastic and the screw and barrel, provide sufficient heat to raise the PLA polymer above its melting point (170–180°C) by the time it reaches the end of the barrel.

PLA with l-lactide contents of 92–98% have been successfully extruded using conventional extruders. The production of PLA film and sheet is practically identical; the main difference between them is their stiffness and flexibility due to the difference in their thicknesses. Typically, films are $\leq 0.076\text{mm}$ (0.003 in.) in thickness, while sheets are typically $\geq 0.25\text{mm}$ (0.01 in.). In cast film extrusion, the molten PLA is extruded through a sheet die and quenched on polished chrome rollers that are cooled with circulating water. Usually, the die gap is set to 10% or 25–50 μm (1–2 mils) greater than the target sheet thickness. Ljungberg et al. [64] extruded neat PLA using the temperatures for the feeding zone, the barrel and the die were 160, 180, and 175°C, respectively. Similar extruder temperature profiles were used by Gruber et al [65].

Sheet and film forming can be achieved on a three-roll stack. Because of the low melt strength of PLA, horizontal roll stacks configuration is preferred. To avoid slippage of web on the rollers, relatively high roller temperatures (25–50°C) are usually used. Nevertheless, extreme high temperatures should be avoided as the web will stick to the rollers, resulting in poor quality sheet. To reduce the chance of trapping air and reduce film or sheet defects, one resin supplier recommended that the

die be positioned as close as possible to the entrance nip and slightly higher than the nip to accommodate the slight drooping of the molten PLA web. Generally, hydraulic rolls stands, capable of producing pressure around 800–900 lbs/linear inch of die is required to prevent floating of the rolls which would result in uneven PLA surfaces, edge instability, and neck-in. Casting of PLA film usually requires edge pinning (electrostatic or low pressure air) to eliminate streaking, reduce neck-in, and improve edge stability. Slitting and web handling of PLA is similar to PS. Edge trimming of PLA should be carried out with rotary shear knives since razor knives may yield rough edges and web breaks. Winding of the PLA web should be done with good tension control in order to obtain a consistent gauge. Similar to PP, PET and PS films, the physical properties of PLA films can be enhanced through orientation. Uniaxial orientation of PLA is achieved in conventional machine direction orientation (MDO) rolls. Since PLA tends to neck in during drawing, nipped rolls are usually required. Through mechanical drawing, it is possible to improve thermal and impact resistance of the PLA film or sheet to a level similar as oriented polystyrene (OPS), oriented polypropylene (OPP) or polyester. An oriented PLA film can be obtained by stretching it to two to ten times its original length at 60–80°C, which is much lower compared with OPP and PET [63].

Miyata and Masuko studied [66] the crystallization characteristics of poly(l-lactide) (PLLA) films of different molecular. In non-isothermal crystallization modes from the isotropic melt, the crystallinity of PLLA films increased remarkably with a decrease in the cooling rate, accompanied by a kind of annealing effect. Overall isothermal crystallization rates of the polymer determined by d:l isomers in the range from 90°C to 140°C indicated the maximum value at 105°C. This temperature is lower than that (120°C) at which the maximum spherulite growth rate is observed.

Komatsuka et. al. [8] studied the gas transport properties (i.e., permeability, diffusivity, and solubility) of PLA blend membranes were systematically investigated. PLA blends had a glass transition temperature of 60°C, a crystallization temperature of 116°C, and a melting temperature of 149°C. The membrane density increased with increasing crystallinity. In contrast, the fractional free volume determined using a group contribution method of van Krevelen decreased with increasing crystallinity. The ranking of the gas permeability at 35°C in all PLA blend membranes used in this study was hydrogen > carbon dioxide > oxygen > nitrogen. In general, as the crystallinity in a polymer membrane increases, gas permeability decreases. Interestingly, the permeability coefficient of some gases in the PLA blend membrane with higher crystallinity was larger than that with lower crystallinity. This result suggests that the size and distribution of free volume in the crystalline PLA blend membrane are different from those in other crystalline polymer membrane.

3. Poly(lactic acid) composites

Most polymer are mixed together and with other substances to confer specific characteristics to the final products such as mechanical strength, flexibility, color, resistance to ultra-violet radiation, to chemical and heat damage [67]. A vast number of additives are available and being developed continuously to impart special features. Modern composite materials evolved from the simplest mixtures of two or

more materials to gain a property that was not there before resulting in the high performance of the end product [68].

Examples of additives are: [67]

1. Stabilizers: they protect against thermal degradation during processing, act as fire retardants, and shield the final product against ultraviolet radiation.
2. Colorants: they are used for aesthetic reasons but are useful also in the absorption of light of specific wavelengths.
3. Reinforcing agents: these are essential for demanding applications where fibers (usually glass or graphite) are arranged in the polymer matrix to improve the dimensional stability of an article, its mechanical properties, and the limits of temperature of usage.
4. Fillers: some are inexpensive additions of materials which reduce cost, while others such as calcium carbonate soften the polymer, improve dielectric properties, and reduce its thermal expansion.
5. Plasticizer: these weaken the structure of polymeric material and give it flexibility and flow properties.
6. Lubricants: these act by migrating out of the bulk of the material and helping its flow and ease of processing near solid walls- for example, of extruder- and though dies.

There are many works that study PLA composites approach by blending polymer with various organic/ inorganic fillers to enhance mechanical and thermal properties of the bioplastics.

3.1 Blending of PLA and other polymers

The aim of blending PLA with other polymers is to create greater application with increased mechanical properties, mainly for improving flexible and toughness of this biodegradable polymer.

Chen et al. [69] developed ductile PLA by modified with methacryloyloxyalkyl isocyanate. In this study, urethane structure polymer materials were prepared. PLA was reacted with a small amount of methacryloyloxyethyl isocyanate (MOI) to obtain a ductile PLA with markedly improved mechanical properties. Elongation at break increased by 20 times and impact resistance (notched) improved by 1.6 times when compared to neat PLA.

Chen et.al. [7] made an effort to fine and tune mechanical properties of high molecular-weight poly-l-lactic acid (PLLA), especially to increase its toughness without sacrificing too much of its original strength. The products are more suitable to use in orthopedic or dental applications. Blends of biodegradable poly-l-lactic acid (PLLA) and poly-dl-lactic acid (PDLLA) or polycaprolactone (PCL), in addition to a third component, the surfactant (a copolymer of ethylene oxide and propylene oxide), were prepared by blending these three polymers at various ratios using dichloromethane as a solvent. The weight percentages of PLLA/PDLLA (or PCL) blends were varied. DSC data indicated that PLLA/PDLLA blends without the surfactant had two T_g 's. With the addition of the surfactant, there was a linear shift of the single T_g as a function of composition, with lower percentages of PLLA

producing lower glass transition temperatures indicating that better miscibility had been achieved. DMA data showed that the 40/60 PLLA/PDLLA blends without the surfactant had high elastic modulus and elongation, and similar results were observed after adding 2% surfactant into the blends. The 50/50 PLLA/PDLLA/2% surfactant blend had the highest elastic modulus, yield strength, and break strength compared with other ratios of PLLA/PDLLA/2% surfactant blends. The elongation at break of 50/50 PLLA/PDLLA was similar to that of PLLA. Again, the elongation at break of 50/50 PLLA/PDLLA/2% surfactant was almost 1.2-1.9 times higher than that of 50/50 PLLA/PDLLA and PLLA. Elongation of PLLA increased with the addition of PCL, but the strength decreased at the same time.

Finkenstadt et al. [70] optimized cost and properties of Poly(lactic acid) by using oilseed co-products as fillers. Agricultural co-products of the alternative oilseed crops, cuphea (C), lesquerella (L) and milkweed (M), were collected after the oil was recovered. PLA and various levels of co-product (0–45%, w/w) were compounded by twin-screw extrusion and injection molded. They found that tensile strength of PLA composites decreased with co-product content increased. PLA-C exhibited increased stiffness. In contrast, the modulus of PLA-M and PLA-L decreased slightly. Unexpectedly, PLA-M showed extensive stress-cracking under tensile stress and exhibited an elongation value 50–200% greater than the neat PLA. Moreover, acoustic emission showed ductile behavior of the PLA-M composites.

Signori et al. [71] investigated the thermal degradation of Poly(lactic acid) (PLA) and poly(butylene adipate-*co*-terephthalate) (PBAT) and their blends. The blend of PLA with PBAT give interesting materials for industrial packaging applications, due to their increased ductility as PBAT content increases. However, like many aliphatic polyesters, the PLA matrix degrades upon melt processing thus affecting the thermo-mechanical features of the blended material. They studied the effect of processing at high temperature on the molecular weight distribution, morphology, and thermo-mechanical properties of both homopolymers, as well as the PLA/PBAT 75/25 blend. Notably, different processing conditions were adopted in terms of temperature (range 150–200 °C) and other relevant processing parameters (moisture removal and nitrogen atmosphere). Analysis of PLA/PBAT blends indicated that intermolecular chain reactions took place under strong degradative conditions of PLA, yielding PLA/PBAT mixed chains (copolymers). Increasing amounts of copolymers resulted in improved phase dispersion and increased ductility, as SEM and mechanical tests indicated. Conversely, reduced PLA degradation with less copolymer formation, afforded higher modulus materials, owing to poorer dispersion of the soft phase (PBAT) into the PLA matrix.

3.2 Compounding PLA with plasticizers

The flexibility, ductility, and toughness of polymers may be improved with the aid of additives called plasticizer. Plasticizers are generally liquids having low vapor pressures and low molecular weights. The small plasticizer molecules occupy positions between the large secondary intermolecular bonding [72]. Plasticizers can decrease melt viscosity, glass transition temperature and the modulus of elasticity of product without altering the fundamental chemical character of the plasticized material [73]. In the other purpose, plasticizers can improve some

properties of polymers such as workability, heat resistance, low-temperature resistance, weathering resistance, insulation properties and oil resistance [74]. There is a report that the adding small amounts of plasticizer (1.5-3%) can enhance the anticorrosion properties of polymer [75]. There are some theories of plasticizing and plasticizer effect. In the lubrication theory the plasticizer is viewed as a lubricant that exhibits no bonding force with polymer. Lubricants only lower intermolecular forces and therefore only cause partial plasticizing. In the early days of plastics technology, relatively ineffective plasticizers have been used in small quantities as processing aids. They decreased melt viscosity thereby facilitating processing while generally affecting the properties of polymer only insignificantly. In contrast, effective plasticizers lower the glass transition temperature of polymers and can no longer be described as processing aids.

The solvation theory is based on concepts of colloid chemistry. The polymer/plasticizer system is regarded as a lyophilic colloid in which the plasticizer forms solvation shells around the polymer particles. For summarizing of the solvation theory, a plasticizer must have molecules, which are not too small otherwise it would be too volatile. It should also not be too poor a solvent as it could then only use in small quantities and the danger of separation and exudation would be great.

The thermodynamic theory uses solution and swelling as explanation of gelling but views plasticizing of brittleness of polymers. The effect of a plasticizer is now treated as that of reducing the intermolecular forces as much as possible and loosening the bonding of polymer molecules with each other, i.e. shielding the force centers which hold together the polymer chain. Plasticizers are only absorbed into the amorphous region of polymers, they do not remain permanently firmly bond (secondary bond formation). It is more likely that there is a continuous exchange of plasticizer molecules. At solvation/desolvation equilibrium, when a certain proportion of the force centers of the polymer chain remain shielded, the gel is stable [73].

According to the polarity theory, the intermolecular force between the plasticizer molecules, the polymer molecules and the polymer/plasticizer molecules must be well balance to ensure that the gel is stable. Therefore, plasticizers contain one or more of both polar and nonpolar groups, which must match the polarity of the particular polymer. The polar, directional and orientating groups of a plasticizer interact with dipoles of polymer. The purpose of the aromatic, polarizable part of the molecule is to conduct further the attractive forces of dipoles and thereby to promote the polar character of plasticizer molecule. The aliphatic, nonpolar portions shield the dipoles of the polymer from one another. Substance which consist of polar groups only associate and exude [73].

In the case of semicrystalline polymers like PLA, an efficient plasticizer has to reduce the glass transition temperature but also to depress the melting point and the crystallinity. The most common plasticizers used for PLA are polyethylene glycols and citrate derivatives.

(a) Polyethylene glycols

Polyethylene glycols (PEGs) are high molecular weight polymers of ethylene oxide. PEGs are designated by a number that roughly represents the average molecular weight of the polymers. At room temperature, PEG with molecular weights

below approximately 600 are clear, viscous liquids; above an approximate molecular weight of 1000, PEGs are white, waxy solids. PEGs possess an ideal array of properties: very low toxicity, excellent solubility in aqueous solutions, extremely low immunogenicity and antigenicity. It is readily excreted after administration into living organisms. PEGs are generally water-soluble and do not typically hydrolyze or deteriorate. The blandness and wide range of solubility and compatibility of these compounds render them useful in a variety of applications, including the pharmaceutical and cosmetics industries [75,76].

PEGs are water-soluble synthetic polymers with a general formula $\text{HO}-(\text{CH}_2\text{CH}_2\text{O})_n-\text{H}$ and have been utilized in various applications in the biotechnology industry [77]. The average number of repeating oxyethylene groups typically range from 4 to about 180. The low molecular weight members from $n=2$ to $n=4$ are diethylene glycol, triethylene glycol and tetraethylene glycol respectively, which are produced as pure compounds. The low molecular weight compounds up to 700 are colorless, odorless viscous liquids with a freezing point from $-10\text{ }^\circ\text{C}$ (diethylene glycol), while polymerized compounds with higher molecular weight than 1,000 are waxlike solids with melting point up to $67\text{ }^\circ\text{C}$ for $n=180$.

PEG 400 was chosen for this research because PEGs, including PEG 400, are generally considered to be inert and possess a low order of toxicity. Many published studies confirm these conclusions in several species including humans. Another reason is the molecular weight is relatively compared to another plasticizer, tributyl citrate, which is also used in this study. Some properties of PEG 400 are listed in Table 9.

Table 9. Properties of PEG 400 [78].

Properties	
Molecular weight	380-420
Appearance	Clear liquid
Moisture	0.2%, max
Hydroxy value	265-295 mg KOH/g
pH	5-7
Specific gravity	1.12-1.13
Viscosity	90 cP at $25\text{ }^\circ\text{C}$

One common feature of PEGs appears to be the water-soluble. It is soluble also in many organic solvents including aromatic hydrocarbons (not aliphatic). They are used to make emulsifying agents and detergents, and as plasticizers, humectants, and water-soluble textile lubricants. The wide range of chain lengths provide identical physical and chemical properties for the proper application selections PEGs is non-toxic, odorless, neutral, lubricating, nonvolatile and nonirritating and is used in a variety of pharmaceuticals and in medications as a solvent, dispensing agent, ointment and suppository bases, vehicle, and tablet excipient [78]. Many researches using PEG to improve properties of polymers are listed as following.

Johnson et al. [79] used free film techniques to study the effect of plasticizers polyethylene glycol 400 (PEG 400), on the properties of hydroxypropyl methylcellulose (HPMC) free films cast from aqueous solutions. PEG 400 was found to enhance water vapor permeability of the free films. Furthermore, it had no significant effect water absorption. The results of these studies can be applied for designing soluble aqueous film coating systems when one or more of the tablet components is sensitive to water.

Heinämäki et al. [80] investigated the effects of polyethylene glycols (PEG 400, 1500 and 4000) used as plasticizers on the moisture permeability and mechanical properties of aqueous hydroxypropyl methylcellulose (HPMC) films. The free films were prepared by using a pneumatic spraying technique similar to that used in fluidized-bed coaters. The mechanical strength of the films was shown to be more dependent on the concentration than on the molecular weight of the PEGs, while the ductility of the films was mainly dependent on the molecular weight of the PEGs. The addition of PEGs at a concentration of 10% resulted in relatively hard and strong films with a moderate elongation (ductility), especially when lower molecular weight plasticizers (PEG 400 or 1500) were used. The moisture permeability and mechanical properties resulted that the addition of PEGs at a concentration in the range of 10–20% of the polymer weight seems to be beneficial for aqueous-based HPMC film coats.

Sakellariou et al. [81] evaluated the plasticizing efficiency of the polyethylene glycols when added to both ethyl cellulose and hydroxypropyl methylcellulose films by measuring the glass transition temperatures of formulations using the torsional braid pendulum. Compared to hydroxypropyl methylcellulose, where there was a significant reduction in the glass transition temperature with increasing concentration for all the polyethylene glycols, the effect in the case of ethyl cellulose was relatively small. In both cases, the plasticizing efficiency of the polyethylene glycols decreased with increasing molecular weight with the high molecular weight solid members exhibiting phase separation.

Srinivasa et al. [82] investigated the effect of plasticizers and fatty acids on mechanical and permeability characteristics of chitosan films. Chitosan films were prepared by blending with polyols (glycerol, sorbitol and polyethylene glycols) and fatty acids (stearic and palmitic acids) and their mechanical and barrier properties studied. The tensile strength of the blended films decreased with the addition of polyols and fatty acids, whereas the percent elongation was increased in polyol blend films, but fatty acid blend films showed no significant differences. Glycerol blend films showed decrease, whereas sorbitol and PEG blend films showed increase in the water vapor permeability (WVP) values. No considerable differences in WVP were observed in fatty acid blend films.

Parra et al. [83] studied influence of polyethylene glycols on the thermal, mechanical, morphological, physical–chemical and biodegradation properties of poly(3-hydroxybutyrate) (PHB). Blends of PHB with PEGs (PHB/PEGs), in different proportions, were investigated for their thermal properties, tensile properties, water vapor transmission rate, enzymatic biodegradation (using light microscopy) and mass retention. They found that the addition of plasticizer did not alter the thermal stability of the blends, although an increase in the PEG content reduced the tensile strength and increased the elongation at break of pure PHB.

Pillin et al. [34] investigated some properties of plasticized PLA. Agreed plasticizers for food contact poly(1,3-butanediol), dibutyl sebacate, acetyl glycerol monolaurate and polyethylene glycols were melt mixed with L-PLA and then, the glass transition, melting, crystallization and mechanical properties of the blends were investigated. The experimental results were compared to the predicted results found through empirical interaction parameters and Fox equations. Molecular scale miscibility is assumed in the amorphous phase whatever the plasticizer. The mobility gained by the PLA chains in the plasticized blends yields crystallization, which is the driving force for various scale phase separations.

Byun et al. [84] developed and investigated an antioxidant poly(lactic acid) (PLA) film prepared with α -tocopherol, BHT and polyethylene glycol (PEG 400). Three different PLA films were fabricated for this study: pure PLA film, PLA film with BHT and PEG 400 (BP-PLA film), PLA film with α -tocopherol, BHT, and PEG 400 (ABP-PLA film). The result showed that the addition of PEG 400 into the pure PLA film decreased the glass transition temperature (T_g) of the film. The BP-PLA and ABP-PLA film had around 51 °C of T_g while pure PLA film had 66 °C. Due to the decreased T_g of both the BP-PLA and ABP-PLA film, both films had an increased elongation at break (%E). The addition of plasticizer into pure PLA film also caused increased water vapor permeability (WVP) and decreased oxygen permeability (OP).

For new approach, Hassouna [85] created the development of plasticized poly(lactic acid) (PLA) by grafting of polyethylene glycols via reactive extrusion. In this work, new ways of plasticizing poly(lactic acid) (PLA) with low molecular PEGs were developed to improve the ductility of PLA while maintaining the plasticizer content at maximum 20 wt.% PLA. To this end, a reactive blending of anhydride-grafted PLA (MAG-PLA) copolymer with PEGs, with chains terminated with hydroxyl groups, was performed. During the melt-processing, a fraction of PEGs was grafted into the anhydride-functionalized PLA chains. The role of the grafted fraction was to improve the compatibility between PLA and PEGs. Reactive extrusion and melt-blending of neat and modified PLA with PEGs did not induce any dramatic drop of PLA molecular weight. It was demonstrated by DSC that the mobility gained by PLA chains in the plasticized blends yielded crystallization. The grafting of a fraction of PEGs into PLA did not affect this process. However, DSC results obtained after the second heating showed an interesting effect on the T_g when 20 wt.% PEGs were melt blended with neat PLA or 10 wt.% MAG-PLA. In the latter case, the T_g displayed by the reactive blend was shifted to even lower temperatures at around 14 °C, while the T_g of neat PLA and PLA blended with 20 wt.% PEGs was around 60 and 23 °C, respectively. Regarding viscoelastic and viscoplastic properties, the presence of MAG-PLA did not significantly influence the behavior of plasticized PLA. Indeed, with or without MAG-PLA, elastic modulus and yield stress decreased, while ultimate strain increased with the addition of PEG into PLA.

(b) Tributyl citrate

For 30 years, Morflex, Inc., has been manufacturing and marketing four citric acid ester, primarily for use in food-contract films and molding compounds [86]. Citric acid esters are use very little because they are expensive and only in part good plasticizer. The following citrate ester as shown in Table 10 are available commercially.

Citrate plasticizers are free of volatile organic compound (VOC's) have a low order of toxicity, high flash point, and are rapidly biodegradable [87]. They are interested to use with biodegradable plastics. There was a report that tributyl citrate (TbC) oligomeric plasticizers drastically lowered the glass transition temperature of PLA, thus creating homogeneous and flexible materials [35]. Therefore, TbC is an interested plasticizer to use in this study. It is insoluble in body fluid resulting in low toxicity. Initial toxicity tests conducted by the Pfizer Drug Safety Evaluation Department proved citrates to be safe through acute dermal toxicity and ocular irritation tests in rabbits, and acute oral toxicity tests in mice and rabbits [88]. FDA approved 1998 as a component of food contact adhesives to be used safety as a component of articles intended for us in packaging, transporting, or holding food [87].

Table 10. The commercial esters and their compatible used materials [73].

Plasticizer	Used with/Compatible with
Triethyl citrate	/ CA, CAB, CN, EC, PVAC, PVB, PVC, VC/VAC
Tributyl citrate	/ CA, CAB, CN, EC, PVAC, PVB, PVC, VC/VAC
Acetyl triethyl citrate	/ CA, CAB, CN, EC, PVAC, PVB, PVC, VC/VAC
Acetyl tri(n-butyl) citrate	/ CA, CAB, CN, EC, PVAC, PVB, PVC, VC/VAC
Acetyl tri(n-hexyl) citrate	PVC /
Acetyl tri(2-ethyl-hexyl) citrate	PVC /
n-Butyl tri(n-hexyl) citrate	PVC /
Acetyl tri(n-octyl-decyl) citrate	PVC /

Tributyl citrate (TbC) has the chemical names as 2 hydroxy-1,2,3-propanetricarboxylic acid., tributyl ester. And there are some other names as butyl citrate, citric acid, tributyl ester and tributyl 2-hydroxy-1,2,3-propanetricarboxylate [87]. The chemical formula is $C_{18}H_{32}O_7$ [89] and molecular structure is shown in Figure 15. Tributyl citrate is a high boiling substance and low toxicity. Some properties of TbC are listed in Table 11.

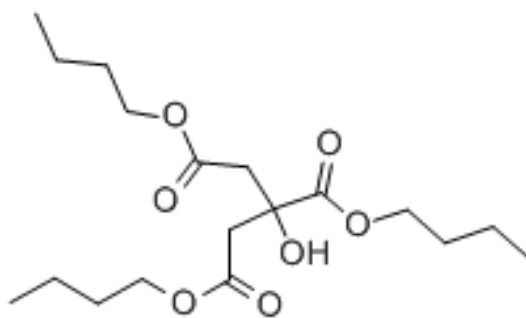


Figure 15. The chemical structure of tributyl citrate (TbC) [90].

Table 11. Properties of tributyl citrate (TbC) [87,89,91].

Properties	
Molecular weight	360.45
Appearance	Clear to yellow, viscous liquid
Solubility	
- Water	< 0.1 g/100 mL at 20 °C
- MeOH	40-80 g/100 mL at 20 °C
- EtOH	40-80 g/100 mL at 20 °C
- Hexane	40-80 g/100 mL at 20 °C
Boiling point	234 °C
Flash point	157 °C
Specific gravity	1.035-1.045
Reflective index	1.444

Citrates are used in food, cosmetics, pharmaceutical and medicine industries as well as in plastic industry; nutrient or food additives having functions of acidity regulator, sequestering and stabilizing agent, antioxidants synergist, firming agent; anticoagulant for stored whole blood and red cells and also for blood specimens as citrates chelate metal ions and saline cathartics, effervescent medicines; high boiling solvent, plasticizer and resin for food contact plastics. Citrates are best suited for medical plastics. They are being used as plasticizers in packaging and medical devices for years. However, health effects arising from long-term exposure to citrates in medical devices have not been widely studied [87,88,91].

TbC is used as a plasticizer that does not fungal growth in cellulosic and vinyl resins (especially, PVC), poly(lactic acid) resins (as a biodegradable component), and furniture coatings. TbC is also a plasticizer permitted in the field of food additives, food contact material, medical, and pharmaceutical application. It is also used as a solvent for nitrocellulose and lacquers intended for food contact application. Tributyl Citrate is effective to keep stable color maintain when processed with resins due to the property of heat-stable. Additional applications include a defoaming agent in

proteinaceous solutions [87,91]. Some researches on using of TbC as plasticizers in plastics are list as following.

Ljungberg and Wessle'n [35] investigated the thermo-mechanical properties of PLA film using Tributyl citrate oligomers as plasticizers. PLA was blended with tributyl citrate (TbC) and two oligomers of TbC that were synthesized by transesterification of tributyl citrate (TbC) and diethylene glycol (DEG). Dynamic mechanical analysis (DMA) and differential scanning calorimetry (DSC) were used to investigate the dynamic mechanical and thermal properties of the blends. All the plasticizers investigated decreased the glass transition temperature of PLA, and the reduction was the largest with the plasticizer having the lowest molecular weight. The PLA matrix became saturated with plasticizer at a certain concentration and phase separation occurred; the higher the molecular weight of the plasticizer, the lower the saturation concentration. Aging of the blends at room temperature for several months induced partial phase separation in the material. It was observed that the morphological stability of the blends was enhanced when the plasticizer concentration was reasonably low (i.e. 10–15 wt%).

Ljungberg et al. [64] developed the flexibility of PLA film by incorporation of a plasticizer in the material. PLA was plasticized with triacetin (TAc) and tributyl citrate (TbC). Storage of the plasticized films resulted in an increased crystallinity and changes in the film properties, rendering constant heat welding difficult. The welding process had no influence on thermal properties, such as cold crystallization temperature, melting temperature, crystallization temperature, and degree of crystallinity, of neat PLA but caused significant changes in the crystallinity of the plasticized materials.

Plasticization of poly(lactide) with blends of tributyl citrate and low molecular weight poly(d,l-lactide)-b-poly(ethylene glycol) copolymers was prepared by Lemmouchi et al. [92] In the process, PLA was melt-mixed with blends of tributyl citrate and more thermally stable low molecular weight block copolymers based on poly(d,l-lactide) and poly(ethylene glycol) of different molecular weights and topologies. The degradation test results show that the presence of plasticizers accelerates the degradation of the PLA matrix.

Lin et al. [93] investigated the effect of organic esters of plasticizers on the water absorption, adhesive property, glass transition temperature and plasticizer permanence of Eudragit acrylic films. The materials used in film coating technology are very important tools for pharmaceutical applications. The effects of four organic esters used as plasticizers (triacetin, diethyl phthalate (DeP), dibutyl phthalate (DbP) and tributyl citrate (TbC)) on the water absorption behavior and adhesive property of Eudragit films and on the glass transition temperature (T_g) and plasticizer permanence of Eudragit E film were investigated. The results indicate that TbC may be the best choice of plasticizer for Eudragit film, particularly for the Eudragit E film.

Andreuccetti et al. [94] studied the effect of hydrophobic plasticizers on functional properties of gelatin-based films using hydrophobic plasticizers derived from citric acid and soy lecithin as emulsifier. The results showed that tensile strength values (TS) varied from 36 to 103 MPa, however, the increase in the concentration of plasticizers (acetyltributyl citrate and tributyl citrate) reduced TS by 57% and no relation was observed between plasticizer quantities and the elongation. Water vapor

permeability varied between 0.17 and 0.34 g mm/m² h kPa, slightly increasing with the increase in concentration of plasticizers.

3.3 Compounding of PLA with fillers

Filler are solid additives, different from plastics matrices in composition and structure, which are added to polymers to increase bulk or improve properties [73] as tensile and compression strength, abrasion resistance, toughness, dimensional and thermal stability, and other properties [72]. In general, the following properties of mineral additives have the greatest influence on the final mechanical properties of a composite: average particle size, particle-size distribution, particle shape, particle integrity (friability), and surface properties. Other properties, such as residue-grit level, color or electrical properties, can be very important in specific applications [86]. Particles come in a variety of shapes and sizes. The size required for most resin applications is under 40 microns. Very fine particle (less than 5 microns), when properly dispersed in a resin, generally provide the best mechanical properties, since the composite is more uniform [86].

3.3.1 PLA/clay nanocomposites

Polymer nanocomposites have attracted enormous interest worldwide from both academic and industrial. Nanosized (1-100 nm) inorganic fillers are used as dispersed phases in polymer matrix (continuous phase) making higher performance of nanocomposites than those of conventional composite. It is believed that the properties improvement in nanocomposites is caused by the reactive end groups of polymer can interact with the nano-particles surface. The interaction such as hydrogen or covalent bonds can be formed resulting in the increasing of the adhesion of nano-particles with the polymer matrix. This, in most cases, leads to enhancement of thermal properties and mechanical properties. For biocomposites, filler (inorganic or biodegradable) was added into bioplastics matrix. Nanocomposites was obtained by adding nanofillers to biopolymers, resulting in very promising materials since they showed improved properties with preservation of the material biodegradability, without eco-toxicity [95-104]. Many publications of nano-biocomposites are list as following.

Jiang et al. [21] studied the properties as morphologies, tensile mechanical properties, dynamic mechanical and rheological properties, polymer nano-particles interactions, and toughening mechanisms of the PLA/NPCC and PLA/MMT nanocomposites were compared. MMT and NPCC showed significantly different effects on the strength, modulus and elongation of the PLA nanocomposites. Different toughening mechanisms were first elucidated for the two types of nanocomposites based on the evidence from both macroscopic and microscopic observations. Under uniaxial tension, large quantities of microvoids were created in both PLA nanocomposites. The microvoids in PLA/NPCC caused massive crazing, while in PLA/MMT they resulted in shear yielding, particularly in the nanocomposite with 2.5 wt% MMT. The MMT stacks and platelets were found to be located between the microvoids in the extended specimens and prevented them from collapsing and coalescing.

Chang et al. [105] investigated the thermo-mechanical properties, morphology, and gas permeability of hybrids prepared with three types of organoclays. Hexadecylamine–montmorillonite (C16–MMT), dodecyltrimethyl ammonium bromide–montmorillonite (DTA–MMT), and Cloisite 25A were used as organoclays in the preparation of nanocomposites. From morphological studies, TEM showed that most clay layers were dispersed homogeneously in the matrix polymer, although some clusters or agglomerated particles were also detected. The initial degradation temperature (at a 2% weight loss) of the poly(lactic acid) (PLA) hybrid films with C16–MMT and Cloisite 25A decreased linearly with an increasing amount of organoclay. For hybrid films, the tensile properties initially increased but then decreased with the introduction of more of the inorganic phase. The O₂ permeability values for all the hybrids for clay loadings up to 10 wt % were less than half the corresponding values for pure PLA, regardless of the organoclay.

The study of Chang et al. [24] also clarify the intercalation of polymer chains to organoclays and to improve the thermo-mechanical properties. Two organoclays were synthesized. One was a montmorillonite modified with hexadecylamine (C16–MMT); the other was a fluorinated-mica modified with hexadecylamine (C16–Mica). Dispersions of organoclays with poly(lactic acid) (PLA) were by using the solution intercalation method at different organoclay contents to produce nano-scale composites. The maximum ultimate tensile strength was observed for blends containing 4 wt% of either of the two organoclays and decreased with further increases in the organoclay content. The initial modulus increased with increasing organoclay content up to 4 wt% for C16–MMT. When the C16–MMT content was greater than this critical wt%, the modulus of the hybrids started to decrease. In contrast, the initial modulus of the hybrids using C16–Mica increased continually with increasing clay content from 2 to 8 wt%. The tensile properties of the C16–Mica hybrids were higher than those of the hybrids containing C16–MMT. The optical translucency was not affected by the organoclay content up to 6 wt%; however, the films containing 8 wt% organoclays were slightly more cloudy.

Wu et al. [106] investigated rheology and thermal stability of poly(lactic acid)/clay nanocomposites. Poly(lactic acid)/clay nanocomposites (PLACNs) were prepared by melt intercalation. The intercalated structure of PLACNs was investigated using XRD and TEM. Both the linear and nonlinear rheological properties of PLACNs were measured by parallel plate rheometer. The results reveal that percolation threshold of the PLACNs is about 4 wt%, and the network structure is very sensitive to both the quiescent and the large amplitude oscillatory shear (LAOS) deformation. The stress overshoots in the reverse flow experiments were strongly dependent on the rest time and shear rate but showed a strain-scaling response to the startup of steady shear flow, indicating that the formation of the long-range structure in PLACNs may be the major driving force for the reorganization of the clay network. The thermal behavior of PLACNs was also characterized. However, the results showed that with the addition of clay, the thermal stability of PLACNs decreases in contrast to that of pure PLA.

Ogata et al. [107] studied on structure and thermal/mechanical properties of poly(l-lactic acid)-clay blend. Organophilic montmorillonite was obtained by the reaction of montmorillonite (MON) and distearyldimethylammonium chloride (DSAC). The modified clay and poly(l-lactic acid), (PLLA), were solvent-cast

blended using chloroform as co-solvent. The structure and properties of the PLLA-clay blends were investigated. Thermal measurements revealed that cold crystallization took place in the as-cast PLLA, and that the clay served as a nucleating agent. From small and wide-angle x-ray scattering measurements, it was found that silicate layers forming the clay could not be individually well dispersed in the PLLA-clay blends prepared by the solvent-cast method. In other words, the clay existed in the form of tactoids, which consist of several stacked silicate monolayers. However, these tactoids formed a remarkable geometrical structure in the blend films. That is, their surfaces lay almost parallel to the film surface, and were stacked with the insertion of PLLA crystalline lamellae in the thickness direction of the film. During the blend drawing process, fibrillation took place with the formation of plane-like voids developed on the plane parallel to the film surface. Furthermore, delamination of the silicate layers did not occur even under the application of a shearing force. Finally, Young's modulus of the blend increased with the addition of a small amount of the clay.

Balakrishnan et al. [108] developed a novel toughened poly(lactic acid) (PLA) nanocomposites. The effects of linear low density polyethylene (LLDPE) and organophilic modified montmorillonite (MMT) on mechanical, thermal and morphological properties of PLA were investigated. LLDPE toughened PLA nanocomposites consisting of PLA/LLDPE blends, of composition 100/0 and 90/10 with MMT content of 2 phr and 4 phr were prepared. The Young's and flexural modulus improved with increasing content of MMT indicating that MMT is effective in increasing stiffness of LLDPE toughened PLA nanocomposite even at low content. LLDPE improved the impact strength of PLA nanocomposites with a sacrifice of tensile and flexural strength. The tensile and flexural strength also decreased with increasing content of MMT in PLA/LLDPE nanocomposites. The impact strength and elongation at break of LLDPE toughened PLA nanocomposites also declined steadily with increasing loadings of MMT. The crystallization temperature and glass transition temperature dropped gradually while the thermal stability of PLA improved with addition of MMT in PLA/LLDPE nanocomposites. The storage modulus of PLA/LLDPE nanocomposites below glass transition temperature increased with increasing content of MMT. X-ray diffraction and transmission electron microscope studies revealed that an intercalated LLDPE toughened PLA nanocomposite was successfully prepared at 2 phr MMT content.

Thellen et al. [109] studied the influence of montmorillonite layered silicate (MLS) on plasticized poly(l-lactide) blown films. PLA was mixed with 10 wt% acetyltriethyl citrate ester plasticizer and 5 wt% of an organically modified montmorillonite at various screw speeds. Wide-angle X-ray diffraction (WAXD) and transmission electron microscopy (TEM) determined that the compounded pellets and the blown film PLA/MLS nanocomposites were intercalated. Nanocomposite films showed a 48% improvement in oxygen barrier and a 50% improvement in water vapor barrier in comparison to the neat PLA. The TGA showed an increase in the decomposition temperature. DSC has determined that the glass transition, cold crystallization and melting point temperatures were not significantly influenced by the presence of MLS. Mechanical properties of the nanocomposites showed that the Young's modulus increased by 20%. Biodegradation rates in soil were slightly greater for the PLA/MLS nanocomposite than the pure PLA.

Paul et al. [110] developed new nanocomposite materials based on plasticized poly(l-lactide) and organo-modified montmorillonites. Plasticized poly(l-lactide) (PLA) based nanocomposites were prepared by melt blending of the matrix with 20 wt% of polyethylene glycol 1000 (PEG 1000) and different amounts of montmorillonite, organo-modified. At constant filler level, it appears that from all the clays studied, the montmorillonite organo-modified by bis-(2-hydroxyethyl) methyl (hydrogenated tallowalkyl) ammonium cations brings the greater effect in terms of thermal stability. Increasing the amount of clay allowed to delay the onset of thermal degradation of the plasticized polymer matrix. It was also pointed out, by WAXS and DSC analyses, that it exist a real competition between PEG 1000 and PLA for the intercalation into the interlayer spacing of the clay.

Liu et al. [111] prepared and investigated some properties of biodegradable polyesteramide composites reinforced with ordinary CaCO_3 , nano- CaCO_3 and nano- SiO_2 . They found that the ordinary filler as well as the nano-filler had a negative effect on the stability of the polymer melt, and an improved mechanical property was obtained around a critical concentration of the filler where a percolation phenomenon appeared. When the composites underwent hydrolysis, the inert filler played a role as a mechanical obstacle in the matrix and retarded the hydrolysis; on the other hand, the interfacial area between the filler particle and the matrix resin increased with the filler, which would accelerate the hydrolysis. As a result of these two inverse effects, a minimum and a maximum value appeared in the plot of the degradation rate-filler content graph. For the ordinary filler filled polymer, the filler retarded the hydrolysis; in great contrast, the hydrolysis rate of nanocomposites showed a maximum value around the critical concentration of the filler, and was much higher than the neat resin.

Yan et al. [112] investigated structural characteristics and thermal properties of plasticized poly(l-lactide)-silica nanocomposites that was synthesized by sol-gel method. IR measurements showed that vibration of C-O-C group is confined by silica network. Also the crystallization of poly(l-lactide) was partly confined by silica network. The presence of even small amount of silica largely improved the tensile strength of the samples. TGA results revealed that the thermal stability of samples is improved with silica loading.

Ray et al. [113,114] studied the nanocomposite of PBSA with organically modified synthetic fluorine mica (OSFM) has been prepared by melt-mixing in a batch mixer. Results demonstrate substantial enhancement in the mechanical properties of PBS, for example, at room temperature, storage flexural modulus increased from 0.5 GPa for pure PBS to 1.2 GPa for the nanocomposites, an increase of about 120% in the value of the elastic modulus and the thermal stability of PBSA was increased moderately in the presence of OSFM. Moreover, they studied thermal properties of poly(ethylene succinate) nanocomposite. The nanocomposite of PES with organically modified montmorillonite (o-mmt) has been prepared by solution-intercalation-film-casting technique. Results showed that the incorporation of o-mmt stops the super-cooling effect and accelerates the mechanism of nucleation and crystal growth of PES matrix significantly. The incorporation of o-mmt also improved the thermal stability of neat PES dramatically

Zhu et al. [115] studied the crystallization behavior and thermal property of biodegradable poly(butylene succinate) that was filled with the functional multi-

walled carbon nanotubes nanocomposite. They found that the presence of f-MWNTs had a significant heterogeneous nucleation effect on the crystallization and morphology of PBSU, resulting in that the crystallization is enhanced during both nonisothermal and isothermal crystallization in the nanocomposite. Moreover, thermal stability of PBSU by around 100C in the presence of f-MWNTs was compared with that of neat PBSU.

3.3.2 Blending of PLA with calcium carbonate

Calcium carbonate is a common substance found in rocks in all parts of the world, and is the main component of shells of marine organisms, snails, coal balls, pearls, and eggshells [31]. It is one of the most abundant white mineral (15%) in the earth's sedimentary crust. Carbonaceous rocks are widely exploited around the world [86]. There are two major commercial grades of calcium carbonate are use by the plastics industry; ground (ordinary) calcium carbonate and precipitated calcium carbonate.

(a) *Ground (ordinary) calcium carbonate*

Naturally occurring calcium carbonates are sedimentary rocks of origin. A rough distinction is made between [73]:

Chalk:	Loosely coherent, consistion of fine calcite crystals and fragment, originating from shells and skeletons of nanofossils.
Limestone:	More highly coherent, consisting of macrofossils of sea shells.
Marble:	Formed by metamorphosis of sedimentary rock, i.e. recrystallization in the earth's interior at high pressure and temperature of about 600 °C. The resultant rock is relatively hard with a dense, coarse-grained structure.

Ground calcium carbonate can be separated into two types, coarse ground and fine ground. The coarse ground is process by dry grinding techniques. The process is simple and consists of crushing, pulverizing, and air classification to remove the oversize particles. Alternatively, The wet griding technique is use to produce the fine ground [86].

(b) *Precipitated Calcium carbonate*

Precipitated calcium carbonate has been produce over the years by several different methods. All methods begin with calcium carbonate as a raw material. The carbonation process is the most important and it is also the simplest and most direct. The following three steps are involved [86].

Calcination:	CaCO_3	\rightarrow	$\text{CaO} + \text{CO}_2$	scheme 2.1
Hydration:	$\text{CaO} + \text{H}_2\text{O}$	\rightarrow	$\text{Ca}(\text{OH})_2$	scheme 2.2
Carbonation:	$\text{Ca}(\text{OH})_2 + \text{CO}_2$	\rightarrow	$\text{CaCO}_3 + \text{H}_2\text{O}$	scheme 2.3

The special properties of precipitated are small particle size and high degree of purity [73]. Compared with finely ground calcium carbonate, precipitated calcium carbonate incur much higher energy costs in their manufacture, and thus the benefits of higher-purity precipitated calcium carbonate also carry a higher price [86].

Calcium carbonate is a chemical compound with the formula CaCO_3 [31]. It has an idea chemical composition of 40.0% calcium, 12.0% carbon and 48.0% oxygen. Ground limestones generally are 94% calcium carbonate of higher, while precipitated grades are over 98% calcium carbonate [86]. Typical percent elemental oxide values of commercial materials are given in Table 12. Particle-size distributions is depended on various grades of ground and precipitated calcium carbonate. The physical properties and thermal properties of ground and precipitated calcium carbonate are listed in Table 13.

Table 12. Typical percent oxide composition of commercial calcium carbonate [86].

Chemical	Ground		Precipitated
CaCO_3	97.4	96.5	99.0
MgCO_3	1.5	2.3	0.2
SiO_2	0.6	0.9	0.1
Al_2O_3	0.18	0.18	0.2
Fe_2O_3	0.08	0.08	0.02
CaSO_4	-	0.02	-

Table 13. Physical and thermal properties of calcium carbonate [86].

Properties	Units	Ground		Precipitated
		Fine	Coarse	
Average particle size	micron, esd ^a	3-14	17	0.07
Specific gravity	g/cm^3	2.71	2.71	2.55-2.65
Surface area, BET N_2	m^2/g	0.9-2.2		11-26
Oil absorption, ASTM D 281		5-21	5-6	28-58
Mohs hardness		2.5-3	3	2.5-3
Thermal conductivity $\times 10^3$	$\text{Cal/g}\cdot\text{s}\cdot^\circ\text{C}$	5.6	-	5.6
Specific heat	$\text{Cal/g}\cdot^\circ\text{C}$	0.205	-	0.21
Coefficient of thermal expansion	$^\circ\text{C}\times 10^{-6}$	10	9-12	10

^aesd = equivalent spherical diameter.

On the weight basis, ground calcium carbonate is the most important filler in plastics. The inert filler calcium carbonate plays an important role in the search balance between low price and the retention of physical and mechanical properties [73].

One of the highest volume uses for calcium carbonate in plastics is for incorporation in polyvinyl chloride (PVC). Calcium carbonate is commercially used in all types of PVC, including flexible and rigid PVC. Cost reduction is primary driving force for its use. Calcium carbonate is generally used at loading level of 20 to 60 parts by weight of ingredient per 100 parts resin by weight (phr). The loading level varies depending on the end-use application. Precipitated grades in general yield better physical properties in flexible PVC than ground grade. Ultrafine precipitated calcium carbonate has report to act as an effective binding agent for hydrogen chloride when PVC burns. In film application, ultrafine calcium precipitated carbonate can be used at loading levels, they do not impair transparency [86].

Calcium carbonate is primarily used in polyolefin as polyethylene and polypropylene to reduce cost. As in most resin systems, the carbonate, because of its low aspect ratio, generally reduce mechanical properties. Low-density polyethylene (LDPE) and high-density polyethylene (HDPE) can be filled with ground calcium carbonate, however, the drop off in mechanical properties has limited this use. Alternatively, calcium carbonate interacts better with polypropylene than polyethylene, but still has a density disadvantage. The addition of calcium carbonate to polypropylene at levels ranging from 20% to 40% by weight can increase the impact strength, but reduce flexural properties and moldability. In crystal and impact styrene, calcium carbonate does serve as a flexural modulus enhancer. Stiffness and impact properties are also improved by incorporating a treated precipitated calcium carbonate. In addition, calcium carbonate is used as processing aids and to reduce heat built up resulting from abrasion in thermoplastic elastomer (TPEs). The finer precipitated grades, both coated and uncoated, are used as reinforcement in TPE and they with silicas [86]. Here is an example of research using CaCO_3 in some polymer to optimize cost and improve properties for applying in needed application.

Lam et al. [22] studied the effect of nanosized and surface-modified precipitated calcium carbonate on properties of CaCO_3 /PP nanocomposites. In order to increase the dispersion of PCC in the PP matrix, nanosized PCC was prepared using sodium tripolyphosphate as a crystallization inhibitor and then surface-modified with stearic acid to prevent it from agglomerating. The higher ability to disperse surface-modified ns-PCC compared with that of n-PCC in PP matrix was believed to stem from a better interfacial interaction of the former with PP matrix. Due to surface modification, a good dispersity of nano PCC in PP matrix was achieved and therefore thermal stability was increased. Strong interaction of ns-PCC with PP matrix also caused an increase in yield and tensile strength and the maxima were reached when loading 15-20 wt% of ns-PCC.

Dangtungee et al. [116] studied on melt rheology and extrudate swell of isotactic polypropylene (iPP) that was filled with uncoated and stearic acid-coated CaCO_3 nano-particles. The wall shear stress for both neat iPP and iPP compounds increased in a non-linear manner with increasing apparent shear rate. The apparent shear viscosity of the samples investigated was found to decrease in a non-linear manner with increasing apparent shear rate. Addition of uncoated CaCO_3 nano-particles was responsible for increasing the apparent shear viscosity of the

compounds, while stearic acid-coated ones did not affect the apparent shear viscosity of the iPP matrix as much. The percentage of extrudate swell was found to increase with increasing apparent shear rate in a non-linear manner, while it was found to increase linearly with increasing wall shear stress. Lastly, the percentage of extrudate swell was found to be a decreasing function of the filler loading.

Supaphol and Harnsiri [117] investigated about the steady-state and oscillatory shear behavior of three neat syndiotactic polypropylene (s-PP) resins and a s-PP resin filled with CaCO_3 particles of varying content, size, and type of surface modification. The inclusion of CaCO_3 particles of varying content, size, and type of surface modification, to a large extent, affected both the steady-state and oscillatory shear behavior of s-PP/ CaCO_3 compounds, with the property values being found to increase with increasing content, decreasing size, and surface coating of the CaCO_3 particles. The observed half-time of crystallization decreased with increasing CaCO_3 content and increased with increasing CaCO_3 particle size. Coating the surface of CaCO_3 particles with either stearic acid or paraffin reduced the ability of the particles to effectively nucleate s-PP resin filled with CaCO_3 particles.

Rungruang et al. [118] built up surface-modified calcium carbonate particles by admicellar polymerization to be used as filler for isotactic polypropylene. The behavior of these coated particles in an isotactic polypropylene (iPP) matrix was compared to that of uncoated and stearic acid-coated ones. Non-isothermal crystallization studies indicated that surface treatment of CaCO_3 particles reduced the ability for CaCO_3 particles to nucleate the iPP matrix. Compared to composites made from the uncoated material, composites made with stearic acid-coated and admicellar-treated CaCO_3 particles had lower tensile strength, Young's modulus, and flexural strength, but higher impact strength. Observation of the fractured surfaces of the composites by scanning electron microscopy (SEM) revealed an improvement in the dispersion and distribution of the CaCO_3 particles within the iPP matrix as a result of the surface treatment.

Avella et al. [119] studied the effect of calcium carbonate nano-particles on crystallization of isotactic polypropylene (iPP) is reported in this contribution. CaCO_3 nano-particles with different crystal modifications (calcite and aragonite) and particle shape were added in small percentages to iPP. The nano-particles were coated with two types of compatibilizers (either polypropylene-*g*-maleic anhydride copolymer, or fatty acids) to improve dispersion and adhesion with the polymer matrix. They found that the type of coating agent used largely affects the nucleating ability of calcium carbonate towards formation of polypropylene crystals. CaCO_3 nano-particles coated with maleated polypropylene can successfully promote nucleation of iPP crystals, whereas the addition of nanosized calcium carbonate coated with fatty acids delays crystallization of iPP, the effect being mainly ascribed to the physical state of the coating in the investigated temperature range for crystallization of iPP, as well as to possible dissolution by fatty acids of heterogeneities originally present in the polypropylene matrix.

Chan et al. [120] prepared Polypropylene/calcium carbonate nanocomposites. The average primary particle size of the CaCO_3 nano-particles was measured to be about 44 nm. The dispersion of the CaCO_3 nano-particles in PP was good for filler content below 9.2 vol%. They found that the CaCO_3 nano-particles are a very effective nucleating agent for PP. Tensile tests showed that the modulus of the

nanocomposites increased by approximately 85%, while the ultimate stress and strain, as well as yield stress and strain were not much affected by the presence of CaCO₃ nano-particles. The results of the tensile test can be explained by the presence of the two-counter balancing forces—the reinforcing effect of the CaCO₃ nano-particles and the decrease in spherulite size of the PP. Impact strength of composite was increased. They believe that the large number of CaCO₃ nano-particles can act as stress concentration sites, which can promote cavitations at the particle–polymer boundaries during loading. The cavitations can release the plastic constraints and trigger mass plastic deformation of the matrix, leading to much improved fracture toughness.

Zuiderduin et al. [27] investigated the toughening of polypropylene with calcium carbonate particles. Polypropylene-CaCO₃ composites were prepared on a twin screw extruder with a particle content of 0-32 vol%. The influence of particle size (0.07–1.9 μm) and surface treatment of the particles (with and without stearic acid) on the toughening properties were studied. The matrix molecular weight of the polypropylene was also varied (MFI 0.3-24 dg/min). The experiments included tensile tests, notched Izod impact tests, differential scanning calorimetry (DSC), scanning electron microscopy and rheology experiments. The modulus of the composites increased, while the yield stress was lowered with filler content. This lowering of yield stress was connected to the debonding of the particles from the polypropylene matrix. From DSC experiments it was shown that the particle content had no influence on the melting temperature or crystallinity of the PP phase, also particle size showed no effect on the thermal properties. The impact resistance showed large improvement with particle content. The brittle-to-ductile transition was lowered from 90 to 40 °C with the addition of CaCO₃ particles. Notched Izod fracture energy was increased from 2 up to 40-50 kJ/m². The stearic acid coating on the particle surface showed a large positive effect on the impact strength. This was mainly due to the improved dispersion of the CaCO₃ particles. Aggregates of particles clearly had a detrimental effect on the impact behavior of the composites. The smaller particle sizes (< 0.7 μm) showed coarse morphologies and this lowered the toughening efficiency. The molecular weight of the polypropylene matrix had a profound effect on the toughening properties. A higher molecular mass shifted the brittle-to-ductile transition towards lower temperatures. At the higher filler loads (> 20 vol%), however, still problems seem to occur with dispersion, lowering the toughening efficiency. Of all particle types used in this study the stearic acid treated particles of 0.7 μm were found to give the best combination of properties. From the study of the micro-toughening mechanism it was shown that at low strain the particles remain attached to the matrix polymer. At higher strain the particles debond and this leads to a change in stress state at the particle size level. This prevents crazing of the matrix polymer and allows extensive plastic deformation, resulting in large quantities of fracture energy.

Gai et al. [30] reported the successful preparation of composite mineral particles, coated by nano-particles of calcium carbonate of 20-100 nm particle size, by chemical reaction using the Ca(OH)₂–H₂O–CO₂ system. The degree of nano-particles coverage can reach 100% if the operating parameters are effectively controlled, and the specific surface area can be increased to three times the value before modification. Mechanical testing of polypropylene containing composite wollastonite powder as filler showed an increase in the impact strength of 65% compared to similar samples prepared using conventional filler powder.

Bartczak et al. [25] studied the toughness mechanism in HDPE that was toughened with calcium carbonate filler particles. HDPE was modified by rigid particulate fillers consisting of three different sizes of CaCO_3 particles of 3.50, 0.70 and 0.44 μm weight average diameter in various volume fractions. Mechanical properties including notched Izod impact energy of the extrusion-blended/injection-molded samples were examined as a function of filler particle size and filler volume fraction. The toughness of the CaCO_3 -filled materials increased dramatically when the mean interparticle ligament thickness of the matrix polyethylene dropped to values below 0.6 μm . The stiff fillers used in this study provided the unusual additional benefit of substantially increasing the Young's modulus of the compounds while also dramatically improving their impact energy.

Osman and Atallah [121] investigated the Effect of the particle size on the viscoelastic properties of filled polyethylene composites of surface treated and non-treated colloidal calcium carbonate and high-density polyethylene with different filler loading were prepared. In nanocomposites, more and stronger filler clusters are formed than in microcomposites due to the large contact area between the particles. The clusters have different shapes and maximum packing than the nearly spherical primary particles, thus enhance the moduli and viscosity of the composites. The obtained results indicate that the higher moduli and viscosity of the nanocomposites is not a direct consequence of the particle size but is due to the presence of more agglomerates and aggregates.

Ma et al. [122] applied a soapless emulsion polymerization method to synthesize CaCO_3 /PMMA spherical composite with different loading of CaCO_3 . CaCO_3 nano-particles were pretreated with oleic acid after the carbonation process of $\text{Ca}(\text{OH})_2$ slurry by CO_2 , in order to improve the compatibility between the CaCO_3 particles and MMA monomer in emulsion system. The results of photon correlation spectroscopy (PCS) showed the particles size of composites were bigger than the pure PMMA. And the size increased with the increase of the content of CaCO_3 nano-particles. TEM images showed that the morphology of the composite microspheres was uniform and CaCO_3 nano-particles can be well encapsulated in the polymeric microsphere, and were located at the edge of the spheres. The results of DTG and TG indicated that the CaCO_3 nano-particles could improve the thermal stability of PMMA. Moreover, capsulation of CaCO_3 by PMMA can increase the acid-resistant of CaCO_3 nanofillers.

Jiang et al. [28] reported the effect of nano-sized and micron-sized calcium carbonate on strengthening of acrylonitrile-butadiene-styrene (ABS). ABS was reinforced by both micron-sized (MCC) and nano-sized precipitated calcium carbonate (NPCC) particles through melt compounding. The MCC/ABS composites were found to have higher modulus but lower tensile and impact strength than neat ABS. In contrast, NPCC increased modulus of ABS whilst maintained or even increased its impact strength for a certain NPCC loading range. SEM examinations revealed that NPCC particles/agglomerates were distributed in much smaller sizes in the composites than its MCC counterparts. The larger interfacial area between NPCC and ABS and cavitations-induced shear yielding in the ligament are believed to be the main reasons of the mechanical property improvement of the NPCC/ABS composites. NPCC/ABS also showed completely different rheological behavior from MCC/ABS, such as the loss of Newtonian region, high G^0 at low frequencies and the appearance

of yield phenomenon. A NPCC network structure was believed to be formed in the composites and induced these pseudo-solid-like rheological behaviors.

Zuiderduin et al. [123] studied the influence of precipitated calcium carbonate particles on the toughening behavior of aliphatic polyketone. The calcium carbonate particles had a particle size of 0.7 μm and a stearic acid coating (1%). Composites of 0 – 31.5 vol% CaCO_3 content have been compounded and injection molded. Studied are the morphology of the composites, the modulus, yield strength, the notch Izod impact strength and the temperature development in the deformation zone by infrared thermography. The thermal properties of the matrix remained unchanged upon addition of CaCO_3 . With increasing particle content the modulus increased and the yield strength decreased. This decrease in yield strength is due to the debonding of the particles and was similar as with rubber particles. With increasing particle content the notched impact resistance increased strongly. The notched impact energy at room temperature was increased from 10 to 80 kJ/m^2 and the brittle-to-ductile transition temperature was lowered to 80 $^\circ\text{C}$. At calcium carbonate contents higher than 16 vol% no further impact improvement was observed. The calcium carbonate particles seemed to debond quite well despite the expected thermal contraction of the matrix polymer. The temperature development in the deformation zone was strong, as strong as with rubber particles.

Xie et al. [124] prepared poly(vinyl chloride) (PVC)/calcium carbonate (CaCO_3) nanocomposites via situ polymerization of vinyl chloride (VC) in the presence of CaCO_3 nano-particles. They reported that CaCO_3 nano-particles were uniformly distributed in the PVC matrix during in situ polymerization of VC with 5.0 wt% or less nano-particles. The glass transition and thermal decomposition temperatures of PVC phase in PVC/ CaCO_3 nanocomposites are shifted toward higher temperatures by the restriction of CaCO_3 nano-particles on the segmental and long-range chain mobility of the PVC phase. The nanocomposites showed shear thinning and power law behaviors. The ‘ball bearing’ effect of the spherical nano-particles decreased the apparent viscosity of the PVC/ CaCO_3 nanocomposite melts, and the viscosity sensitivity on shear rate of the PVC/ CaCO_3 nanocomposite is higher than that of pristine PVC. Moreover, CaCO_3 nano-particles stiffen and toughen PVC simultaneously, and optimal properties were achieved at 5 wt% of CaCO_3 nano-particles in Young's modulus, tensile yield strength, elongation at break and Charpy notched impact energy.

Wang et al. [125] investigated the influence of calcium carbonate (CaCO_3) nano-particles on the rheology enhancement of polycarbonate (PC) melt. The PC/ CaCO_3 nanocomposites with different compositions of CaCO_3 were prepared by melt-compounding. Characterizations via energy-dispersive X-ray spectrometer (EDS) and field-emission scanning electron microscopy (FE-SEM) confirm the random dispersion of CaCO_3 in the PC/ CaCO_3 masterbatch. The rheological experiments showed the remarkable rheology enhancement of PC melt due to the addition of CaCO_3 nano-particles. Mechanical tests showed that, upon incorporation of only 1 wt% CaCO_3 , the tensile modulus, the bending modulus, and the bending strength of PC are improved; however, the tensile strength and elongation at break are depressed.

Jiang et al. [126] studied the influence of CaCO_3 nano-particles (NPCC) with fatty acid coating on the rheological and mechanical properties of thermoplastic

polyurethane (TPU) nanocomposites. They found that NPCC tend to agglomerate into micron size. Tensile modulus and toughness were increase with increasing of NPCC concentration. The free fatty acid in NPCC code name NPCC 401 induced its unique rheological behavior such as the decrease of viscosity with increasing particle concentration.

Jin and Park [127] used several techniques to investigate the thermal stabilities and mechanical interfacial properties of butadiene rubber (BR) reinforced with nano-CaCO₃. They found that thermal stabilities of BR/nano-CaCO₃ composites were significantly increased by increasing the nano-CaCO₃ content. With increasing the nano-CaCO₃ content, the glass transition temperature of the composites remained approximately constant. Meanwhile, the mechanical interfacial properties of BR/nano-CaCO₃ composites also were increased by the addition of nano-CaCO₃. The addition of nano-CaCO₃ also had the effect of increasing the tensile strength and elongation of the composites.

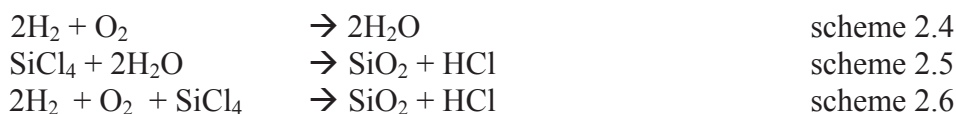
3.3.3 Blending of PLA with silicon dioxide

Silicon dioxide (silica) and silicate minerals make up 95% of earth's crust. There are two major types of silica, ground silica and synthetic silica. Ground silica is separate into three categories: crystalline, microcrystalline, and diatomaceous. The chemical compound silicon dioxide, also known as silica (from the Latin silex), is an oxide of silicon with the chemical formula SiO₂. Commercial reserves must be light in color and easy to process to grain size of between 20 to 140 meshes. Beneficial involves washing, milling, and classification. A typical oxide chemical analysis, as given in Table 14, indicates the high purity of such grades.

Table 14. Typical percent oxide composition of ground silica [86].

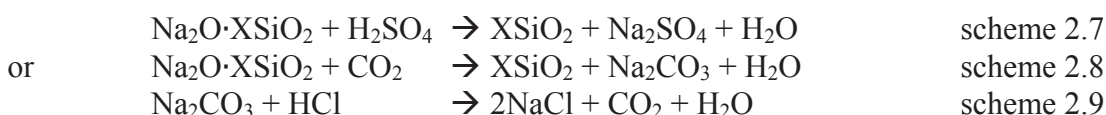
Chemical	Crystalline	Micro crystalline	Diatomaceous
SiO ₂	99.7	99.9	86.9
Al ₂ O ₃	0.101	0.18	3.1
Fe ₂ O ₃	0.023	0.02	1.1
CaO	< 0.01	0.04	0.41
MgO	< 0.01	0.01	0.65
TiO ₂	0.019	-	0.18
LOI	0.25	0.25	3.8

Synthetic silica are very fine amorphous white powders. They are very different in structure and properties from the natural ground silica. Fumed silica is prepared by high-temperature vapor process in which silicon tetrachloride is hydrolyzed in the flame of hydrogen and oxygen. The reactions are simplified in the following chemical equation:



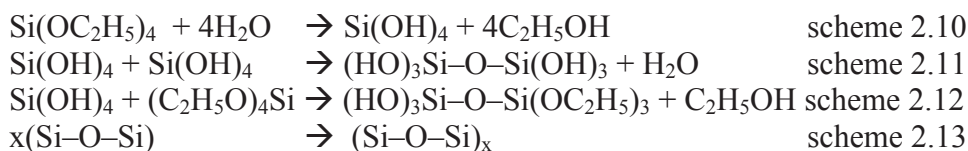
The particle size and surface area of fumed silica can be controlled by varying the ratio of reactant in the process [86].

Less expensive synthetic silica processes involve liquid rather than vapor techniques. Precipitated silica is processed by sol-gel process of sodium silicate.



The sodium silicate in this process may originate from variety of sources. A standard route is to fuse high-purity silica sand with sodium carbonate, yielding by-product carbon dioxide that can be recycled back into the precipitated process [86].

The reaction of tetraethyl orthosilicate (TEOS) is alternative process to produce silica. The hydrolysis of TEOS would happen in the presence of water, and $\text{Si}(\text{OH})_4$ was formed as one of the hydrolyses. Then, $\text{Si}(\text{OH})_4$ molecule would polymerize with other $\text{Si}(\text{OH})_4$ or TEOS molecule. The product of this step was the monomer or oligomers of polysiloxane. Finally, the monomers or oligomers of polysiloxane continue to polymerize and form a film of high relative molecular mass polysiloxane with a three-dimensional network structure [128].



Because water and TEOS are immiscible, a mutual solvent such as ethanol is normally used as a homogenizing agent [128].

The physical properties of precipitated silica are controlled through process variables, such as reactant concentration, rate of addition, temperature, order of addition, pH, and drying condition. Five different categories of precipitated silica are arbitrarily defined by oil-absorption as shown in Table 15

Table 15. Definition of silica structure level [86].

Level	Oil absorption ($\text{cm}^3/100 \text{ g}$)
Very high structure	Above 200
High structure	175-200
Medium structure	125-175
Low structure	75-125
Very low structure	Less than 75

In the vast majority of silicates, the Si atom shows tetrahedral coordination, with 4 oxygen atoms surrounding a central Si atom. The most common example is seen in the quartz crystalline form of silica. In each of the most thermodynamically stable crystalline forms of silica, on average, all 4 of the vertices (or oxygen atoms) of the SiO₄ tetrahedral are shared with others, yielding the net chemical formula of SiO₂ as shown in Figure 16 [129].

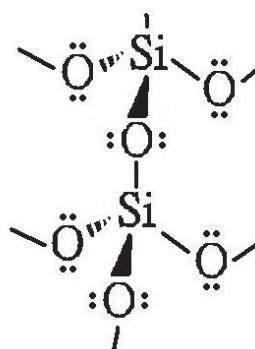


Figure 16. Molecular structure of SiO₂ [130].

Crystalline silica is silicon dioxide that has a theoretical composition of SiO₂. At atmospheric pressures, there are three major forms of silica: quartz (stable below 870°C), tridymite (stable from 870 °C to 1470 °C) and cristobalite (stable from 1470 °C to 1723 °C). Typical physical properties of natural/ground and synthetic silica are given in Table 16 and 17 [86].

Table 16. Physical and thermal properties of natural silica [86].

Property	Units	Crystalline	Microcrystalline	Diatomaceous
Average particle size	micron, esd ^a	1.9-8.8	2.1-8.2	3-8
Specific gravity	g/cm ³	2.65	2.05	-
Surface area, BET N ₂	m ² /g	0.54-2.06	3.6-6	
Oil absorption, ASTM D 281		24.1-36.2	26-30	105-135
Mohs hardness		6.5-7	6.5-7	6.5-7
Thermal conductivity × 10 ³	Cal/g·s·°C	7	-	-
Specific heat	Cal/g·°C	0.19	-	-
Coefficient of thermal expansion	°C×10 ⁻⁶	-	10	-

^aesd = equivalent spherical diameter.

Silica glass sphere generally lead to increase in tensile strength, compressive strength and flexural modulus. Because of spherical shape, stress cracking in finished parts occurs to lesser extent than with ground fillers. Although hollow sphere lower the apparent density, the usually impair the mechanical properties [73].

Table 17. Physical properties of synthetic silica [86].

Property	Units	Fumed	Precipitated	Gel
Primary particle size	Micron	0.007-0.04	0.01-0.30	-
Average particle size	micron, esd ^a	0.8	8-10	4-8
Specific gravity	g/cm ³	2.2	2.2	2.2
Surface area, BET N ₂	m ² /g	50-400	60-300	100-800
Oil absorption, ASTM D 281		150-250	160-200	150-250
Mohs hardness		6.5-7	6.5-7	6.5-7
Percent moisture		< 1.5	6.0	5.0
Silanol groups/nm ²		2-4	1.5-10	4-10

^aesd = equivalent spherical diameter.

Silica glass sphere generally lead to increase in tensile strength, compressive strength and flexural modulus. Because of spherical shape, stress cracking in finished parts occurs to lesser extent than with ground fillers. Although hollow sphere lower the apparent density, the usually impair the mechanical properties [73].

Silica is used for a variety of reason in polyvinyl chloride (PVC) resin system. In soft PVC, silica is used to control thixotropy, improve dielectric properties, prevent plate-out, and add antiblocking and flattening properties. Synthetic silica is a poor conductor of heat and electricity and, therefore, can be used only in low voltage PVC insulation applications. In PVC films, fumed and gel silica are used for antiblocking, antislip, and plate-out properties. For some systems, partial replacement of mineral (CaCO₃) by silica can be made to increase hardness, elastic recovery, resistance to heat distortion, and scratch resistance [86].

In polyethylene and polypropylene blown film, fumed, diatomaceous, and gel-silica grades are used for antiblocking and free-flow purposes. Silica is also used to reduce plate-out in polyethylene, polypropylene, and polystyrene resins. In low-density polyethylene, silica is sometimes used to improve the surface printability of the plastic. Rubber applications are a major market for silica, but its usefulness has not extended into thermoplastic elastomer. It can be used at levels from 2.5% to 25% in elastomer to give reinforcement [86].

There are some publications that use silica nano-particles to improve tensile strength, modulus, hardness, abrasion resistance and thermal properties of polymer. Ma et al. [131] prepared polyacrylate/silica nanocomposite by sol-gel process via in situ emulsion polymerization. DSC results showed that the glass transition temperature of polyacrylate/nano-SiO₂ was higher than that of polyacrylate.

Zhang et al. [132] developed a novel biodegradable nanocomposite based on poly (3-hydroxybutyrate-co-3-hydroxyhexanoate) (PHBHHx) and silane-modified kaolinite/silica core-shell nano-particles (SMKS), via solution-casting method using chloroform as solvent. Unmodified (ORK) and glycidoxypropyltrimethoxysilane (G-silane) surface-modified kaolin (SMK) were also introduced into PHBHHx matrix for comparison. SMKs significantly improved the mechanical properties of the PHBHHx

compared to that of ORK and SMK. The composite filled with a low loading of SMKS increased the tensile strength and toughness. TEM micrographs indicated that SMKS was finely distributed in the PHBHHx matrix compared with the other two kinds of fillers. These significant improvements in these mechanical properties were attributed to the fine dispersion of SMKS into the polymer and covalent interaction between polymer chains and the surface of SMKS.

Wen et al. [133] investigated the effect of spherical nanofillers (SiO_2) on the thermal stability of PLA. The nanocomposites displayed improved thermal stability both under nitrogen and in air. The stabilization mechanism was attributed mainly to the barrier effect of the network formed, which was demonstrated by the improved barrier properties and rheological performance. FTIR spectroscopy and TGA indicated that hydroxyl groups on SiO_2 surfaces and PLA chain-ends reacted during melt processing. The resulting grafted SiO_2 and entangled PLA chains formed a dense network, which hindered the diffusion of oxygen and volatile decomposition products. Furthermore, the improvement in thermal stability resulted from the restraining effect on the mobility of active hydroxyl end-groups, so that some related thermal decomposition reactions were inhibited.

Chrissafis et al. [134] prepared nanocomposites of poly(L-lactic acid) (PLLA) containing 2.5 wt% of fumed silica nano-particles (SiO_2) and organically modified montmorillonite (OMMT) by solved evaporation method. The results showed that all nanocomposites exhibited higher mechanical properties compared to neat PLLA, except elongation at break. Nano-particles also affect the thermal properties of PLLA and especially the crystallization rate.

Bikiaris [135] reviewed about the effect of nano-particles on the thermal properties of polycondensation polymers. The results in most cases showed enhancement thermal stability at low loading (4–5 wt%) of nano-particles. In case of thermal decomposition from TGA for the PLA/ SiO_2 nanocomposites gradually increases for SiO_2 contents up to 5 wt%, then decreases slowly with further increase of filler loading. PLA/ SiO_2 nanocomposite with 5 wt% SiO_2 exhibits the highest T_{onset} (365.1 °C), which is shifted approximately 35 °C towards higher temperature compared to T_{onset} for neat PLA.

In advance, silica was use as a filler enhancing the permeability of polymer membrane. Wahab et al. [136] investigated the use of nanosized fumed silica (Aerosil® R106) as fillers in the production of asymmetric hollow fiber mixed matrix membrane (HFMMM) where polysulfone was the host polymer matrix. The presence of fumed silica particles were found to stimulate the flow of CO_2 as indicated by an increase (> 12%) in CO_2 permeability for all HFMMMs. At low loading of 0.1% (w/w), the permeability of CO_2 and CH_4 were 90.04 and 2.75 GPU, respectively, and the selectivity was higher than the neat PSf hollow fiber membrane. The selectivities of CO_2/CH_4 and O_2/N_2 significantly improved with an average value of 32.74 and 6.35, respectively. The HFMMM also showed an increase in glass transition temperature and thermal stability.

The effects of different particle shapes of ultrafine silica used as a filler were also investigated Idrus et al [137]. Three shapes of filler (cubical, elongated and irregular) were produced using the Hosokawa Alpine classifier mode with a 50 ATP-forced vortex classifier. Each filler was loaded into SMR-L natural rubber at four different loadings, 10 to 40 parts per hundred of rubber (phr). However, at higher

loading, elongated-shaped filler showed a higher maximum torque compared with cubical or irregular shaped fillers. Because of better filler–rubber interaction, irregular shaped fillers showed the highest tensile strength, elongation at break and hardness compared with the cubical and elongated shapes.

For increasing the efficiency of filler, combing filler or making composite filler is interesting. There are some reports about the combination of CaCO_3 and Silica filler as a core-shell particle than be use as plastic filler.

Chen et al. [138] invented the method to produce $\text{CaCO}_3/\text{SiO}_2.n\text{H}_2\text{O}$ nanocomposite particles, a template nucleus is used calcium carbonate and the surface of nucleus is encapsulated by a $\text{SiO}_2.n\text{H}_2\text{O}$ nanolayer. The nanocomposite particles were prepared by concept that polymers have larger contact area with silica particles than with calcium carbonate, benefits to form linkage at the interface of two materials (plastic and filler), thereby improving mechanical properties of materials.

Tanabe and Mitsuhashi [139] invented the method to produce silica-calcium carbonate particles by forming calcium carbonate with synthetic silica was added 95% conversion of carbonation reaction. The silica-calcium carbonate particles have both excellent characteristics of synthetic silica and calcium carbonate. Synthetic silica is fixed on the surfaces of calcium carbonate particles as it is while keeping the characteristics of the synthetic silica that has good properties such as a high specific surface area, high gas absorbability, high oil absorption and the like.

Zhang and Li [140] studied the synthesis of $\text{CaCO}_3@/\text{SiO}_2$ core–shell nanoparticles. The cubic core–shell particles were created using a surface precipitation procedure using cubic calcite as seeds on which a silica layer was grown. Moreover, the calcite of core–shell nano-particles can be dissolved leaving silica shells. The characterizations of composite and silica shells were made. The results showed that the silica layer was continuously coated on the surface of CaCO_3 core with a thickness of about 5 nm. After coated with silica shells, the thermal stability decreases for its reaction with silica. The shape and size of pores of silica shells were similar to that of the CaCO_3 cores.

CHAPTER 3

RESEARCH METHODOLOGY

1. Phase I: The effect of particle size and particle loading on the mechanical, physical and thermal properties of CaCO₃-PLA biocomposites

1.1 Materials

Poly(lactic acid) (PLA) Extrusion/Thermoforming (Natureworks®2002D) grade, with L/D isomer ratio of 96:4, glass transition temperature (T_g) of 58 °C and melting temperature (T_m) of 153 °C, weight-average molecular weight (M_w) of 212,300 Da and polydispersity (M_w/M_n) of 3.06 was used in this research. Prior processing, differential scanning calorimeter (DSC) measurement of PLA pellet was performed under nitrogen atmosphere by Perkin Elmer, Pyris 1. Samples were heated from 40 to 180 °C at 5 °C/min (1st heating), cooled to 40 °C at 5 °C/min, and then heated again to 180 °C at 5 °C/min (2nd heating).

There were three kind of CaCO₃ used in the research; CaCO₃ micro-particle (1QC, Quality Mineral Co., Ltd., Thailand), and two grades of CaCO₃ nano-particle by precipitation method (CNANO P-23, BRS Intertrade Co., Ltd., Thailand and NPCC 101, Behn Meyer Chemical Co., Ltd., Thailand). Morphology of CaCO₃ was analyzed by Scanning Electron Microscopy (SEM). The agglomerate particles size was evaluated by sized analysis and dynamic light scattering technique. The characteristics of CaCO₃ were analyzed by XRD, FT-IR and TGA. Their code names in the experiment were developed as Micro-CaCO₃-1740, Nano-CaCO₃-1041, and Nano-CaCO₃-280, respectively.

1.2 Specimen preparation

PLA and all kinds of CaCO₃ as mention above were used as filler. PLA and CaCO₃ was blended in En Mach SHJ-25 co-rotating twin-screw extruder and extruded throughout a T-slit die and drawn by nip rolls at speed of 15 Hz to cast flat sheet. The screw speed was 130 rpm and extruder temperature profile was in the range of 150°C, 150 °C, 155 °C, 155 °C, 160 °C, 160 °C, 165 °C, 165 °C in the feeding zone down to metering zone and the temperature of die was controlled at 170 °C. Neat PLA was also processed under the same condition to be the reference. The amounts of each CaCO₃ in PLA biocomposites were varied in the range of 0-20 wt% of biocomposites.

1.3 Experiments

1.3.1 Thermal stability studies

Thermal Gravimetric Analysis (TGA) of neat PLA, extruded PLA and CaCO₃-PLA biocomposites samples was performed under nitrogen atmosphere with Mettler Toledo TGA model 1. Samples were heated from 50 °C to 500 °C at 10 °C/min. The T_{onset}, T_d and T_{end} were calculated from the TGA curve.

1.3.2 Thermal properties studies

The melting and crystallization behavior of the CaCO₃-PLA biocomposites were studied by Differential Scanning Calorimeter (DSC) (Perkin Elmer, Pyris 1) under nitrogen atmosphere. The heating scan cycle was performed between the temperature of 40 and 180 °C at the heating/cooling rate of 5 °C/min (heat-cool-heat) and the data was collected.

1.3.3 Mechanical properties studies

Tensile tests were carried out according to ASTM D882 standard using a universal testing machine (LR50K, Lloyd Instruments, UK) under ambient conditions with 100 mm initial grip separation at crosshead speeds of 10 mm/min. The high-speed tensile test as 600 mm/min (limitation of the machine) was performed to imitate the impacted force situation.

1.3.4 Dynamic mechanical properties studies

Dynamic mechanical properties of PLA and its biocomposites with different CaCO₃ particle sizes and loading were studied. The storage modulus (E') of thin sheets extruded PLA, and CaCO₃-PLA biocomposites were determined as a function of temperature by dynamic mechanical analysis using Dynamic Mechanical Analyzer (DMA) Gabo Eplexor QC 25 instrument. Thermal properties as glass transition temperature and crystallization temperature were also discussed in this section. DMA spectra were taken in the tension mode, at a frequency of 1 Hz and various temperatures in the range of 25-140 °C at heating rate of 2 °C/min.

1.3.5 Morphology studies

Wide-angle X-ray diffraction (WAXD) analyzer, Rigaku miniflex II, was employed to study crystallization pattern and crystallinity of CaCO₃-PLA biocomposite sheet. The diffraction patterns were collected from 3.0 to 60.0° with the step size of 0.01°. Scanning Electron Microscopy (SEM) was used to investigate morphology of the CaCO₃-PLA biocomposites. The samples were fractured in liquid nitrogen and sputtered with gold. Then the phase morphology was observed in an SEM instrument, Jeol JSM-6301f, operating at low voltage (5 KV and 10 KV) for high magnification of 10,000X and 50,000X.

1.3.6 Rheology studies

Rheology behavior was studied by three techniques; melt flow indexer, capillary rheometer and rotational rheometer. CaCO₃-PLA biocomposites were characterized by melt flow indexer with testing temperature of 170 °C and 2.16 kg piston load according to ASTM D1238 to investigate the effect of filler size and filler loading on viscosity. The in-depth rheological of the biocomposites were then investigated by a capillary rheometer (Bohlin Instrument Company), the correction for true viscosity was built up by using a capillary die with the L/D ratio of 16/1 mm/mm in right barrel and a zero die as a reference in left barrel. In addition, the melt behavior of biocomposite at low shear rate was investigated by rotational rheometer (plat & plate rheometer, Rheometric Scientific, TA Instruments) with steady shear rate sweep range of 0.01 – 150.0 s⁻¹. The temperature of the test was fixed at 170 °C as same as die temperature in the processing.

2. Phase II: The effect of plasticizers on the CaCO₃-PLA nanocomposites

2.1 Materials

Poly(lactic acid) (PLA) Extrusion/Thermoforming (Natureworks®2002D) grade, with L/D isomer ratio of 96:4, glass transition temperature (T_g) of 58 °C and melting temperature (T_m) of 153 °C, weight-average molecular weight (M_w) of 212,300 Da and polydispersity (M_w/ M_n) of 3.06 was used in this phase. Nano-CaCO₃-280 (NPCC 101, Behn Meyer Chemical Co., Ltd., Thailand) was selected to use as filler. In addition, polyethylene glycol (PEG, M_w~400, Fluka), and Tributyl citrate (TbC, M_w~360, Fluka) were used as plasticizer. The chemical structure and some properties of plasticizers are shown in Figure 17 and Table 18, respectively.

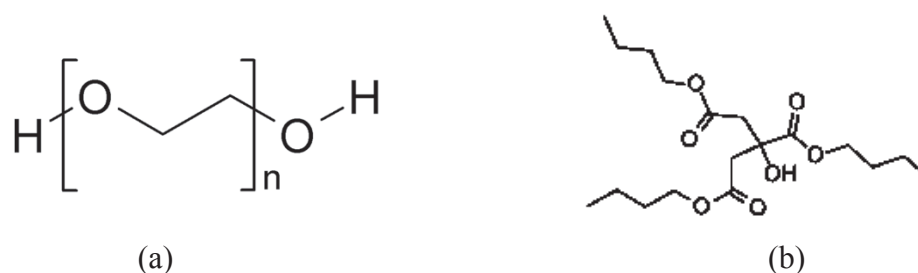


Figure 17. Chemical structure of plasticizers; (a) polyethylene glycol and (b) tributyl citrate [90,141].

Table 18. Some properties of polyethylene glycol and tributyl citrate plasticizer.

Properties	Polyethylene glycol	Tributyl citrate
Molecular weight	M _n 380-420, Average M _n 400	360.44
Refractive index	n ₂₀ /D 1.466	n ₂₀ /D 1.445
Density	1.128 g/mL	1.043 g/mL

2.2 Specimen preparation

In this phase, PLA and CaCO₃ were dried overnight at 60 °C before they were brought into the process. The nanocomposites, as shown in Table 19, were compounded by adding of all components to En Mach SHJ-25 co-rotating twin-screw extruder. PLA and CaCO₃ blends were prepared in weight percentage of while PEG and TbC were added as parts per hundred (phr) in the blends. The barrel temperature profile adopted during blending was ranged from 150 °C in the feed zone to 170 °C in metering zone at the fixed screw speed of 130 rpm. Then the extruded materials were compression molded into standard tensile and impact specimens according to ASTM D638 and ASTM D256 using LabTech compression molding with mold temperature of 170 °C and mold pressure of 20,000 psi for 5 min.

Table 19. Designations of materials and their compositions used in phase II.

Names	Designations	Ratio (PLA : CaCO ₃ : plasticizer)
PLA	PLA	100.0 : 0.0 : 0.0
CaCO ₃ -PLA nanocomposite	PLA/CaCO ₃	95.0 : 5.0 : 0.0
10 phr PEG plasticized PLA nanocomposite	PLA/10PEG	90.9 : 0.0 : 9.1
10 phr PEG plasticized CaCO ₃ -PLA nanocomposite	PLA/CaCO ₃ /10PEG	86.8 : 4.5 : 8.7
20 phr PEG plasticized PLA nanocomposite	PLA/20PEG	83.3 : 0.0 : 16.7
20 phr PEG plasticized CaCO ₃ -PLA nanocomposite	PLA/CaCO ₃ /20PEG	79.8 : 4.2 : 16.0
10 phr TbC plasticized PLA nanocomposite	PLA/10TbC	90.9 : 0.0 : 9.1
10 phr TbC plasticized CaCO ₃ -PLA nanocomposite	PLA/CaCO ₃ /10TbC	86.8 : 4.5 : 8.7
20 phr TbC plasticized PLA nanocomposite	PLA/20TbC	83.3 : 0.0 : 16.7
20 phr TbC plasticized CaCO ₃ -PLA nanocomposite	PLA/CaCO ₃ /20TbC	79.8 : 4.2 : 16.0

2.3 Experiments

2.3.1 Thermal stability studies

Thermal Gravimetric Analysis (TGA) measurements were performed to measure the thermal stability of nanocomposite under nitrogen atmosphere. In this phase, Mettler Toledo TGA model 1 was used to investigate thermal property of PLA and plasticized CaCO₃-PLA nanocomposites. Samples were heated from 50 °C to 500 °C at 10 °C/min. The T_{onset}, T_d and T_{end} were calculated from the TGA curve.

2.3.2 Thermal properties studies

The melting and crystallization behavior of the nanocomposites were studied by Differential Scanning Calorimeter (DSC) (Mettler Toledo DSC822e) under nitrogen atmosphere. The temperature was raised from -20 to 180 °C at the heating ramp of 10 °C/min.

2.3.3 Mechanical properties studies

Tensile test was carried out according to ASTM D638 type V using a universal testing machine (LR50K, Lloyd Instruments, UK) under ambient conditions with crosshead speeds of 10 mm/min. Izod impact test, according to ASTM D256, were done on notched impact specimens, by using an instrument impact tester (Radmana Model ITR2000).

2.3.4 Dynamic mechanical properties studies

Dynamic mechanical properties of PLA and its plasticized-nanocomposites were studied. The storage modulus (E') of PLA, and plasticized CaCO_3 -PLA nanocomposites were determined as a function of temperature by dynamic mechanical analysis using Dynamic Mechanical Analyzer (DMA) Gabo Eplexor QC 25 instrument. Some thermal properties as glass transition temperature and crystallization temperature were also discussed in this section. DMA spectra were taken in the tension mode, at a frequency of 1 Hz and various temperatures in the range of 25-140 °C at heating rate of 2 °C/min.

2.3.5 Morphology studies

Wide-angle X-ray diffraction (WAXD) analyzer, Rigaku miniflex II, was employed to study crystallization pattern and crystallinity of PLA and plasticized PLA nanocomposites. The diffraction patterns were corrected from 3.0 to 60.0° with the step size of 0.01°. The morphology of nanocomposites was investigated by Scanning Electron Microscopy (SEM). The fractured surfaces of samples were sputtered with platinum, then the morphology was observed in an SEM instrument (Hitachi Model S3400N).

2.3.6 Rheology studies

Because of the incorporation with plasticizer, the viscosity of PLA dropped dramatically. The capillary rheometer was limited to measure viscosity of the melt that has very low viscosity. Therefore, the rheology behavior was only tested by rotational rheometer (plat & plate rheometer, Rheometric Scientific, TA Instruments) with steady shear rate sweep range of 0.01 – 1,000.0 s^{-1} . The temperature of the test was fixed at 170 °C as same as the die temperature in the extrusion process.

3. Phase III: The effect of SiO₂ surface treatment on CaCO₃ nano-particles on PLA nanocomposite

3.1 Materials

Poly(lactic acid) (PLA) Extrusion/Thermoforming (Natureworks®2002D) grade, with L/D isomer ratio of 96:4, glass transition temperature (T_g) of 58 °C and melting temperature (T_m) of 153 °C, weight-average molecular weight (M_w) of 212,300 Da and polydispersity (M_w/M_n) of 3.06 was used in this phase. Nano-CaCO₃-280 (NPCC 101, Behn Meyer Chemical Co., Ltd., Thailand) was selected to use for the preparation of SiO₂ coated CaCO₃ particles. Distilled water ethanol and ammonium hydroxide (NH₄OH, 35%NH₃, Mallinckrodt Chemical) were also used adjust the condition of the reaction. In addition, polyethylene glycol (PEG, $M_w \sim 400$, Fluka), and Tributyl citrate (TbC, $M_w \sim 360$, Fluka) were used as plasticizer.

3.2 Preparation of silica coated calcium carbonate composite particles

The [SiO₂-CaCO₃].nH₂O nano-particles were prepared by hydrolysis-condensation polymerization of TEOS on the surface of CaCO₃ particles. The CaCO₃ particles were dispersed into the mixture of TEOS, 200 ml ethanol and 300 ml distillation water. The mole ratios of TEOS to CaCO₃ were vary as 1:30, 1:20 and 1:10 then, 100 ml NH₄OH was added slowly, and the mixture was vigorously stirred at 40 °C for 6 h. After the reaction, the hydrophilic silica modified calcium carbonate ([SiO₂-CaCO₃].nH₂O) were filtrated and washed with ethanol followed by distillation water for several times to remove dissociative polysiloxane, unreacted monomer, and polysiloxane oligomers. The [SiO₂-CaCO₃].nH₂O nano-particles were then dried at 60°C in the oven.

3.3 Particle characterization

The characteristics of the [SiO₂-CaCO₃].nH₂O particles were characterized by wide-angle X-ray diffraction (WAXD) analyzer (Rigaku miniflex II) and Bruker vector-22 Fourier Transform Infrared (FT-IR) using KBr disk technique. Morphology of [SiO₂-CaCO₃].nH₂O particles was investigated by Transmission Electron Microscopy (TEM, Jeol model JEM-1230). The elemental content of [SiO₂-CaCO₃].nH₂O nano-particle was analyzed by X-ray fluorescence spectrometer (XRF, Phillips PW-2404). Particle size of fillers was determined by dynamic light scattering technique (Malvern Instrument, Zetasizer nano ZS). The BET surface area and pore size analyzer (BET, Quantachrome instrument model Nova 2000e) was also used to investigate the surface and porosity of [SiO₂-CaCO₃].nH₂O nano-particles.

3.4 Specimen preparation

Prior to compounding, PLA, CaCO₃ and [SiO₂-CaCO₃].nH₂O were dried overnight at 60 °C in order to remove the moisture. The nanocomposites, according to Table 20, were compounded by adding of all components to En Mach SHJ-25 co-rotating twin-screw extruder. The barrel temperature profile adopted during

blending was ranged from 150 °C in the feed zone to 170 °C in metering zone at the fixed screw speed of 130 rpm. Then the extruded materials were compression molded into standard tensile and impact specimens according to ASTM D638 and ASTM D256 using LabTech compression molding with mold temperature of 170 °C and mold pressure of 20,000 psi for 5 min. In addition, sheet specimen of PLA and its nanocomposites were fabricated by LabTech cast film and sheet chill rolls line. The temperature profile was ranged from 90 °C in the feed zone to 170 °C in metering zone at the fixed screw speed of 170 rpm. Extruded was throughout a T-slit die and drawn by chill rolls of the calendaring line at speed of 0.6 m/min to cast flat sheet of which had 7.5 cm width. Finally, these sheets were then investigated the gas permeability.

Table 20. Designations of materials and their compositions used in phase III.

Names	Designation	Ratio (wt%)
		(PLA : Filler : plasticizer)
PLA	PLA	100.0 : 0.0 : 0.0
CaCO ₃ -PLA nanocomposite	PLA/CaCO ₃	95.0 : 5.0 : 0.0
[SiO ₂ -CaCO ₃](1:30)-PLA nanocomposite	PLA/[SiO ₂ -CaCO ₃](1:30)	95.0 : 5.0 : 0.0
[SiO ₂ -CaCO ₃](1:20)-PLA nanocomposite	PLA/[SiO ₂ -CaCO ₃](1:20)	95.0 : 5.0 : 0.0
[SiO ₂ -CaCO ₃](1:10)-PLA nanocomposite	PLA/[SiO ₂ -CaCO ₃](1:10)	95.0 : 5.0 : 0.0
10 phr PEG plasticized PLA nanocomposite	PLA/10PEG	90.9 : 0.0 : 9.1
10 phr PEG plasticized CaCO ₃ -PLA nanocomposite	PLA/CaCO ₃ /10PEG	86.8 : 4.5 : 8.7
10 phr PEG plasticized [SiO ₂ -CaCO ₃](1:30)-PLA nanocomposite	PLA/[SiO ₂ -CaCO ₃](1:30)/10PEG	86.8 : 4.5 : 8.7
10 phr PEG plasticized [SiO ₂ -CaCO ₃](1:20)-PLA nanocomposite	PLA/[SiO ₂ -CaCO ₃](1:20)/10PEG	86.8 : 4.5 : 8.7
10 phr PEG plasticized [SiO ₂ -CaCO ₃](1:10)-PLA nanocomposite	PLA/[SiO ₂ -CaCO ₃](1:10)/10PEG	86.8 : 4.5 : 8.7
10 phr TbC plasticized PLA nanocomposite	PLA/10TbC	90.9 : 0.0 : 9.1
10 phr TbC plasticized CaCO ₃ -PLA nanocomposite	PLA/CaCO ₃ /10TbC	86.8 : 4.5 : 8.7
10 phr TbC plasticized [SiO ₂ -CaCO ₃](1:30)PLA nanocomposite	PLA/[SiO ₂ -CaCO ₃](1:30)/10TbC	86.8 : 4.5 : 8.7
10 phr TbC plasticized [SiO ₂ -CaCO ₃](1:20)-PLA nanocomposite	PLA/[SiO ₂ -CaCO ₃](1:20)/10TbC	86.8 : 4.5 : 8.7
10 phr TbC plasticized [SiO ₂ -CaCO ₃](1:10)-PLA nanocomposite	PLA/[SiO ₂ -CaCO ₃](1:10)/10TbC	86.8 : 4.5 : 8.7

3.5 Experiment

3.5.1 Thermal stability studies

Thermal Gravimetric Analysis (TGA) measurements were performed to measure the thermal stability of nanocomposite under nitrogen atmosphere. In this phase, Mettler Toledo TGA model 1 was used to investigate that property. Samples were heated from 50 °C to 500 °C at 10 °C/min. The T_{onset} , T_{d} and T_{end} were calculated from the TGA curve.

3.5.2 Thermal properties studies

The melting and crystallization behavior of the nanocomposites were studied by Differential Scanning Calorimeter (DSC) (Mettler Toledo DSC822e) under nitrogen atmosphere. The temperature was raised from -20 to 180 °C at the heating ramp of 10 °C/min.

3.5.3 Mechanical properties studies

Tensile test was carried out according to ASTM D638 type V using a universal testing machine (Instron 5969) under ambient conditions with crosshead speed of 10 mm/min. Izod impact test, according to ASTM D256, were done on notched impact specimens, by using an instrument impact tester (Swick Pendulum Impact Tester B5102.202 4 J).

3.5.4 Dynamic mechanical properties studies

Dynamic mechanical properties of PLA and its plasticized-nanocomposites were studied. The storage modulus (E') of PLA, CaCO₃-PLA, [SiO₂-CaCO₃]-PLA and plasticized [SiO₂-CaCO₃]-PLA nanocomposites were determined as a function of temperature by dynamic mechanical analysis using Dynamic Mechanical Analyzer (DMA) Gabo Eplexor QC 25 instrument. Some thermal properties as glass transition temperature and crystallization temperature were also discussed in this section. DMA spectra were taken in the tension mode, at a frequency of 1 Hz and various temperatures in the range of 25-140 °C at heating rate of 2 °C/min.

3.5.5 Morphology studies

Wide-angle X-ray diffraction (WAXD) analyzer, Rigaku miniflex II, was employed to study crystallization pattern and crystallinity of PLA, PLA nanocomposites and plasticized PLA nanocomposites. The diffraction patterns were corrected from 3.0 to 60.0° with the step size of 0.01°. The morphology of nanocomposites was investigated by Scanning Electron Microscopy (SEM). The fractured surfaces of samples were sputtered with platinum, then the morphology was observed in an SEM instrument (Hitachi Model S3400N).

3.5.6 Rheology studies

The rheology behavior was tested by rotational rheometer (plat & plate rheometer, Rheometric Scientific, TA Instruments) with steady shear rate sweep range of $0.01 - 1000.0 \text{ s}^{-1}$. The temperature of the test was fixed at $170 \text{ }^\circ\text{C}$ as same as the die temperature in the process.

3.5.7 Permeability studies

The gas permeation properties as oxygen transmission rate (O_2TR), carbon dioxide transmission rate (CO_2TR) and water vapor transmission rate (WVTR) of the sheet specimens were investigated. O_2TR was tested by Illinois model 8500 using ASTM D 3985 at 50% R.H. and temperature of $25 \text{ }^\circ\text{C}$. CO_2TR was investigated by Brugger GDP-C using ASTM D 1434-82 at 0% R.H. and temperature of $23 \text{ }^\circ\text{C}$. WVTR was evaluated by Mocon Permatran-W model 398 using ASTM E 398-03 at 90% R.H. and temperature of $37.8 \text{ }^\circ\text{C}$.

CHAPTER 4

RESULTS AND DISCUSSION

1. Phase I: The effect of particle size and particle loading on the mechanical, physical and thermal properties of CaCO₃-PLA biocomposites

PLA bioplastic offers a potential alternative to petrochemical plastics in many applications. Adding fillers into plastics are usually implemented not only confined to cost reduction, but also to control their physical and mechanical properties. A fairly new area of composites has emerged in which the reinforcing materials have the dimensions in nanometric scale. Nano-reinforcements of biodegradable polymers have strong promises in designing eco-friendly green nanocomposites for several applications. Properties of filler-filled composites are closely related to the dispersion of the particles in polymer matrix.

Consideration of various fillers, calcium carbonate (CaCO₃) is the most popular filling material, due to its high amount of loading in plastics and low cost. The particle size, particle loading and the distribution of CaCO₃ affect properties of polymers. Many research found that the incorporation of CaCO₃ into polymers could improve some properties of the composites, especially in PP [22,27,116-120].

Thus, this phase aimed to investigate the effect of CaCO₃ particle size and particle loading on mechanical, physical and thermal properties of CaCO₃-PLA biocomposites that were fabricated by extrusion sheet process. Moreover, the other aim of this phase was to test feasibility of PLA sheet fabrication using the simple two casting rolls that was connected to the extrusion sheet line. The outcome of phase I will be used as a guideline for the research in phase II and phase III.

1.1. Materials characterization

Poly(lactic acid) (PLA) pellet used in this research was characterized by DSC at the heating/cooling rate of 5 °C /min. DSC thermograms as shown in Figure 18, show that there was T_g at about 57.06 °C and single peak of T_m at about 149.18 °C in 1st heating scan. In 2nd heating scan, T_g was found at about 56.75 °C while the signal of T_m was not revealed.

The morphology and particle size of micro-sized CaCO₃ and both grades of nano-sized CaCO₃ were characterized by SEM and sized analysis technique. SEM micrographs of all CaCO₃ used in this research are shown in Figure 19 and the average agglomeration size are shown in Table 21. Their code names in this research were developed as Micro-CaCO₃-1740, Nano-CaCO₃-1041, and Nano-CaCO₃-280, respectively.

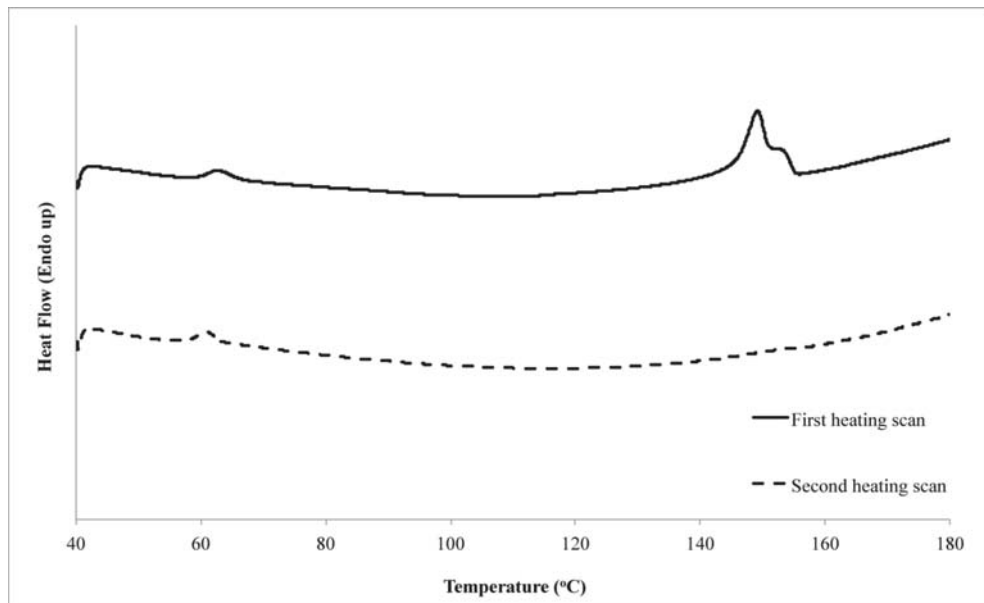


Figure 18. DSC thermograms of PLA pellet (Natureworks®2002D).

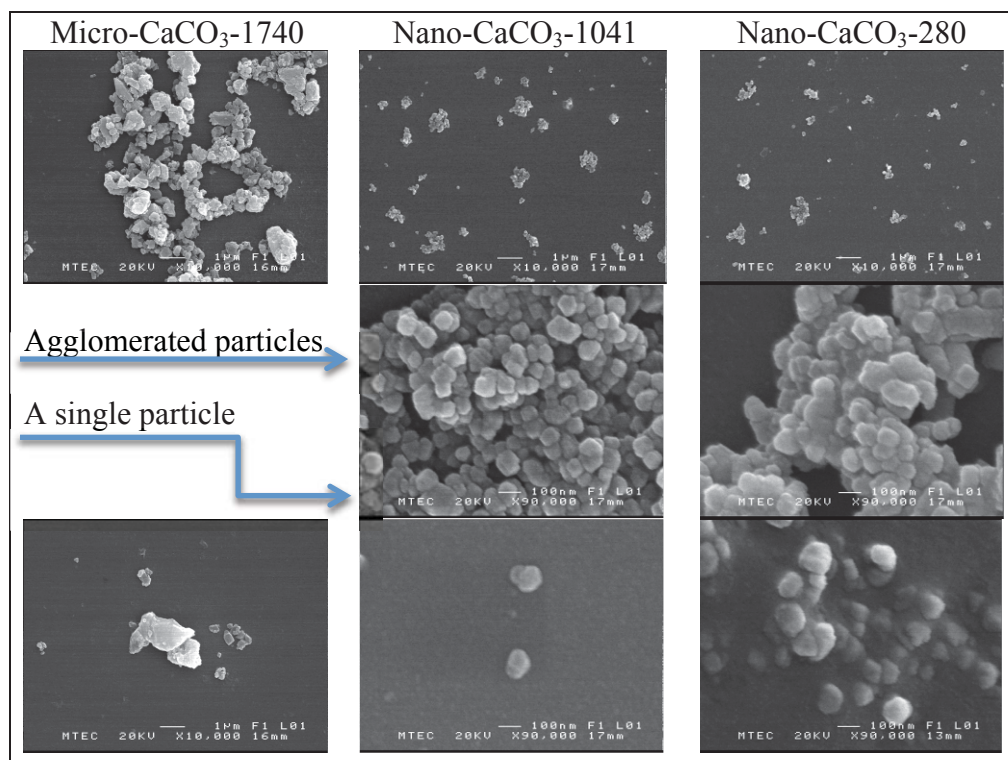
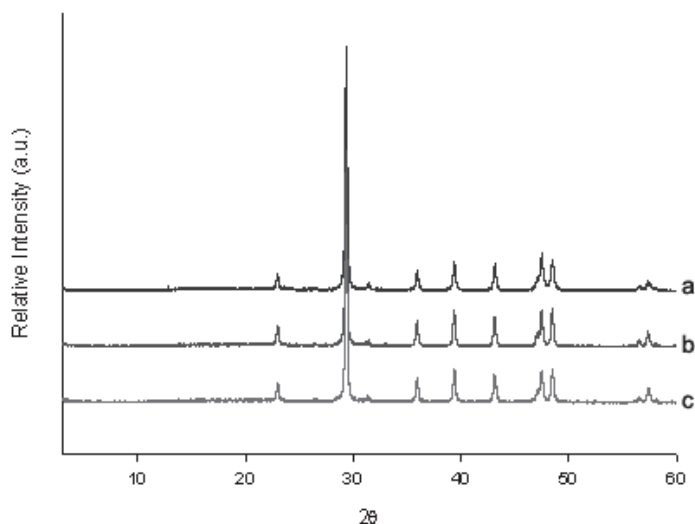


Figure 19. SEM micrographs of Micro-CaCO₃-1740, Nano-CaCO₃-1041 and Nano-CaCO₃-280 particles.

Table 21. Single particle and agglomeration size of CaCO₃.

Type of CaCO ₃	Single Particle Size (nm)	Agglomeration Size (nm)
Micro-CaCO ₃ -1740	1,600	1,746.7 ± 5.8
Nano-CaCO ₃ -1041	40-60	1,066 ± 37.4
Nano-CaCO ₃ -280	40	278.4 ± 1.7

The characteristics of CaCO₃ particles were analyzed by XRD, FT-IR and TGA. Figure 20 shows the XRD patterns of various CaCO₃ particles used in the research. There were no differences in characteristics of all types of CaCO₃ particles. The sharp peaks were shown at $2\theta \approx 23.03^\circ$, 29.36° , 35.94° , 39.35° , 43.14° , 47.49° and 48.51° .

**Figure 20.** XRD patterns of (a) Micro-CaCO₃-1740, (b) Nano-CaCO₃-1041 and (c) Nano-CaCO₃-280 particles.

Infrared spectra of CaCO₃ are presented in Figure 21. The FT-IR absorption peaks of all CaCO₃ were qualitatively similar. All types of CaCO₃ displayed the absorption peak of crystal at about 875 cm^{-1} and 710 cm^{-1} . The absorption peak at 875 cm^{-1} indicated the $[\text{CO}_3]^{2-}$ out-of-plane deformation mode of the aragonite form while the absorption peak of 710 cm^{-1} showed the calcite form [142]. This implied that the product was the mixture of calcite and aragonite. In addition, there were interested absorption peaks appeared at about $1,780\text{ cm}^{-1}$, $2,950\text{--}2,850\text{ cm}^{-1}$ and $3,600\text{--}3,200\text{ cm}^{-1}$. These peak indicated C=O stretching in carboxylic acid, alkyl C-H stretching and O-H stretching, respectively [143]. These absorption peaks proved that all types of CaCO₃ were treated by some fatty acid on the surface for preventing the re-agglomeration of particles.

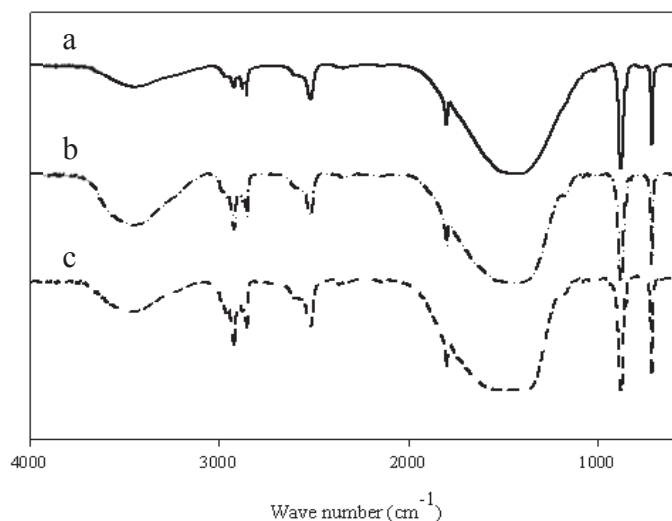


Figure 21. FT-IR spectra of (a) Micro- CaCO_3 -1760, (b) Nano- CaCO_3 -1041 and (c) Nano- CaCO_3 -280 particles.

Figure 22 shows TGA curves of all CaCO_3 used in this research. It was found that the content of fatty acid treated on the surface of two types of nano-sized CaCO_3 was nearly at the same amount (at about 4.2 wt%). The onset of degradation temperature showed that fatty acid treated on the Nano- CaCO_3 -1041 degraded at lower temperature with the faster rate than the fatty acid treated of the Nano- CaCO_3 -280. The content of fatty acid treated on the Micro- CaCO_3 -1760 (about 0.7 wt%) was less than those of nano-sized CaCO_3 . However, the onset of degradation temperature showed that fatty acid treated on the Micro- CaCO_3 -1760 was more stable than fatty acid treated on both nano-sized CaCO_3 particles.

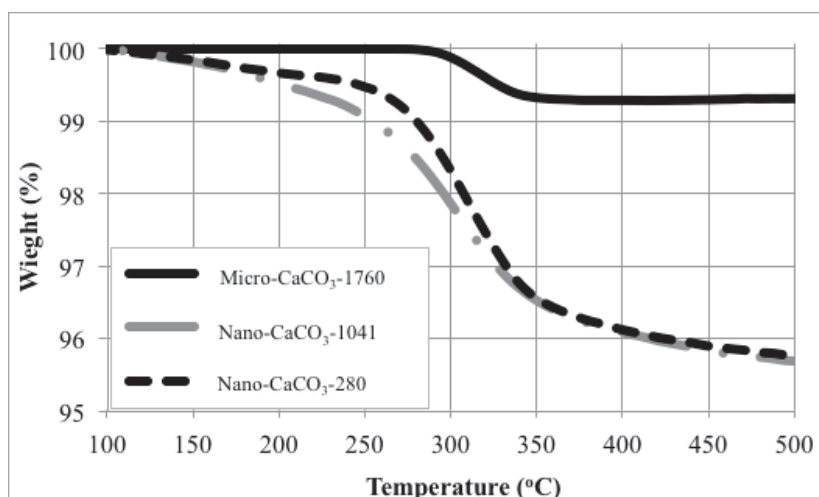


Figure 22. TGA curves of CaCO_3 used in this research; Micro- CaCO_3 -1740, Nano- CaCO_3 -1041 and Nano- CaCO_3 -280 particles.

1.2 Thermal stability studies

TGA was used to investigate the thermal stability of CaCO₃-PLA biocomposites in N₂ atmosphere. The TGA curves of the filled and unfilled biocomposites are shown in Figure 23 and the onset of degradation temperature (T_{onset}), degradation temperature (T_d), and the end of degradation (T_{end}) are reported in Table 22. The adding of CaCO₃ with fatty acid sizing agent had negative effect on thermal stability of PLA polyester. The effect of CaCO₃ is different from the other research on additional polymers and rubber such as poly(vinyl chloride), poly(methyl methacrylate), polypropylene and butadiene rubber [101,122,124,127]. PLA has a functional group of ester linkage, which is susceptible to chemical reaction in elevated temperature. The decrease of T_d in polyester when adding more fillers was also found in the research of Evans et al. and Liu et al. They found that the addition of CaCO₃ would lower the stability of PLA melt, and the negative effect of the nano-CaCO₃ was greater than that of the ordinary CaCO₃ [102,111]. In this research, CaCO₃ was coated by fatty acid to prevent re-agglomeration during storage and handling. The chemical reaction between fatty acid and ester linkage of PLA caused chain scission and induced thermal degradation of PLA, therefore, T_d of CaCO₃-PLA biocomposites decreased from 392 °C (neat PLA) to around 295-355 °C. It was found that T_d of PLA with Nano-CaCO₃-1041 and Nano-CaCO₃-280 were much lower than that of Micro-CaCO₃-1740 due to higher amount of fatty acid coating (larger surface area of the nano-sized particles).

Table 22. Thermal stability analysis of the unfilled and filled PLA biocomposites with various loading of CaCO₃.

Materials	$T_{\text{onset}}(^{\circ}\text{C})$	$T_d(^{\circ}\text{C})$	$T_{\text{end}}(^{\circ}\text{C})$
Neat PLA	376.24	392.54	412.98
Extruded PLA	346.33	365.47	375.11
5% Micro-CaCO ₃ -1740	335.61	356.70	362.89
10% Micro-CaCO ₃ -1740	330.43	348.81	353.48
15% Micro-CaCO ₃ -1740	312.58	339.47	346.93
20% Micro-CaCO ₃ -1740	308.91	331.55	340.24
5% Nano-CaCO ₃ -1041	329.08	347.06	351.60
10% Nano-CaCO ₃ -1041	313.78	333.86	337.65
15% Nano-CaCO ₃ -1041	284.98	309.75	314.94
20% Nano-CaCO ₃ -1041	277.29	296.20	306.20
5% Nano-CaCO ₃ -280	330.05	347.77	351.47
10% Nano-CaCO ₃ -280	311.93	333.60	337.68
15% Nano-CaCO ₃ -280	280.52	306.35	311.28
20% Nano-CaCO ₃ -280	278.14	295.24	304.42

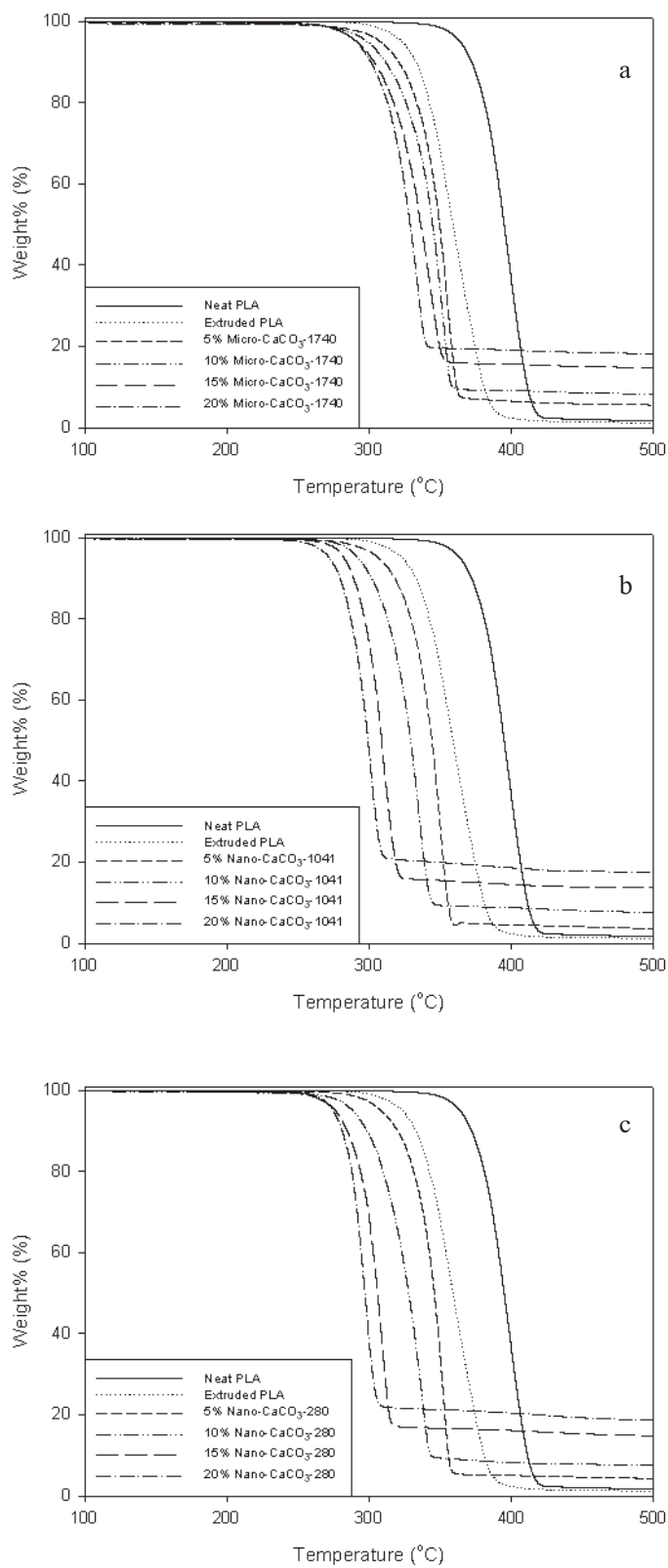


Figure 23. TGA curves of the CaCO₃-PLA biocomposites with various loading of CaCO₃; a) Micro-CaCO₃-1740, b) Nano-CaCO₃-1041 and c) Nano-CaCO₃-280.

1.3 Thermal properties studies

The DSC technique was used to study effect of adding micro- and nano-sized CaCO_3 on thermal properties of the biocomposites. Figure 24 shows DSC thermograms (Endo.) of CaCO_3 -PLA biocomposites extruded sheet at the heating/cooling rate of $5\text{ }^\circ\text{C}/\text{min}$. Table 23 shows glass transition temperature (T_g), melting temperature (T_m) and co-crystallization (T_{cc}) of the CaCO_3 -PLA biocomposite extrusion sheet. It was found that PLA and CaCO_3 -PLA biocomposites had one T_m but no T_{cc} in the first heating scan. However, in the second heating scan, both PLA and CaCO_3 -PLA biocomposites showed one T_{cc} and two T_m . In this research, compounding of CaCO_3 -PLA was calendared by casting rolls after extruded from die. The orientation of PLA polymer chains by this process caused no T_{cc} to be detected in the first heating scan. Moreover, drawing of the extrusion sheet caused stress-induced crystallization [144], so there was one broad T_m about $151\text{ }^\circ\text{C}$ in all CaCO_3 -PLA biocomposites sheets in the first heating scan.

Moreover, some researches mentioned that PLA could be found to exhibit four crystalline structures as α , β , γ and stereo-complex, upon the condition of processing and the tendency to crystallize upon purity of PLA polymer. The orthorhombic α crystal structure is the most commonly observed structure, in which the chains are in $-10/3$ left helical conformation. The values provided vary a little from group to group as: $a = 10.34\text{-}10.7\text{ \AA}$, $b = 5.97\text{-}6.45\text{ \AA}$, $c = 27.8\text{-}28.8\text{ \AA}$. Under high stress, β crystal orthorhombic ($a = 10.31\text{ \AA}$, $b = 6.1\text{ \AA}$, $c = 9\text{ \AA}$) structure with chains exhibiting more extended $3/1$ helical conformations can be formed. β crystals are found to transform into α crystal when annealed above T_g . The triclinic stereo-complex can only be obtained with 1:1 mixture of PLLA and PDLA. The hexagonal γ crystals are grown on a special substrate [21,30,144].

In the second heating scan, two T_m of both PLA and CaCO_3 -PLA biocomposites was founded. In general, commercial PLA contains D-form as impurity. The two melting peak were built from one imperfect crystalline showed as lower T_m (around $146\text{-}148\text{ }^\circ\text{C}$) and another more perfect crystalline showed as higher T_m (around $153\text{-}154\text{ }^\circ\text{C}$). These crystalline were explained based on melt-recrystallized model that small and imperfect crystals changed successively into more stable crystals through the melting and re-crystallization. Moreover, CaCO_3 could act as a nucleating agent to create more stable crystals.

Interestingly, T_{cc} was detected in all types and all loading of CaCO_3 in the second heating scan of the CaCO_3 -PLA biocomposite extrusion sheets. As PLA was thermally degraded in the melt process and the presence of fatty acid coating on CaCO_3 particles could accelerate chain scission of PLA. Thus, shorter polymer chains could be re-oriented and showed co-crystallization at T_{cc} around $105\text{-}112\text{ }^\circ\text{C}$. However, the T_{cc} of the PLA increased when it was blended with Micro- CaCO_3 -1740 and Nano- CaCO_3 -1041, and decreased when it was blended with smaller sized Nano- CaCO_3 -280. The decrease of co-crystallization temperature in Nano- CaCO_3 -280-PLA nanocomposite was due to large surface area of the nano-particle giving more reactivity of fatty acid to chain scission of PLA. These short chains of PLA could move and re-orientate easier than those long chains of high molecular weight PLA. Thus, T_{cc} of PLA nanocomposites were decreased with the increasing of CaCO_3 loading. It was found that by adding of smaller Nano- CaCO_3 -280 at 20 phr could

lower T_{cc} to the lowest temperature of 105°C, which would help in handling of the biocomposite melts in casting rolls.

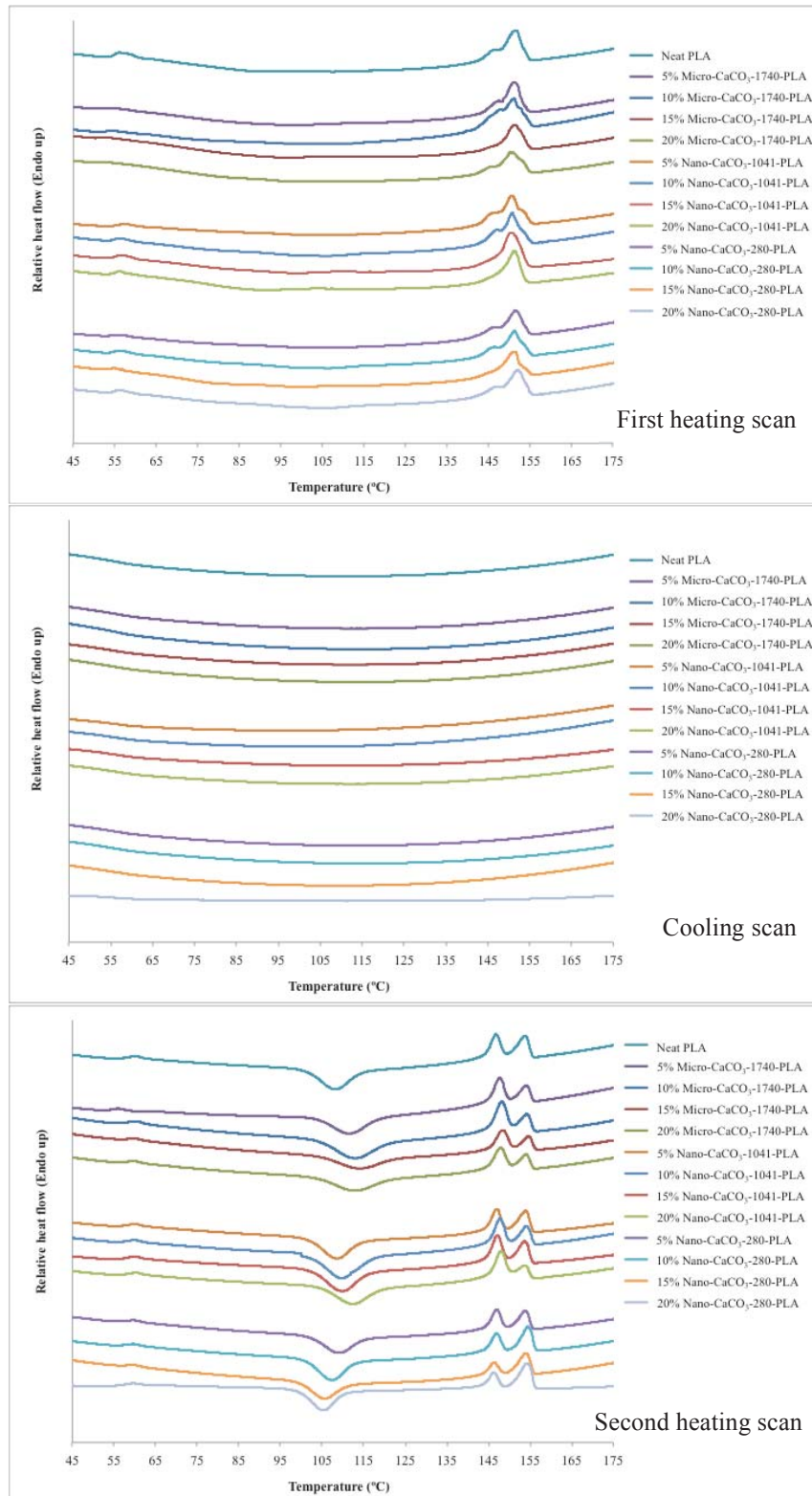


Figure 24. DSC thermograms of CaCO₃-PLA biocomposite extrusion sheet.

Table 23. Thermal properties of CaCO₃-PLA biocomposite extrusion sheet.

CaCO ₃	Filler ratio (%)	First heating scan			Second heating scan			
		T _g (°C)	T _{cc} (°C)	T _m (°C)	T _g (°C)	T _{cc} (°C)	T _m (°C)	
							peak 1	peak 2
Micro-CaCO ₃ -1740	0	54.38	-	151.27	58.01	108.15	146.77	153.77
	5	53.41	-	151.10	54.59	111.33	147.69	154.11
	10	52.57	-	151.10	56.75	112.83	148.19	154.76
	15	51.95	-	151.19	56.78	113.92	148.36	154.61
	20	51.31	-	150.19	55.94	112.66	147.85	154.03
Nano-CaCO ₃ -1041	5	55.22	-	150.53	56.82	108.41	146.94	153.95
	10	54.82	-	150.61	58.39	109.19	147.71	154.21
	15	54.19	-	150.28	56.06	109.92	147.11	153.62
	20	54.85	-	151.12	57.26	112.36	147.96	153.80
Nano-CaCO ₃ -280	5	53.45	-	151.38	56.95	108.02	146.97	153.80
	10	53.77	-	151.23	56.06	107.42	146.95	154.54
	15	53.10	-	151.04	58.09	105.58	146.28	154.03
	20	52.54	-	152.95	56.25	105.32	146.28	154.28

1.4 Mechanical properties studies

Tensile properties of PLA and CaCO₃-PLA biocomposites were tested according to ASTM D882 standard. The results in Figure 25 show that Young's modulus of CaCO₃-PLA biocomposites decreased with the increasing of CaCO₃ content. This trend could also be found in percentage of strain and high-speed tensile strength. The nano-sized CaCO₃ had more negative effect on mechanical properties of PLA than micro-sized CaCO₃. The decrease of the mechanical properties of CaCO₃-PLA biocomposites would cause from the lower crystallinity of PLA in agreement with XRD results. Lorenzo et al. [119] also reported that the addition of nano-sized calcium carbonate coated with fatty acids delayed crystallization of iPP. PLA polyester can undergo thermal degradation, causing lower molecular weight. Therefore, the mechanical properties of PLA after melt process were reduced. In addition, fatty acid coating on CaCO₃ surface could react with ester linkage of PLA and accelerated the degradation of PLA during melt process, causing lower molecular weight of PLA. Therefore, the increase of CaCO₃ content, which is also the increase of fatty acid content in the compound, resulted in the decrease of modulus of the biocomposites.

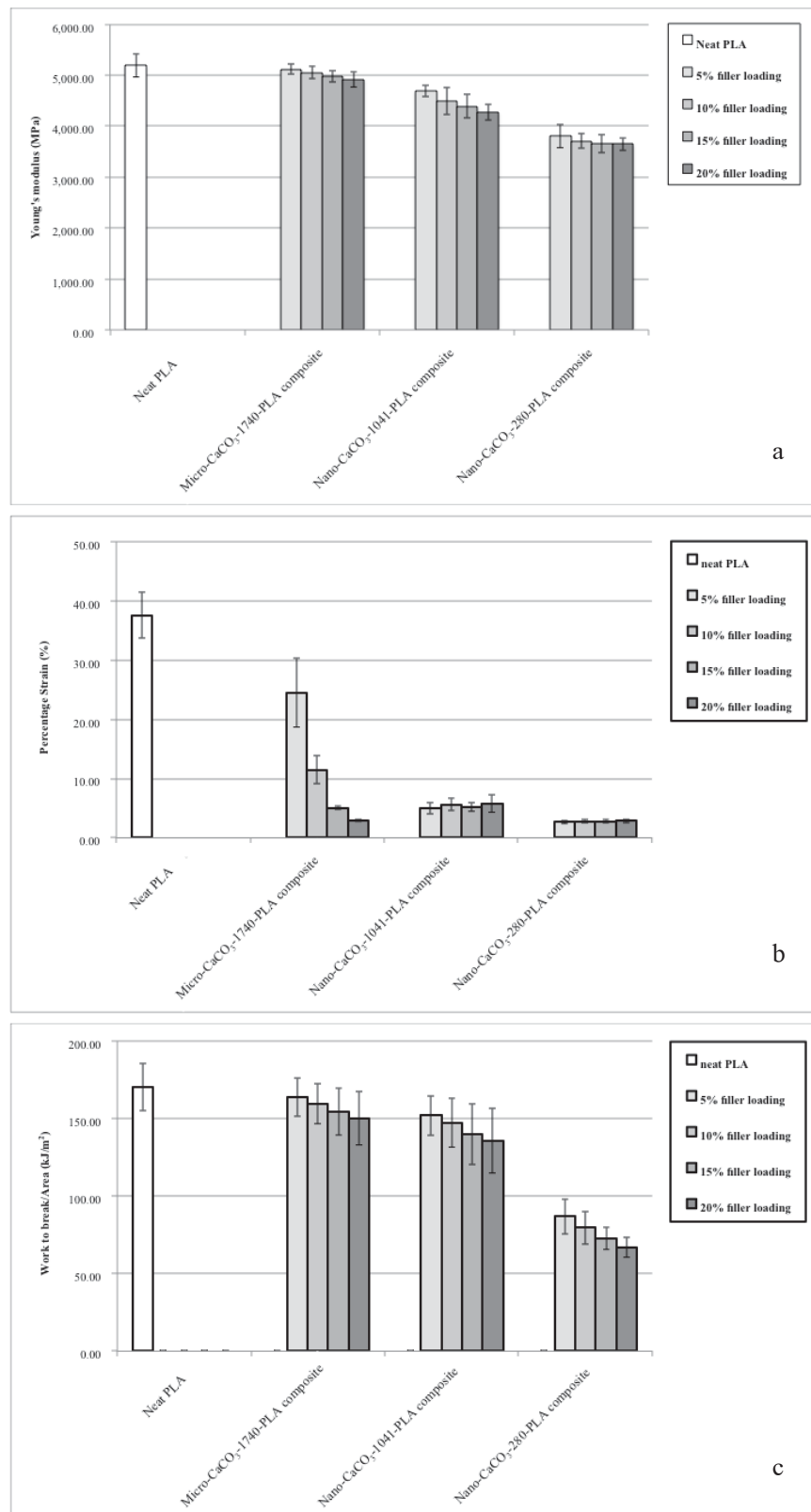


Figure 25. Mechanical properties of PLA and CaCO₃-PLA biocomposite; a) Young's modulus, b) Percentage of strain and c) High-speed tensile strength.

The decrease of elongation at break of PLA biocomposites demonstrated that the interfacial interaction between PLA matrix and CaCO_3 was so poor. The fillers induced a definite decrease in elongation [25], because they acted as stress concentrator to promote crack initiation. Therefore, the increase of particle loading and the decrease of particle size resulted the decreasing of elongation at break. However, the increasing content of nano-sized CaCO_3 in CaCO_3 -PLA nanocomposite had no significant effect on the percentage of stain.

Moreover, high-speed tensile test showed that the presence of CaCO_3 nano-particles could act as a stress concentration in the PLA matrix causing them to premature breakage. Zuiderduin et al. [27] also found that some coarse morphologies of smaller particle sizes ($< 0.7 \mu\text{m}$) lowered the toughening efficiency of fillers. Therefore, the smaller particle size and higher loading of CaCO_3 gave the lower high-speed tensile strength of the biocomposites.

1.5 Dynamic mechanical properties studies

Figure 26 shows the storage modulus (E') of extruded PLA and CaCO_3 -PLA biocomposite sheet over a temperature range of 25-140 °C. Normally, the E' of extruded PLA and CaCO_3 -PLA biocomposite sheet was slightly dropped when the temperature increased from 25 to 55 °C. Subsequently, E' dropped rapidly after temperature of about 55 °C because it was subjected to temperature higher than its glass transition temperature (T_g). For CaCO_3 -PLA biocomposite sheet at lower temperature range (25-55 °C), E' decreased with increasing CaCO_3 content. Similar to the reducing of Young's modulus, the E' decreased with decreasing size of fillers and increasing of filler contents. The Nano- CaCO_3 -280 that has the smallest size made the lowest E' of the biocomposite sheet. As discussed earlier in mechanical properties studies, the fatty acid coated on CaCO_3 , enhanced chain scission and caused shorter polymer chains. Therefore, the low molecular weight PLA caused the reduction of E' .

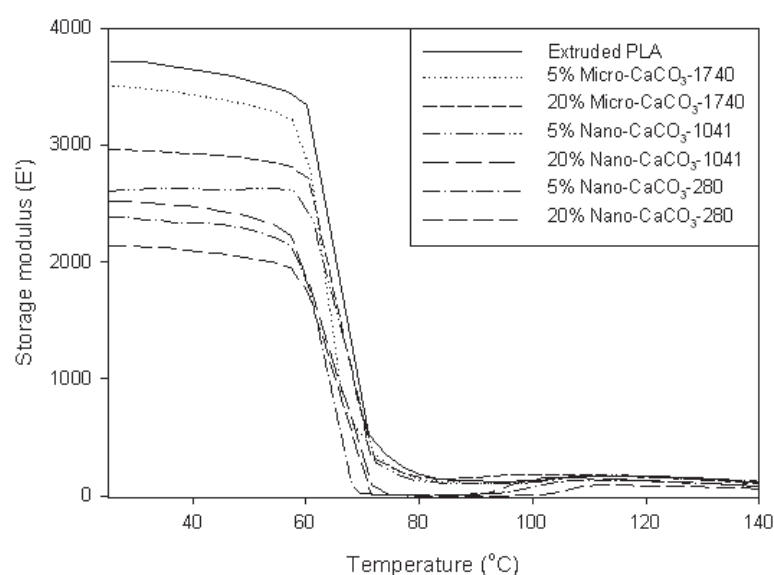


Figure 26. Storage modulus of extruded PLA and CaCO_3 -PLA biocomposite sheet.

The slightly increase in storage modulus (E') at temperature above T_g was due to co-crystallization of PLA. As PLA can undergo chain scissions depolymerization in melting process, the shorter chain of PLA could re-orientate and T_{cc} (around 110°C) of PLA was also found in the second heating scan of DSC. Hassan et al. reported the similar observation on E' of PLA/MMT nanocomposites. The increase of PLA's rigidity resulted from the crystallization [109]. There were no significant difference in type and content of CaCO_3 that affected the shift of E' around these temperature because almost all segments of PLA that could be crystallized, were oriented completely from the process. Finally, at the higher temperature, the E' of extruded PLA and CaCO_3 -PLA biocomposite sheet dropped again because of softening and melting of PLA matrix [124].

In consideration of T_g from DMA test, $\tan \delta$ in Figure 27 shows that there was no significant difference in T_g between the biocomposites consisting 5 wt% micro-sized and 5 wt% nano-sized CaCO_3 and that of extruded PLA. However, the increasing of the CaCO_3 loading to 20 wt% dramatically decreased T_g of PLA, since the higher amount of fatty acid coated on CaCO_3 surface could react with PLA, causing chain scission and enhancing movement of polymer chains. Therefore, the high content of the CaCO_3 fillers gave the high content of coating substance, resulting in the decreasing of T_g .

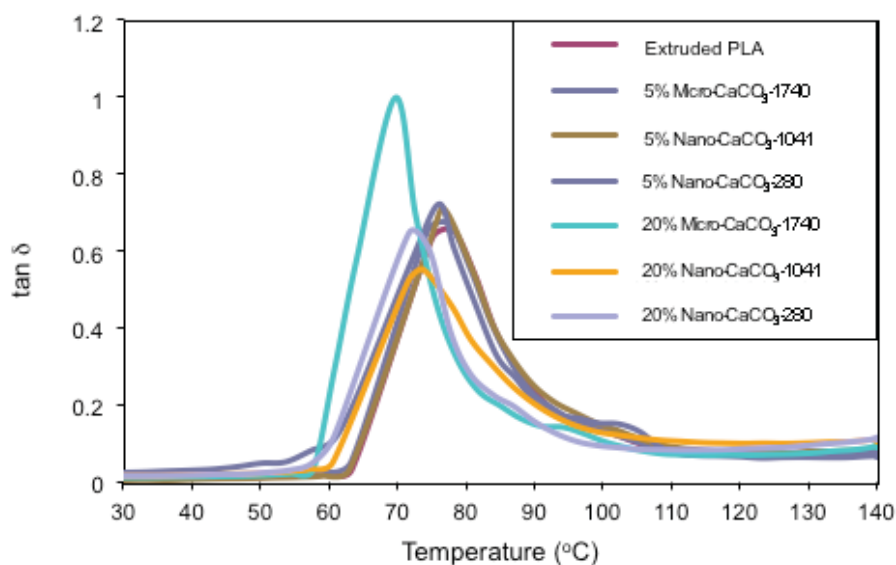


Figure 27. $\tan \delta$ of extruded PLA and CaCO_3 -PLA biocomposite sheet.

1.6 Morphology studies

The XRD patterns of extruded PLA, melt-pressed sheet PLA and CaCO_3 -PLA biocomposites sheets are illustrated in Figure 28-30.

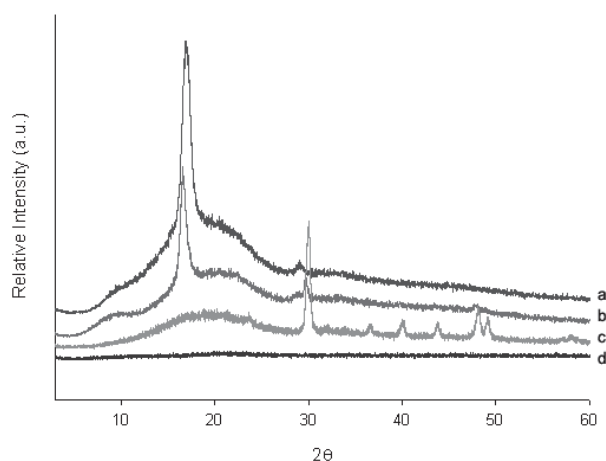


Figure 28. XRD patterns of (a) extruded sheet PLA, (b) 5 wt% Micro-CaCO₃-1740-PLA sheet, (c) 20 wt% Micro-CaCO₃-1740-PLA sheet and (d) melt-pressed PLA sheet.

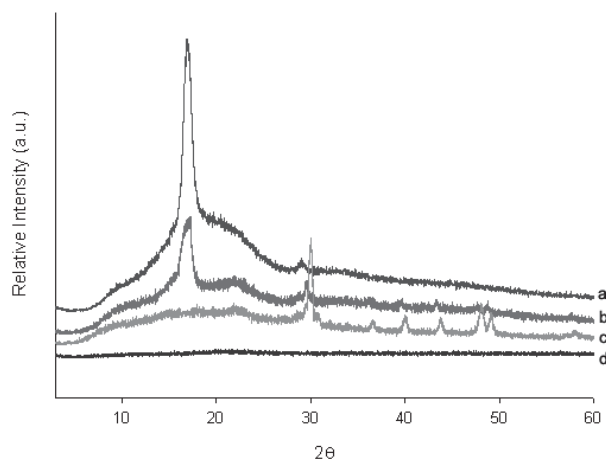


Figure 29. XRD patterns of (a) extruded sheet PLA, (b) 5 wt% Nano-CaCO₃-1041-PLA sheet, (c) 20 wt% Nano-CaCO₃-1041-PLA sheet and (d) melt-pressed PLA sheet.

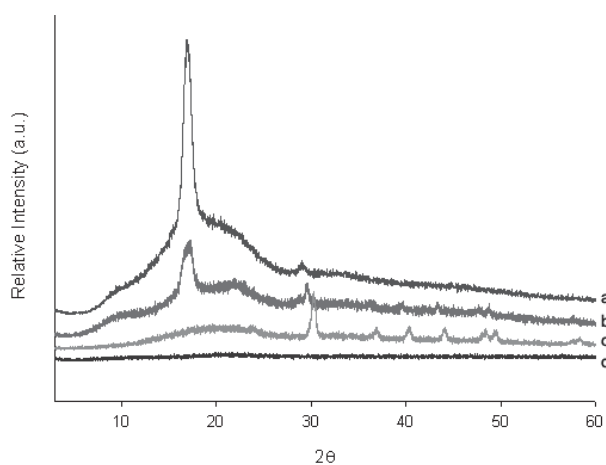


Figure 30. XRD patterns of (a) extruded sheet PLA, (b) 5 wt% Nano-CaCO₃-280-PLA sheet, (c) 20 wt% Nano-CaCO₃-280-PLA sheet and (d) melt-pressed PLA sheet.

The crystalline PLA showed the broad peak between $2\theta \approx 6^\circ$ to $2\theta \approx 30^\circ$ and the characteristic peak of PLA extrusion sheet was illustrated at $2\theta \approx 17^\circ$. However, there was no characteristic XRD pattern of melt-pressed PLA sheet. These mean that there were crystallization of PLA and PLA biocomposites during the extrusion sheet process. When the loading of CaCO_3 increased the characteristic of CaCO_3 in CaCO_3 -PLA biocomposites sheets were obviously more intense but the characteristic peak at $2\theta \approx 17^\circ$ was weaker. This evidence showed that the crystallization of PLA was decreased when the CaCO_3 were added into the biocomposites. Fatty acid coating on the CaCO_3 surface lowered crystallinity of PLA because it induced chain scission of PLA due to thermal degradation. The effect was clearly supported the decreasing of modulus in mechanical properties of the biocomposites as discussed previously.

To investigate phase morphology of CaCO_3 -PLA biocomposites, the fractured surface of the extrusion sheets were observed by SEM after being gold coated. As shown in Figure 31, agglomerated particles of both micro- and nano-sized CaCO_3 were broken down into small aggregates and single-particles after extrusion process. Therefore, CaCO_3 particles were well dispersed and distributed in PLA matrix. However, in the case of higher nano-sized CaCO_3 at higher loading, the SEM micrographs show the agglomeration of CaCO_3 particles in the polymer matrix. This could be the evidence to support the decreasing of energy to break in high-speed tensile test due to crack initiation as discussed previously.

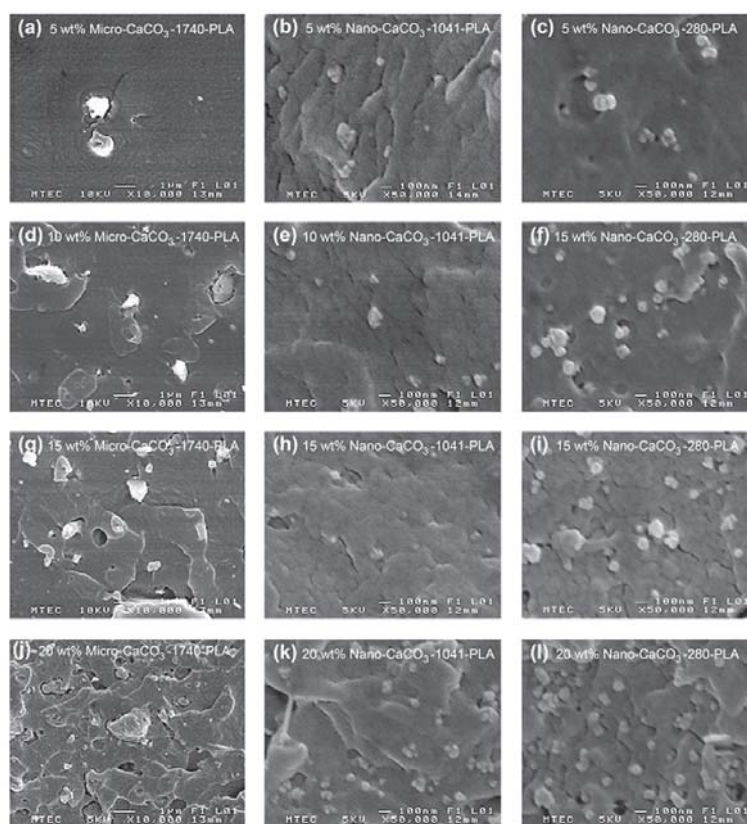


Figure 31. The distribution of CaCO_3 particles in the PLA matrix; Micro- CaCO_3 -1740 (10,000X) and Nano- CaCO_3 -1041 (50,000X) and Nano- CaCO_3 -280 (50,000X).

1.7 Rheology studies

In order to understand the melt behavior in the process, the rheology of materials was investigated in term of the relation of materials viscosity and shear rate. The rheological behavior of CaCO₃-PLA biocomposites was characterized by melt flow indexer. The melt flow index (170°C/2.16 kg) values of neat PLA before and after processing are 2.50 and 4.07 g/10 min, respectively. The viscosity of neat PLA after melt processing decreased significantly. The decrease of viscosity was due to PLA was melted in high temperature and high shear rate, causing chain scission and lowering its molecular weight.

When incorporating PLA with CaCO₃, the nano-size CaCO₃ had profound effect on melt viscosity more than the micro-size CaCO₃ did. As shown in Figure 32, the melt flow index indicated that viscosity of PLA biocomposite decreased with respect to CaCO₃ loading. Decrease of viscosity when adding micro- or nano-sized CaCO₃ in PLA would be attributed from characteristics of CaCO₃ particles in the polymer matrix. As seen in SEM images, the single particle of CaCO₃ and their particle agglomeration was sphere-like and rigid, which would lubricate PLA polymeric chains during flow. Moreover, the fatty acid sizing agents coated on CaCO₃ surface caused chain scission of PLA by thermal degradation and lowering its molecular weight. Therefore, MFI of PLA increased with respect to the decreasing of CaCO₃ particle size and increasing of CaCO₃ loading.

Eq. 3.1 predicts that a plot between $1/\log a_{MFI}$ and $1/\Phi$ should be linear, and the propriety of this experimental data [145].

$$\frac{1}{\log a_{MFI}} = -2.303f(T,0) + \frac{2.303f^2(T,0)}{b(T)} \frac{1}{\Phi} \quad \text{Eq. 3.1}$$

Where a_{MFI} is $MFI(T,0)/MFI(T, \Phi)$ and Φ is mass fraction of fillers.

Figure 33 shows the relation of $1/\log a_{MFI}$ and $1/\Phi$. It clearly shows that micro- and nano-sized CaCO₃ influenced biocomposite viscosity in different degree. Nano-sized CaCO₃ lowered the biocomposite viscosity than micro-sized CaCO₃ did. This is due to smaller size of sphere-like and rigid particle (as well as agglomerated particles) can lubricate the movement of polymer chain better during melt flow. It was also found that filler loading of micro-sized CaCO₃ affects the biocomposite viscosity more pronouncedly than those of nano-sized particles. Higher loading of micro-sized filler would create lubricating effect during flow.

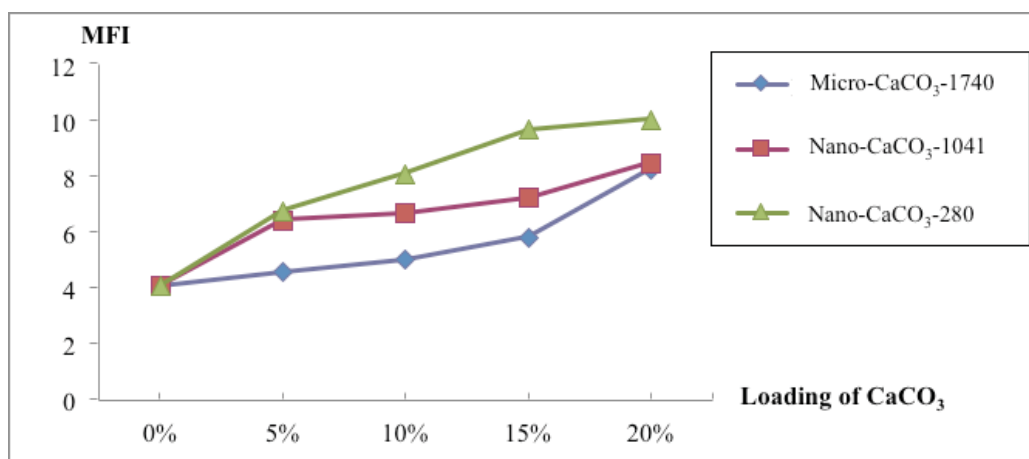


Figure 32. The melt flow index of pure PLA after extrusion process and those of micro- and nano-sized CaCO₃-PLA biocomposite sheet at 5-20 wt% loading of CaCO₃.

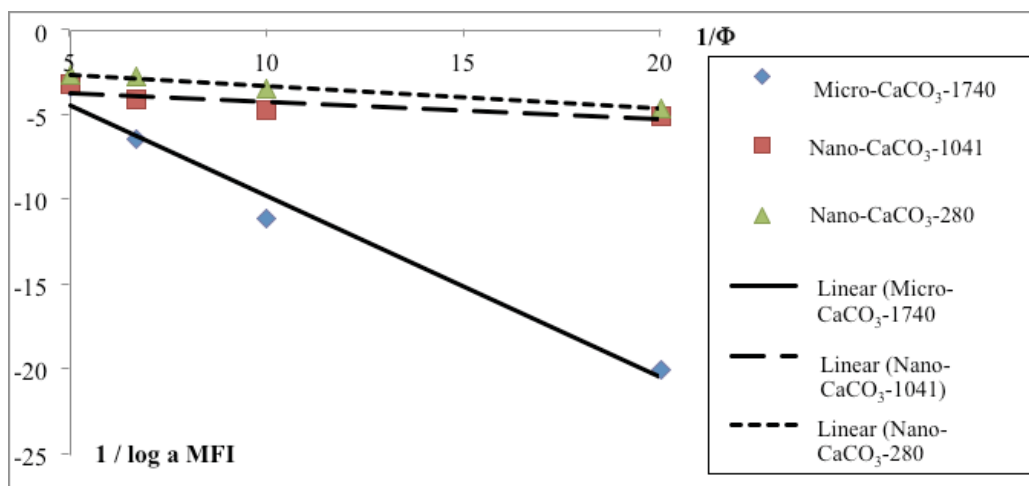


Figure 33. The melt flow index variation with filler loading fraction of micro- and nano-sized CaCO₃-PLA biocomposite sheet (170 °C and 2.16 kg test load condition).

The rotational rheometer (plate & plate rheometer) was used to investigate true viscosity of material at low shear rate. As seen in the Figure 34, shear viscosity of PLA biocomposites were relatively constant at low shear rate. Generally, viscosity of extruded PLA is lower than neat PLA because of the reduction of PLA molecular weight by thermal degradation during melt processing. The additions of CaCO₃ particles reduced the viscosity of PLA as lubricating effect and reduction of PLA molecular weight by transesterification with the presence of fatty acid. However, the opposite effect occurred when PLA was incorporated with high content of nano-sized CaCO₃. Viscosity of PLA nanocomposites was increased with the addition of Nano-CaCO₃-1041 loading over than 5 wt%, or the addition of Nano-CaCO₃-280 over than 15 wt%. This was due to agglomeration of small particles at high loading of nano-particle fillers in nanocomposite obstructed the flow.

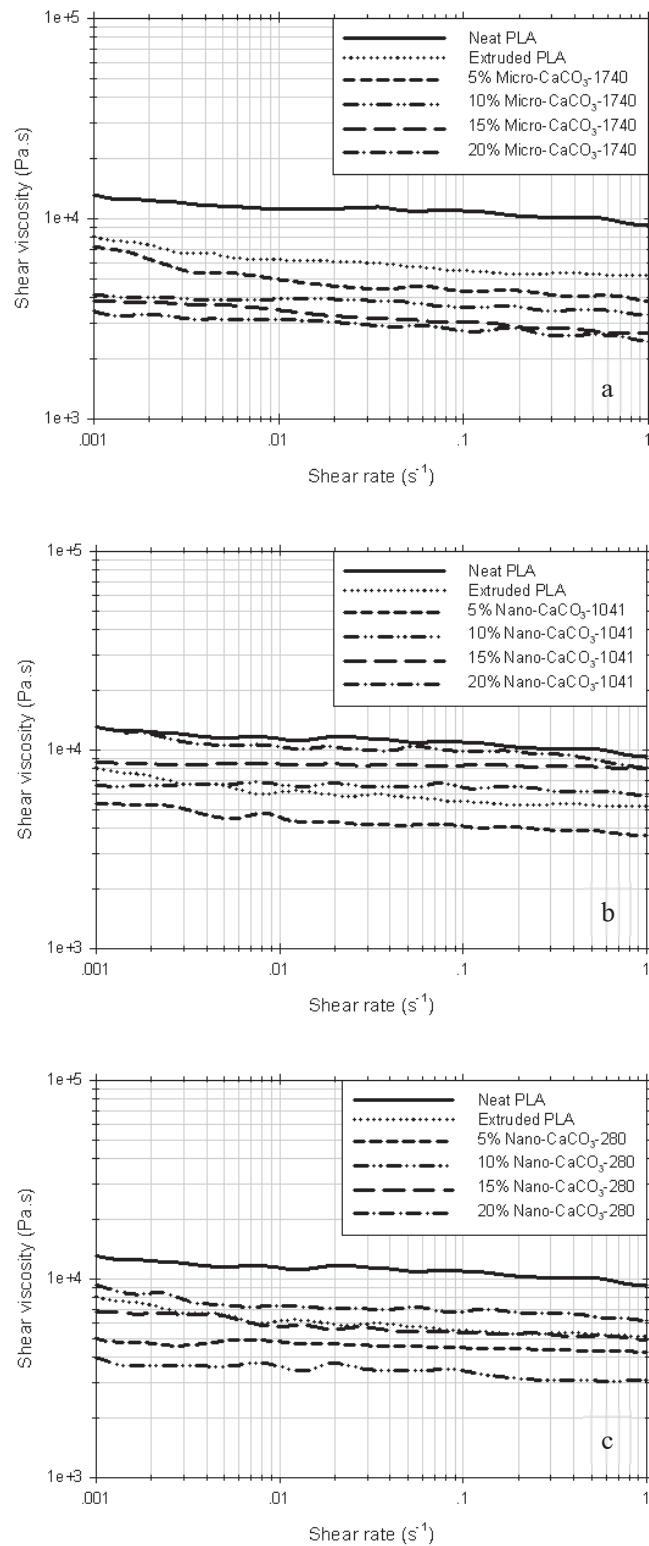


Figure 34. Viscosity properties of CaCO₃-PLA biocomposite at low shear rate; a) Micro-CaCO₃-1740-PLA biocomposite, b) Nano-CaCO₃-1041-PLA biocomposite and c) Nano-CaCO₃-280-PLA biocomposite.

Generally, polymers are fabricated at high shear rate melt processing. Capillary rheometer is typically used to investigate the melt properties in high shear rate range. For a given type and loading of CaCO₃ particles, Figure 35 shows that the shear stress of the melt increased with respect to increasing shear rate from 100 s⁻¹ to 2500 s⁻¹ in non-linear behavior. Viscosity of the micro-sized CaCO₃ biocomposites was higher than those of extruded PLA because of the obstacle from fillers during shear flow as observed in typical filled composites. Although adding nano-sized CaCO₃ into PLA increased shear viscosities marginally, incorporating nano-sized CaCO₃ with lower agglomeration into PLA, surprisingly reduced shear viscosity at low shear rate. Rigid fillers of CaCO₃ did not deform under stretching and hence exerted more resistance to flow deformation under extensional strain in a capillary rheometer. It was found that the micro-sized CaCO₃ obstructed movement of the polymer chains more than the nano-sized CaCO₃ did, even though PLA adding Nano-CaCO₃-1041 and Nano-CaCO₃-280 had higher number of particles than PLA adding Micro-CaCO₃-1740 at the same loading weight of CaCO₃. Thus, the nano-sized CaCO₃ presented profound lubricating effect. This was due to particle-particle interaction. It is expected that the lubricating effect of nano-particles on viscosity becomes more prominent with increasing loading of CaCO₃. This lubricating effect of spherical rigid particles was found in CaCO₃-PVC nanocomposite melts, reported by Xie et al [124]. In addition, Wang et al. observed the same result in the case of CaCO₃ filled polycarbonate. It was found that the shear viscosity of polycarbonate was decreased when increasing the CaCO₃ content in polycarbonate [146].

Moreover, there was high content of fatty acid at the high loading of CaCO₃. Mw of PLA tended to decrease with the increasing of fatty acid content and this reduction of molecular weight could be revealed via the reduction of CaCO₃-PLA biocomposite viscosity. This effect also enhanced the decreasing of viscosity of CaCO₃-PLA biocomposites at high content of fillers.

In this research, when nano-sized CaCO₃ re-agglomerated at higher loading, the longer distance between agglomerate particles caused less lubricating effect and hindered the movement of polymer chains. Thus, viscosity of PLA with 20 wt% Nano-CaCO₃-1041 was nearly the same value as that of PLA with 10 wt% Nano-CaCO₃-1041. Osman and Atallah also reported that higher viscosity of the nanocomposites was due to the presence of more agglomerates and aggregates in polymer matrix [121].

In order to compare rheological behavior of the unfilled and filled PLA melts under steady shear, the data were fitted to the well-known power law model (eq. 3.2). This model is used extensively to describe the flow properties of non-Newtonian liquids in theoretical analysis as well as in practical engineering applications [121,124,125,147].

$$\eta = k\dot{\gamma}^{n-1} \quad \text{Eq. 3.2}$$

where η is shear viscosity, k is a constant, $\dot{\gamma}$ is shear rate and n is the power law index.

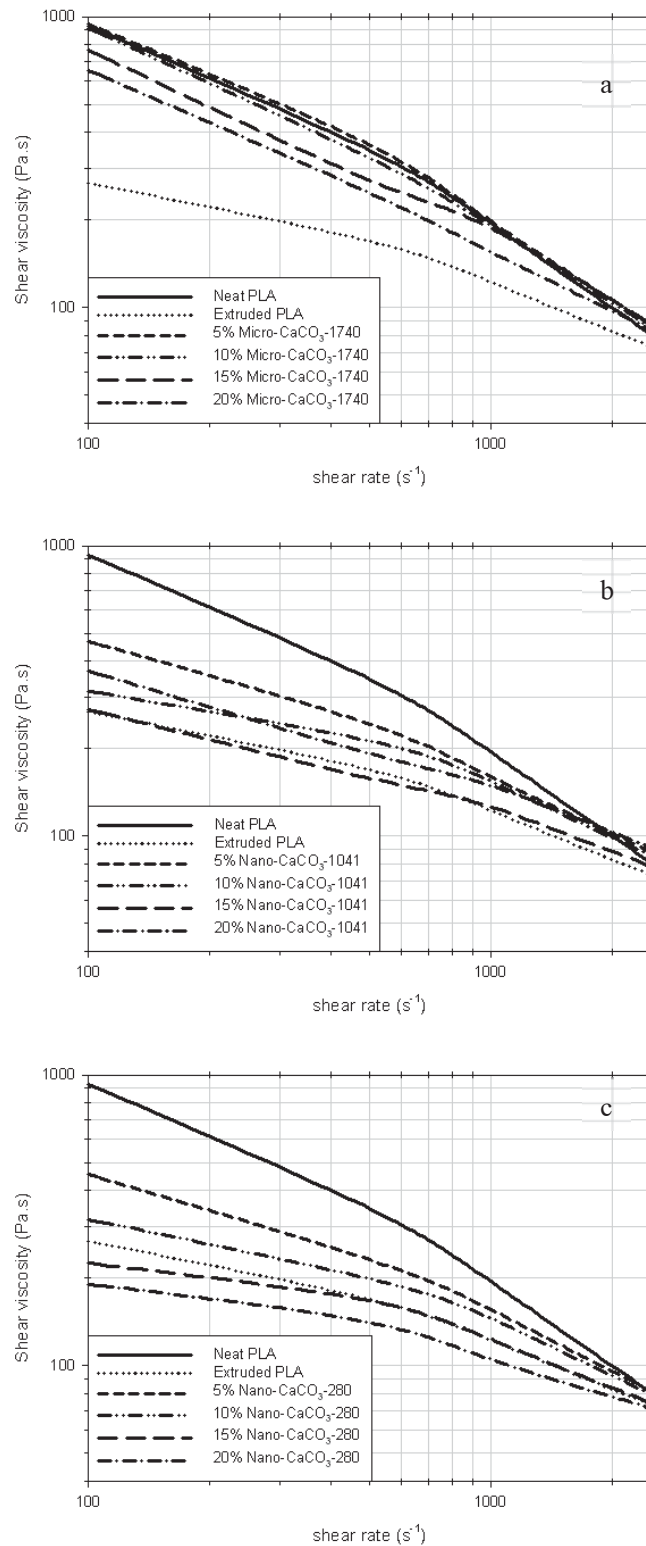


Figure 35. Viscosity properties of CaCO₃-PLA biocomposite at high shear rate; a) Micro-CaCO₃-1740-PLA biocomposite, b) Nano-CaCO₃-1041-PLA biocomposite and c) Nano-CaCO₃-280-PLA biocomposite.

When shear viscosity and true shear rate of the melt are plotted in log scale, the slope of the graph relates to the power law index (n), which $n < 1$ indicates pseudoplastic behavior (or shear thinning) of the melt. Figure 35 shows that plots of shear viscosity of filled PLA melts were not linear in the full range of shear rates, thus the slopes of graph were separated into 2 steps; the range of low shear rate of $100\text{-}500\text{ s}^{-1}$ and that of high shear rate $500\text{-}2500\text{ s}^{-1}$.

Extruded PLA had the power law index higher than neat PLA at both low and high shear rate ranges. When power law index is closed to 1, it means that polymer melt viscosity is less sensitive to shear rate. It is clearly seen that viscosity of extruded PLA decreased tremendously because of thermal degradation [71] causing polymer chains to be shorter and less entanglement during shear flow. At low particle loading, micro-sized CaCO_3 increased shear sensitivity of filled PLA biocomposites more than nano-sized ones since agglomerate could be broken from shear stress. In contrast, high loading of nano-sized CaCO_3 with less agglomeration (Nano- $\text{CaCO}_3\text{-}280$) reduced shear sensitivity of extruded PLA in addition to its lubricating effect and the reduction of PLA molecular weight due to fatty acid coating as discussed earlier.

2. Phase II: The effect of plasticizers on the $\text{CaCO}_3\text{-PLA}$ nanocomposites

One important requirement for packaging materials is high flexibility at room temperature during storage time. However, PLA is comparatively brittle and stiff at room temperature so modification by adding plasticizers is needed for PLA in order to apply it for flexible-desired applications such as food packaging. Plasticizers are materials used in polymer to reduce T_g of materials. Some researches have shown that addition of plasticizers such as polyethylene glycol (PEG), glucosemonoesters, and partial fatty acid esters had successfully improved the brittleness and widen applications of PLA [108,110]. Tributyl citrate is also used as a plasticizer for bioplastics such as PLA. Ljungberg and Wesslén showed that tributyl citrate oligomeric plasticizers drastically lowered the T_g of PLA, thus creating homogeneous and flexible materials. Tributyl citrate plasticizers, even at low molecular weight, had plasticizing effect as same as PEG did [35]. Although as shown in phase I, adding of super fine nano-sized CaCO_3 (Nano- $\text{CaCO}_3\text{-}280$) into PLA reduced mechanical properties due to the induction of thermal degradation of PLA but it could improve processability of this commercialized biopolymer by lowering T_{cc} to around 105°C , resulting in maintaining melt strength of the biocomposite throughout the casting rolls. Thus, in phase II, the effects of two plasticizers, polyethylene glycol (PEG) and tributyl citrate (TbC), on properties of $\text{CaCO}_3\text{-PLA}$ nanocomposite were investigated, used only Nano- $\text{CaCO}_3\text{-}280$ particles at 5 wt%.

2.1 Thermal stability studies

Thermal stability of PLA and $\text{CaCO}_3\text{-PLA}$ nanocomposites with and without plasticizers were also tested in this phase of research. TGA curves are showed in Figure 36 and the onset of degradation temperature (T_{onset}), degradation temperature (T_d), and the end of degradation (T_{end}) are reported in Table 24.

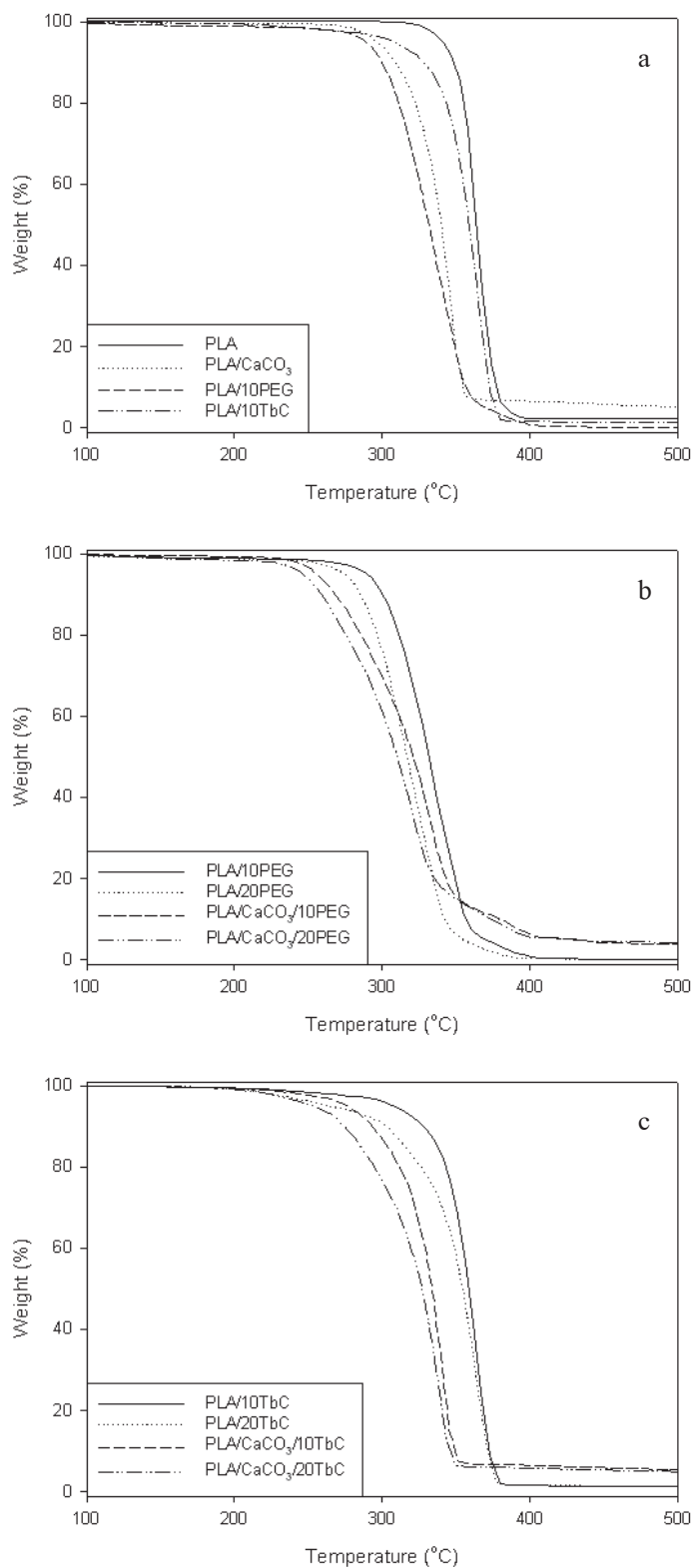


Figure 36. TGA curves of a) Neat PLA, 5 wt% CaCO₃-PLA nanocomposite and plasticized CaCO₃-PLA nanocomposite, b) PEG plasticized PLA and plasticized CaCO₃-PLA nanocomposite, c) TbC plasticized PLA and plasticized CaCO₃-PLA nanocomposite.

In Figure 36a, TGA curve shows that thermal stability of CaCO₃-PLA nanocomposite was lower than that of neat PLA. The addition of plasticizers induced PLA to degrade at lower temperature. PEG plasticized PLA had lower thermal stability compared to TbC plasticized PLA. D'Antone et al. also found that T_d of PLA-PEG block copolymer decreased with the length of the PEG blocks [148]. This indicated that PEG could induce the degradation of PLA by reducing PLA molecular weight via transesterification during the melt process.

Table 24. Thermal stability analysis of the unfilled and filled PLA nanocomposite without and with PEG/TbC plasticizers.

Materials	T _{onset} (°C)	T _d (°C)	T _{endset} (°C)
PLA	351.61	366.67	376.56
PLA/CaCO ₃	320.64	341.60	357.56
PLA/10PEG	306.86	338.84	357.81
PLA/20PEG	292.62	321.69	338.29
PLA/CaCO ₃ /10PEG	291.74	331.61	351.73
PLA/CaCO ₃ /20PEG	278.56	320.64	342.24
PLA/10TbC	344.09	365.58	375.04
PLA/20TbC	335.49	364.20	374.35
PLA/CaCO ₃ /10TbC	319.46	342.07	348.53
PLA/CaCO ₃ /20TbC	310.53	339.68	346.21

The molecular weight of neat PLA, extruded PLA and plasticized PLA as shown in Table 25 were determined by Gel Permeation Chromatography (GPC). It was found that the Mw of PLA decreased due to thermal degradation of PLA after melt process. The addition of PEG reduced Mw of PLA from 1.6×10^5 to 7.4×10^4 and Mn of PLA from 7.5×10^4 to 3.7×10^4 . The large reduction of molecular weight was occurred via transesterification reaction. Moreover, it was also observed by Essa et al. that Mw of PEG-graft-PLA decreased from 56,171 (neat PLA) to 8,392 [149].

In addition, GPC result shows that TbC plasticizer could also reduce the Mw of PLA from 1.6×10^5 to 1.3×10^5 and Mn of PLA from 7.5×10^4 to 5.9×10^4 . Transesterification could also occur as it occurred in PEG case. In the contrast, TbC is a branch molecule while PEG is a linear molecule. Ljungberg and Wesslén explained that the tertiary hydroxyl group on TbC would be quite unreactive and not participate in the transesterification reaction. They reported that out of the three ester groups present in TbC, two would be transesterified and the third one would be less reactive because of sterical hindrance after the first two ester groups reacted. However, the tertiary OH-group as well as the third ester group would have participated in the reaction to some extent, causing uncontrolled branching and increasing of molecular weight [35]. This reason could explain why Mw of TbC plasticized PLA was reduced less than those with

PEG plasticizer. Furthermore, TbC could induce the entanglement of PLA, thus TbC plasticized PLA had a higher viscosity than PEG plasticized PLA.

Table 25. Molecular weight determination of PLA and plasticized PLA.

Type	Mn	Mw	Mz	PDI
PLA pellet	8.2×10^4	1.7×10^5	3.0×10^5	2.0
Extruded PLA	7.5×10^4	1.6×10^5	3.1×10^5	2.1
PLA/10PEG	3.7×10^4	7.4×10^4	1.2×10^5	2.0
PLA/10TbC	5.9×10^4	1.3×10^5	2.2×10^5	2.1

The results in Figure 36b and 36c show that the incorporation of nano-sized CaCO_3 with plasticizers dramatically reduced thermal stability of PLA more than the addition of solely plasticizer into PLA. This results from the synergistic effect of chemical reaction of sizing agent and the transesterification of plasticizers on PLA molecules. As agreement with GPC analysis, molecular weight of PLA decreased dramatically when PEG/TbC plasticizers and nano-sized CaCO_3 were incorporated into PLA. Figure 37 presents TGA curve of nano-sized CaCO_3 (Nano- CaCO_3 -280 particles) showing the amount of fatty acid coated on the nano-sized CaCO_3 surface was about 4.2%. It began to degrade at low temperature (about 250°C), resulting in lower thermal stability of plasticized CaCO_3 -PLA nanocomposite than neat PLA and plasticized PLA.

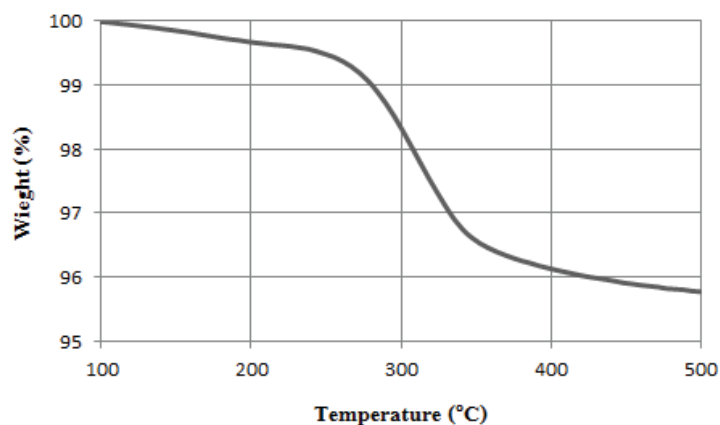


Figure 37. TGA curve of CaCO_3 nano-particles (Nano- CaCO_3 -280).

2.2 Thermal properties studies

Thermal properties of unfilled and filled PLA nanocomposites without and with PEG/TbC plasticizers at 10 and 20 phr, were investigated by DSC analysis. The DSC thermograms (Exo.) of the nanocomposites are showed in Figure 38 and the glass transition temperature (T_g), melting temperature (T_m), co-crystallization (T_{cc}) and crystallization temperature (T_c) of the nanocomposites are reported in Table 26. It

was also found that PLA and PLA nanocomposites had one T_m in the first heating scan. However, in the second heating scan, both PLA and PLA nanocomposites showed two T_m (with small split peak). In this phase, specimen preparation was fabricated by compression molding because CaCO_3 -PLA nanocomposites at high amount of plasticizers was difficult to handle by extrusion sheet process. The poor orientation of PLA polymer chains by this compression molding process caused one broad T_m about 150 °C in the first heating scan.

The addition of nano-sized CaCO_3 had potential to lower T_{cc} of PLA as also seen in phase I because the presence of fatty acid on the CaCO_3 surface could accelerate chain scission of PLA. Thus, shorter polymer chains could re-orientate and crystallize easier. When PEG/TbC plasticizer was incorporated into PLA, T_{cc} was dramatically reduced because plasticizers could enhance the movement of PLA polymer chains to fold and crystallize. It was reported that the crystallization rate of PLA was very slow [108]. It is interesting that the T_c peak for PLA appeared during cooling only in PEG plasticized CaCO_3 -PLA nanocomposite. Moreover, T_{cc} of PLA decreased dramatically with the addition of PEG plasticizer. These were due to plasticized effect on the mobility of PLA macromolecules and the low molecular weight of PLA in the presence of this plasticizer and fatty acid coated CaCO_3 . This enhancement of the PLA molecular mobility is claimed to be the major factor acting on the crystallization kinetic of this polymer [34].

It can be seen from Table 26 that the T_g of PLA had dropped dramatically with respect to the amount of plasticizers. Many research also found the same effect in various polymers [150-153]. This was due to better mobility of PLA molecules when it was plasticized. Moreover, molecular weight of PLA was decreased when PEG and TbC plasticizers were incorporated due to transesterification with PLA. The short chains of PLA could be vibrated and rotated easier than long chains of PLA, resulting in the large reduction of T_g .

The results show that T_m of plasticized PLA had the shoulder peak in the first heating scan and double peaks in the second heating scan. This resulted from the incorporation of plasticizers into PLA, made PLA crystallize easier. Nevertheless, due to specimen prepared by compression molding, some crystals of plasticized PLA were not completely formed or different crystal structures were present resulting in the presence of shoulder of T_m peak and another small peak at lower melting temperature. Furthermore, the unfavorable transesterification of both plasticizers reduced T_m of PLA and CaCO_3 -PLA nanocomposite obviously and T_m of PLA and CaCO_3 -PLA nanocomposite was decreased with respect to amount of plasticizers. This was due to the reduction in molecular weight of plasticized PLA, which made lower crystallinity of PLA.

It was found that the additions of 20 phr of plasticizers could reduce T_m of PLA to about 5 °C implying that PLA was subjected to thermal degradation. In addition, the results show that T_g , T_{cc} and T_m of PLA were dropped dramatically when plasticizers and nano-sized CaCO_3 were both incorporated. This was the synergist effect of fatty acid coated on CaCO_3 surface and the effect of plasticizers on chain scission of PLA. Moreover, plasticizers could enhance the movement of PLA polymer chains as well as the short chains of degraded PLA could move easily resulting in the sharp decrease of T_g , T_{cc} and T_m of PLA.

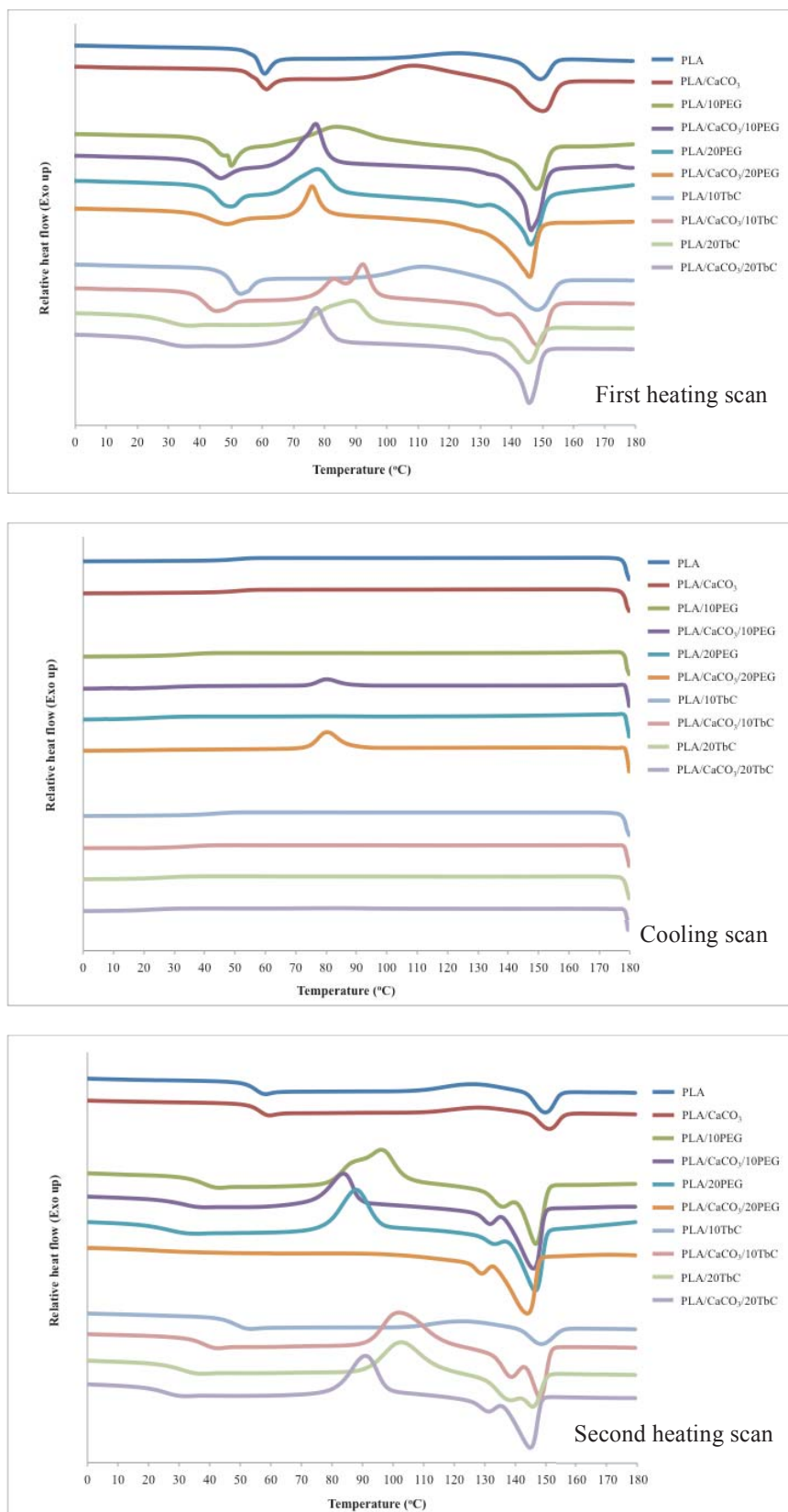


Figure 38. DSC thermograms of plasticized CaCO₃-PLA nanocomposites.

Table 26. Thermal properties of plasticized CaCO₃-PLA nanocomposites.

Materials	First heating scan				Cooling scan	Second heating scan				
	T _g (°C)	T _{cc} (°C)	T _m (°C)			T _c (°C)	T _g (°C)	T _{cc} (°C)	T _m (°C)	
			Peak 1	Peak 2					Peak 1	Peak 2
PLA	56.16	123.07	-	149.13	-	56.01	126.14	-	149.9	
PLA/CaCO ₃	55.75	109.10	-	150.09	-	55.07	125.97	-	150.22	
PLA/10PEG	43.34	83.79	136 (shoulder)	148.25	-	36.54	95.99	135.83	146.54	
PLA/CaCO ₃ /10PEG	39.98	77.19	134 (shoulder)	146.29	81.63	28.61	83.66	131.65	145.82	
PLA/20PEG	42.13	77.80	129.84	146.20	-	24.52	87.84	133.18	146.37	
PLA/CaCO ₃ /20PEG	40.74	76.15	128 (shoulder)	145.99	80.42	23.13	-	128.99	143.68	
PLA/10TbC	47.44	111.92	-	148.42	-	47.20	122.73	-	148.48	
PLA/CaCO ₃ /10TbC	38.50	92.34 (shoulder)	136.20	148.28	-	36.53	101.83	138.49	147.93	
PLA/20TbC	27.35	88.80	133 (shoulder)	145.57	-	27.13	102.48	138.29	145.59	
PLA/CaCO ₃ /20TbC	25.50	77.51	130 (shoulder)	145.83	-	22.06	90.84	131.16	144.69	

2.3 Mechanical properties studies

The mechanical properties of the CaCO₃-PLA nanocomposites were performed by tensile test and Izod impact test, which were carried out according to the ASTM D638 and ASTM D256 standard, respectively. Figure 39a and 39b reveal the tensile properties of unfilled and filled nanocomposites without and with PEG/TbC plasticizer at 10 and 20 phr. The results show that elastic modulus of PLA was not improved by the incorporation of nano-sized CaCO₃ due to the effect of fatty acid coating as discussed earlier. The addition of plasticizers further decreased elastic modulus of PLA because of transesterification, causing lower molecular weight of PLA. Interestingly, elastic modulus of 20 phr TbC plasticized PLA nanocomposite decreased dramatically.

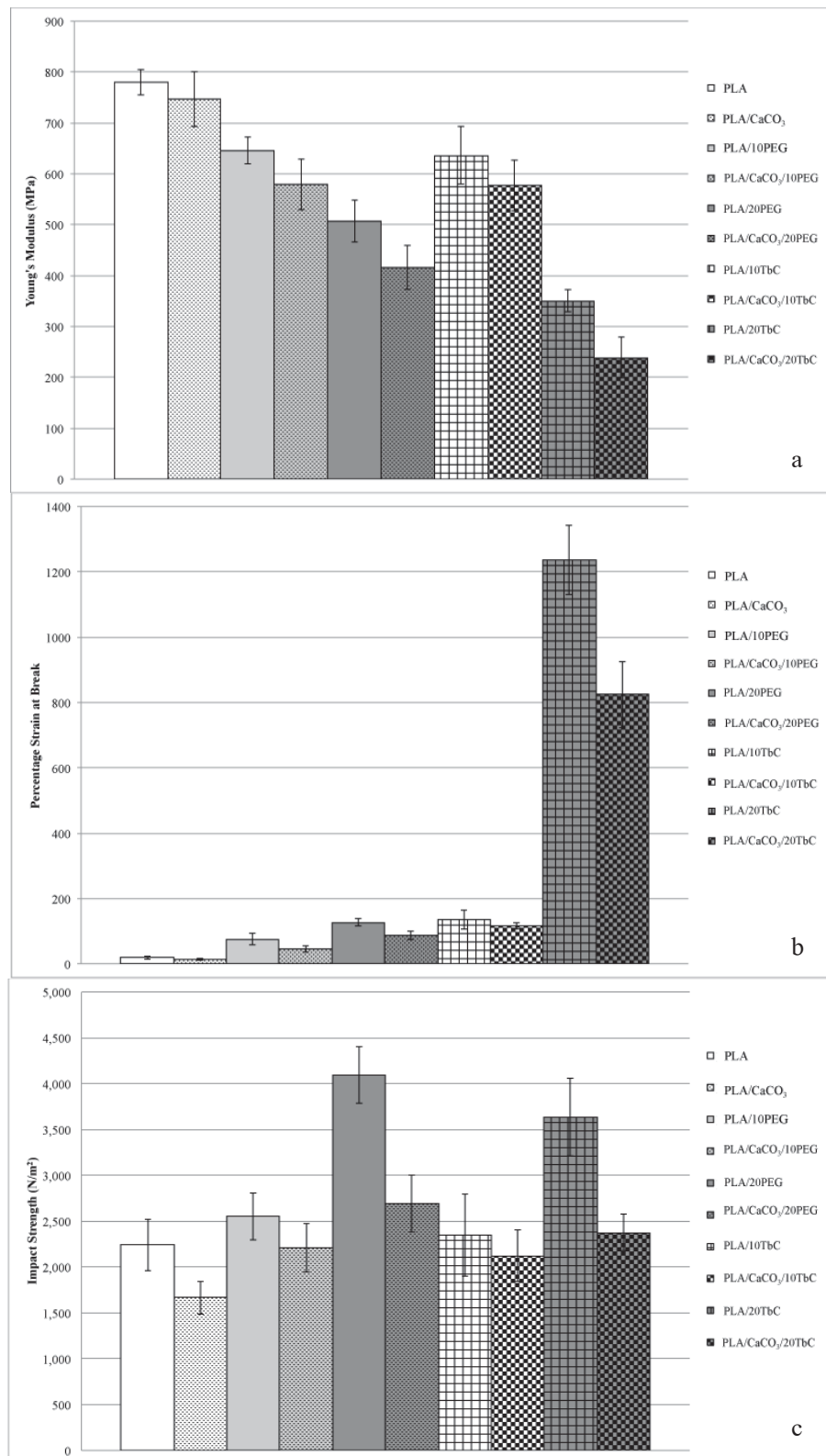


Figure 39. Mechanical properties of PLA, PLA nanocomposite and plasticized PLA nanocomposite; a) Young's modulus, b) Percentage of strain and c) Impact Strength.

In the presence of nano-sized CaCO_3 , the decrease of percentage of strain at break of PLA demonstrated that this filler induced a definite decrease in elongation [33]. However, plasticizers could toughen neat PLA and CaCO_3 -PLA nanocomposites. The addition of plasticizers increased percentage of strain at break largely when compared to neat PLA and un-plasticized PLA nanocomposites. The decreasing of Young's modulus and increasing of percentage of strain was performed by the plasticizing effect and also the reduction of PLA molecular weight because of transesterification with these plasticizers. From the plasticizing effect, the small molecules of plasticizers penetrated into the polymer matrix and reduced the intermolecular force between the polymer chains. PEG has chemical linkage as ether linkage and and TbC has chemical linkage as ester linkage in their molecule. Both functional groups of linkage are compatible with the ester linkage in PLA polymer chain. Therefore, they can enhance the mobility of PLA polymer chains when subjected to load. The results from this study implied that TbC had more effect on molecular mobility of PLA when compared to PEG. This was due to the differences of chemical structure of the type of linkage, the molecular weight and structure of molecule of these plasticizers. TbC had ester linkage as same as PLA, therefore it was compatible with PLA polymer chains more than PEG was. The solubility parameter of PLA and both plasticizers are shown in Table 27. TbC and PLA have similar solubility parameters, which indicated that they should be miscible and therefore that TbC is efficient as plasticizer for PLA. In addition, the branch molecular structure of TbC kept further distance between PLA polymer chains than that linear structure of PEG did. Moreover, it could induce some entanglement between PLA polymer chains causing the high performance of the enhancing in elongation at break when the high content of TbC was incorporated.

Table 27. Solubility parameters (δ) for PLA and PEG/TbC plasticizers [34,35].

Type	Solubility parameter, δ (J.cm^{-3}) ^{1/2}
PLA	20.1
PEG	23.5
TbC	19.6

The decrease in notched impact strength of CaCO_3 -PLA nanocomposites as shown in Figure 39c proved that CaCO_3 acted as stress concentrator to promote crack initiation. It can be seen that nano-sized CaCO_3 reduced the impact strength of neat PLA to about 0.75 times. This might cause from some coarse morphologies of smaller particle sizes ($< 0.7 \mu\text{m}$) lowered the toughening efficiency [27]. However, the impact resistance of CaCO_3 -PLA nanocomposites was improved by the addition of plasticizers. The increasing content of plasticizer in PLA and CaCO_3 -PLA nanocomposite increased their impact resistance. It was found that adding 20 phr of these two plasticizers improved impact strength of PLA to over 1.5 times, compared to neat PLA. The incorporation of plasticizer into the brittle CaCO_3 -PLA nanocomposite could improve its flexibility obviously.

2.4 Dynamic mechanical properties studies

Figure 40 shows the dynamic mechanical analysis results of plasticized CaCO₃-PLA nanocomposites over a temperature range of 25-160 °C. Figure 40a shows the E' of the nanocomposites as a function of temperature. It can be seen that the E' of the nanocomposites were slightly dropped as the temperature increased from 25 to 50 °C. Subsequently, the E' dropped rapidly designated at their T_g. The slightly increase in E' at the temperature above T_g was due to the co-crystallization of PLA matrix [35,66]. This situation can also be observed and discussed as in phase I. Additionally, from Figure 40a, the incorporation of nano-sized CaCO₃ particles in the nanocomposites resulted in the reduction of the E', but did not affect T_g of PLA. This was due to lubricating effect of fatty acid sizing agent coated CaCO₃ surface [112]. Moreover, as discuss earlier in phase I, the fatty acid coated CaCO₃ surface induced thermal degradation of PLA. Furthermore, the growth of spherulitic structure might be obstructed by the CaCO₃ nano-particles. As large spherulites are believed to have a much higher load-bearing capability as mention in the study of Chan et al. and Way et al [120,154]. A decrease in the spherulite size and crystallinity decreased the modulus of polymer. Moreover, the additions of plasticizer into the nanocomposites reduce storage modulus in agreement with the results on decreasing of tensile modulus as discussed earlier.

Figure 40b and 40c show tan δ of the nanocomposites as a function of temperature. The addition of only CaCO₃ nano-particles did not affect T_g of PLA. However, when PEG/TbC plasticizer was blended into PLA, T_g of all samples was dropped significantly with respect to the amount of plasticizers. Other research attributed that the plasticizer can enhance the mobility of PLA polymer chains at low temperature [35,108]. Moreover, the short chains of degraded PLA in the presence of PEG/TbC plasticizer could move easier than those long chains of neat PLA supporting in the reduction of T_g of PLA. In addition, the incorporation of CaCO₃ nano-particles and plasticizers reduced T_g of PLA more than adding solely plasticizer. The large reducing of T_g of plasticized CaCO₃-PLA nanocomposite was expected from prompting synergism of plasticizing effect of plasticizer and reduction of molecular weight of PLA from transesterification with plasticizers and chain scission by the enhancement of fatty acid coated on CaCO₃. Fatty acid has the carbonyl groups in the molecule, which is similar to TbC plasticizer but differs from those PEG, which has ether linkage. Therefore, this could explain why synergism of TbC with nano-sized CaCO₃ filler was more dominant than PEG.

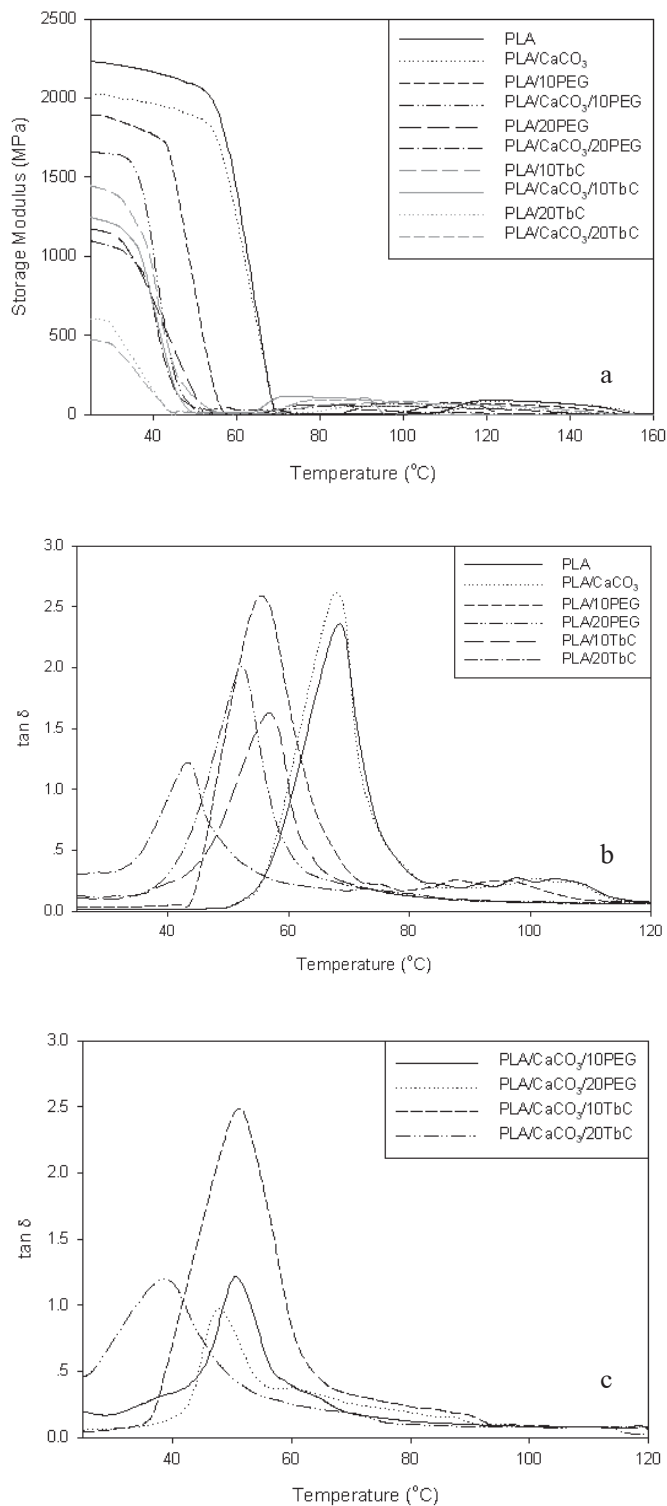


Figure 40. Dynamic mechanical properties of PLA, PLA nanocomposite and plasticized PLA nanocomposite; a) Storage modulus, b) $\tan \delta$ of PLA, CaCO₃-PLA nanocomposite and plasticized PLA and c) $\tan \delta$ of plasticized PLA nanocomposite.

2.5 Morphology studies

XRD results in Figure 41 show the crystallinity and crystal structure of PLA compared to CaCO₃-PLA nanocomposite with and without plasticizers. All XRD patterns did not show the sharp peak at 2 θ about 17° contrasted to the patterns seen in phase I. This was attributed to the different process of specimen preparation. The compression molding process was used to fabricate specimens in phase II. This result confirmed that the characteristic peak at 2 θ about 17° was the characteristic of crystal structure, which was developed by the drawing in casting rolls in extrusion sheet process, used in phase I. Figure 41 shows that the characteristic peaks of CaCO₃ were found in CaCO₃-PLA and plasticized CaCO₃-PLA nanocomposites. CaCO₃ reduced crystallinity of PLA as seen via the lower area of broad peak at 2 θ of about 20°. However, there was no shift of broad peak in CaCO₃-PLA nanocomposite, compared to neat PLA. This implied that CaCO₃ did not change the crystal structure of PLA.

In Figure 41a, there was no significant difference in the area of broad peak at 2 θ at about 20° implying the equivalence in crystallinity of PLA and 10 phr plasticized PLA. Furthermore, the same XRD pattern implied the same crystal structure of PLA and 10 phr plasticized PLA. Figure 41b and 41c showed that XRD of 10 phr PEG plasticized PLA and 20 phr PEG plasticized PLA were not different. This means that the increasing of PEG plasticizer content in PLA did not affect the crystallinity and crystal structure of PLA. Likewise, the XRD patterns in Figure 41c show that XRD of 10 phr TbC plasticized PLA and 20 phr TbC plasticized PLA were the same, implying that the crystallinity and crystal structure were not different.

However, incorporation of CaCO₃ and PEG plasticizer affected the crystallinity of PLA as shown in Figure 41b. The crystallinity of 10 phr PEG plasticized CaCO₃-PLA nanocomposite was lower than those of neat PLA and PEG plasticized PLA, but it was still higher than those of CaCO₃-PLA nanocomposite. This was due to the negative effect of fatty acid sizing agent that coated on CaCO₃ surface, induced chain scission of PLA resulting in the reduction of PLA crystallinity. However, the crystallinity of 20 phr PEG plasticized CaCO₃-PLA was higher than 10 phr PEG plasticized CaCO₃-PLA nanocomposite, since PLA and PEG are more compatible.

In the case of TbC plasticized CaCO₃-PLA nanocomposite as shown in Figure 41c, the crystallinity of TbC plasticized CaCO₃-PLA nanocomposites was at the same amount to those of neat PLA. However, the increasing of content of plasticizer had not much effect in crystallization of PLA. It was found that the crystallinity of 20 phr plasticized CaCO₃-PLA was the same range of those in PLA, plasticized PLA and 10 phr plasticized CaCO₃-PLA nanocomposite.

Figure 42 shows SEM micrographs of PLA and plasticized CaCO₃-PLA nanocomposite. It was found that nano-sized CaCO₃ were dispersed well by compounding in a twin-screw extruder and fabricated in a compression molding process. The smooth surface in Figure 42a showed that CaCO₃ was compatible with PLA matrix. In addition, there was no phase separation of plasticizers even in the high content of PEG and TbC plasticizer as 20 phr. Furthermore, the surface of plasticized CaCO₃-PLA nanocomposites was still smooth, showing the better compatibility of PLA and CaCO₃ due to plasticizers.

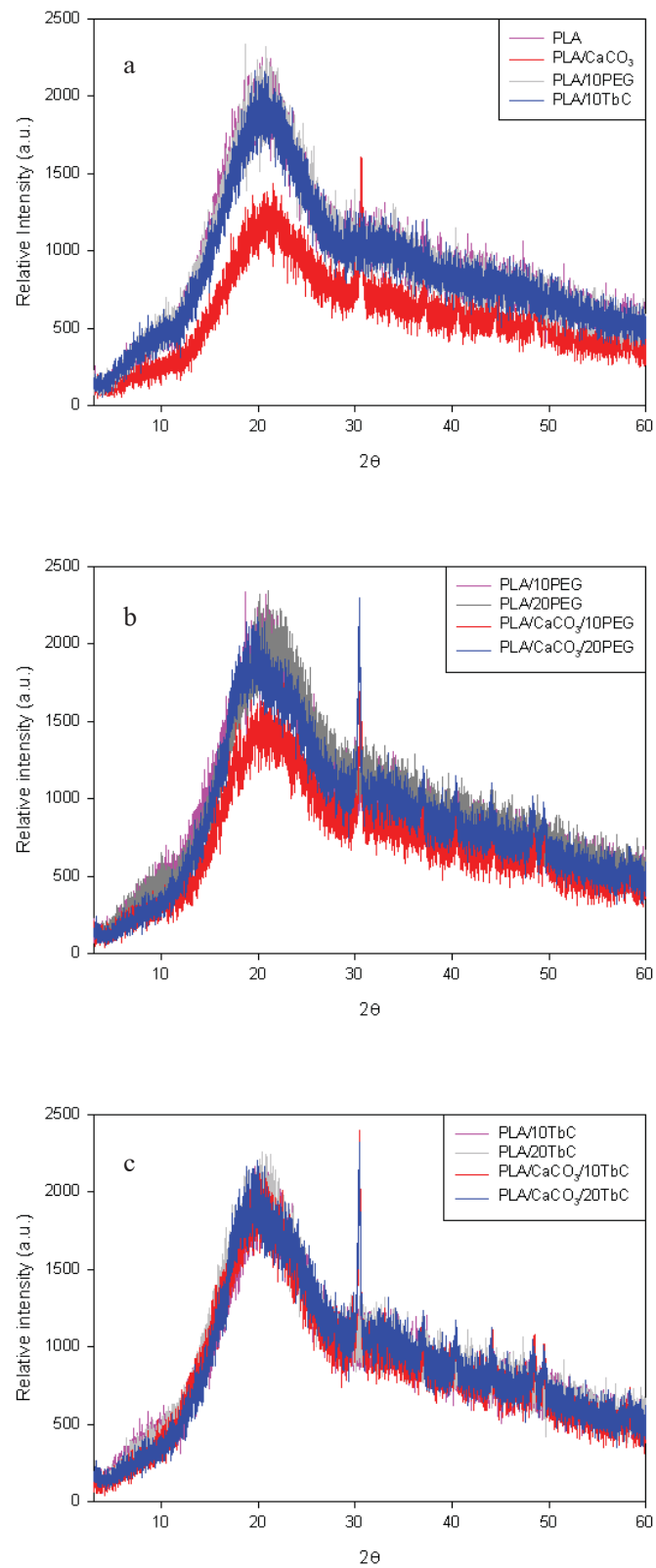


Figure 41. X-Ray diffraction pattern of PLA, CaCO₃-PLA nanocomposite and plasticized CaCO₃-PLA nanocomposite.

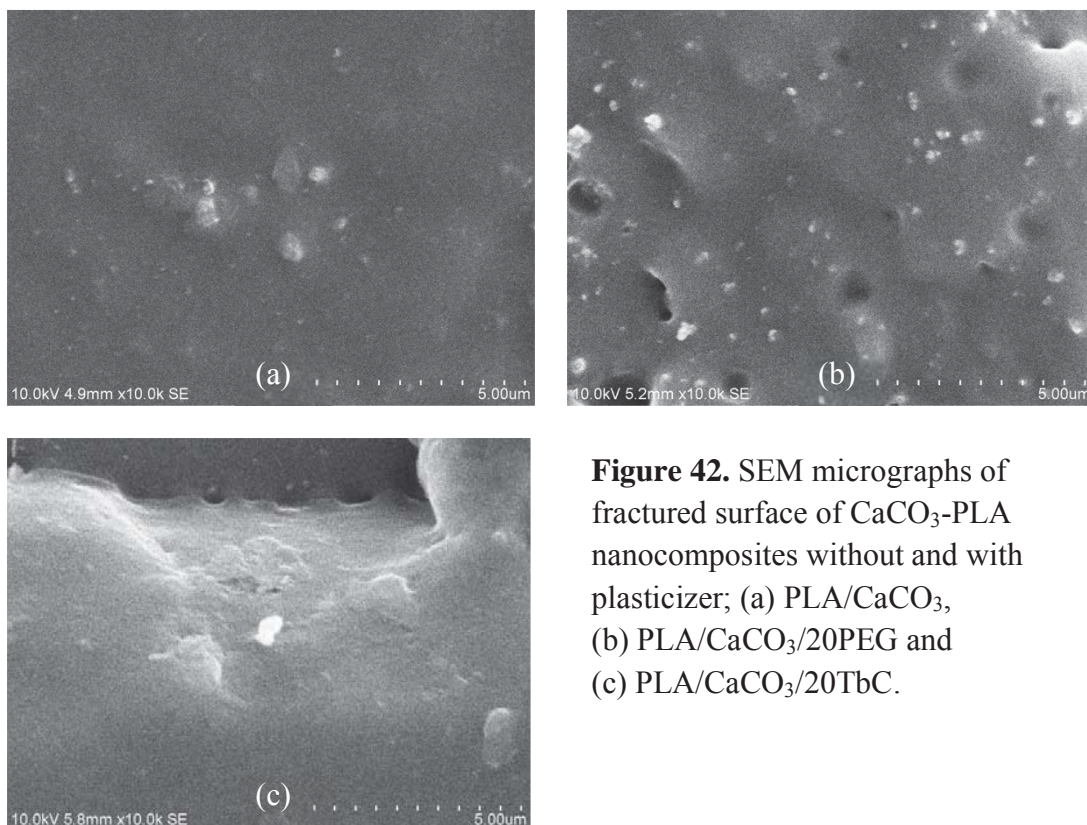


Figure 42. SEM micrographs of fractured surface of CaCO₃-PLA nanocomposites without and with plasticizer; (a) PLA/CaCO₃, (b) PLA/CaCO₃/20PEG and (c) PLA/CaCO₃/20TbC.

SEM micrographs of the fractured surface of impact tested specimen in Figure 43 show that the fracture behavior of CaCO₃-PLA nanocomposites changed from brittle to ductile behavior after incorporating with plasticizers. Fractured surface of neat PLA was smooth with local ductile breaking as craze and crack propagation occurred during the fast breaking. When CaCO₃ was added into polymer matrix, the fractured surface of CaCO₃-PLA was smooth as same as fractured surface of neat PLA. However, the local ductile breaking like fibril as seen in neat PLA fractured surface was not found. This implies that nano-sized CaCO₃ behaved as stress concentrators promoting crack initiation, and thus local ductile breaking diminished.

When plasticizers were blended into PLA, the CaCO₃-PLA nanocomposites were tougher and broken in favor of ductile failure. Stripes of locally extension in polymer matrix were presented in fractured surface of 10 phr plasticized PEG nanocomposite, and these stripes became more randomly distributed when adding 20 phr PEG. Meanwhile, fractured surface of TbC plasticized PLA nanocomposites were smoother comparing to PEG plasticized PLA. This was due to branch molecule of TbC induced PLA to be entangled with other molecules via transesterification reaction during the thermal process. And thus, when specimen was plunged by impact force, it was broken mainly in ductile behavior, even CaCO₃ nano-particles were added.

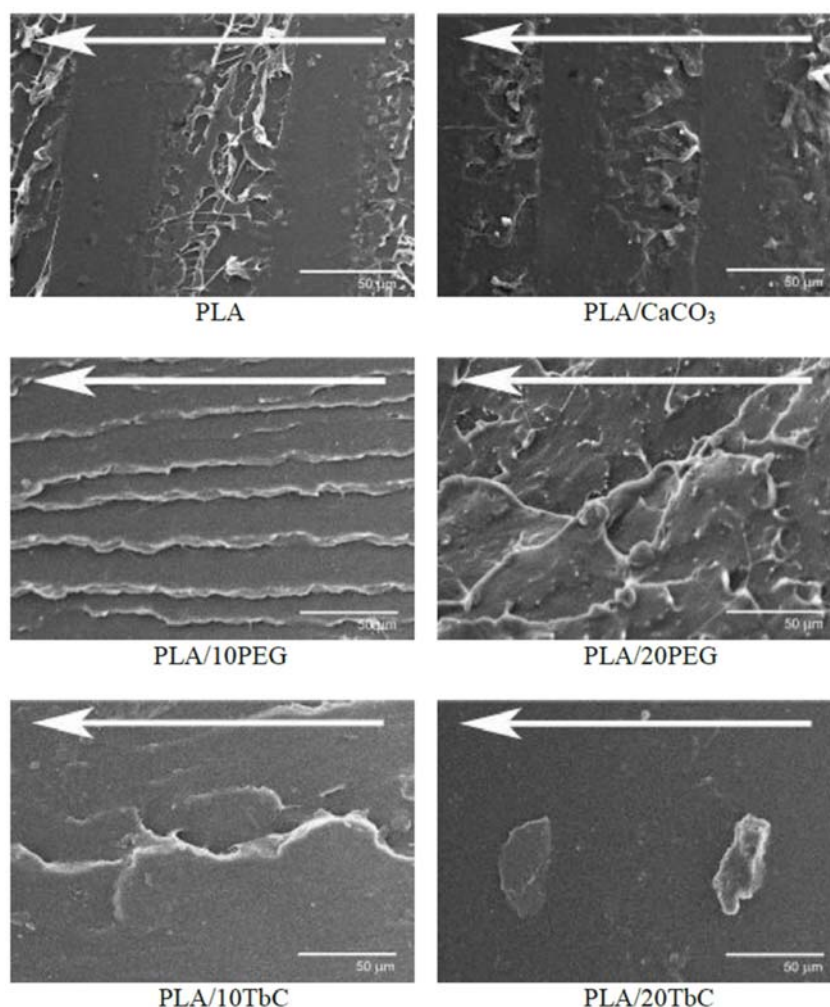


Figure 43. SEM micrographs of impact fractured specimen of PLA/CaCO₃/plasticizers nanocomposites. The white arrow indicates stress direction in the impact test.

2.6 Rheology studies

Melt viscosity of CaCO₃-PLA nanocomposites without and with PEG/TbC plasticizer of 10 and 20 phr was also investigated. However, in phase II, PLA and its nanocomposites were compounded in extrusion process and fabricated in compression molding process, giving them subjected to two-time thermal processes consecutively. The viscosity of PLA decreased from about 6×10^3 Pa.s to be about 2×10^3 Pa.s due to thermal history. Moreover, the addition of PEG plasticizer reduced PLA viscosity drastically due to acceleration of PLA thermal degradation. Since the viscosity was dramatically reduced, the capillary rheometer was not suitable to differentiate effect of plasticizer on PLA and its nanocomposites. The rotational rheometer was then employed for the rheology studies in phase II.

The viscosity of PLA and its nanocomposites at various shear rates are illustrated in Figure 44. The viscosity of CaCO₃-PLA nanocomposite was lower than PLA because the nano-sized CaCO₃ induced the lubricating effect and the reduction of PLA molecular weight due to fatty acid sizing agent as mention earlier in phase I.

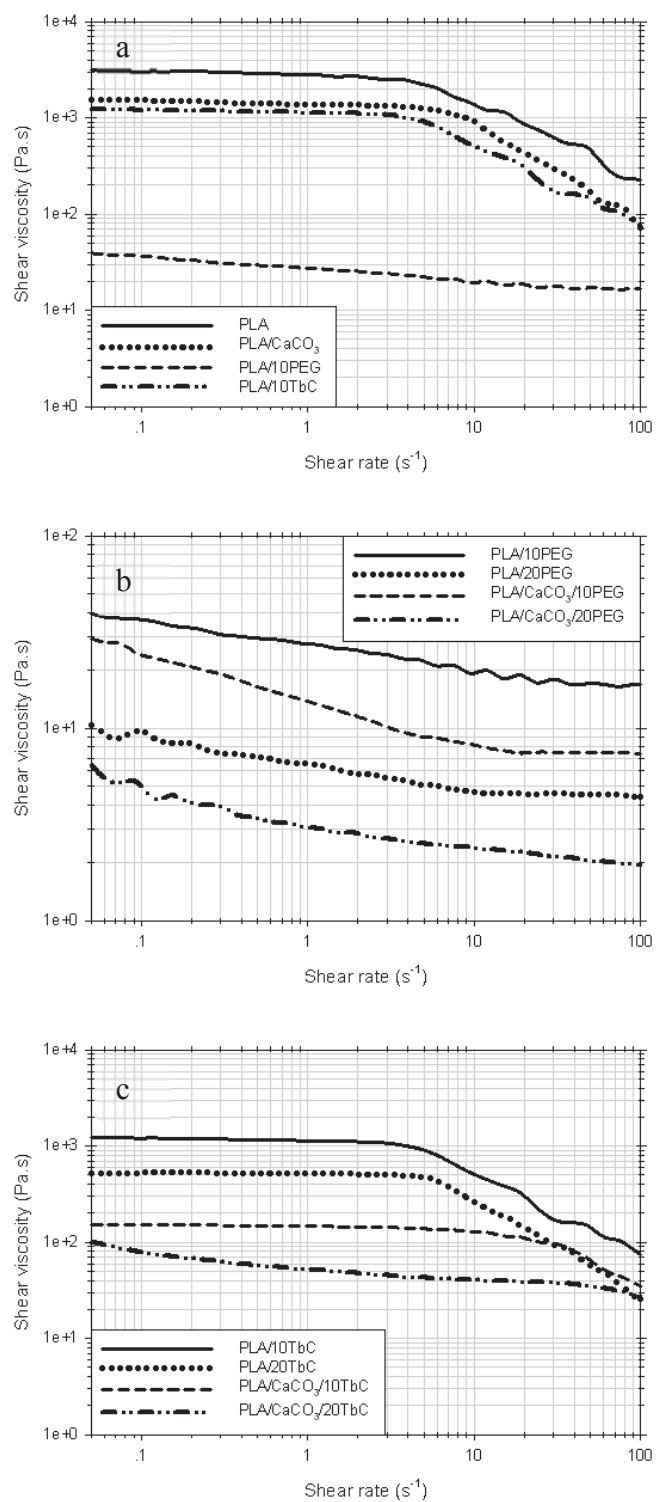


Figure 44. Viscosity properties at low shear rate range of a) Neat PLA, 5 wt% CaCO₃-PLA nanocomposite and plasticized CaCO₃-PLA nanocomposite, b) PEG plasticized PLA and plasticized CaCO₃-PLA nanocomposite, c) TbC plasticized PLA and plasticized CaCO₃-PLA nanocomposite.

As seen in Figure 44a, the addition of both PEG and TbC plasticizers reduced viscosity of neat PLA. Plasticizers penetrated into the PLA matrix, enhancing the chain mobility and flow. Furthermore, PEG plasticized PLA showed very low viscosity compared to TbC. This resulted from the addition of PEG reduced Mw of PLA due to transesterification, resulting in the decrease of melt viscosity of PEG plasticized PLA and the change in its melt rheology behavior. The large reduction of molecular weight occurred via transesterification reaction was also observed by Essa et al. They found that Mw of PEG-graft-PLA was 8,392 while Mw of their neat PLA was 56,171 [149]. The low Mw of PEG plasticized PLA can flow easier and the shear sensitivity was reduced. Thus, the incorporation of plasticizers and CaCO₃ enhanced the decreasing of viscosity of PLA due to the synergistic effect of the molecular weight reduction of PLA in the presence of fatty acid coated on CaCO₃ and transesterification with plasticizers as mention earlier as well as the plasticizing effect of plasticizers.

Transesterification reaction of TbC and PLA could occur as well as it occurred in PEG case. In contrast, the branch molecule of TbC could induce the entanglement of PLA polymer chain while the PEG did not. Therefore, viscosity of TbC plasticized PLA was slightly decreased, compared to PEG plasticized PLA. Figure 44b and 44c show that the viscosity of PLA decreased with respect to the content of PEG and TbC plasticizers, respectively. The higher content of plasticizers caused the lower viscosity of CaCO₃-PLA nanocomposites. Since TbC was a branch molecule, TbC-reacted PLA would entangle with the others, giving TbC slightly lowered shear viscosity. This caused the antagonism of thermal degradation effect due to fatty acid coated on CaCO₃ fillers and transesterification of TbC plasticizers on rheology behavior of CaCO₃-PLA nanocomposites.

3. Phase III: The effect of SiO₂ surface treatment on CaCO₃ nano-particles on PLA nanocomposite

The effects of particle size and loading of CaCO₃ on mechanical and thermal properties of PLA were investigated and reported in phase I. In addition, the effects of PEG and TbC plasticizers on mechanical and thermal properties of PLA and CaCO₃-PLA nanocomposites were investigated in phase II. Adding of micro-sized CaCO₃ could maintain viscosity of extruded PLA to be close to that of neat PLA, while adding of nano-sized CaCO₃ caused easier flow of PLA due to lubricating effect of spherical-like rigid particles. The addition of plasticizer into system promotes the chain flexibility and extends the ability to elongate before breaking. The plasticizer as PEG and TbC could improve mechanical properties of PLA, especially in tensile elongation at break and impact strength.

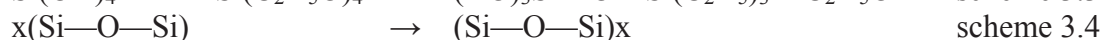
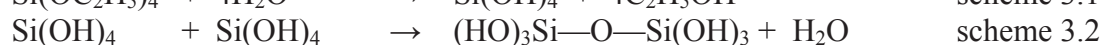
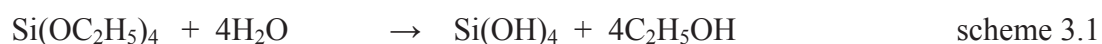
SiO₂ reinforcing filler is widely used in polymer composites. There are many publications that used silica nano-particles to improve mechanical properties and thermal properties of polymer. Ma et al. reported that the glass transition temperature of nano-sized SiO₂-polyacrylate was higher than that of neat polyacrylate [131]. Zhang et al. illustrated that the silane-modified kaolinite/silica core-shell nano-particles (SMKS) significantly improved mechanical properties of the poly(3-hydroxybutyrate-co-3-hydroxyhexanoate) (PHBHHx). The low loading of SMKs could increase the tensile strength and toughness of this polymer [132]. Moreover,

Wen et al. showed that nano-sized SiO₂ improved thermal stability of PLA both under nitrogen and in air [133]. Chrissafis et al. exhibited that nanocomposites of PLLA containing 2.5 wt% of fumed silica nano-particles (SiO₂) and organically modified montmorillonite (OMMT) illustrated the higher mechanical properties compared to neat PLLA, except elongation at break [134]. Bikiaris also reported that thermal decomposition from TGA for the SiO₂-PLA nanocomposites gradually increased when adding SiO₂ up to 5 wt%, then decreased slowly with further increase of filler loading [135].

Moreover, good breathability and gas absorbability of food packaging materials are highly considerate. In this phase, nano-sized CaCO₃ particle was surface-treated by silicon dioxide, resulting in hydrophilic filler as [SiO₂-CaCO₃].nH₂O (hydrophilic silica modified calcium carbonate nano-particle). Synthetic SiO₂ fixed on the surfaces of CaCO₃ particles provide desired properties such as a high specific surface area and high absorbability, as well as a potential benefit to improve mechanical properties of polymers [138,139].

3.1 SiO₂-CaCO₃ nano-particle characterization

The hydrolysis of TEOS would be occurred in the presence of water and alkaline catalysts, and then Si(OH)₄ was formed as one of the of hydrolysates. The adding of NH₄OH was to promote the hydrolysis of TEOS. Then, Si(OH)₄ molecule would polymerize with other Si(OH)₄ or TEOS molecule. The product of this step was the monomer or oligomers of polysiloxane. Finally, the oligomers of polysiloxane continue to polymerize and form a film of high relative molecular mass polysiloxane with a three-dimensional network structure as shown in scheme 3.1-3.4. Because water and TEOS are immiscible, a mutual solvent such as ethanol is normally used as a homogenizing agent. Fine particles CaCO₃ can provide nucleation centers and decrease the kinetic barrier to nucleation of hydrophilic silica. The polymerization of silica occurs on the surface of the CaCO₃ particles and the silica film thus covers around the particles tightly.



The infrared spectra of the particles from FT-IR characterization were analyzed in the range of 400 cm⁻¹ to 4,000 cm⁻¹ as shown in Figure 45. It can be seen that the spectrum of blank CaCO₃ nano-particles was quite the same as the spectrum of SiO₂-CaCO₃ but there was transmitting bands at about 1,100 cm⁻¹ of Si—O—Si asymmetric stretching [128] of SiO₂-CaCO₃ nano-particles. This revealed that the SiO₂ was occurred in the reaction, proved the successful of the preparation of SiO₂-CaCO₃ nano-particles. Morphologies of CaCO₃ nano-particles and SiO₂-CaCO₃ nano-particles are shown in Figure 46.

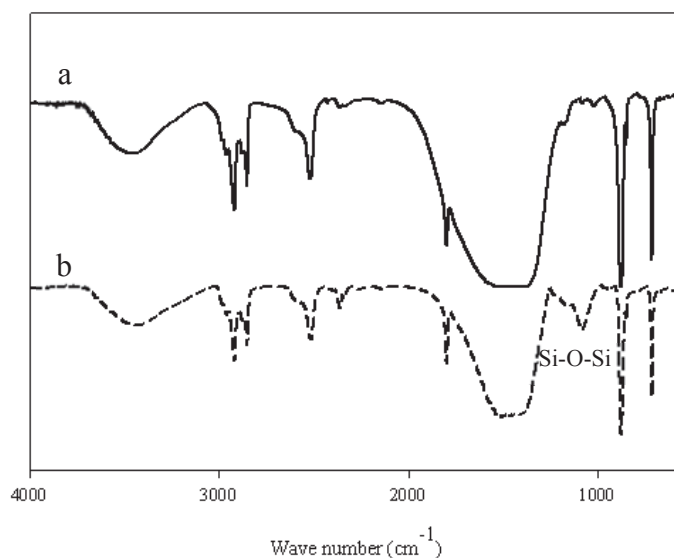


Figure 45. FT-IR spectra of (a) CaCO_3 nano-particle and (b) $\text{SiO}_2\text{-CaCO}_3$ nano-particles.

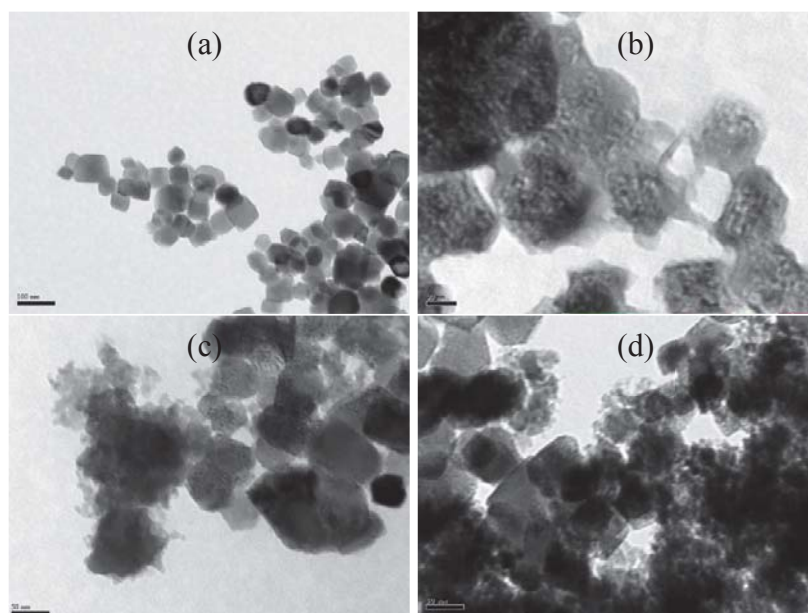


Figure 46. Morphologies of (a) CaCO_3 nano-particles and (b-d) $\text{SiO}_2\text{-CaCO}_3$ nano-particles.

The XRD pattern of nano-sized CaCO_3 is shown in Figure 47. In addition, the diffraction pattern of synthesized SiO_2 in the same procedure but without CaCO_3 is shown in Figure 48. It showed the broad peak of amorphous structure of SiO_2 at about $2\theta \approx 22^\circ$ as reported in the research of Cheng et al. [128] and research of Zhang and Li [140]. Figure 49 shows the X-ray diffraction results of the $\text{SiO}_2\text{-CaCO}_3$ nano-particles. The coating of SiO_2 layer on CaCO_3 surface did not change the crystal structure of CaCO_3 core. Furthermore, it should be considered that the broad peak of SiO_2 at $2\theta \approx 22^\circ$ was also found in the XRD pattern of $\text{SiO}_2\text{-CaCO}_3$ nano-particles. This shows that there was amorphous silica in $\text{SiO}_2\text{-CaCO}_3$ nano-particles in agreement with the results from FT-IR characterization.

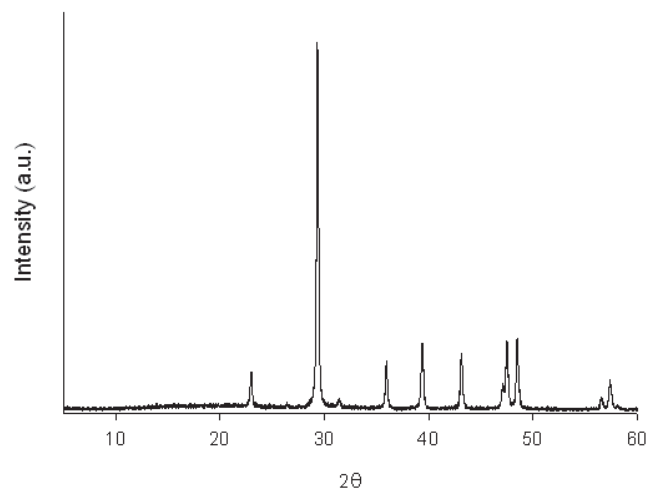


Figure 47. XRD pattern of CaCO₃ nano-particles.

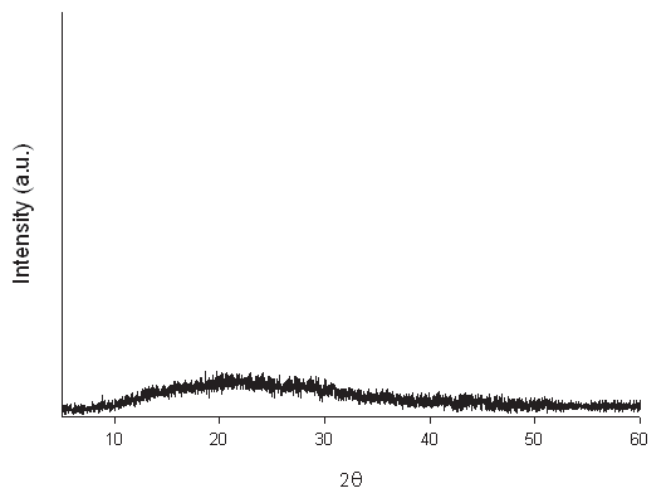


Figure 48. XRD pattern of synthesized SiO₂ particles.

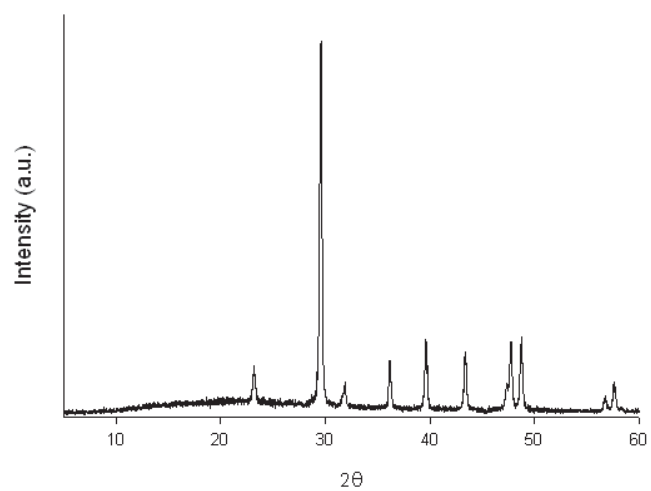


Figure 49. XRD pattern of amorphous SiO₂-CaCO₃ nano-particles.

Dynamic light scattering was used to measure the agglomeration size of CaCO_3 and $\text{SiO}_2\text{-CaCO}_3$ nano-particles. Water was used as a medium in the characterization. The results of this characterization are shown in Figure 50. It was found that the agglomeration sizes of filler particles, reduced with the increasing of SiO_2 content in the filler particles. When SiO_2 coated CaCO_3 surface, it hindered the effect of hydrophobic fatty acid coated on CaCO_3 surface and particles were more hydrophilic and compatible with water. Therefore, $\text{SiO}_2\text{-CaCO}_3$ surface was more hydrophilic than CaCO_3 surface due to the influence of hydrophilicity of $\text{SiO}_2\cdot n\text{H}_2\text{O}$.

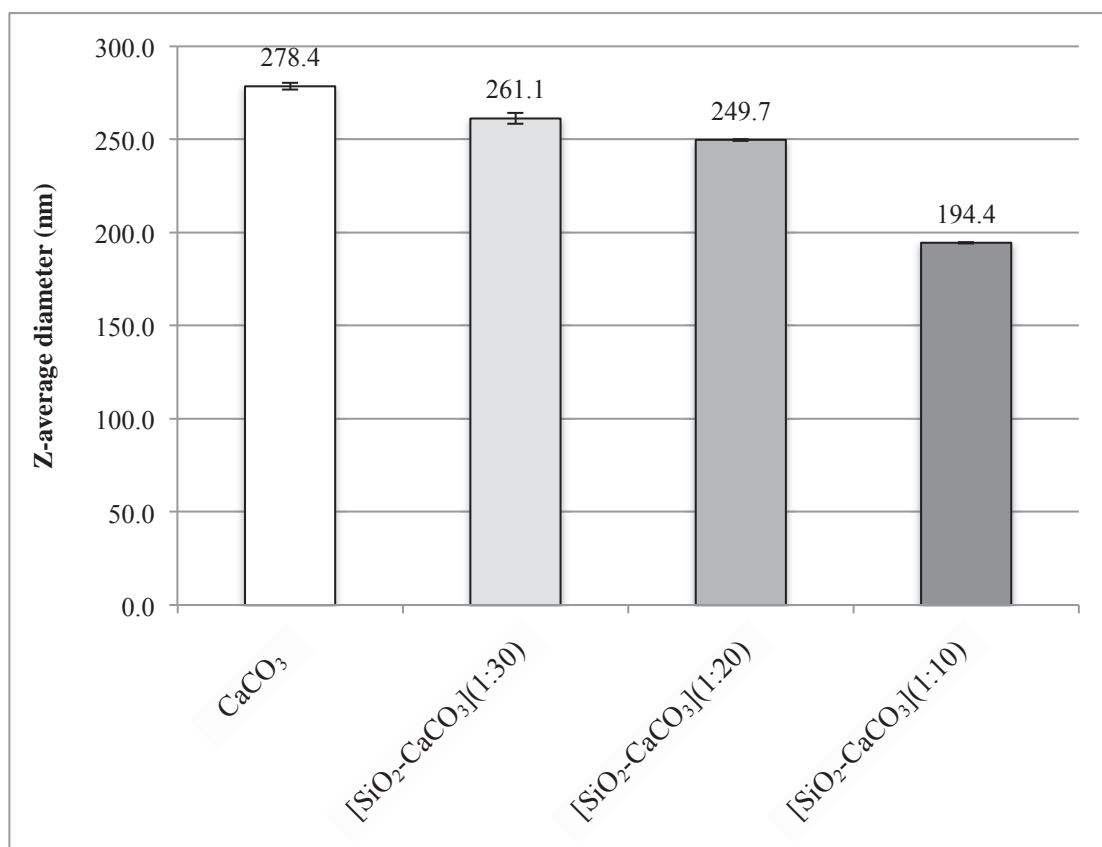


Figure 50. Z-average diameter of CaCO_3 and $\text{SiO}_2\text{-CaCO}_3$ nano-particles.

Table 28 shows the elemental analysis of $\text{SiO}_2\text{-CaCO}_3$ nano-particles by X-ray fluorescence spectrometer (XRF). The major elements of the nano-particles are Oxygen (O) and Calcium (Ca) with small amount of Silica (Si) according to Si : Ca mole ratio in the reactants. Table 29 showed relative Si : Ca ratio of synthesized $\text{SiO}_2\text{-CaCO}_3$ nano-particles. It was found that mole ratio of Si : Ca of synthesized $\text{SiO}_2\text{-CaCO}_3$ nano-particles, increased according to the increase of Si : Ca mole ratio in the reactants and the value of Si : Ca ratio of synthesized $\text{SiO}_2\text{-CaCO}_3$ nano-particles, were relatively close to the Si : Ca mole ratio in the reactants. Thus, the mole ratio of Si : Ca in synthesized $\text{SiO}_2\text{-CaCO}_3$ nano-particles could be controlled by this preparation procedure.

Table 28. The elemental analysis of SiO₂-CaCO₃ nano-particles.

Element	Concentration (wt%)		
	[SiO ₂ -CaCO ₃](1:30)	[SiO ₂ -CaCO ₃](1:20)	[SiO ₂ -CaCO ₃](1:10)
O	58.72	53.83	50.83
Na	0.02	0.04	0.07
Mg	0.13	0.16	0.13
Al	0.04	0.05	0.07
Si	0.87	1.92	3.91
P	N/D	N/D	N/D
S	0.02	0.02	0.01
Cl	N/D	N/D	N/D
K	N/D	N/D	N/D
Ca	40.11	43.89	44.9
Fe	0.05	0.05	0.04
Sr	0.04	0.04	0.04
Total	100	100	100

Table 29. The Si : Ca mole ratio in synthesized SiO₂-CaCO₃ nano-particles.

Particles	Ratio of Si : Ca
[SiO ₂ -CaCO ₃](1:30)	0.93 : 30
[SiO ₂ -CaCO ₃](1:20)	1.25 : 20
[SiO ₂ -CaCO ₃](1:10)	1.24 : 10

In Figure 51, BET results show that nano-sized CaCO₃ had the lowest surface area and pore volume and the SiO₂-CaCO₃ nano-particles had higher surface area and pore volume with respect to higher SiO₂ contents. When SiO₂ was adhered on the surface of CaCO₃, giving the nano-particles higher surface area and pore volume. However, pore size of SiO₂-CaCO₃ nano-particles decreased with the increasing of SiO₂ contents because SiO₂ has smaller pore size than CaCO₃. The lower pore size particle, giving SiO₂-CaCO₃ nano-particles higher amount of pore in the equivalent volume, thus, higher surface area.

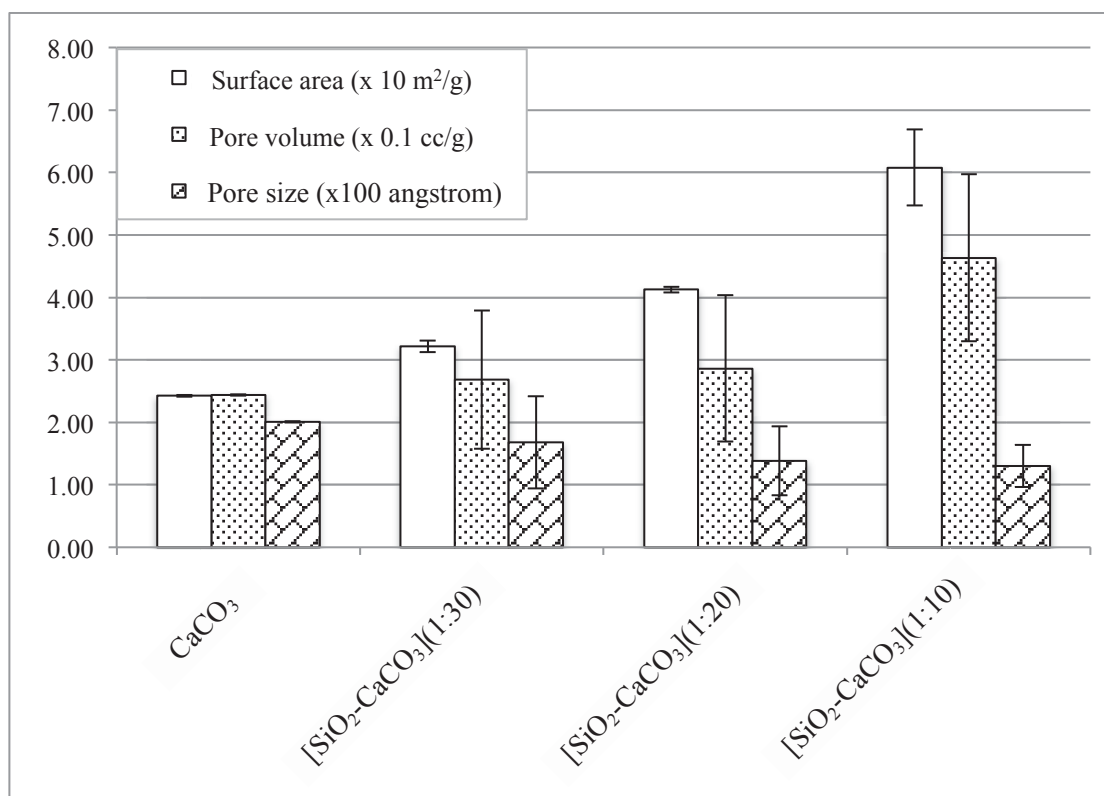


Figure 51. Surface areas, pore volume and pore size of CaCO₃ and SiO₂-CaCO₃ nano-particles.

3.2 Thermal stability studies

Thermal stability of PLA and SiO₂-CaCO₃ nano-particles with PEG/TbC plasticizer of 10 phr were studied in this phase of research. TGA curves are shown in Figure 52 and the onset of degradation temperature (T_{onset}), degradation temperature (T_d), and the end of degradation (T_{end}) are reported in Table 30. Thermal stability of CaCO₃-PLA nanocomposite was lower than that of neat PLA because the chemical reaction between fatty acid coated on CaCO₃ enhanced chain scission and induced thermal degradation of PLA as discussed earlier in phase I and phase II.

In this phase, SiO₂-CaCO₃ was added as filler in PLA polymer matrix. The TGA results show that thermal stability of [SiO₂-CaCO₃]-PLA nanocomposite was improved, compared to CaCO₃-PLA nanocomposite. SiO₂ on the surface of CaCO₃ could extend the onset of degradation temperature. It was also reported that SiO₂ enhanced thermal stability at low loading (4–5 wt%) in most cases of polycondensation polymers. The optimum content of SiO₂ could exhibit the high T_{onset} which was shifted approximately 35 °C towards higher temperature compared to T_{onset} for neat PLA [135].

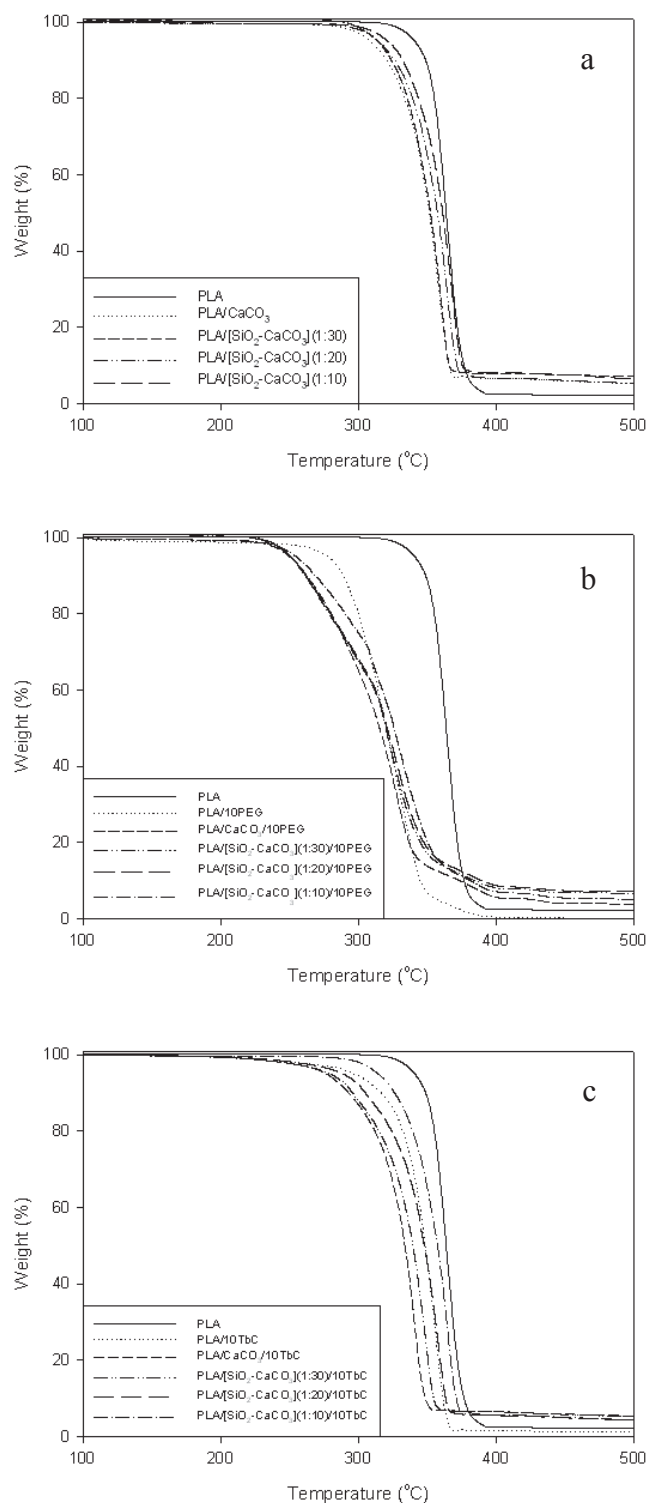


Figure 52. TGA curves of a) Neat PLA, 5 wt% [SiO₂-CaCO₃]-PLA nanocomposite and plasticized [SiO₂-CaCO₃]-PLA nanocomposite, b) PEG plasticized PLA and plasticized [SiO₂-CaCO₃]-PLA nanocomposite at various Si : Ca mole ratio, c) TbC plasticized PLA and plasticized [SiO₂-CaCO₃]-PLA nanocomposite at various Si : Ca mole ratio.

In this study, thermal degradation temperature of SiO₂-PLA nanocomposites increased when adding SiO₂-CaCO₃ nano-particles with higher amount of Si. Inorganic SiO₂ could absorb more heat, thus retard thermal degradation of PLA during melt process. It was found that adding of SiO₂-CaCO₃ nano-particles could maintain T_{onset} and T_d of SiO₂-CaCO₃ nano-particles to the same temperature as that of neat PLA. Although, the addition of plasticizers induced the thermal degradation, causing low molecular weight of PLA, thus the thermal stability of PEG plasticized PLA and TbC plasticized PLA were lower than neat PLA. The adding of SiO₂-CaCO₃ nano-particles also maintained thermal stability of plasticized PLA to the same temperature with that of neat PLA nanocomposite, especially when adding [SiO₂-CaCO₃](10:1) nano-particle.

Table 30. Thermal stability analysis of PLA, CaCO₃-PLA nanocomposite and [SiO₂-CaCO₃]-PLA nanocomposite with and without PEG/TbC plasticizer.

Material	T _{onset} (°C)	T _d (°C)	T _{endset} (°C)
PLA	346.33	365.46	375.31
PLA/CaCO ₃	330.05	347.81	351.52
PLA/[SiO ₂ -CaCO ₃](1:30)	331.56	348.23	353.13
PLA/[SiO ₂ -CaCO ₃](1:20)	339.97	359.69	364.92
PLA/[SiO ₂ -CaCO ₃](1:10)	342.78	363.15	367.15
PLA/10PEG	291.68	331.53	351.72
PLA/CaCO ₃ /10PEG	277.07	232.14	339.60
PLA/[SiO ₂ -CaCO ₃](1:30)/10PEG	277.56	309.61	338.32
PLA/[SiO ₂ -CaCO ₃](1:20)/10PEG	283.84	315.65	343.40
PLA/[SiO ₂ -CaCO ₃](1:10)/10PEG	289.97	324.30	351.24
PLA/10TbC	334.01	355.55	365.07
PLA/CaCO ₃ /10TbC	307.04	339.37	347.69
PLA/[SiO ₂ -CaCO ₃](1:30)/10TbC	324.33	347.62	358.41
PLA/[SiO ₂ -CaCO ₃](1:20)/10TbC	332.99	359.02	363.17
PLA/[SiO ₂ -CaCO ₃](1:10)/10TbC	341.16	362.99	367.36

3.3 Thermal properties studies

The DSC thermograms (Exo.) of plasticized [SiO₂-CaCO₃]-PLA nanocomposites are shown in Figure 53 and the glass transition temperature (T_g), melting temperature (T_m), co-crystallization (T_{cc}) and crystallization temperature (T_c) of the nanocomposites are reported in Table 31.

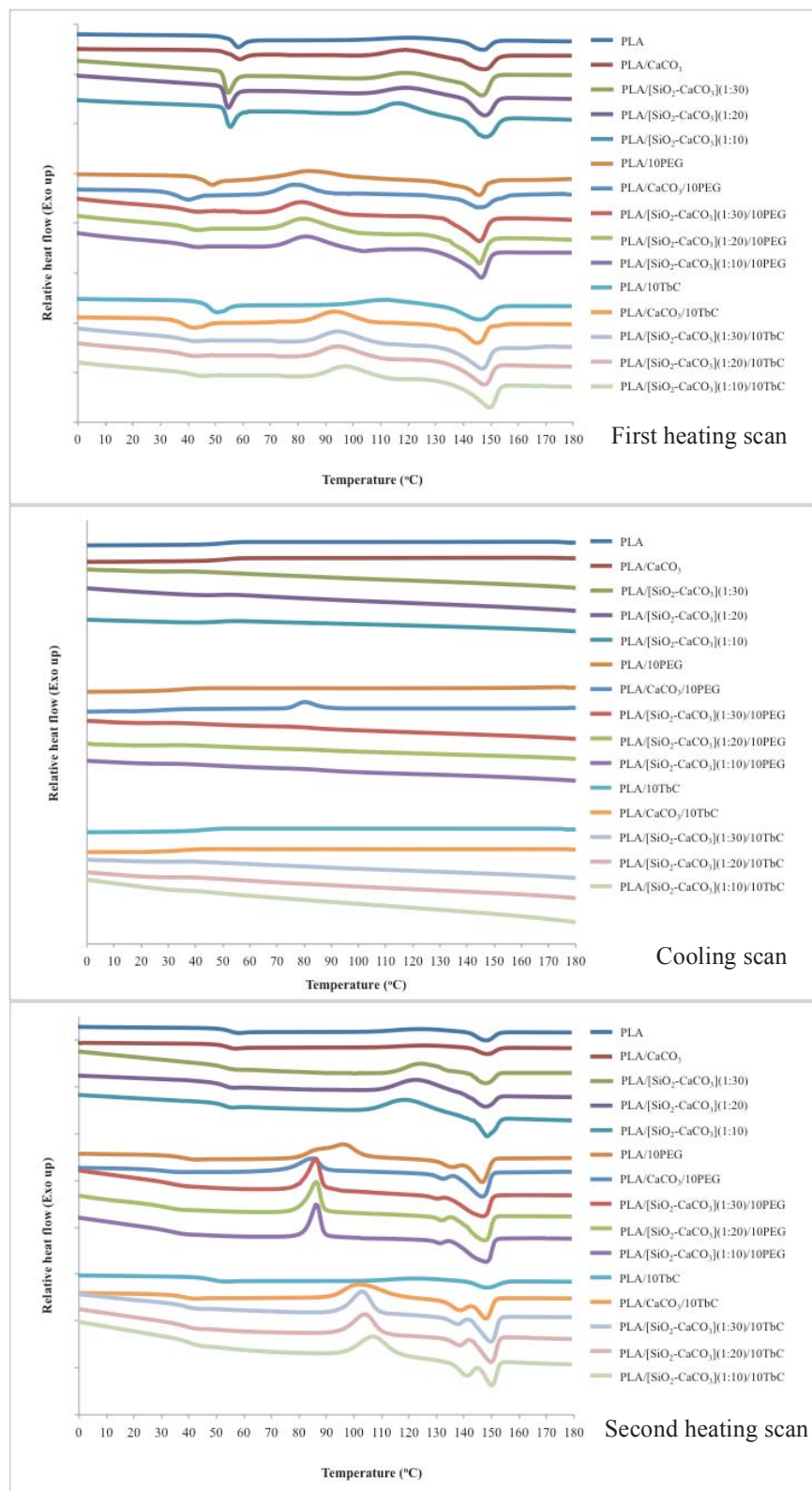


Figure 53. DSC thermograms of [SiO₂-CaCO₃]-PLA nanocomposites without and with PEG/TbC plasticizer of 10 phr.

Table 31. Thermal properties of [SiO₂-CaCO₃]-PLA nanocomposites without and with PEG/TbC plasticizer of 10 phr.

Materials	First heating scan				Cooling scan	Second heating scan				
	T _g (°C)	T _{cc} (°C)	T _m (°C)			T _c (°C)	T _g (°C)	T _{cc} (°C)	T _m (°C)	
			Peak 1	Peak 2					Peak 1	Peak 2
PLA	52.06	120.28	-	147.13	-	51.98	123.70	-	147.48	
PLA/CaCO ₃	52.27	119.94	-	147.22	-	52.22	123.53	-	147.80	
PLA/ [SiO ₂ -CaCO ₃](1:30)	52.15	119.81	-	148.87	-	51.77	123.35	-	148.52	
PLA/ [SiO ₂ -CaCO ₃](1:20)	52.64	118.17	-	148.90	-	52.38	120.18	-	148.73	
PLA/ [SiO ₂ -CaCO ₃](1:10)	53.41	115.12	-	149.84	-	52.34	117.43	-	149.71	
PLA/10PEG	42.23	83.27	136 (shoulder)	145.92	-	35.02	94.48	134.33	145.46	
PLA/CaCO ₃ /10PEG	34.89	78.82	134 (shoulder)	145.35	81.79	27.09	82.15	131.48	144.44	
PLA/[SiO ₂ - CaCO ₃](1:30)/10PEG	36.44	79.17	136 (shoulder)	146.10	-	30.53	83.80	131.04	145.65	
PLA/[SiO ₂ - CaCO ₃](1:20)/10PEG	37.16	80.04	136 (shoulder)	146.32	-	31.84	84.88	131.87	145.78	
PLA/[SiO ₂ - CaCO ₃](1:10)/10PEG	38.03	80.62	136 (shoulder)	146.37	-	33.17	85.39	131.90	145.98	
PLA/10TbC	45.34	112.27	-	146.98	-	45.72	121.60	-	146.96	
PLA/CaCO ₃ /10TbC	35.20	91.76	136 (shoulder)	146.72	-	35.05	100.70	137.23	146.41	
PLA/[SiO ₂ - CaCO ₃](1:30)/10TbC	36.94	92.30	138 (shoulder)	148.84	-	36.84	102.30	136.84	148.36	
PLA/[SiO ₂ - CaCO ₃](1:20)/10TbC	37.92	92.68	138 (shoulder)	148.92	-	37.69	103.09	137.76	148.77	
PLA/[SiO ₂ - CaCO ₃](1:10)/10TbC	39.03	93.04	138 (shoulder)	149.52	-	38.63	105.24	139.27	149.48	

The addition of SiO₂-CaCO₃ nano-particles did not affect T_g of PLA similarly to the addition of CaCO₃. It was also found that PLA, CaCO₃-PLA nanocomposites and [SiO₂-CaCO₃]-PLA nanocomposites had one T_m in the first heating scan. However, in the second heating scan, PLA and both PLA

nanocomposites showed two T_m (with small split peak). In this phase, specimen preparation was fabricated by compression molding. The poor orientation of PLA polymer chains by this compression molding process caused one broad T_m about 150 °C in the first heating scan.

The addition of $\text{SiO}_2\text{-CaCO}_3$ nano-particles slightly increased T_{cc} of plasticized PLA in contrast to the addition of nano-sized CaCO_3 as discussed in phase I and II. When PEG/TbC plasticizer was incorporated into PLA, T_{cc} was dramatically reduced because plasticizers could enhance the movement of PLA polymer chains to fold and crystallize. On contrary, SiO_2 on the surface of CaCO_3 could extend the degradation temperature of PLA, therefore molecular weight of PLA could maintain during the thermal process and T_{cc} of plasticized PLA increased slightly with SiO_2 content on the $\text{SiO}_2\text{-CaCO}_3$ filler. It is interested that the T_c peak for PLA appeared during cooling only in PEG plasticized $\text{CaCO}_3\text{-PLA}$ nanocomposite because plasticized effect on the mobility of PLA macromolecules and the low molecular weight of PLA in the presence of this plasticizer and fatty acid coated CaCO_3 enhanced crystallization of PLA. However, T_c was not found in PEG plasticized $[\text{SiO}_2\text{-CaCO}_3]\text{-PLA}$ nanocomposites because the synergistic effect of PEG and fatty acid coated CaCO_3 was retarded by the implement of SiO_2 on the surface of CaCO_3 nano-particles.

It can be seen from Table 31 that the T_g of plasticized PLA slightly increased when adding $\text{SiO}_2\text{-CaCO}_3$ nano-particle, compared to nano-sized CaCO_3 . As SiO_2 is more rigid than CaCO_3 , $\text{SiO}_2\text{-CaCO}_3$ nano-particles retard the movement of degraded PLA short chain, causing improvement of its mechanical strength. Furthermore, $\text{SiO}_2\text{-CaCO}_3$ nano-particles improved T_m of $[\text{SiO}_2\text{-CaCO}_3]\text{-PLA}$ nanocomposite according to the SiO_2 contents.

3.4 Mechanical properties studies

The mechanical properties of the plasticized $\text{CaCO}_3\text{-PLA}$ and $[\text{SiO}_2\text{-CaCO}_3]\text{-PLA}$ nanocomposites at various Si : Ca mole ratio as shown in Figure 54-56 were performed by tensile test and Izod impact test. Figure 54 shows that the Young's modulus of PLA was not improved by the addition of nano-sized CaCO_3 and it was decreased obviously when plasticizers was added into PLA. Furthermore, the incorporation of both nano-sized CaCO_3 and plasticizers reduced modulus of PLA dramatically because of the acceleration of PLA thermal degradation and plasticized effect as discussed in phase I and phase II. However, the successful surface modification of nano-sized CaCO_3 with SiO_2 , benefited $[\text{SiO}_2\text{-CaCO}_3]\text{-PLA}$ nanocomposites with the improvement in Young's modulus of both unplasticized and plasticized PLA, compared to adding of nano-sized CaCO_3 . Young's modulus of $[\text{SiO}_2\text{-CaCO}_3]\text{-PLA}$ nanocomposite increased according to the increasing of SiO_2 content on the filler surface. Moreover, TGA results showed that SiO_2 surface modified CaCO_3 could reduce the negative effect of fatty acid coated on CaCO_3 nano-particle, thus thermal degradation of PLA during melt process was retarded and PLA molecular weight was maintained. It was found that Young's modulus of TbC plasticized $[\text{SiO}_2\text{-CaCO}_3]\text{-PLA}$ nanocomposites was slightly higher than that of PEG plasticized $[\text{SiO}_2\text{-CaCO}_3]\text{-PLA}$ nanocomposites because the branching molecule of TbC gave the lower reduction in molecular weight of PLA.

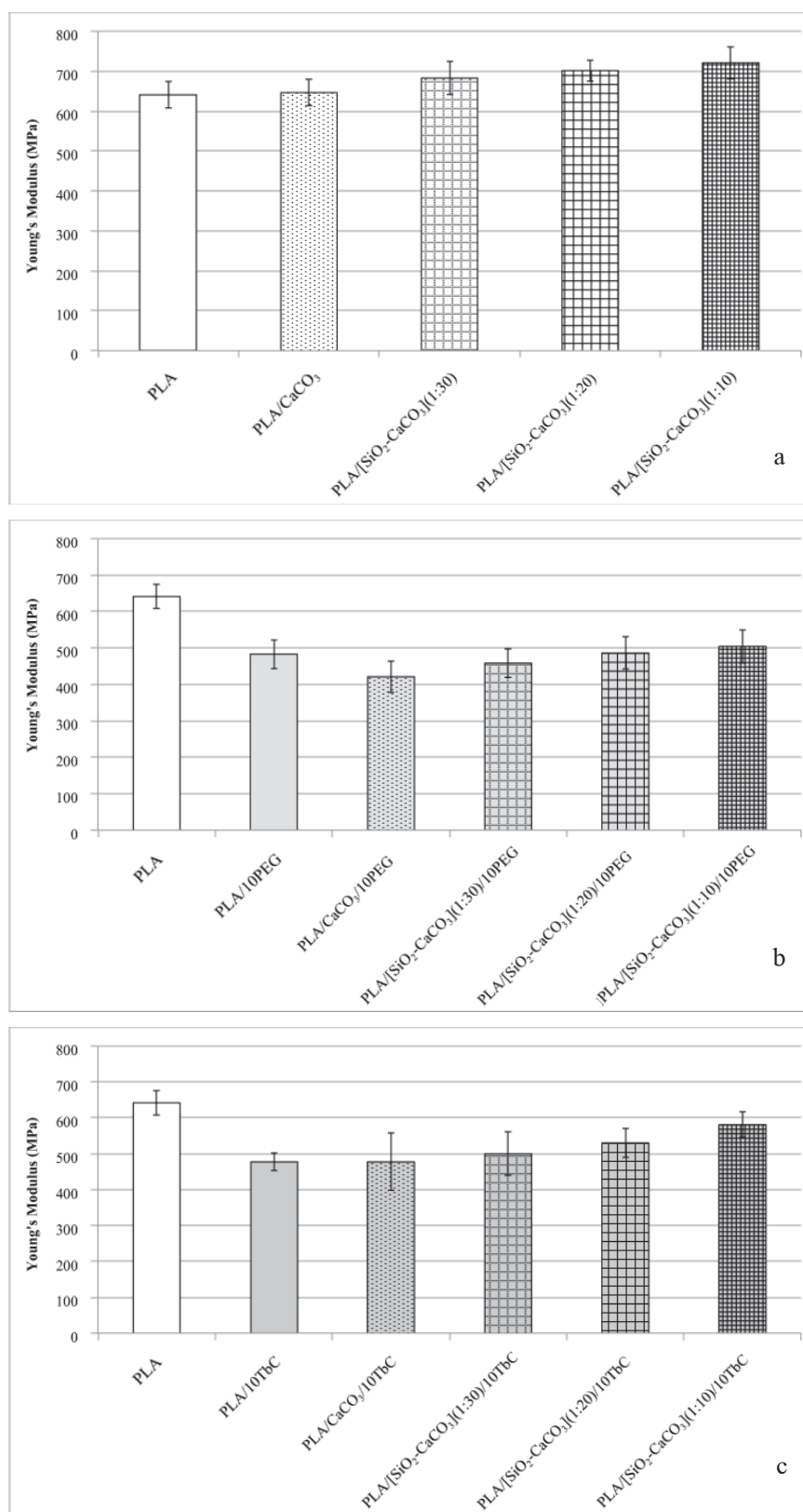


Figure 54. Young's modulus of PLA, plasticized PLA, plasticized CaCO₃-PLA and [SiO₂-CaCO₃]-PLA nanocomposites at various Si : Ca mole ratio.

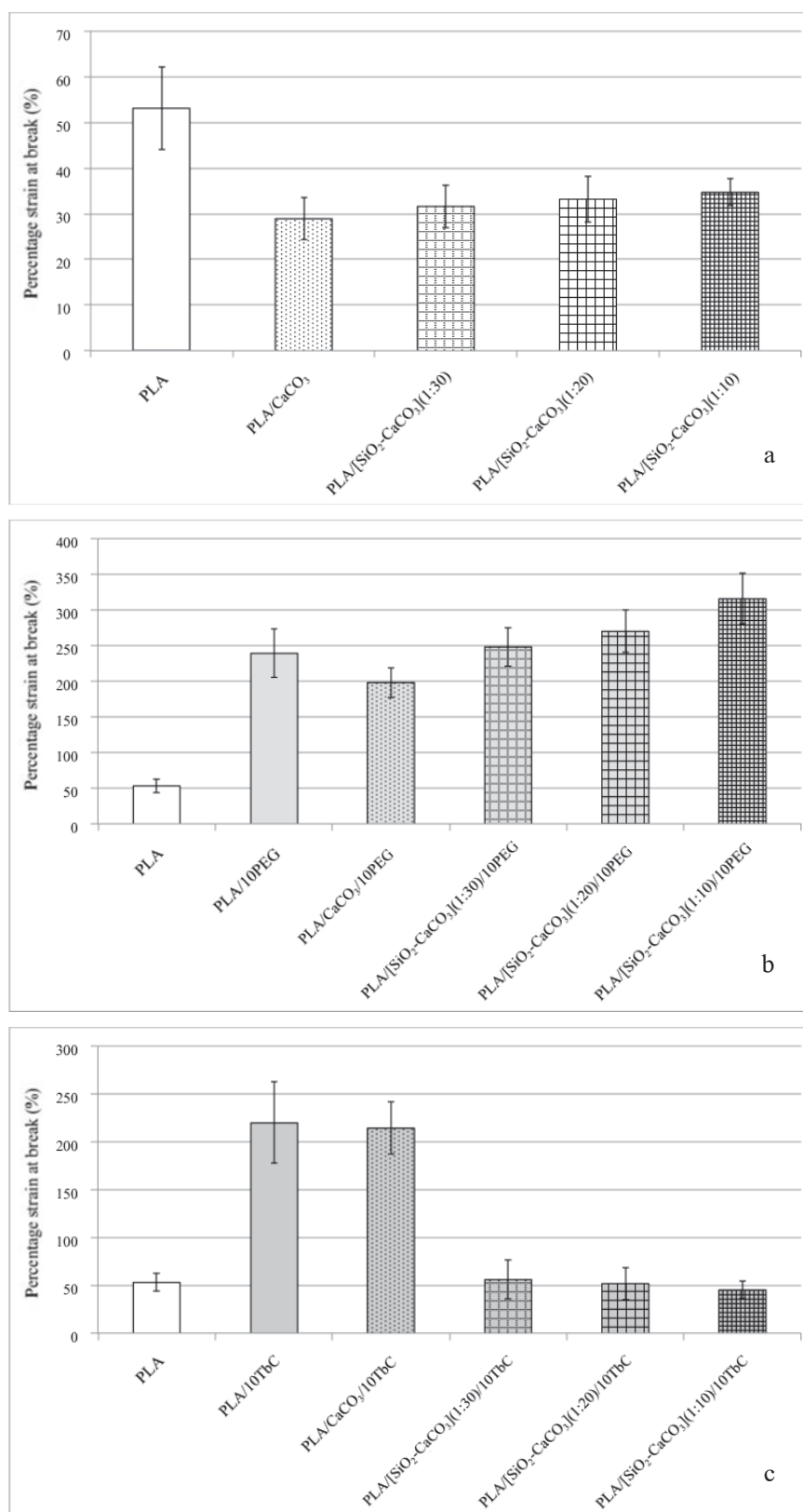


Figure 55. Percentage of strain at break of PLA, plasticized PLA, plasticized CaCO₃-PLA and [SiO₂-CaCO₃]-PLA nanocomposites at various Si : Ca mole ratio.

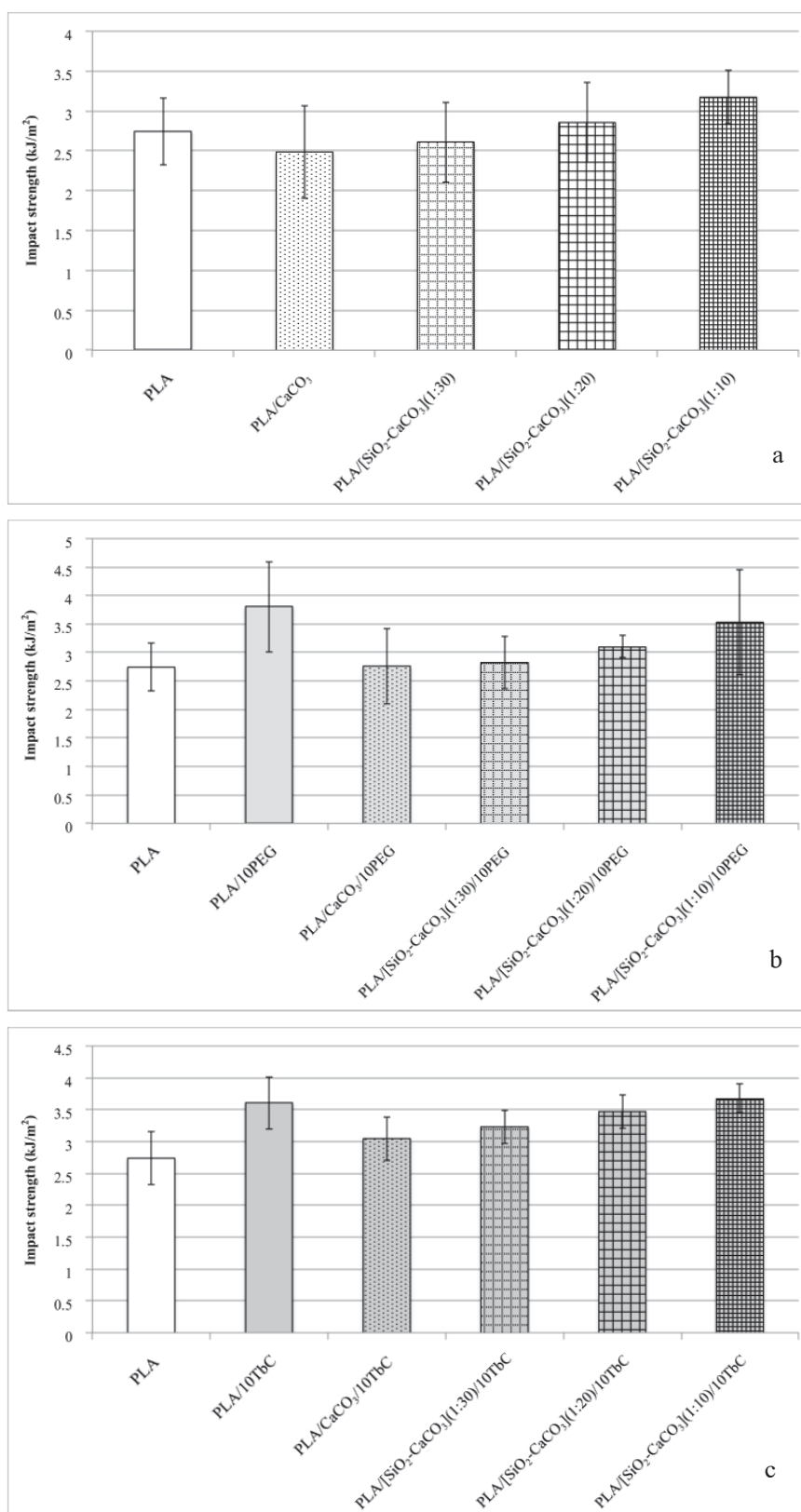


Figure 56. Impact strength of PLA, plasticized PLA, plasticized CaCO₃-PLA and [SiO₂-CaCO₃]-PLA nanocomposites at various Si : Ca mole ratio.

As nano-sized CaCO_3 acted as a stress concentrator to promote crack initiation as well as the interfacial interaction between PLA matrix and CaCO_3 nanoparticles was poor. Figure 55 shows that the percentage of strain at break of unplastified $[\text{SiO}_2\text{-CaCO}_3]\text{-PLA}$ nanocomposite improved because of the better compatibility between polymer matrix and $\text{SiO}_2\text{-CaCO}_3$ nano-particles. Furthermore, the percentage of strain at break of PEG plasticized $[\text{SiO}_2\text{-CaCO}_3]\text{-PLA}$ nanocomposite was increased according to the increasing of SiO_2 content on the surface of CaCO_3 . However, the percentage of strain at break of TbC plasticized $[\text{SiO}_2\text{-CaCO}_3]\text{-PLA}$ nanocomposite was the same as that of neat PLA. The reason was due to some agglomeration of $\text{SiO}_2\text{-CaCO}_3$ that was found in SEM micrograph of fractured surface. These particles agglomerations promoted crack initiation of PLA and induced PLA to break at low elongation.

Figure 56 illustrates that impact strength of PLA was decreased by the addition of nano-sized CaCO_3 because of introducing crack initiator. However, impact strength of PLA increased by the incorporation of plasticizers into PLA because of improvement in flexibility. It was found that adding of $\text{SiO}_2\text{-CaCO}_3$ nano-particles could improve impact strength of unplastified and plasticized PLA nanocomposites, and the impact strength of unplastified and plasticized $[\text{SiO}_2\text{-CaCO}_3]\text{-PLA}$ nanocomposite was increased according to the increasing of SiO_2 content on the surface of CaCO_3 nano-particles due to the better compatibility of $\text{SiO}_2\text{-CaCO}_3$ nano-particles with PLA matrix.

3.5 Dynamic mechanical properties studies

Figure 57 shows that storage modulus of $\text{CaCO}_3\text{-PLA}$ and plasticized $\text{CaCO}_3\text{-PLA}$ nanocomposite were lower than those of neat PLA as discussed in phase I and phase II. The incorporation of $\text{SiO}_2\text{-CaCO}_3$ nano-particles increased storage modulus of PLA. In the dynamic tension mode of DMA testing, the rigid surface of $\text{SiO}_2\text{-CaCO}_3$ inhibited the movement of PLA matrix resulting that PLA was not deformed easily when it was added by $\text{SiO}_2\text{-CaCO}_3$ nano-particle. Moreover, molecular weight of PLA could be maintained during the melt process as the surface modification of SiO_2 on CaCO_3 , retarded the negative effect of fatty acid sizing agent on thermal degradation of PLA. Thus, the storage modulus of PLA was increased with the increasing of SiO_2 content on the surface of CaCO_3 as shown in Figure 57a. The addition of both PEG and TbC plasticizers enhanced the molecular movement of PLA polymer chain resulting in the decreasing of storage modulus as seen in Figure 57b and 57c. Unfortunately, the effect of high content plasticizers were dominant, therefore the storage modulus did not improve obviously in $[\text{SiO}_2\text{-CaCO}_3]\text{-PLA}$ nanocomposite.

As well as phase I and phase II, the storage modulus decreased sharply at the temperature about T_g and it slightly increased again at about T_{cc} because of co-crystallization of PLA. Figure 58 shows peak of $\tan \delta$ curve, illustrated the T_g of materials. The results show that the small content of CaCO_3 did not affect T_g of PLA but T_g of PLA with plasticizers decreased dramatically.

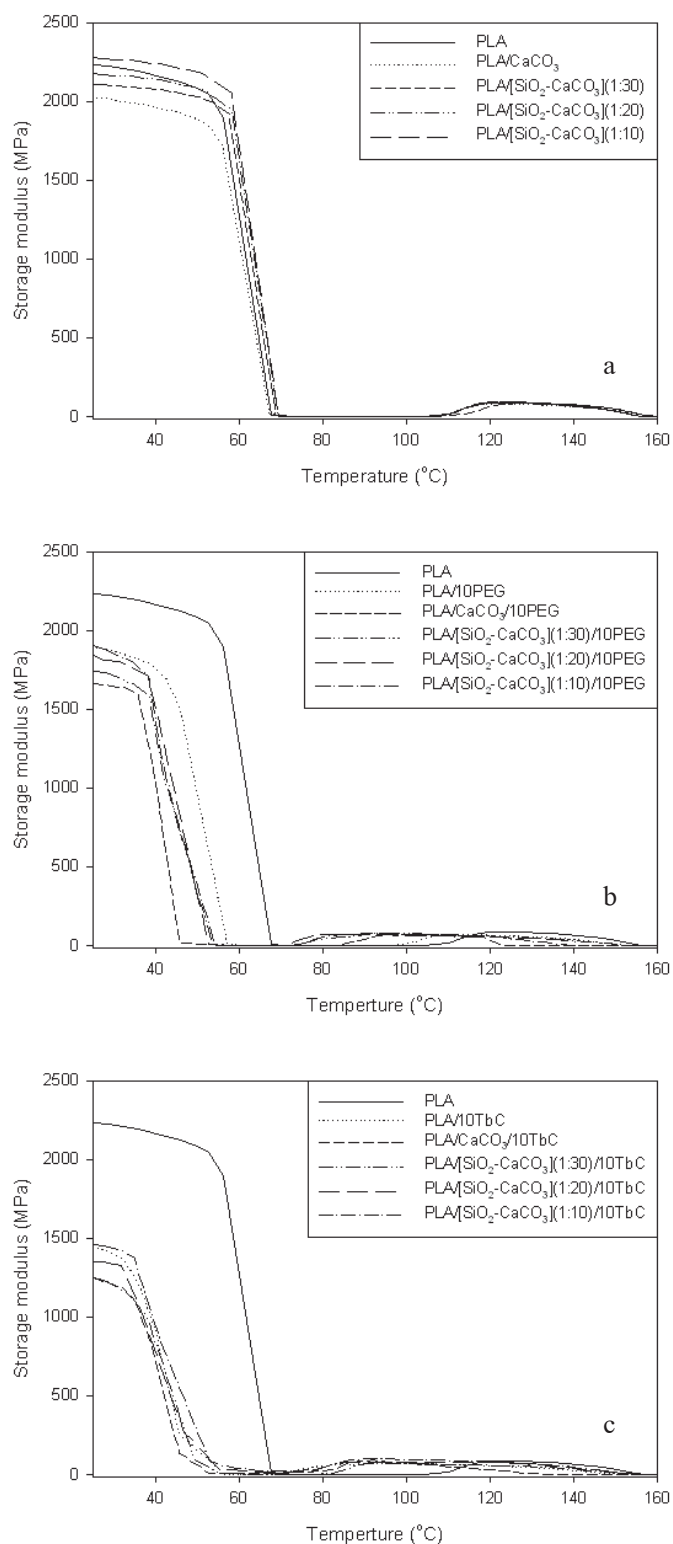


Figure 57. Storage modulus of PLA, plasticized PLA, plasticized CaCO₃-PLA and [SiO₂-CaCO₃]-PLA nanocomposites at various Si : Ca mole ratio.

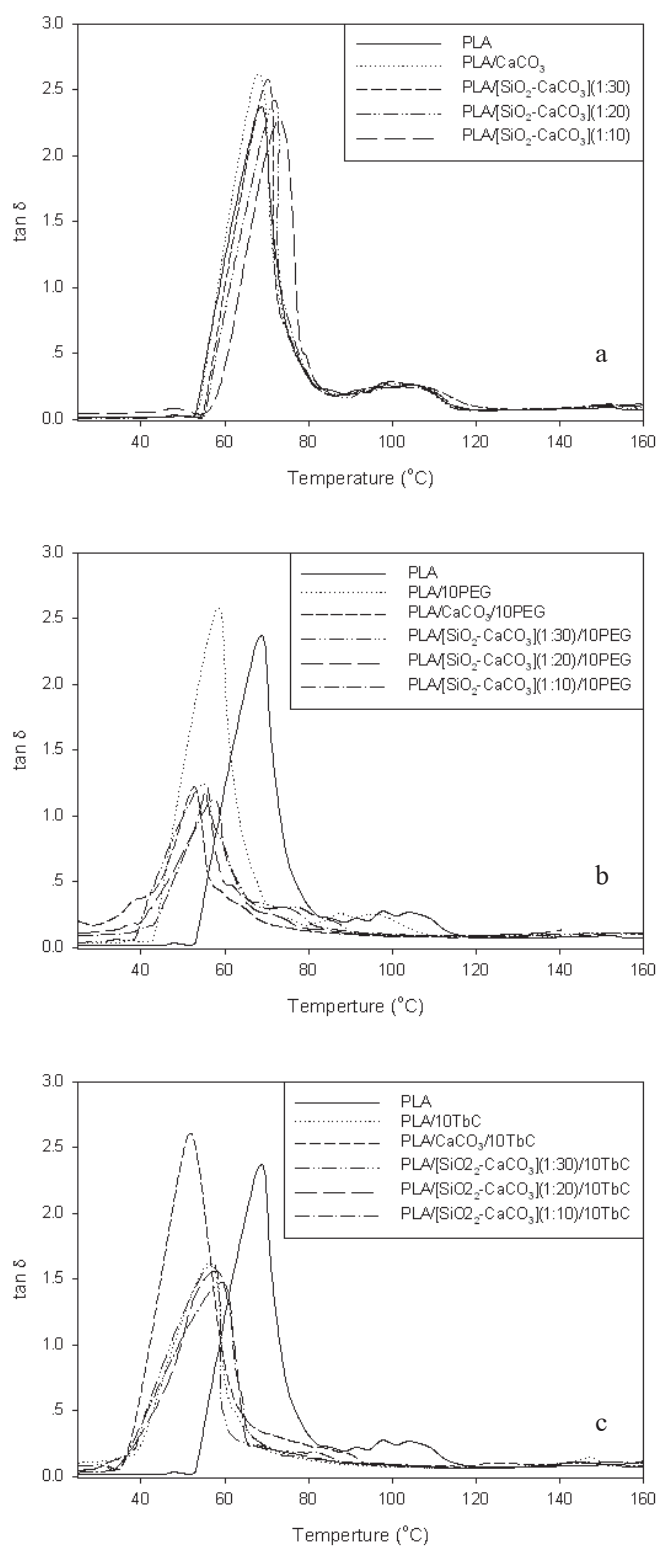


Figure 58. Tan δ of PLA, plasticized PLA, plasticized CaCO_3 -PLA and $[\text{SiO}_2\text{-CaCO}_3]$ -PLA nanocomposites at various Si : Ca mole ratio.

The T_g of [SiO₂-CaCO₃]-PLA nanocomposite was higher than those neat PLA as seen in Figure 58a. SiO₂ could retard the thermal degradation of PLA and plasticized PLA during the melt process. Moreover, the rigid surface of SiO₂ on the smooth surface of CaCO₃ inhibited the movement of polymer chain. Therefore, T_g of [SiO₂-CaCO₃]-PLA nanocomposite was increased with respect to the content of SiO₂ on CaCO₃ surface. This situation was also occurred in the case of plasticized [SiO₂-CaCO₃]-PLA nanocomposite as shown in Figure 58b and 58c. The increasing in content of SiO₂ enhanced the shift of T_g of plasticized-PLA to occur at higher temperature.

In addition, the value of $\tan \delta$ was calculated from storage modulus divided by loss modulus. Storage modulus implies the elastic part of materials, while the loss modulus represent the viscous part of solid materials. In physical meaning, a material that has high $\tan \delta$ is deformed easier like a viscos fluid. Figure 58 shows that $\tan \delta$ of plasticized [SiO₂-CaCO₃]-PLA nanocomposite tended to decrease with the increasing of SiO₂ content. This implied that SiO₂ that treated on CaCO₃ surface retarded the deformation of PLA and the stability of PLA shape at the temperature about T_g was increased according to the increasing of SiO₂ content.

3.6 Morphology studies

The X-ray diffraction patterns in Figure 59 show that nano-sized CaCO₃ reduced degree of crystallinity of PLA but the addition of SiO₂-CaCO₃ nano-particles could improve crystallinity of PLA. As shown in Figure 59a, the degree of crystallinity of PLA tended to increase according to the content of SiO₂ on CaCO₃ surface. This implied that the compatibility between polymer matrix and SiO₂-CaCO₃ nano-particle could enhance the crystallization of PLA. In the plasticized system as shown in Figure 59b and 59c, the degree of crystallinity of plasticized PLA decreased when it was incorporated with nano-sized CaCO₃. In contrast, SiO₂-CaCO₃ nano-particles could enhance crystallization of PLA and the degree of crystallinity of PLA was increased again. However, the degree of crystallinity of PLA was not increased with the increasing of SiO₂ content. This was due to dominant effect of plasticizers, enhanced the movement of PLA molecular chain. In plasticized system, polymer chain could move and fold in crystal structure, while it also moved out of the fold chain easily. Therefore, this might be the reason that the degree of crystallinity of plasticized PLA nanocomposites was limited.

SEM micrographs in Figure 60 reveal the fracture behavior of PLA and plasticized PLA nanocomposites. As well as explain in phase II, fractured surface of neat PLA was smooth with local ductile breaking as craze and crack propagation occurred during the impact loading. When nano-sized CaCO₃ was added into PLA matrix, they became stress concentrators promoting crack initiation, thus local ductile breaking diminished causing the decreasing of impact strength. When PEG and TbC plasticizers that were blended into PLA, plasticizers could enhance the movement of PLA molecular chain resulting that nanocomposites were tougher and broken in favor of ductile failure. There were many stripes of locally extension in polymer matrix in fractured surface of 10 phr plasticized nanocomposite. These strips line were in the line of impact force direction causing the higher impact strength.

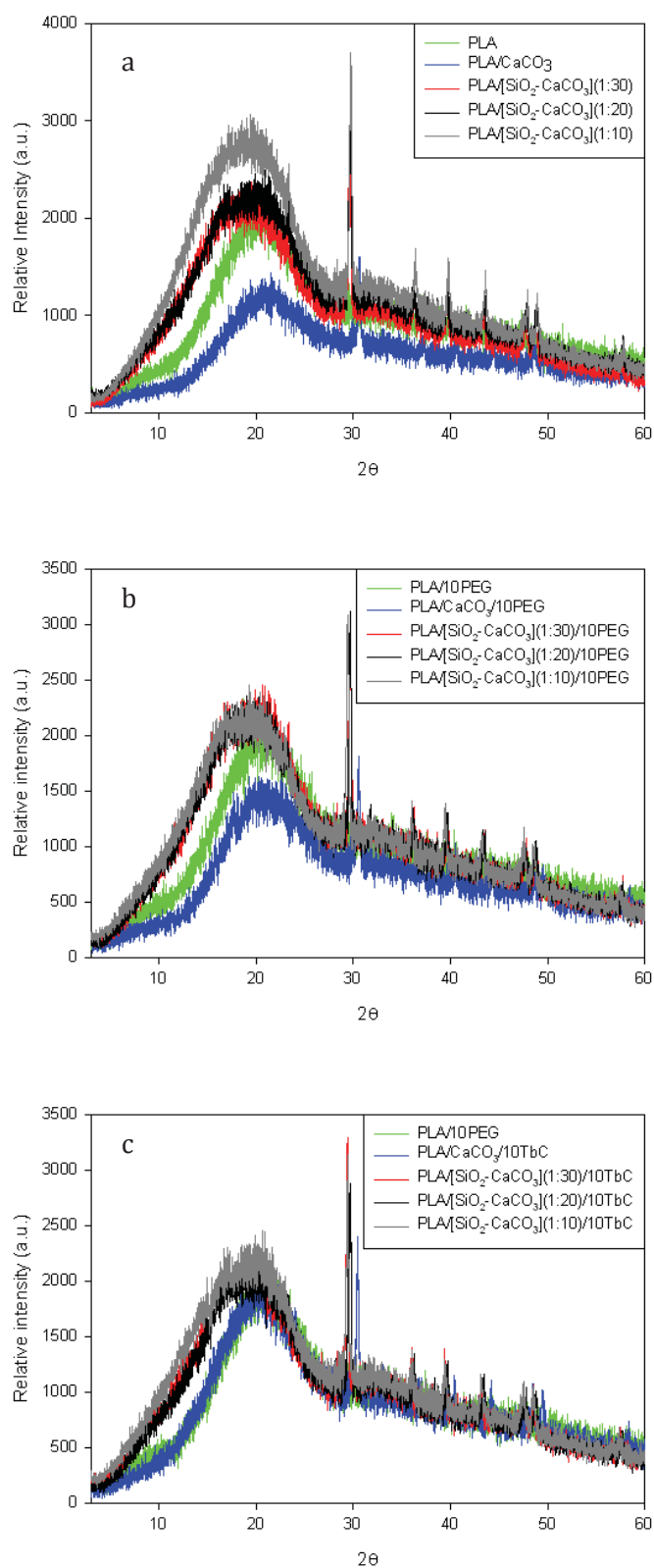


Figure 59. X-Ray diffraction patterns of PLA, plasticized PLA, plasticized CaCO₃-PLA and [SiO₂-CaCO₃]-PLA nanocomposites at various Si : Ca mole ratio.

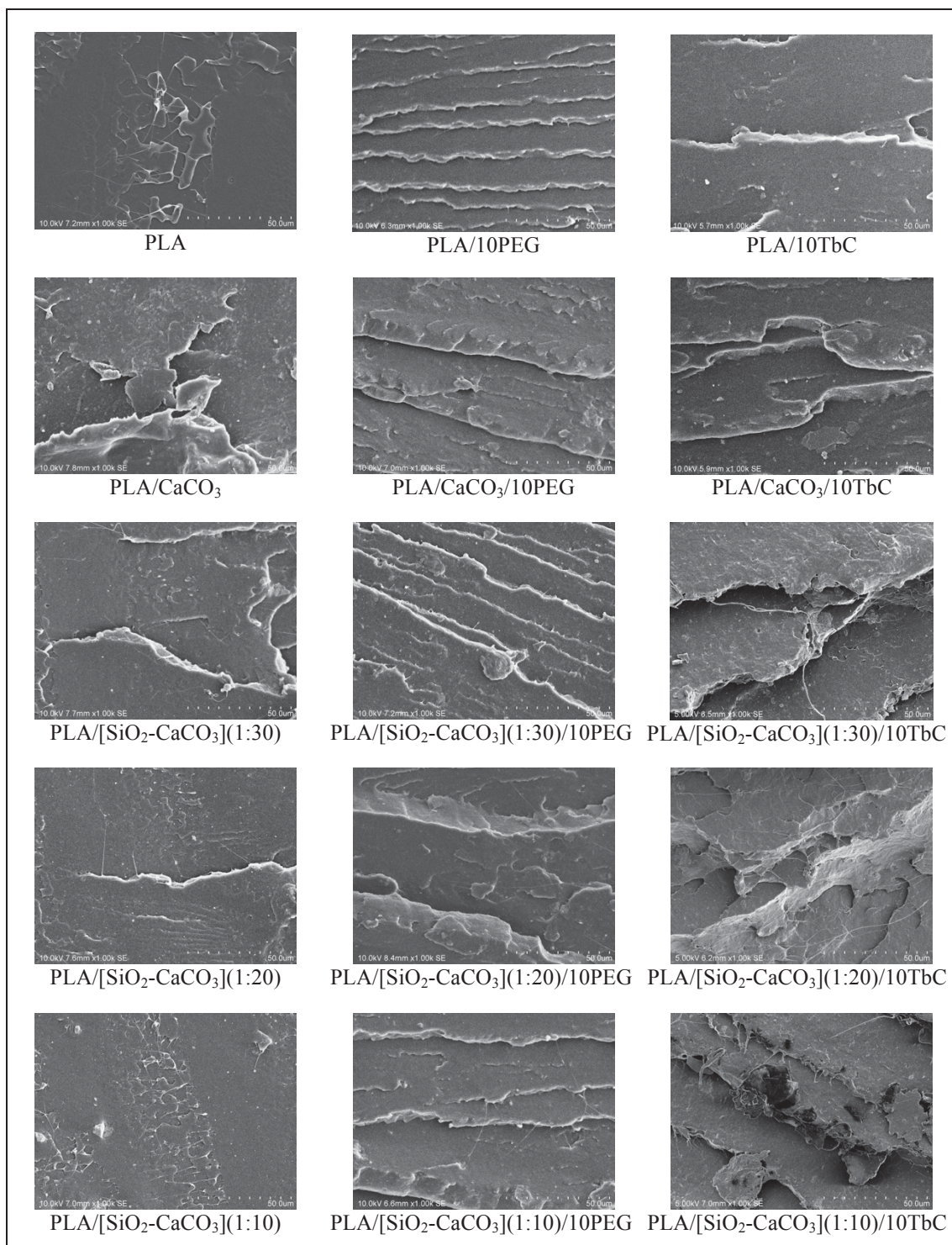


Figure 60. SEM micrographs of fractured surface of PLA, plasticized PLA, plasticized CaCO₃-PLA and [SiO₂-CaCO₃]-PLA nanocomposites at various Si : Ca mole ratio.

It was found that fractured surface of [SiO₂-CaCO₃]-PLA nanocomposites looked smooth similar to that of neat PLA. However, it presented finer local ductile breaking indicating that crack initiation occurred at the CaCO₃ nano-particles but

crack propagation occurred with higher extension. This situation also occurred in the case of plasticized PLA resulting that impact strength of plasticized $[\text{SiO}_2\text{-CaCO}_3]$ -PLA nanocomposites were higher than plasticized CaCO_3 -PLA nanocomposites.

In consideration of SEM micrographs of $[\text{SiO}_2\text{-CaCO}_3]$ -PLA and plasticized $[\text{SiO}_2\text{-CaCO}_3]$ -PLA nanocomposites as shown in Figure 61, it was found that some agglomerations of $\text{SiO}_2\text{-CaCO}_3$ nano-particles occurred in the case of 10 phr TbC plasticized $[\text{SiO}_2\text{-CaCO}_3]$ -PLA nanocomposites. This was the reason of the low percentage of strain at break of this $[\text{SiO}_2\text{-CaCO}_3]$ -PLA nanocomposite. The large agglomerated particles promoted crack initiation and crack propagation during the tensile loading and $[\text{SiO}_2\text{-CaCO}_3]$ -PLA nanocomposite were broken at low elongation.

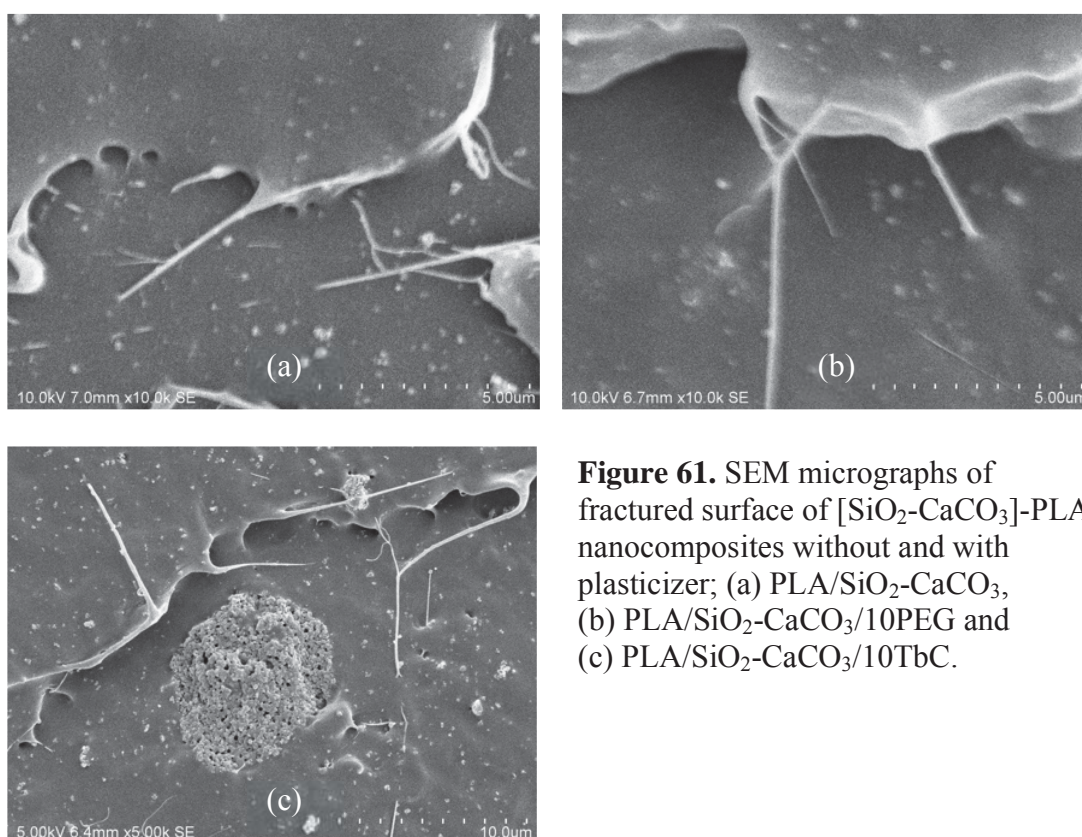


Figure 61. SEM micrographs of fractured surface of $[\text{SiO}_2\text{-CaCO}_3]$ -PLA nanocomposites without and with plasticizer; (a) PLA/ $\text{SiO}_2\text{-CaCO}_3$, (b) PLA/ $\text{SiO}_2\text{-CaCO}_3/10\text{PEG}$ and (c) PLA/ $\text{SiO}_2\text{-CaCO}_3/10\text{TbC}$.

3.7 Rheology studies

The viscosity of PLA and its plasticized nanocomposites at various shear rates are illustrated in Figure 62. The viscosity of CaCO_3 -PLA nanocomposite was lower than PLA as it occurred in phase I and phase II. The main reasons of the decreasing of viscosity are the sizing agent on filler surface and self-lubrication of filler as mentioned in phase I.

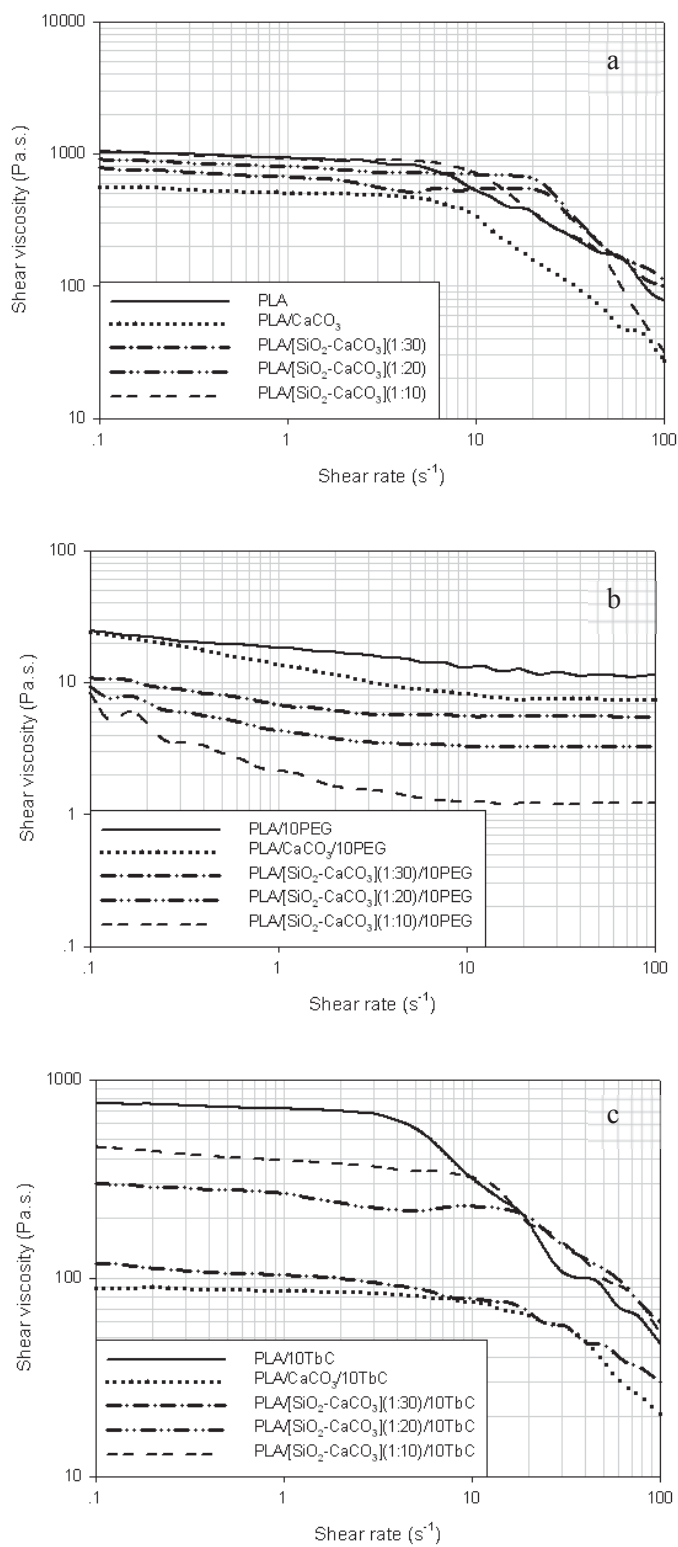


Figure 62. Viscosity of plasticized PLA nanocomposite at various shear rate range.

As seen in Figure 62a, addition of SiO₂-CaCO₃ nano-particle increased viscosity of PLA. Viscosity of [SiO₂-CaCO₃]-PLA nanocomposite was increased according to SiO₂ content on CaCO₃ surface. Rigid surface and porous of SiO₂-CaCO₃ nano-particle inhibited the flow of PLA molecules in melt state as well as the mobility of molecular chains in solid state. Another aspect was the compatibility between PLA and hydrophilic SiO₂-CaCO₃ nano-particle that would induce good adhesion between PLA molecular chains and the particles. SiO₂-CaCO₃ nano-particle thus could obstruct the flow of PLA and the higher content of SiO₂ would cause the higher viscosity of nanocomposite. Furthermore, SiO₂-CaCO₃ nano-particle could retard the reduction of molecular weight of PLA during melt process due to the reaction with fatty acid sizing agent of CaCO₃.

Adding PEG and TbC reduced viscosity of PLA and PLA nanocomposites as shown in Figure 62b and 62c. This was due to plasticizers could penetrate between PLA molecules, enhancing the chain mobility and flow. PEG plasticized PLA showed very low viscosity compared to others due to the transesterification. In PEG plasticized PLA nanocomposite, the addition of SiO₂-CaCO₃ reduced viscosity of PLA obviously. This implied that PEG plasticizer was compatible well with SiO₂ on the surface of CaCO₃. Low molecular weight PEG plasticizer covered the rigid surface of SiO₂, enhancing the flow of PLA by lubricating effect of filler particles. Therefore, the viscosity of PEG plasticized [SiO₂-CaCO₃]-PLA was decreased with respected to the increasing of SiO₂ content. In contrast, the entanglement of PLA polymer chain induced by the branch molecule of TbC decreased viscosity slightly, comparing to PEG plasticized PLA nanocomposite melt. The addition of SiO₂-CaCO₃ nano-particle inhibited the movement of entangled PLA molecular chain. Therefore, the viscosity of TbC plasticized [SiO₂-CaCO₃]-PLA nanocomposites were increased according to the amount of SiO₂ on the CaCO₃ surface.

3.8 Permeability studies

While a package serves as a barrier between the product and the environment to which the product/package system is exposed, the degree of protection varies. This variation is particularly important in connection with the transport of gases, water vapor, or other low molecular weight compounds between the external environment and the internal package environment, which is controlled by the packaging material. Freshly cut vegetables and fruit continue to respire during storage and transportation. The packaging should allow O₂ from outside to diffuse in for breathability. However, by-product of respiration such as CO₂ and water vapor must be removed from inside the package to make it more difficult for bacteria or mould to grow and help the product last longer.

In this phase, PLA, CaCO₃-PLA nanocomposite and plasticized [SiO₂-CaCO₃]-PLA nanocomposite sheet were fabricated using extrusion sheet process as shown in Figure 63. PLA and it plasticized [SiO₂-CaCO₃]-PLA nanocomposites were first compounded by twin-screw extruder and then the compounding pellet was use as materials in the extrusion sheet process. These sheets

were then studied the gas permeability of these PLA and plasticized PLA nanocomposite sheets as Oxygen transmission (O_2TR), carbon dioxide transmission (CO_2TR) and water vapor transmission ($WVTR$).



Figure 63. Extrusion sheet process and PLA, $CaCO_3$ -PLA nanocomposite and plasticized $[SiO_2-CaCO_3]$ -PLA nanocomposite sheets.

Figure 63 illustrates the O_2TR , CO_2TR and $WVTR$ of PLA and its plasticized $[SiO_2-CaCO_3]$ -PLA nanocomposites. The gases transmission values of neat PLA were close to the report of Auras et al [155]. The results revealed that gas permeability of PLA increased with the addition of $CaCO_3$. Generally, The permeation phenomenon is governed by diffusivity and solubility. The higher diffusivity and solubility of gas can result in the higher permeability of gas through the polymer matrix. Moreover, filler does strongly affect achievable crystallinity in melt processing operations. Under such conditions, permeability should be dominated by the level of crystallinity in the samples [55]. As a result of the study, PLA extrusion sheet had low O_2 , CO_2 and water vapor permeability, giving it not suitable for breathable packaging application. However, XRD result showed that the degree of crystallinity of PLA was decreased according to the increasing of the nano-sized $CaCO_3$ content. The effect of fatty acid sizing agent on chain scission of PLA, retarded the crystallization of PLA as discussed in phase I. The good permeation of gases occurred in amorphous $CaCO_3$ -PLA nanocomposite. The gases could diffuse well through amorphous region better than the crystalline region. When fresh fruit and vegetable products were contained in the package, this showed that O_2 , CO_2 gases and water vapor could move through the package easier, thus breathability of the fresh fruits and vegetables products kept in the package must continue to extend their shelf life during transportation or storage.

Plasticizers tended to promote the permeability of PLA. XRD result illustrated that the degree of crystallinity of neat PLA and plasticized PLA were the same. However, T_g of PLA was decreased by the addition of plasticizers. This made PLA more ductile in the rubbery state of polymer. The flexible of polymer matrix enhanced the transmission of gases. Figure 64a and 64b reveal that branch molecule of TbC plasticizer gave the larger gap between PLA polymer chain, therefore O_2TR

and CO₂TR of TbC plasticized PLA nanocomposite were relatively higher than that of PEG plasticized PLA nanocomposite. However, WVTR of TbC plasticized PLA nanocomposites were relatively lower than PEG plasticized PLA nanocomposite. This was due to a hydroxyl group and some carbonyl group in citrate molecule was attached by water vapor and then some hydrogen bonding was occurred, thus the WVTR was retarded. Therefore, the WVTR of TbC plasticized PLA nanocomposite was lower than PEG plasticized PLA and the values of gas permeability was the same as those of neat PLA sheet.

The synergistic effect of SiO₂-CaCO₃ nano-particle and plasticizers could increase breathability of PLA packaging. The gas from the breathing of fruit and vegetable products could move out and the fresh gases in the air surrounded the package could move in through the packaging conveniently. In addition, too-high water vapor permeability is not favor in fruits and vegetables packaging because it make the products inside look withered. WVTR value of TbC plasticized [SiO₂-CaCO₃]-PLA nanocomposite sheet increased slightly, while it contained the highest O₂TR and CO₂TR. Water vapor molecule could not easily move out of the TbC plasticized [SiO₂-CaCO₃]-PLA nanocomposite package, when compared to PEG plasticized [SiO₂-CaCO₃]-PLA nanocomposite package, while the O₂ and CO₂ could easily move pass these package. Consequently, packed fruits and vegetables in the TbC plasticized [SiO₂-CaCO₃]-PLA nanocomposite package could breathe conveniently. Thus, this package could keep fruits and vegetables fresh on shelves and shelf life of fresh products were expanded.

Gas permeability of [SiO₂-CaCO₃]-PLA nanocomposite tended to decrease with respected to the increasing of SiO₂ content on the CaCO₃ surface. As mention earlier, permeability of PLA was controlled by crystallinity of samples. Degree of crystallinity of PLA tended to increase according to the content of SiO₂ in [SiO₂-CaCO₃]-PLA nanocomposite. The high crystallinity polymer had good barrier properties but poor gas permeability. It was found that O₂ permeability dramatically decreased while CO₂ and water vapor permeability slightly decreased with the increase of SiO₂ content on CaCO₃ surface. However, compounding with plasticizers, gave advantage of this [SiO₂-CaCO₃]-PLA nanocomposite as a potential for packaging materials to allow breathability of fruits and vegetables. Moreover, the high porosity of SiO₂ as revealed by BET result implied that gases could be trapped in the porous of SiO₂ and gas permeability was decreased according to the content of SiO₂. This situation could lead to a potential that ethylene gas, produced by ripening of fruits and vegetables in the package, which caused further ripening and spoilage of products, was absorbed in SiO₂ porous. Therefore, the absorption of this gas in porous of SiO₂ on the SiO₂-CaCO₃ nano-particle was able to extend the shelf life of fruits and vegetable. Furthermore, the BET showed that surface area of SiO₂-CaCO₃ nano-particle was increase according to the SiO₂ content on the surface of CaCO₃ particles. This implied that filler with higher content of SiO₂ was likely to absorb gases in higher amount and the packaging was able to extend fresh fruits and vegetables shelf life effectively.

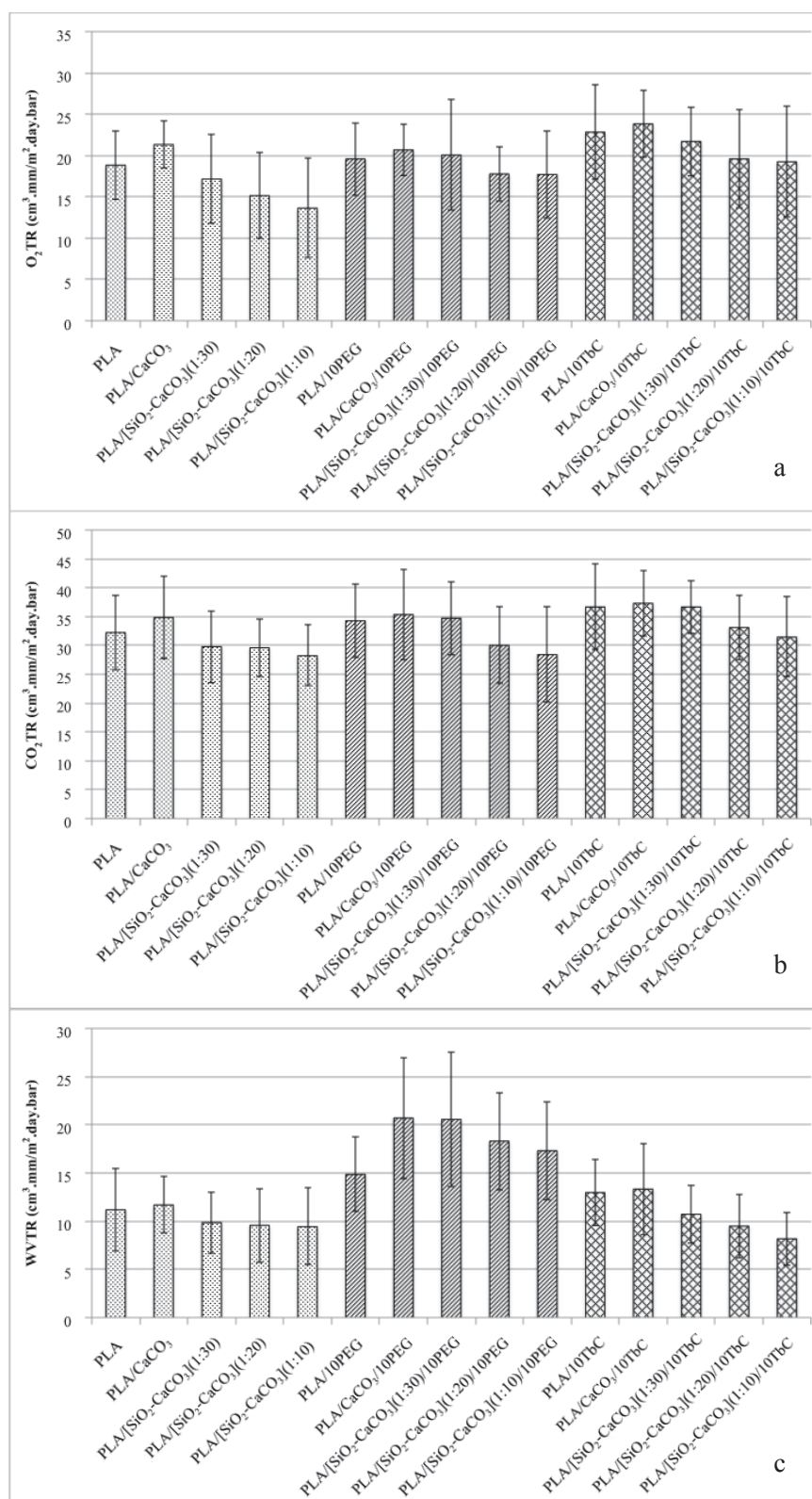


Figure 64. Gas permeability of PLA, CaCO₃-PLA nanocomposite and plasticized [SiO₂-CaCO₃]-PLA nanocomposite sheets; a) O₂TR, b) CO₂TR and c) WVTR.

TbC plasticized [SiO₂-CaCO₃]-PLA nanocomposite, especially in TbC plasticized [SiO₂-CaCO₃](1:30)-PLA nanocomposite, was applicable for active food packaging because it had both absorbability and breathability properties. This plasticized nanocomposite sheet gave highest O₂ and CO₂ permeability but water vapor permeability slightly increased. O₂ and CO₂ molecules could pass through the TbC plasticized [SiO₂-CaCO₃]-PLA nanocomposite easier than neat PLA sheet, while the water vapor permeability were comparable to neat PLA. As a result, gases from the breathing of fruits and vegetables could pass through the TbC plasticized [SiO₂-CaCO₃]-PLA nanocomposite easier than neat PLA package, while the water vapor still pass the package comparable to neat PLA. Thus, the combination between SiO₂-CaCO₃ and TbC plasticizers enhanced the performance in extending of fresh fruits and vegetables. Furthermore, in some applications, which the controlled value of gas permeation was needed, the permeability properties of PLA could be optimized by varying the SiO₂ content on the filler surface and plasticizer content in the plasticized PLA nanocomposite.

CHAPTER 5

CONCLUSIONS AND SUGGESTION

1. Conclusions

In phase I of this research, micro- and nano-sized calcium carbonate were well dispersed and distributed when compounding with poly(lactic acid) (PLA) in a co-rotating twin-screw extruder to produce casting sheets of CaCO₃-PLA biocomposites. However, some agglomeration of nano-sized CaCO₃ was observed due to lab-scale processability. TGA showed that fatty acid as a sizing agent of CaCO₃ induced PLA to degrade at lower temperature. It was found that Yong's modulus of the biocomposites decreased as the size of CaCO₃ decreased, and the content of CaCO₃ increased because of higher content of fatty acid coating on CaCO₃ which caused thermal degradation of PLA during melt process. Moreover, high-speed tensile test showed that the presence of CaCO₃ nano-particles could act as a stress concentration to promote crack initiation in the biocomposites. The slightly increase in storage modulus (E') at temperature above T_g was due to co-crystallization of PLA. As PLA can undergo thermal degradation in melting process, causing chain scission, the shorter chain of PLA could re-orient and T_{cc} (around 110 °C) of PLA was also found in the second heating scan of DSC. Moreover, XRD patterns indicated that CaCO₃ coated with fatty acid lowered the crystallinity of PLA, which was due to thermal degradation of PLA at the presence of fatty acid. Melt flow index test revealed that both micro- and nano-sized CaCO₃ reduced viscosity of PLA due to lubricating effect of rigid particles. In low shear rate range as investigated by the plate and plate rheometer, the additions of small content of CaCO₃ tended to decrease viscosity of CaCO₃-PLA biocomposites but the viscosity of the biocomposites increased again at higher content of CaCO₃. It was found that true viscosity of the unfilled and filled PLA melts decreased with increasing shear rate in a non-linear behavior. Shear sensitivity of filled biocomposites were affected by CaCO₃ particle size and loading, considering from change of power law index in both low and high shear rate ranges. Higher contents of micro-sized CaCO₃ loading could maintain viscosity of extruded PLA to be close to neat PLA, therefore, the adding of micro-sized CaCO₃ could help sheet process of PLA easier. Although adding of super fine nano-sized CaCO₃ (Nano-CaCO₃-280) into PLA reduced mechanical properties due to the induction of thermal degradation of PLA but it could improve processability of this commercialized biopolymer by lowering T_{cc} to around 105 °C, resulting in maintaining melt strength of the biocomposites throughout the casting rolls.

One important requirement for packaging materials is high flexibility at room temperature during storage time. However, PLA is comparatively brittle and stiff at room temperature so modification by adding plasticizers is needed for PLA in order to apply it for flexible-desired applications such as food packaging. In phase II, PLA, nano-CaCO₃-280 and plasticizers was compounded in plasticized CaCO₃-PLA nanocomposites by a co-rotating twin-screw extruder, then the specimens were prepared by compression molding because of low viscosity by adding plasticizers.

It was found that polyethylene glycols (PEGs) and tributyl citrate (TbC) plasticizers could improve tensile elongation at break and flexibility of CaCO₃-PLA nanocomposites as well as caused good dispersion of CaCO₃ in plasticized PLA matrix. There was no phase separation in plasticized PLA even at the high contents of plasticizers as 20 phr. Furthermore, the fracture behavior of CaCO₃-PLA nanocomposites changed from brittle to ductile behavior after plasticizers were incorporated. DMA results showed that both plasticizers lowered T_g of PLA nanocomposites to below 50 °C, causing higher flexibility. The slightly increase in storage modulus (E') of plasticized PLA nanocomposites at temperature above T_g, which was due to co-crystallization of PLA, was also founded. XRD analysis showed that PEG and TbC plasticizers could improve crystallinity of CaCO₃-PLA nanocomposite because plasticizers could enhance the movement of PLA polymer chains to fold and crystallize. DSC results revealed that the plasticizers could reduce T_{cc} and T_m of PLA, which was in good agreement with rheology studies that viscosity of plasticized CaCO₃-PLA nanocomposites was dramatically lower than those of neat PLA. Moreover, GPC analysis showed that Mw of plasticized PLA was lower than PLA and Mw of PEG plasticized PLA was dramatically lower than TbC plasticized PLA. PEG plasticizer reacted with PLA at elevated temperature, causing further reduction of PLA molecular weight. The shorter chain of PLA was the cause of lower mechanical properties and melting temperature. While, TbC plasticizer could also react with PLA by transesterification. However, as TbC was a branch molecule so it caused reacted PLA to entangle with the others. Thus, TbC slightly lowered shear viscosity at higher shear rate. This caused the antagonism of thermal degradation effect due to fatty acid coated on CaCO₃ fillers and transesterification of TbC plasticizers on rheology behavior of CaCO₃-PLA nanocomposites. TGA also showed that thermal stability of PLA nanocomposites was dramatically dropped when the content of plasticizers increased. Most nano-sized CaCO₃ available in the global market was treated with some sizing agent as fatty acid to protect them from re-agglomeration during storage and handling. Thus, adding TbC plasticizer could improve flexibility as well as maintain processability of CaCO₃-PLA nanocomposites, especially handling in casting rolls.

Moreover, good breathability and gas absorbability of food packaging materials are highly considerate. The successful preparation of high porosity and hydrophilic modification of CaCO₃ surface was performed in phase III of this research. Only nano-CaCO₃-280 nano-particles was surface modified by SiO₂ via sol gel-process using TEOS as precursor. Modified SiO₂-CaCO₃ nano-particles were prepared with different Si : Ca ratios. SEM micrographs illustrate that SiO₂ layers coated around the CaCO₃ nano-particles causing the slightly increase in particle sizes, however, the particle size of SiO₂-CaCO₃ particles were still in the range of nano-scale. XRD did not illustrate the shift of CaCO₃ characteristic peak, however the characteristic broad diffraction of amorphous SiO₂ was also revealed in SiO₂-CaCO₃ diffraction pattern. Agglomerated particle sized of SiO₂-CaCO₃ was decreased because the hydrophilic SiO₂ coating surface enhanced good dispersion in water medium of the test. It was found that the Si : Ca wt% ratio was increased with respect to the Si : Ca mole ratio used in the reaction. Adding of SiO₂-CaCO₃ nano-particles had positive effect on mechanical properties and thermal properties of PLA. Compared to CaCO₃-PLA and plasticized CaCO₃-PLA nanocomposite, incorporating

SiO₂-CaCO₃ at the same content increased elastic modulus, the percentage of strain at break and notched impact strength of PLA nanocomposites. These properties of [SiO₂-CaCO₃]-PLA nanocomposite increased with respect to increasing of SiO₂ content on the surface of CaCO₃ nano-particles. This implies that better compatibility between polymer matrix and filler was achieved after modification surface of CaCO₃ with SiO₂. Moreover, TGA showed that thermal stability of CaCO₃-PLA nanocomposites and its plasticized nanocomposites was increased according to SiO₂ content in the CaCO₃ surface because SiO₂ could absorb more heat, thus retarded thermal degradation of PLA and maintained PLA molecular weight during melt process. DSC showed in a good agreement that T_{cc} and T_m of the plasticized [SiO₂-CaCO₃]-PLA nanocomposites increased due to improvement in thermal stability of PLA. However, flexibility of the plasticized [SiO₂-CaCO₃]-PLA nanocomposite decreased as T_g of the nanocomposites increased according to SiO₂ content on the surface of CaCO₃. The rigidity of SiO₂ surface inhibited the movement of PLA polymer chain enhancing the increase of T_g, T_{cc} and T_m. SEM micrographs show good dispersion of SiO₂-CaCO₃ in PLA and plasticized PLA nanocomposites. Moreover, XRD results showed the improvement of crystallinity of plasticized PLA nanocomposites due to the compatibility between polymer matrix and SiO₂-CaCO₃ nano-particles. However, some agglomeration of filler were found in TbC plasticized [SiO₂-CaCO₃]-PLA nanocomposite. SEM also illustrated that the fracture behavior of [SiO₂-CaCO₃]-PLA nanocomposite was ductile, causing the increase of impact strength. The addition of porous filler as SiO₂-CaCO₃ retarded the movement of PLA polymer chain as well as the flow of PLA melt, resulting in the increase of PLA viscosity. Thus, adding SiO₂-CaCO₃ could maintain the viscosity of PLA and help handling process in casting rolls.

Finally, these nanocomposite extrusion sheets had high potential to use as packaging materials to maintain freshness of fruits and vegetables. Freshly cut vegetables and fruit continue to respire during storage and transportation. The packaging should allow O₂ from outside to diffuse in for breathability. However, by-product of respiration such as CO₂ and water vapor must be removed from inside the package to make it more difficult for bacteria or mould to grow and help the product last longer. As a result of the study, PLA extrusion sheet had low O₂, CO₂ and water vapor permeability, giving it is not suitable for breathable packaging application. It was found that adding nano-sized CaCO₃ gave PLA higher O₂, CO₂ and water vapor permeability than neat PLA because of lower crystallinity, which allowed gas to diffuse through PLA sheet matrix. Moreover, adding PEG and TbC plasticizers gave PLA a slightly higher O₂ and CO₂ but much higher water vapor permeability than CaCO₃-PLA nanocomposite because of better mobility of PLA polymer chains. In this research, adding SiO₂-CaCO₃ nano-particles lower O₂, CO₂ and water vapor permeability of PLA due to higher crystallinity. It was found that O₂ permeability dramatically decreased while CO₂ and water vapor permeability slightly decreased with the increase of SiO₂ content on CaCO₃ surface. However, compounding with plasticizers, gave advantage of this [SiO₂-CaCO₃]-PLA nanocomposite as a potential for packaging materials to allow breathability of fruits and vegetables. In case of PEG and TbC plasticized PLA, adding SiO₂-CaCO₃ nano-particles increased O₂ and CO₂ permeability but showed different effect on water vapor permeability. It was found that [SiO₂-CaCO₃]-PLA nanocomposites with PEG plasticizer had higher water vapor

permeability due to hydrophilic hydroxyl groups. However, too-high water vapor permeability is not favor in fruits and vegetables packaging because it make the products inside look withered. $[\text{SiO}_2\text{-CaCO}_3]$ -PLA nanocomposites with TbC plasticizer, which gave higher O_2 and CO_2 permeability but slight increase in water vapor permeability, were suitable for this application, especially, the $[\text{SiO}_2\text{-CaCO}_3](1:30)$ gave highest O_2 and CO_2 permeability but maintain water vapor permeability to neat PLA. Therefore, the TbC plasticized $[\text{SiO}_2\text{-CaCO}_3]$ -PLA nanocomposite could be alternative packaging materials to extend the shelf life of the products. CO_2 and water vapor gas from breathing of fruits and vegetables could diffuse throughout the packaging and fresh gases in the air as O_2 surrounded the package could diffuse through the plasticized $[\text{SiO}_2\text{-CaCO}_3]$ -PLA nanocomposite package easier than neat PLA package. Thus, the combination of $\text{SiO}_2\text{-CaCO}_3$ nanoparticles and plasticizers could enhance the performance of active packaging in extending shelf life of fresh fruits and vegetables. In addition, TbC plasticizers can be used as a processing aid agent because it is able to reduce viscosity of PLA and enhance PLA processability in the industrial scale process. The plasticized PLA packaging will be softer and tougher. SiO_2 content on the surface of CaCO_3 filler will enhance the plasticized PLA nanocomposite packaging to be stronger and more stable at high temperature. Furthermore, the permeability value of PLA can be optimized for tailor-made application by adjusting the SiO_2 contents on CaCO_3 surface and plasticizer contents in the plasticized PLA nanocomposites. Therefore, the high performance active packaging can be innovated.

2. Suggestion for future study

From this research, in order to optimize breathability and gas absorbability of PLA packaging films by adding $\text{SiO}_2\text{-CaCO}_3$ nano-particles in plasticized PLA, the controlling ratio of the SiO_2 content and plasticizer loading should be considered for each desired application. The plasticized PLA packaging films will be softer and tougher. As a result, this packaging can be kept in low temperature as the storage temperature of fruits and vegetables, preventing the risk of breaking films in refrigerator. Generally, plasticizers can act as a processing aid to reduce viscosity of PLA but causing the difficulty in handling of casting rolls. Adding $\text{SiO}_2\text{-CaCO}_3$ nano-particles into PLA nanocomposite, make it can be fabricated into the uniform sheet by extrusion sheet process, following by casting rolls.

The mechanical properties of PLA can be optimized by adjusting the content of SiO_2 and plasticizers. In food packaging application, a package is used as a barrier between the packed product and the environment outside. This package is used to cover the products in connection with the transport of gases, water vapor, or other low molecular weight compounds between the external environment and the internal package environment, which is controlled by the packaging material. Plasticizers and CaCO_3 particles promoted the permeability of gases in PLA while $\text{SiO}_2\text{-CaCO}_3$ nanoparticles inhibited it. The barrier properties and permeability of each food packaging materials are different. Thus, the optimum permeability of each food packaging can be proper by adjusting the content of these additives. The addition of TbC plasticizer and $\text{SiO}_2\text{-CaCO}_3$ in PLA gave better advantage for PLA application in packaging film. This nanocomposite was more flexible than neat PLA with the less reduction in

modulus. In addition, the porosity of SiO_2 showed the possibility to trap gas resulting in keeping the fruits and vegetable fresh. The breathability of fruits and vegetable after collecting can keep going on, while gas is trapped and water vapor is retained in the package. This packaging can extend storage and logistic time of fruits and vegetables.

This research can be extent by studying the fabrication in other processing methods such as thermoforming, injection and blow film process. This knowledge of research can be innovated to use for food packaging. However, each food has different requirements for barrier and permeability, therefore the in-depth study of packaging for each food should be done to perform the innovative packaging materials.

REFERENCES

1. Bioplastics [online]. Accessed 7 November 2008. Available from <http://www.nia.or.th/bioplastics/>
2. National Innovation Agency. Ministry of Science and Technology. National Roadmap for the Development of Bioplastic Industry, Approved pursuant to the Cabinet Resolution no. 24/2551, Tuesday 22 July 2008.
3. Plastic Production [online]. Accessed 22 July 2011. Available from <http://www.plasticseurope.org>
4. Kuhlke, B. and T. Walsh. World Plastics Market Review [online]. Accessed 22 July 2011. Available from <http://www.polymerplace.com/articles/WorldPlasticsReview.pdf>
5. Methods of Processing Plastic [online]. Accessed 22 July 2011. Available from <http://www.plasticsindustry.com/plastic-processing-methods.asp>
6. Ray, S. S. and M. Bousmina. "Biodegradable Polymers and Their Layered Silicate Nanocomposites: In Greening the 21st Century Materials World." Progress in Materials Science 50, 8 (November 2005): 962-1079.
7. Chen, C.-C. et al. "Preparation and Characterization of Biodegradable PLA Polymeric Blends." Biomaterials 24, 7 (March 2003): 1167-1173.
8. Komatsuka, T., A. Kusakabe, and K. Nagai. "Characterization and Gas Transport Properties of Poly(lactic acid) Blend Membranes." Desalination 234, 1-3 (December 2008): 212-220.
9. Bioplastic Capacity [online]. Accessed 7 November 2008. Available from <http://www.thaibioplast.com/doc/chapter2.doc>
10. Bioplastic [online]. Accessed 7 November 2008. Available from <http://www.thaibioplast.com>
11. Biocompostable-Bioplastic [online]. Accessed 7 November 2008. Available from <http://www.worldcentric.org/biocompostables/bioplastics.html>
12. Science-Bioplastic [online]. Accessed 7 November 2008. Available from <http://web-japan.org/trends/science/sci031212.html>
13. Life-Cycle Economy [online]. Accessed 20 July 2011. Available from <http://www.eurokamczech.com/Biokam/Biokam/web/Life-CycleEconomy.html>
14. Asia's Future Bioplastics Hub [online]. Accessed 26 January 2011. Available from <http://www.chemanager-online.com/en/topics/chemicalsdistribution/asia-s-future-bioplastics-hub>
15. Natureworks Attracts \$150 Million Equity Investment from Leading Thailand Company PTT Chemical [online]. Accessed 26 January 2012. Available from <http://www.natureworkslc.com/News-and-Events/Press-Releases/2011/10-12-11-NatureWorks-attracts-PTT-Chemical-equity-investment.aspx>
16. Green ABS [online]. Accessed 28 January 2012. Available from http://www.irpc.co.th/?page_id=2660&lang=en

17. Ali, S. R. and K. Pakistan. THAILAND: Trial for Fully Compostable Plastics in Q3. SCG Unit Foresees Viability in Three Years [online]. Accessed 28 January 2012. Available from <http://www.gupta-verlag.com/general/news/industry/10042/THAILAND-Trial-for-fully-compostable-plastics-in-Q3-SCG-unit-foresees-viability-in-three-years>
18. An "Educational" Seminar on The Chemicals Industry [online]. Accessed 28 January 2012. Available from http://www1.siamcement.com/pdf/Presentation/SCG_Chemicals.pdf
19. Siriaoutan, A. Puff & Pie Bioplastic Bags: Pilot Cooperation Project by Thai Airways and SCG Chemicals Supported by NIA to Encourage Environmental Awareness [online]. Accessed 29 January 2012. Available from [http://www.nia.or.th/2009/pr/images/2010/6/bioplastic/Press Release - Puff Pie.pdf](http://www.nia.or.th/2009/pr/images/2010/6/bioplastic/Press%20Release%20-%20Puff%20Pie.pdf)
20. Kanjanasoon, T. Thai Airways Launches Biofuels Flight [online]. Accessed 29 January 2012. Available from <http://www.thailandoutlook.tv/tan/ViewData.aspx?DataID=1050990>
21. Jiang, L., J. Zhang, and M. P. Wolcott. "Comparison of Polylactide/Nano-sized Calcium Carbonate and Polylactide/Montmorillonite Composites: Reinforcing Effects and Toughening Mechanisms." Polymer 48, 26 (December 2007): 7632-7644.
22. Lam, T. D. et al. "Effect of Nanosized and Surface-Modified Precipitated Calcium Carbonate on Properties of CaCO₃/Polypropylene Nanocomposites." Materials Science and Engineering: A 501, 1-2 (February 2009): 87-93.
23. Sorrentino, A., G. Gorrasi, and V. Vittoria. "Potential Perspectives of Bio-Nanocomposites for Food Packaging Applications." Trends in Food Science & Technology 18, 2 (February 2007): 84-95.
24. Chang, J.-H. et al. "Poly(lactic acid) Nanocomposites: Comparison of Their Properties with Montmorillonite and Synthetic Mica (II)." Polymer 44, 13 (June 2003): 3715-3720.
25. Bartczak, Z. et al. "Toughness Mechanism in Semi-Crystalline Polymer Blends: II. High-Density Polyethylene Toughened with Calcium Carbonate Filler Particles." Polymer 40, 9 (April 1999): 2347-2365.
26. Wilbrink, M. W. L. et al. "Toughenability of Nylon-6 with CaCO₃ Filler Particles: New Findings and General Principles." Polymer 42, 26 (December 2001): 10155-10180.
27. Zuiderduin, W. C. J. et al. "Toughening of Polypropylene with Calcium Carbonate Particles." Polymer 44, 1 (January 2003): 261-275.
28. Jiang, L. et al. "Strengthening Acrylonitrile-Butadiene-Styrene (ABS) with Nano-sized and Micron-sized Calcium Carbonate." Polymer 46, 1 (January 2005): 243-252.
29. CaCO₃ [online]. Accessed 25 April 2011. Available from <http://www.bikudo.com>
30. Gai, G.-S. et al. "Preparation and Properties of Composite Mineral Powders." Powder Technology 153, 3 (June 2005): 153-158.
31. Calcium carbonate [online]. Accessed 20 July 2011. Available from http://en.wikipedia.org/wiki/calcium_carbonate

32. Xun-qiu, W. and J. Deng-gao. "Modification of Nanometer Calcium Carbonate for Water-Borne Architectural Coatings." Journal of China University of Mining & Technology 18, 1 (March 2008): 78-81.
33. Fu, S.-Y. et al. "Effects of Particle Size, Particle/Matrix Interface Adhesion and Particle Loading on Mechanical Properties of Particulate-Polymer Composites." Composites Part B: Engineering 39, 6 (September 2008): 933-961.
34. Pillin, I., N. Montrelay, and Y. Grohens. "Thermo-Mechanical Characterization of Plasticized PLA: Is the miscibility the only significant factor?" Polymer 47, 13 (June 2006): 4676-4682.
35. Ljungberg, N. and B. Wesslén. "Tributyl Citrate Oligomers as Plasticizers for Poly(lactic acid): Thermo-Mechanical Film Properties and Aging." Polymer 44, 25 (December 2003): 7679-7688.
36. Van Tuil, R. et al. Properties of Biobased Packaging Materials in Biobased Packaging Materials for the Food Industry: Status and Perspectives. Frederiksberg: KVL, 2000.
37. Weber, C. J. Biobased Packaging Materials [online]. Accessed 5 September 2011. Available from [http://www.biodeg.net/fichiers/Book on biopolymers \(Eng\).pdf](http://www.biodeg.net/fichiers/Book on biopolymers (Eng).pdf)
38. Plackett, D. Biopolymers-New Materials for Sustainable Films and Coatings. John Wiley & Sons, Inc., 2011.
39. Yu, L. Biodegradable Polymer Blends and Composites from Renewable Resources. New Jersey: John Willey & Sons, Inc., 2009.
40. Idealised Closed Loop Life Cycle [online]. Accessed 20 July 2011. Available from <http://en.european-bioplastics.org/press/press-pictures/labelling-logos-charts/>
41. Smith, R. Biodegradable Polymers for Industrial Applications. Cambridge: Woodhead Publishing Ltd., 2005.
42. Jérôme, C. and P. Lecomte. "Recent Advances in the Synthesis of Aliphatic Polyesters by Ring-Opening Polymerization." Advanced Drug Delivery Reviews 60, 9 (June 2008): 1056-1076.
43. Global bioplastic consumption [online]. Accessed 5 October 2011. Available from <http://en.european-bioplastics.org/market/>
44. Enomoto, K., M. Ajioka, and A. Yamaguchi. Polyhydroxycarboxylic Acid and Preparation Process Thereof. United States 5310865. 10 May 1994.
45. Gruber, P. R. et al. Continuous Process for Manufacture of Lactide Polymers with Controlled Optical Purity. United States 6005067. 21 December 1999.
46. Gruber, P. R. et al. Continuous Process for Manufacture of Lactide Polymers with Purification by Distillation. United States 5357035. 18 August 1994.
47. Gruber, P. R. et al. Hydroxyl-Terminated Lactide Polymer Composition. United States 5446123. 29 August 1995.
48. Gruber, P. R. et al. Melt-Stable Lactide Polymer Composition and Process for Manufacture Thereof. United States 6143863. 7 November 2000.
49. Deshpande, A. P. Poly lactic acid [online]. Accessed 1 September 2011. Available from http://203.199.213.48/1560/1/pla_apd_nagarjuna.pdf
50. PLA Typical Properties [online]. Accessed 1 September 2011. Available from http://www.ides.com/generics/PLA/PLA_typical_properties.htm

51. Polylactic Acid (PLA): Properties, Market and Perspectives [online]. Accessed 1 September 2011. Available from <http://biopol.free.fr/index.php/polylactic-acid-pla-properties-market-and-perspectives>
52. Solubility [online]. Accessed 4 September 2011. Available from http://www.natureworksllc.com/Technical-Resources/~media/Technical_Resources/Properties_Documents/PropertiesDocument_Solubility-Test-Results_pdf.pdf
53. Rhim, J.-W., S.-I. Hong, and C.-S. Ha. "Tensile, Water Vapor Barrier and Antimicrobial Properties of PLA/Nanoclay Composite Films." LWT - Food Science and Technology 42, 2 (March 2009): 612-617.
54. Biodegradable Polyester [online]. Accessed 3 September 2011. Available from <http://www.biodeg.net/bioplactic.html> - biodegradable
55. Bao, L. et al. "Gas permeation Properties of Poly(lactic acid) Revisited." Journal of Membrane Science 285, 1-2 (November 2006): 166-172.
56. Barrer [online]. Accessed 3 September 2011. Available from <http://en.wikipedia.org/wiki/Barrer>
57. Polylactic acid [online]. Accessed 4 September 2011. Available from http://en.wikipedia.org/wiki/Polylactic_acid
58. Vink, E. T. H. et al. "Applications of Life Cycle Assessment to NatureWorks™ Polylactide (PLA) Production." Polymer Degradation and Stability 80, 3 (2003): 403-419.
59. Enantiomer [online]. Accessed 5 September 2011. Available from <http://en.wikipedia.org/wiki/Enantiomer>
60. Biodegradable and Biorenewable Materials Based on Lactic Acid [online]. Accessed 5 September 2011. Available from <http://www.cem.msu.edu/~smithmr/Lactide.htm>
61. Ikada, Y. and H. Tsuji. "Biodegradable Polyesters for Medical and Ecological Applications." Macromolecular Rapid Communications 21, 3 (February 2000): 117-132.
62. Sagala, F. H. et al. "PLA (Polylactic acid) Nanofibers for Medical Application." Arena Tekstil 24, 2 (December 2009): 94-101.
63. Lim, L. T., R. Auras, and M. Rubino. "Processing Technologies for Poly(lactic acid)." Progress in Polymer Science 33, 8 (August 2008): 820-852.
64. Ljungberg, N., T. Andersson, and B. Wesslén. "Film extrusion and Film Weldability of Poly(lactic acid) Plasticized with Triacetone and Tributyl Citrate." Journal of Applied Polymer Science 88, 14 (June 2003): 3239-3247.
65. Gruber, P. R. et al. Melt-Stable Amorphous Lactide Polymer Film and Process for Manufacturing Thereof. United States 5484881. 16 January 1996.
66. Miyata, T. and T. Masuko. "Crystallization Behaviour of Poly(l-lactide)." Polymer 39, 22 (October 1998): 5515-5521.
67. Simpson, W. G. Plastics and Resin Compositions. Cambridge: The Royal Society of Chemistry, 1995.
68. Harper, C. A. Handbook of Plastics, Elastomers, and Composites. 2nd edition. New York: McGraw-Hill, Inc., 1992.
69. Chen, B.-K. et al. "Ductile PLA Modified with Methacryloyloxyalkyl Isocyanate Improves Mechanical Properties." Polymer 51, 21 (October 2010): 4667-4672.

70. Finkenstadt, V. L. et al. "Poly(lactic acid) Green Composites using Oilseed Coproducts as Fillers." Industrial Crops and Products 26, 1 (June 2007): 36-43.
71. Signori, F., M.-B. Coltelli, and S. Bronco. "Thermal Degradation of Poly(lactic acid) (PLA) and Poly(butylene adipate-co-terephthalate) (PBAT) and Their Blends Upon Melt Processing." Polymer Degradation and Stability 94, 1 (January 2009): 74-82.
72. Callister, W. D. Materials Science and Engineering : An Introduction. New York: John Wiley, 1985.
73. Gachter, R. and H. Muller. Plastics Additives Handbook. Ohio: Hanser/Gardner Publications, Inc., 1993.
74. Plasticizer [online]. Accessed 6 September 2011. Available from <http://www.tciamerica.com/product/materials-chem/F018.shtml>
75. Hermansky, S. J. et al. "Effects of Polyethylene Glycol 400 (PEG 400) Following 13 Weeks of Gavage Treatment in Fischer-344 Rats." Food and Chemical Toxicology 33, 2 (February 1995): 139-149.
76. Zalipsky, S. "Chemistry of Polyethylene Glycol Conjugates with Biologically Active Molecules." Advanced Drug Delivery Reviews 16, 2-3 (September 1995): 157-182.
77. Kumar, V., V. K. Sharma, and D. S. Kalonia. "Effect of Polyols on Polyethylene Glycol (PEG)-Induced Precipitation of Proteins: Impact on Solubility, Stability and Conformation." International Journal of Pharmaceutics 366, 1-2 (January 2009): 38-43.
78. Polyethylene Glycol [online]. Accessed 7 September 2011. Available from <http://chemicaland21.com/industrialchem/organic/POLYETHYLENE GLYCOL.htm>
79. Johnson, K. et al. "Effect of Triacetin and Polyethylene Glycol 400 on Some Physical Properties of Hydroxypropyl Methylcellulose Free Films." International Journal of Pharmaceutics 73, 3 (July 1991): 197-208.
80. Heinämäki, J. T. et al. "The Mechanical and Moisture Permeability Properties of Aqueous-Based Hydroxypropyl Methylcellulose Coating Systems Plasticized with Polyethylene Glycol." International Journal of Pharmaceutics 112, 2 (November 1994): 191-196.
81. Sakellariou, P., R. C. Rowe, and E. F. T. White. "An evaluation of the interaction and plasticizing efficiency of the polyethylene glycols in ethyl cellulose and hydroxypropyl methylcellulose films using the torsional braid pendulum." International Journal of Pharmaceutics 31, 1-2 (July 1986): 55-64.
82. Srinivasa, P. C., M. N. Ramesh, and R. N. Tharanathan. "Effect of Plasticizers and Fatty Acids on Mechanical and Permeability Characteristics of Chitosan Films." Food Hydrocolloids 21, 7 (October 2007): 1113-1122.
83. Parra, D. F. et al. "Influence of Poly(ethylene glycol) on the Thermal, Mechanical, Morphological, Physical-Chemical and Biodegradation Properties of Poly(3-hydroxybutyrate)." Polymer Degradation and Stability 91, 9 (September 2006): 1954-1959.

84. Byun, Y., Y. T. Kim, and S. Whiteside. "Characterization of an Antioxidant Polylactic Acid (PLA) Film Prepared with α -Tocopherol, BHT and Polyethylene Glycol using Film Cast Extruder." Journal of Food Engineering 100, 2 (September 2010): 239-244.
85. Hassouna, F. et al. "New Approach on the Development of Plasticized Polylactide (PLA): Grafting of Poly(ethylene glycol) (PEG) via Reactive Extrusion." European Polymer Journal 47, 11 (November 2011): 2134-2144.
86. Edenbaum, J. Plastics Additives and Modifiers Handbook. New York: Van Nostrand Reinhold, 1992.
87. Bolgar, M. et al. Handbook for The Chemical Analysis of Plastic and Polymer Additives. Boca Raton: CRC Press Taylor & Francis Group, LLC, 2008.
88. Rahman, M. and C. S. Brazel. "The Plasticizer Market: An Assessment of Traditional Plasticizers and Research Trends to Meet New Challenges." Progress in Polymer Science 29, 12 (December 2004): 1223-1248.
89. Tributyl Citrate [online]. Accessed 7 September 2011. Available from http://www.newdruginfo.com/pharmacopeia/usp28/v28230/usp28nf23s0_m84970.htm
90. Tributyl Citrate (TbC) [online]. Accessed 7 September 2011. Available from http://www.chemicalbook.com/ChemicalProductProperty_EN_CB2299345.htm
91. Tributyl Citrate [online]. Accessed 7 September 2011. Available from <http://chemicalland21.com/industrialchem/plasticizer/TRIBUTYL CITRATE.htm>
92. Lemmouchi, Y. et al. "Plasticization of Poly(lactide) with Blends of Tributyl Citrate and Low Molecular Weight Poly(d,l-lactide)-b-Poly(ethylene glycol) Copolymers." European Polymer Journal 45, 10 (October 2009): 2839-2848.
93. Lin, S.-Y., K.-S. Chen, and L. Run-Chu. "Organic Esters of Plasticizers Affecting The Water Absorption, Adhesive Property, Glass Transition Temperature and Plasticizer Permanence of Eudragit Acrylic Films." Journal of Controlled Release 68, 3 (September 2000): 343-350.
94. Andreuccetti, C., R. A. Carvalho, and C. R. F. Grosso. "Effect of Hydrophobic Plasticizers on Functional Properties of Gelatin-Based Films." Food Research International 42, 8 (October 2009): 1113-1121.
95. Bordes, P., E. Pollet, and L. Avérous. "Nano-Biocomposites: Biodegradable Polyester/Nanoclay Systems." Progress in Polymer Science 34, 2 (February 2009): 125-155.
96. Armentano, I. et al. "Biodegradable Polymer Matrix Nanocomposites for Tissue Engineering: A Review." Polymer Degradation and Stability 95, 11 (November 2010): 2126-2146.
97. Huang, M., J. Yu, and X. Ma. "High Mechanical Performance MMT-Urea and Formamide-Plasticized Thermoplastic Cornstarch Biodegradable Nanocomposites." Carbohydrate Polymers 63, 3 (March 2006): 393-399.
98. Jana, S. C. and S. Jain. "Dispersion of Nanofillers in High Performance Polymers using Reactive Solvents as Processing Aids." Polymer 42, 16 (July 2001): 6897-6905.
99. Konwar, U., N. Karak, and M. Mandal. "Mesua Ferrea L. Seed Oil Based Highly Thermostable and Biodegradable Polyester/Clay Nanocomposites." Polymer Degradation and Stability 94, 12 (December 2009): 2221-2230.

100. Dangtungee, R. and P. Supaphol. "Melt Rheology and Extrudate Swell of Titanium (IV) Oxide Nano-particle-Filled Isotactic Polypropylene: Effects of Content and Surface Characteristics." Polymer Testing 27, 8 (December 2008): 951-956.
101. Luyt, A. S. et al. "Morphology, Mechanical and Thermal Properties of Composites of Polypropylene and Nanostructured Wollastonite Filler." Polymer Testing 28, 3 (May 2009): 348-356.
102. Evans, S. J., P. J. Haines, and G. A. Skinner. "The Thermal Degradation of Polyester Resins II. The Effects of Cure and of Fillers on Degradation." Thermochimica Acta 291, 1-2 (April 1997): 43-49.
103. La Mantia, F. P. and M. Morreale. "Green Composites: A Brief Review." Composites Part A: Applied Science and Manufacturing 42, 6 (June 2011): 579-588.
104. Gorna, K. et al. "Amorphous Calcium Carbonate in Form of Spherical Nanosized Particles and Its Application as Fillers for Polymers." Materials Science and Engineering: A 477, 1-2 (March 2008): 217-225.
105. Chang, J.-H., Y. U. An, and G. S. Sur. "Poly(lactic acid) Nanocomposites with Various organoclays. I. Thermomechanical Properties, Morphology, and Gas Permeability." Journal of Polymer Science Part B: Polymer Physics 41, 1 (January 2003): 94-103.
106. Wu, D. et al. "Rheology and Thermal Stability of Polylactide/Clay Nanocomposites." Polymer Degradation and Stability 91, 12 (December 2006): 3149-3155.
107. Ogata, N. et al. "Structure and Thermal/Mechanical Properties of Poly(l-lactide)-Clay Blend." Polymer Degradation and Stability 35, 2 (January 1997): 389-396.
108. Balakrishnan, H. et al. "Novel Toughened Polylactic Acid Nanocomposite: Mechanical, Thermal and Morphological Properties." Materials & Design 31, 7 (August 2010): 3289-3298.
109. Thellen, C. et al. "Influence of Montmorillonite Layered Silicate on Plasticized Poly(l-lactide) Blown Films." Polymer 46, 25 (November 2005): 11716-11727.
110. Paul, M.-A. et al. "New Nanocomposite Materials Based on Plasticized Poly(l-lactide) and Organo-Modified Montmorillonites: Thermal and Morphological Study." Polymer 44, 2 (January 2003): 443-450.
111. Liu, X. et al. "The Preparation and Properties of Biodegradable Polyesteramide Composites Reinforced with Nano-CaCO₃ and Nano-SiO₂." Materials Letters 61, 19-20 (August 2007): 4216-4221.
112. Yan, S. et al. "Structural Characteristics and Thermal Properties of Plasticized Poly(l-lactide)-Silica Nanocomposites Synthesized by Sol-Gel Method." Materials Letters 61, 13 (May 2007): 2683-2686.
113. Ray, S. S., J. Bandyopadhyay, and M. Bousmina. "Thermal and Thermomechanical Properties of Poly[(butylene succinate)-co-Adipate Nanocomposite]." Polymer Degradation and Stability 92, 5 (May 2007): 802-812.
114. Ray, S. S. and M. E. Makhatha. "Thermal Properties of Poly(ethylene succinate) Nanocomposite." Polymer 50, 19 (September 2009): 4635-4643.

115. Zhu, S., Y. Zhao, and Z. Qiu. "Crystallization Kinetics and Morphology Studies of Biodegradable Poly(ethylene succinate)/Multi-Walled Carbon Nanotubes Nanocomposites." Thermochimica Acta 517, 1-2 (April 2011): 74-80.
116. Dangtungee, R., J. Yun, and P. Supaphol. "Melt Rheology and Extrudate Swell of Calcium Carbonate Nano-particle-Filled Isotactic Polypropylene." Polymer Testing 24, 1 (February 2005): 2-11.
117. Supaphol, P. and W. Harnsiri. "Rheological and Isothermal Crystallization Characteristics of Neat and Calcium Carbonate-Filled Syndiotactic Polypropylene." Journal of Applied Polymer Science 100, 6 (June 2006): 4515-4525.
118. Rungruang, P., B. P. Grady, and P. Supaphol. "Surface-Modified Calcium Carbonate Particles by Admicellar Polymerization to be used as Filler for Isotactic Polypropylene." Colloids and Surfaces A: Physicochemical and Engineering Aspects 275, 1-3 (March 2006): 114-125.
119. Avella, M. et al. "Nucleation Activity of Nanosized CaCO₃ on Crystallization of Isotactic Polypropylene, in Dependence on Crystal Modification, Particle Shape, and Coating." European Polymer Journal 42, 7 (July 2006): 1548-1557.
120. Chan, C.-M. et al. "Polypropylene/Calcium Carbonate Nanocomposites." Polymer 43, 10 (May 2002): 2981-2992.
121. Osman, M. A. and A. Atallah. "Effect of The Particle Size on The Viscoelastic Properties of Filled Polyethylene." Polymer 47, 7 (March 2006): 2357-2368.
122. Ma, X. et al. "Study on CaCO₃/PMMA Nanocomposite Microspheres by Soapless Emulsion Polymerization." Colloids and Surfaces A: Physicochemical and Engineering Aspects 312, 2-3 (January 2008): 190-194.
123. Zuiderduin, W. C. J., J. Huétink, and R. J. Gaymans. "Rigid Particle Toughening of Aliphatic Polyketone." Polymer 47, 16 (July 2006): 5880-5887.
124. Xie, X.-L. et al. "Rheological and Mechanical Properties of PVC/CaCO₃ Nanocomposites Prepared by In Situ Polymerization." Polymer 45, 19 (September 2004): 6665-6673.
125. Wang, Z. et al. "Rheology Enhancement of Polycarbonate/Calcium Carbonate Nanocomposites Prepared by Melt-Compounding." Materials Letters 60, 8 (April 2006): 1035-1038.
126. Jiang, L. et al. "The Influence of Fatty Acid Coating on The Rheological and Mechanical Properties of Thermoplastic Polyurethane (TPU)/Nano-sized Precipitated Calcium Carbonate (NPCC) Composites." Polymer Bulletin 57, 4 (2006): 575-586.
127. Jin, F.-L. and S.-J. Park. "Thermo-Mechanical Behaviors of Butadiene Rubber Reinforced with Nano-sized Calcium Carbonate." Materials Science and Engineering: A 478, 1-2 (April 2008): 406-408.
128. Cheng, Z.-p. et al. "Synthesis and Characterization of Aluminum Particles Coated with Uniform Silica Shell." Transactions of Nonferrous Metals Society of China 18, 2 (April 2008): 378-382.
129. Silica [online]. Accessed 9 September 2011. Available from <http://en.wikipedia.org/wiki/Silica>

130. The Carbon Family [online]. Accessed 9 September 2011. Available from http://chemwiki.ucdavis.edu/Inorganic_Chemistry/Descriptive_Chemistry/Main_Group_Elements/Group_14%3A_The_Carbon_Family
131. Ma, J.-Z., J. Hu, and Z.-J. Zhang. "Polyacrylate/Silica Nanocomposite Materials Prepared by Sol-Gel Process." European Polymer Journal 43, 10 (October 2007): 4169-4177.
132. Zhang, Q. et al. "A Novel Biodegradable Nanocomposite Based on Poly(3-hydroxybutyrate-co-3-hydroxyhexanoate) and Silylated Kaolinite/Silica Core-Shell Nano-particles." Applied Clay Science 46, 1 (September 2009): 51-56.
133. Wen, X. et al. "Study of The Thermal Stabilization Mechanism of Biodegradable Poly(L-lactide)/Silica Nanocomposites." Polymer International 60, 2 (February 2011): 202-210.
134. Chrissafis, K. et al. "Enhancing Mechanical and Thermal Properties of PLLA Ligaments with Fumed Silica Nano-particles and Montmorillonite." Journal of Thermal Analysis and Calorimetry 105, 1 (December 2010): 313-323.
135. Bikiaris, D. "Can Nano-particles Really Enhance Thermal Stability of Polymers? Part II: An Overview on Thermal Decomposition of Polycondensation Polymers." Thermochimica Acta 523, 1-2 (August 2011): 25-45.
136. Wahab, M. F. A., A. F. Ismail, and S. J. Shilton. "Studies on Gas Permeation Performance of Asymmetric Polysulfone Hollow Fiber Mixed Matrix Membranes using Nanosized Fumed Silica as Fillers." Separation and Purification Technology 86 (February 2012): 41-48.
137. Idrus, S. S., H. Ismail, and S. Palaniandy. "Study of The Effect of Different Shapes of Ultrafine Silica as Fillers in Natural Rubber Compounds." Polymer Testing 30, 2 (April 2011): 251-259.
138. Chen, J. et al. CaCO₃/SiO₂.nH₂O Nanocomposite Particles and SiO₂.nH₂O Hollow-Structures Nanomaterials and Synthesizing Method. United States 7485367. 3 February 2009.
139. Tanabe, K. and K. Mitsuhashi. Silica-calcium carbonate composite particles. United States 7060127. 13 June 2006.
140. Zhang, S. and X. Li. "Synthesis and Characterization of CaCO₃@SiO₂ Core-Shell Nano-particles." Powder Technology 141, 1-2 (March 2004): 75-79.
141. Polyethylene Glycol [online]. Accessed 10 February 2012. Available from http://en.wikipedia.org/wiki/Polyethylene_glycol
142. Yao, C.-L. et al. "Unusual Morphology of Calciumcarbonate Controlled by Amino Acids in Agarose Gel." Journal of the Chilean Chemical Society 55, 2 (2010): 270-273.
143. Table of IR Absorptions [online]. Accessed 7 December 2011. Available from <http://www.chem.ucla.edu/~webspectra/irtable.html>
144. Ou, X. and M. Cakmak. "Influence of Biaxial Stretching Mode on The Crystalline Texture in Polylactic Acid Films." Polymer 49, 24 (November 2008): 5344-5352.
145. Shenoy, A. V. Rheology of Filled Polymer Systems. Dordrechht: Kluwer Academic Pubishers, 1999.

146. Wang, Z. et al. "Rheology enhancement of polycarbonate/calcium carbonate nanocomposites prepared by melt-compounding." Materials Letters 60, 8 (2006): 1035-1038.
147. Choi, H. M. and B. Yoo. "Steady and Dynamic Shear Rheology of Sweet Potato Starch-Xanthan Gum Mixtures." Food Chemistry 116, 3 (October 2009): 638-643.
148. D'Antone, S. et al. "Thermogravimetric Investigation of Two Classes of Block Copolymers based on Poly(lactic-glycolic acid) and Poly(ϵ -caprolactone) or Poly(ethylene glycol)." Polymer Degradation and Stability 74, 1 (2001): 119-124.
149. Essa, S., J. M. Rabanel, and P. Hildgen. "Effect of Polyethylene Glycol (PEG) Chain Organization on The Physicochemical Properties of Poly(D, L-lactide) (PLA) based Nano-particles." European Journal of Pharmaceutics and Biopharmaceutics 75, 2 (June 2010): 96-106.
150. Martin, O. and L. Avérous. "Poly(lactic acid): Plasticization and Properties of Biodegradable Multiphase Systems." Polymer 42, 14 (June 2001): 6209-6219.
151. Hu, Y. et al. "Crystallization and Phase Separation in Blends of High Stereoregular Poly(lactide) with Poly(ethylene glycol)." Polymer 44, 19 (September 2003): 5681-5689.
152. Hu, Y. et al. "Aging of Poly(lactide)/Poly(ethylene glycol) Blends. Part 1. Poly(lactide) with Low Stereoregularity." Polymer 44, 19 (September 2003): 5701-5710.
153. Hu, Y. et al. "Aging of Poly(lactide)/Poly(ethylene glycol) Blends. Part 2. Poly(lactide) with High Stereoregularity." Polymer 44, 19 (September 2003): 5711-5720.
154. Way, J. L., J. R. Atkinson, and J. Nutting. "The Effect of Spherulite Size on The Fracture Morphology of Polypropylene." Journal of Materials Science 9, 2 (1974): 293-299.
155. Auras, R. A., S. P. Singh, and J. J. Singh. Evaluation of Oriented Poly(lactide) Polymers with Existing PET and Oriented PS for Fresh Food Service Containers [online]. Accessed 10 January 2012. Available from http://www.burchamintl.com/papers/petpapers/46_gpec05.pdf

APPENDICES

APPENDIX A
RESEARCH DATA

The information data of PLA from NatureWork LLC.



NatureWorks® PLA Polymer 2002D

Extrusion/Thermoforming

NatureWorks® PLA polymer 2002D, a NatureWorks LLC product, is a thermoplastic resin derived primarily from annually renewable resources and is specifically designed for extrusion/thermoforming applications. PLA polymer 2002D is a clear extrusion sheet grade and processes easily on conventional extrusion and thermoforming equipment. See table at right for properties.

Applications

Potential applications for PLA polymer 2002D include:

- Dairy containers
- Food serviceware
- Transparent food containers
- Blister pack
- Cold drink cups

Processing Information

PLA polymer 2002D is easily processed on conventional extrusion equipment. The material is stable in the molten state, provided that the drying procedures are followed.

Machine Configuration

PLA polymer 2002D will process on conventional extrusion machinery with the following equipment: General purpose screw with L/D ratios from 24:1 to 30:1 and compression ratio of 2.5:1 to 3:1. Smooth barrels are recommended.

Typical Material & Application Properties ⁽¹⁾		
Physical Properties	PLA Polymer 2002D	ASTM Method
Specific Gravity	1.24	D792
Melt Index, g/10 min (190°C/2.16K)	4-8	D1238
Clarity	Transparent	
Mechanical Properties		
Tensile Strength @ Break, psi (MPa)	7,700 (53)	D882
Tensile Yield Strength, psi (MPa)	8,700 (60)	D882
Tensile Modulus, kpsi (GPa)	500 (3.5)	D882
Tensile Elongation, %	6.0	D882
Notched Izod Impact, ft-lb/in (J/m)	0.24 (12.81)	D256
Shrinkage is similar to PET ⁽²⁾		

- (1) Typical properties; not to be construed as specifications.
 (2) Refer to NatureWorks® PLA Sheet Extrusion Processing Guide

Process Details

Startup and Shutdown

PLA polymer 2002D is not compatible with a wide variety of polyolefin resins, and special purging sequences should be followed:

1. Clean extruder and bring temperatures to steady state with low-viscosity, general-purpose polystyrene or polypropylene.
2. Vacuum out hopper system to avoid contamination.
3. Introduce PLA polymer into the extruder at the operating conditions used in Step 1.
4. Once PLA polymer has purged, reduce barrel temperatures to desired set points.
5. At shutdown, purge machine with high-viscosity polystyrene or polypropylene.

Drying

In-line drying may be required. A moisture content of less than 0.025% (250 ppm) is recommended to prevent viscosity degradation. Typical drying conditions for crystallized granules are 4 hours at 158°F (70°C) or to a dew point of -30°F (-34°C), airflow rate of greater than 0.5 cfm/lbs per hour of resin throughput. The resin should not be exposed to atmospheric conditions after drying. Keep the package sealed until ready to use and

Processing Temperature Profile ⁽¹⁾		
Melt Temperature	410°F	210°C
Feed Throat	113°F	45°C
Feed Temperature	355°F	180°C
Compression Section	375°F	190°C
Metering Section	390°F	200°C
Adapter	390°F	200°C
Die	375°F	190°C
Screw Speed	20-100 rpm	

promptly reseal any unused material.

- (1) NatureWorks® PLA Sheet Extrusion Processing Guide is available at www.natureworkslc.com

The information data of PLA from NatureWork LLC. (Continued)



NatureWorks® PLA Polymer 2002D

Extrusion/Thermoforming

NatureWorks® PLA polymer 2002D, a NatureWorks LLC product, is a thermoplastic resin derived primarily from annually renewable resources and is specifically designed for extrusion/thermoforming applications. PLA polymer 2002D is a clear extrusion sheet grade and processes easily on conventional extrusion and thermoforming equipment. See table at right for properties.

Applications

Potential applications for PLA polymer 2002D include:

- Dairy containers
- Food serviceware
- Transparent food containers
- Blister pack
- Cold drink cups

Processing Information

PLA polymer 2002D is easily processed on conventional extrusion equipment. The material is stable in the molten state, provided that the drying procedures are followed.

Machine Configuration

PLA polymer 2002D will process on conventional extrusion machinery with the following equipment: General purpose screw with L/D ratios from 24:1 to 30:1 and compression ratio of 2.5:1 to 3:1. Smooth barrels are recommended.

Typical Material & Application Properties ⁽¹⁾		
Physical Properties	PLA Polymer 2002D	ASTM Method
Specific Gravity	1.24	D792
Melt Index, g/10 min (190°C/2.16K)	4-8	D1238
Clarity	Transparent	
Mechanical Properties		
Tensile Strength @ Break, psi (MPa)	7,700 (53)	D882
Tensile Yield Strength, psi (MPa)	8,700 (60)	D882
Tensile Modulus, kpsi (GPa)	500 (3.5)	D882
Tensile Elongation, %	6.0	D882
Notched Izod Impact, ft-lb/in (J/m)	0.24 (12.81)	D256
Shrinkage is similar to PET ⁽²⁾		

(1) Typical properties; not to be construed as specifications.

(2) Refer to NatureWorks® PLA Sheet Extrusion Processing Guide

Process Details

Startup and Shutdown

PLA polymer 2002D is not compatible with a wide variety of polyolefin resins, and special purging sequences should be followed:

1. Clean extruder and bring temperatures to steady state with low-viscosity, general-purpose polystyrene or polypropylene.
2. Vacuum out hopper system to avoid contamination.
3. Introduce PLA polymer into the extruder at the operating conditions used in Step 1.
4. Once PLA polymer has purged, reduce barrel temperatures to desired set points.
5. At shutdown, purge machine with high-viscosity polystyrene or polypropylene.

Drying

In-line drying may be required. A moisture content of less than 0.025% (250 ppm) is recommended to prevent viscosity degradation. Typical drying conditions for crystallized granules are 4 hours at 158°F (70°C) or to a dew point of -30°F (-34°C), airflow rate of greater than 0.5 cfm/lbs per hour of resin throughput. The resin should not be exposed to atmospheric conditions after drying. Keep the package sealed until ready to use and

Processing Temperature Profile ⁽¹⁾		
Melt Temperature	410°F	210°C
Feed Throat	113°F	45°C
Feed Temperature	355°F	180°C
Compression Section	375°F	190°C
Metering Section	390°F	200°C
Adapter	390°F	200°C
Die	375°F	190°C
Screw Speed	20-100 rpm	

promptly reseal any unused material.

(1) NatureWorks® PLA Sheet Extrusion Processing Guide is available at www.natureworkslc.com

The information data of PLA from NatureWork LLC. (Continued)



NatureWorks® PLA Polymer 2002D

Safety and Handling Considerations

Material Safety Data (MSD) sheets for PLA polymers are available from NatureWorks LLC. MSD sheets are provided to help customers satisfy their own handling, safety, and disposal needs, and those that may be required by locally applicable health and safety regulations, such as OSHA (U.S.A.), MAK (Germany), or WHMIS (Canada). MSD sheets are updated regularly; therefore, please request and review the most current MSD sheets before handling or using any product.

The following comments apply only to PLA polymers; additives and processing aids used in fabrication and other materials used in finishing steps have their own safe-use profile and must be investigated separately.

Hazards and Handling Precautions

PLA polymers have a very low degree of toxicity and, under normal conditions of use, should pose no unusual problems from incidental ingestion, or eye and skin contact. However, caution is advised when handling, storing, using, or disposing of these resins, and good housekeeping and controlling of dusts are necessary for safe handling of product. Workers should be protected from the possibility of contact with molten resin during fabrication. Handling and fabrication of resins can result in the generation of vapors and dusts that may cause irritation to eyes and the upper respiratory tract. In dusty atmospheres, use an approved dust respirator. Pellets or beads may present a slipping hazard. Good general ventilation of the polymer processing area is recommended. At temperatures exceeding the polymer melt temperature (typically 170°C), polymer can release fumes, which may contain fragments of the polymer, creating a potential to irritate eyes and mucous membranes. Good general ventilation should be sufficient

for most conditions. Local exhaust ventilation is recommended for melt operations. Use safety glasses if there is a potential for exposure to particles which could cause mechanical injury to the eye. If vapor exposure causes eye discomfort, use a full-face respirator. No other precautions other than clean, body-covering clothing should be needed for handling PLA polymers. Use gloves with insulation for thermal protection when exposure to the melt is localized.

Combustibility

PLA polymers will burn. Clear to white smoke is produced when product burns. Toxic fumes are released under conditions of incomplete combustion. Do not permit dust to accumulate. Dust layers can be ignited by spontaneous combustion or other ignition sources. When suspended in air, dust can pose an explosion hazard. Firefighters should wear positive-pressure, self-contained breathing apparatuses and full protective equipment. Water or water fog is the preferred extinguishing medium. Foam, alcohol-resistant foam, carbon dioxide or dry chemicals may also be used. Soak thoroughly with water to cool and prevent re-ignition.

Disposal

DO NOT DUMP INTO ANY SEWERS, ON THE GROUND, OR INTO ANY BODY OF WATER. For unused or uncontaminated material, the preferred options include recycling into the process or sending to an industrial composting facility, if available; otherwise, send to an incinerator or other thermal destruction device. For used or contaminated material, the disposal options remain the same, although additional evaluation is required. (For example, in the U.S.A., see 40 CFR, Part 261, "Identification and Listing of Hazardous Waste.") All disposal methods must be in compliance with Federal, State/Provincial, and local laws and regulations.

Environmental Concerns

Generally speaking, lost pellets are not a problem in the environment except under unusual circumstances when they enter the marine environment. They are benign in terms of their physical environmental impact, but if ingested by waterfowl or aquatic life, they may mechanically cause adverse effects. Spills should be minimized, and they should be cleaned up when they happen. Plastics should not be discarded into the ocean or any other body of water.

Product Stewardship

NatureWorks LLC has a fundamental duty to all those that make and use our products, and for the environment in which we live. This duty is the basis for our Product Stewardship philosophy, by which we assess the health and environmental information on our products and their intended use, then take appropriate steps to protect the environment and the health of our employees and the public.

Customer Notice

NatureWorks LLC encourages its customers and potential users of its products to review their applications for such products from the standpoint of human health and environmental quality. To help ensure our products are not used in ways for which they were not intended or tested, our personnel will assist customers in dealing with ecological and product safety considerations. Your sales representative can arrange the proper contacts. NatureWorks LLC literature, including Material Safety Data sheets, should be consulted prior to the use of the company's products. These are available from your NatureWorks LLC representative.

NOTICE: No freedom from any patent owned by NatureWorks LLC or others is to be inferred. Because use conditions and applicable laws may differ from one location to another and may change with time, Customer is responsible for determining whether products and the information in this document are appropriate for Customer's use and for ensuring that Customer's workplace and disposal practices are in compliance with applicable laws and other governmental enactments. NatureWorks LLC assumes no obligation or liability for the information in this document. NO WARRANTIES ARE GIVEN; ALL IMPLIED WARRANTIES OF MERCHANTABILITY OR FITNESS FOR A PARTICULAR USE ARE EXPRESSLY EXCLUDED.

NOTICE REGARDING PROHIBITED USE RESTRICTIONS: NatureWorks LLC does not recommend any of its products, including samples, for use as: Components of, or packaging for, tobacco products; Components of products where the end product is intended for human or animal consumption; In any application that is intended for any internal contact with human body fluids or body tissues; As a critical component in any medical device that supports or sustains human life; In any product that is designed specifically for ingestion or internal use by pregnant women; and in any application designed specifically to promote or interfere with human reproduction.

For additional information in the U.S. and Canada,
call toll-free 1-877-423-7559
In Europe, call 31-(0)35-699-1344
In Japan, call 81-33-285-0824

NatureWorks®
15305 Minnetonka Blvd., Minnetonka, MN 55345

NatureWorks and the NatureWorks logo are trademarks of NatureWorks LLC
Copyright © 2005 NatureWorks LLC

The information of Micro-CaCO₃-1760

Trade name: **Q-MIN 1QC**

Supplier: **Quality Minerals**

Product performance:

Also used in paint, paper and pharmaceutical industries.

Applications / Recommended for:

- Thermoplastics, other
- Rubbers

TYPICAL PROPERTIES	VALUE	UNIT
Calcium carbonate content	98.5	%
Magnesium (as MgO) content	0.3	%
Aluminum as Al ₂ O ₃ content	0.2	%
Silicon dioxide (SiO ₂) content	0.3	%
Fe ₂ O ₃ content	0.2	%
Brightness	88	%
Moisture content	0.2	%
Bulk density	0.55	g/cm ³
Specific gravity	2.7	
pH	8.8 - 9.2	
Specific surface	35,000-38,000	cm ² /ml
Average particle size	1.6 ± 0.2	μm

Product type:

Calcium Carbonate (Precipitated) >> Calcium carbonate (ground)

Chemical composition: Calcium carbonate

Physical form: Powder

Other products with same trade name: Q-MIN 1Q, Q-MIN 2Q and Q-MIN 2QC

The information of Nano-CaCO₃-1041

EMAX ASIA

Technical Data Sheet

CNANO P-23 **COATING, SEALANT & CABLE**

It is a super ultra fine and very narrow particle size distribution precipitated calcium carbonate specially formulated as functional filler in PVC Coatings or Epoxy Sealants and PVC Cable.

Applications

For use as special functional filler in car under-body PVC coating, epoxy sealant and PVC cable compounds.

It can be added as functional filler in coating or sealant with exceptional rheological and thixotropic properties. Under high shear, it thins out making it flows easily and facilitates the application of the coating onto a surface. Once shear is removed, viscosity returns enabling the coating to adhere to the surface without sagging or running.

It can be used in PVC cable as functional filler and/or to partially replace Titanium Dioxide, while maintaining similar mechanical properties.

Best results can be achieved with good mixing to produce good dispersion and distribution of fine particles in the compound system.

Typical Properties

• Chemical Composition	: Calcium Carbonate
• Appearance	: Dry White Powder
• Moisture Content	: <0.5%
• Whiteness	: >90%
• Specific Gravity	: 2.55
• Particle Size Average	: 40 – 60 nanometer
• Surface Area (BET)	: >20 m ² /g
• pH	: 8.5 - 10.0

Packaging and Storage

It is packed in 25 kg kraft paper bag. Storage life is 180 days in cool and dry condition.

The above information is provided based on our best knowledge and subjected to change. As the circumstances and conditions under which this product would be used are beyond our control, we accept no liability for any loss and damage arising from its use.

The information of Nano-CaCO₃-280



Technical Data Sheet

产品性能指标

Product Name (产品名称):	Nano-precipitated calcium carbonate (纳米碳酸钙)
Product Code (产品代码):	NPCC-101
Tests (测试)	Typical Value (标准值)
Appearance (外观)	White Power (白色粉末)
Particle shape(粒子形状)	Cubic
Particle size(avg) (平均粒径) ,nm	40
Whiteness (白度) , %	>90
Density (密度) , g/ml	2.5-2.6
Moisture Content (湿含量) , %	<0.5
CaCO ₃ (unmodified 未处理) , %	> 97
Surface Modification (表面处理)	yes(有)
pH	8.0-9.5

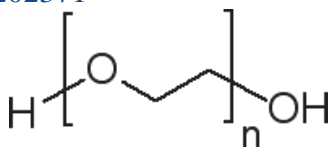
The information of PEG plasticizer used in phase II and phase III

202398 Aldrich

Poly(ethylene glycol) Average M_n 400

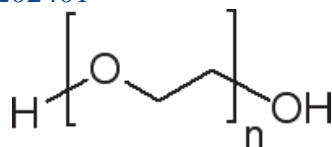
Customers Also Purchased

202371



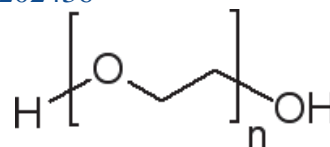
Poly(ethylene glycol)
average M_n 300

202401



Poly(ethylene glycol)
average M_n 600, waxy
solid (moist)

202436



Poly(ethylene glycol)
average M_n 1,305-1,595,
waxy solid

Description

Used in conjunction with carbon black to form a conductive composite.¹

Application Polymer nanospheres of poly(ethylene glycol) were used for drug delivery.²

Packaging 20 kg in poly drum

5, 250, 500 g in glass bottle

Properties

vapor density	>1 (vs air)
vapor pressure	<0.01 mmHg (20 °C)
form	viscous liquid
autoignition temp.	581 °F
mol wt	M_n 380-420, average M_n 400
refractive index	$n_{20/D}$ 1.466
viscosity	7.3 cSt (210 °F)(lit.)
density	1.128 g/mL

Safety

Personal Protective Equipment Eyeshields, Gloves

The information of TbC plasticizer used in phase II and phase III

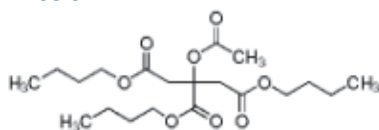
27497 Aldrich

Tributyl citrate ($\geq 97.0\%$)

CAS Number:	77-94-1
Empirical Formula (Hill Notation):	$C_{18}H_{32}O_7$
Molecular Weight:	360.44
Beilstein Registry Number:	1806072
EC Number:	201-071-2
MDL number:	MFCD00027217
PubChem Substance ID:	24856617

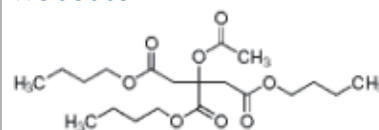
Customers Also Viewed

42858



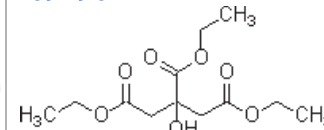
Tributyl 2-acetylcitrate
purum, $\geq 99.0\%$ (GC)

W308005



Tributyl 2-acetylcitrate
 $\geq 98\%$

109290



Triethyl citrate
99%

Properties

assay $\geq 97.0\%$

refractive index $n_{20/D}$ 1.445

density 1.043 g/mL at 20 °C(lit.)

Safety

Personal Protective Equipment Eyeshields, Gloves

Safety Statements 23-24/25

Average agglomeration size of CaCO₃

Type of CaCO ₃	Measure 1	Measure 2	Measure 3	Average	S.D.
Micro-CaCO ₃ -1740	1,740	1,750	1,750	1,746.7	5.8
Nano-CaCO ₃ -1041	1,041	1,048	1,109	1,066.0	37.4
Nano-CaCO ₃ -280	279.5	279.3	276.4	278.4	1.7

Average Young's modulus of PLA biocomposites in phase I

Type of biocomposites	Measure 1	Measure 2	Measure 3	Measure 4	Measure 5	Young's Modulus (MPa)	S.D.
Neat PLA	5,164.01	5,212.63	4,898.52	5,541.22	5,160.60	5,195.39	229.25
5% Micro-CaCO ₃ -1740-PLA	5,252.07	4,974.09	5,165.52	5,140.40	5,069.50	5,120.31	104.61
10% Micro-CaCO ₃ -1740-PLA	4,906.96	4,985.37	5,174.66	5,166.19	5,010.54	5,048.74	117.50
15% Micro-CaCO ₃ -1740-PLA	5,040.81	4,880.86	4,840.60	5,071.67	5,033.24	4,973.44	104.86
20% Micro-CaCO ₃ -1740-PLA	5,025.64	4,789.73	4,886.55	4,771.63	5,116.29	4,917.97	149.81
5% Nano-CaCO ₃ -1041-PLA	4,760.89	4,642.96	4,602.31	4,847.28	4,598.43	4,690.37	109.60
10% Nano-CaCO ₃ -1041-PLA	4,346.49	4,265.15	4,776.43	4,767.20	4,278.67	4,486.79	262.03
15% Nano-CaCO ₃ -1041-PLA	4,168.67	4,127.88	4,441.36	4,618.14	4,618.97	4,395.01	237.00
20% Nano-CaCO ₃ -1041-PLA	4,056.00	4,373.20	4,352.47	4,145.02	4,438.73	4,273.09	163.78
5% Nano-CaCO ₃ -280-PLA	3,650.06	3,602.30	3,941.12	3,698.53	4,143.69	3,807.14	228.94
10% Nano-CaCO ₃ -280-PLA	3,633.65	3,744.68	3,903.26	3,525.32	3,729.00	3,707.18	140.37
15% Nano-CaCO ₃ -280-PLA	3,527.45	3,860.09	3,565.53	3,481.33	3,853.25	3,657.53	184.23
20% Nano-CaCO ₃ -280-PLA	3,718.12	3,819.97	3,536.80	3,611.21	3,545.82	3,646.38	121.07

Average percentage strain at break of PLA biocomposites in phase I

Type of biocomposites	Measure 1	Measure 2	Measure 3	Measure 4	Measure 5	Percentage strain at break (%)	S.D.
Neat PLA	40.97	35.34	41.35	32.15	38.00	37.56	3.89
5% Micro-CaCO ₃ -1740-PLA	25.55	25.19	27.71	29.74	14.62	24.56	5.85
10% Micro-CaCO ₃ -1740-PLA	10.26	14.56	12.71	11.83	8.20	11.51	2.42
15% Micro-CaCO ₃ -1740-PLA	4.85	4.61	5.39	5.19	5.14	5.04	0.31
20% Micro-CaCO ₃ -1740-PLA	2.85	2.90	3.29	2.78	3.04	2.98	0.20
5% Nano-CaCO ₃ -1041-PLA	5.24	6.39	4.72	4.80	3.81	4.99	0.94
10% Nano-CaCO ₃ -1041-PLA	5.70	4.62	4.43	6.83	6.34	5.58	1.05
15% Nano-CaCO ₃ -1041-PLA	5.87	5.69	4.85	5.35	4.14	5.18	0.70
20% Nano-CaCO ₃ -1041-PLA	6.79	5.41	4.39	4.61	7.95	5.83	1.51
5% Nano-CaCO ₃ -280-PLA	2.43	2.87	2.59	3.06	2.43	2.68	0.28
10% Nano-CaCO ₃ -280-PLA	2.86	2.94	3.10	2.44	2.44	2.76	0.30
15% Nano-CaCO ₃ -280-PLA	3.11	2.65	2.80	2.37	3.18	2.82	0.33
20% Nano-CaCO ₃ -280-PLA	2.57	3.29	2.87	2.61	2.88	2.84	0.29

Average high-speed tensile test of PLA biocomposite in phase I

Type of biocomposites	Measure 1	Measure 2	Measure 3	Measure 4	Measure 5	High speed tensile (kJ/m ²)	S.D.
Neat PLA	187.89	184.31	152.16	162.80	163.84	170.20	15.27
5% Micro-CaCO ₃ -1740-PLA	166.04	169.08	180.02	149.41	153.54	163.62	12.33
10% Micro-CaCO ₃ -1740-PLA	170.77	143.06	148.80	170.94	164.60	159.63	12.93
15% Micro-CaCO ₃ -1740-PLA	165.62	154.56	152.23	130.76	169.03	154.44	15.03
20% Micro-CaCO ₃ -1740-PLA	136.10	146.16	142.74	145.76	179.78	150.11	17.07
5% Nano-CaCO ₃ -1041-PLA	142.98	139.15	126.67	130.51	114.48	151.95	12.80
10% Nano-CaCO ₃ -1041-PLA	155.70	137.23	169.35	129.48	144.69	147.29	15.67
15% Nano-CaCO ₃ -1041-PLA	107.64	139.55	158.59	141.84	152.45	140.01	19.69
20% Nano-CaCO ₃ -1041-PLA	116.09	155.13	160.26	118.21	128.56	135.65	20.75
5% Nano-CaCO ₃ -280-PLA	96.31	99.57	86.84	77.81	73.78	86.86	11.22
10% Nano-CaCO ₃ -280-PLA	88.11	82.31	63.42	75.47	88.69	79.60	10.50
15% Nano-CaCO ₃ -280-PLA	76.81	69.87	61.56	77.17	78.23	72.73	7.06
20% Nano-CaCO ₃ -280-PLA	66.21	63.36	61.74	65.64	77.88	66.97	6.36

Average melt flow index of PLA biocomposites in phase I

Type of biocomposites	Measure 1	Measure 2	Measure 3	Measure 4	Measure 5	Melt flow index (g/10min)	S.D.	1/log a MFI
PLA	4.21	3.80	3.92	3.82	4.56	4.06	0.32	-
5% Micro-CaCO ₃ -1760-PLA	5.35	5.11	5.02	3.80	3.54	4.57	0.83	-19.73
10% Micro-CaCO ₃ -1760-PLA	5.89	4.80	5.54	4.23	4.58	5.01	0.69	-11.03
15% Micro-CaCO ₃ -1760-PLA	6.11	6.80	4.58	7.53	4.13	5.83	0.94	-6.38
20% Micro-CaCO ₃ -1760-PLA	7.94	8.24	7.30	8.84	8.88	8.24	0.66	-3.26
5% Nano-CaCO ₃ -1041-PLA	6.38	6.57	6.51	6.29	6.45	6.44	0.11	-4.95
10% Nano-CaCO ₃ -1041-PLA	6.45	6.58	7.39	6.34	6.66	6.69	0.41	-4.58
15% Nano-CaCO ₃ -1041-PLA	7.21	7.91	7.65	6.31	7.00	7.22	0.62	-3.97
20% Nano-CaCO ₃ -1041-PLA	8.22	7.86	9.23	8.64	8.48	8.49	0.49	-3.10
5% Nano-CaCO ₃ -280-PLA	6.04	7.05	7.10	6.65	6.91	6.75	0.43	-4.49
10% Nano-CaCO ₃ -280-PLA	8.66	7.43	8.42	7.84	7.99	8.07	0.49	-3.33
15% Nano-CaCO ₃ -280-PLA	9.77	9.08	8.39	10.48	10.74	9.69	0.97	-2.63
20% Nano-CaCO ₃ -280-PLA	9.15	11.45	8.96	10.59	9.89	10.01	1.01	-2.54

Average Young's modulus of PLA nanocomposite in phase II

Type of nanocomposites	Measure 1	Measure 2	Measure 3	Measure 4	Measure 5	Young's Modulus (MPa)	S.D.
PLA	797.65	748.03	754.75	794.38	799.14	778.79	25.18
PLA/CaCO ₃	798.95	675.50	792.06	730.09	728.01	744.92	51.15
PLA/10PEG	633.25	683.50	611.63	658.70	647.77	646.23	26.97
PLA/CaCO ₃ /10PEG	620.20	629.99	590.31	511.45	546.14	579.62	50.17
PLA/20PEG	492.92	477.12	506.04	576.08	475.48	505.53	41.37
PLA/CaCO ₃ /20PEG	451.88	393.03	393.95	368.26	474.74	416.37	44.80
PLA/10TbC	685.44	689.20	643.01	598.27	561.65	635.51	55.39
PLA/CaCO ₃ /10TbC	557.69	537.05	537.58	654.51	598.55	577.08	49.99
PLA/20TbC	362.23	343.17	374.18	322.84	302.84	350.60	22.49
PLA/CaCO ₃ /20TbC	279.78	258.66	262.30	191.23	202.87	238.97	39.31

Average percentage of strain at break of PLA nanocomposite in phase II

Type of nanocomposites	Measure 1	Measure 2	Measure 3	Measure 4	Measure 5	Percentage strain at break (%)	S.D.
PLA	12.82	23.98	22.21	15.64	20.24	18.98	4.64
PLA/CaCO ₃	14.08	18.13	8.92	17.70	8.87	13.54	4.52
PLA/10PEG	83.57	89.60	70.65	85.15	50.28	75.85	15.94
PLA/CaCO ₃ /10PEG	37.54	51.69	33.47	44.94	59.98	45.52	10.68
PLA/20PEG	139.94	132.51	110.03	121.72	134.87	127.81	11.96
PLA/CaCO ₃ /20PEG	67.45	89.99	81.02	94.97	101.12	86.91	13.13
PLA/10TbC	149.11	132.15	173.85	103.42	110.08	133.72	28.84
PLA/CaCO ₃ /10TbC	127.16	103.19	127.32	115.03	109.69	116.48	10.68
PLA/20TbC	1,297.83	1,345.39	1,113.40	1,184.76	1,204.76	1,235.35	105.58
PLA/CaCO ₃ /20TbC	839.95	940.72	883.97	676.40	779.15	824.04	101.57

Average impact strength of PLA nanocomposite in phase II

Type of nanocomposites	Measure 1	Measure 2	Measure 3	Measure 4	Measure 5	Impact strength (N/m ²)	S.D.
PLA	2,141.40	2,534.97	1,999.04	2,537.43	1,978.15	2,238.20	279.20
PLA/CaCO ₃	1,568.95	1,952.60	1,519.45	1,587.64	1,755.04	1,676.73	177.85
PLA/10PEG	2,741.26	2,825.70	2,202.83	2,594.43	2,390.84	2,551.01	255.16
PLA/CaCO ₃ /10PEG	2,262.24	2,379.56	2,102.93	2,501.13	1,815.92	2,212.36	265.97
PLA/20PEG	4,376.95	3,832.13	3,977.45	3,829.29	4,475.02	4,098.17	307.16
PLA/CaCO ₃ /20PEG	2,772.75	2,820.47	2,969.84	2,751.10	2,157.08	2,694.25	312.18
PLA/10TbC	2,580.62	3,024.23	2,165.32	2,001.37	1,959.51	2,346.21	451.62
PLA/CaCO ₃ /10TbC	2,109.05	2,559.49	1,771.16	2,111.14	2,067.16	2,123.60	281.86
PLA/20TbC	121.4	110.31	90.34	106.46	90.68	3,633.91	419.43
PLA/CaCO ₃ /20TbC	2,266.13	2,659.51	2,367.97	2,132.51	2,454.45	2,376.12	198.72

Preparation of SiO₂-CaCO₃ particle

Specification of precursor

CaCO₃ : Mw = 100

TEOS : Mw = 208, purity 98%, density = 0.933 g/cm³

Calculation

There is 1 atom of Si in 1 molecule of TEOS, so mol ratio of Si : TEOS is 1 : 1

There is 1 atom of Ca in 1 molecule of CaCO₃, so mol ratio of Ca : CaCO₃ is 1 : 1

The mol ratio of Si : Ca are 1 : 30, 1 : 20 and 1:10

For each Si : Ca mol ratio, we prepare these fillers base on 150 g of CaCO₃ (equal to 1.5 mol of CaCO₃) for using in 3 kg of PLA.

So, the mol ratio of Si : Ca are 0.05 : 1.5, 0.075 : 1.5 and 0.15 : 1.5, respectively.

Therefore, the weight of Si : Ca are

$$(0.05 \times 208) : (1.5 \times 100) = 10.4 \text{ g} : 150 \text{ g}$$

$$(0.075 \times 208) : (1.5 \times 100) = 15.6 \text{ g} : 150 \text{ g}$$

$$(0.15 \times 208) : (1.5 \times 100) = 31.2 \text{ g} : 150 \text{ g}$$

$$\text{TEOS } 1 \text{ L} = (933 \times 98)/100 = 914.34 \text{ g}$$

Therefore, we use

$$10.4 \text{ g} / 914.34 \text{ g/L} = 0.0114 \text{ L} = 11.4 \text{ ml}$$

$$15.6 \text{ g} / 914.34 \text{ g/L} = 0.0171 \text{ L} = 17.1 \text{ ml}$$

$$31.2 \text{ g} / 914.34 \text{ g/L} = 0.0341 \text{ L} = 34.1 \text{ ml}$$

for Si : Ca mol ratio as 1 : 30, 1 : 20 and 1:10, respectively.

Average agglomeration size of CaCO₃ and SiO₂-CaCO₃ nano-filler

Type of Filler	Measure 1	Measure 2	Measure 3	Average	S.D.
CaCO ₃	279.5	279.3	276.4	278.4	1.7
[SiO ₂ -CaCO ₃](1:30)	258	263.5	261.9	261.1	2.8
[SiO ₂ -CaCO ₃] (1:20)	249.7	249.1	250.2	249.7	0.6
[SiO ₂ -CaCO ₃](1:10)	194.2	194.9	194.2	194.4	0.4

Surface areas, pore volume and pore size of CaCO₃ and CaCO₃-SiO₂ nano-particles

Type of fillers	Surface area (x10 m ² /g)	S.D.	Pore volume (x 10 ⁻¹ cc/g)	S.D.	Pore size (x 10 ² Angstrom)	S.D.
CaCO ₃	2.425	0.013	2.441	0.013	2.005	0.011
CaCO ₃ -SiO ₂ (1:30)	3.217	0.093	2.686	1.109	1.681	0.739
CaCO ₃ -SiO ₂ (1:20)	4.124	0.044	2.863	1.170	1.385	0.552
CaCO ₃ -SiO ₂ (1:10)	6.080	0.607	4.635	1.337	1.305	0.339

Average Young's modulus of PLA nanocomposite in phase III

Type of nanocomposites	Measure 1	Measure 2	Measure 3	Measure 4	Measure 5	Young's Modulus (MPa)	S.D.
PLA	594	671	675	640	627	641.40	33.40
PLA/CaCO ₃	637	594	657	679	665	646.40	33.00
PLA/[SiO ₂ -CaCO ₃](1:30)	651	715	634	731	683	682.80	41.09
PLA/[SiO ₂ -CaCO ₃](1:20)	743	689	708	697	671	701.60	26.79
PLA/[SiO ₂ -CaCO ₃](1:10)	694	719	779	739	674	721.00	40.71
PLA/10PEG	445	496	509	438	527	483.00	39.53
PLA/CaCO ₃ /10PEG	483	380	414	442	381	420.00	43.62
PLA/[SiO ₂ -CaCO ₃](1:30)/10PEG	487	458	477	391	478	458.20	39.02
PLA/[SiO ₂ -CaCO ₃](1:20)/10PEG	532	437	526	491	444	486.00	44.46
PLA/[SiO ₂ -CaCO ₃](1:10)/10PEG	484	434	536	519	547	504.00	45.82
PLA/10TbC	448	491	506	457	484	477.20	24.12
PLA/CaCO ₃ /10TbC	524	434	389	458	581	477.20	75.79
PLA/[SiO ₂ -CaCO ₃](1:30)/10TbC	587	511	482	503	418	500.20	60.72
PLA/[SiO ₂ -CaCO ₃](1:20)/10TbC	554	582	525	478	511	530.00	39.91
PLA/[SiO ₂ -CaCO ₃](1:10)/10TbC	602	602	608	568	525	581.00	35.06

Average percentage of strain at break of PLA nanocomposite in phase III

Type of nanocomposites	Measure 1	Measure 2	Measure 3	Measure 4	Measure 5	Percentage strain at break (%)	S.D.
PLA	47.1	47.3	68.8	49.5	52.5	53.04	9.08
PLA/CaCO ₃	23.3	29.9	25.8	35.1	30.4	28.90	4.55
PLA/[SiO ₂ -CaCO ₃](1:30)	29.6	38.6	30.9	33.0	25.9	31.60	4.69
PLA/[SiO ₂ -CaCO ₃](1:20)	31.0	28.2	40.5	36.0	30.3	33.20	4.98
PLA/[SiO ₂ -CaCO ₃](1:10)	32.2	35.4	34.8	39.2	31.9	34.70	2.95
PLA/10PEG	243.0	242.0	251.0	184.0	276.7	239.34	33.97
PLA/CaCO ₃ /10PEG	196.0	178.1	212.3	226.0	178.0	198.08	21.15
PLA/[SiO ₂ -CaCO ₃](1:30)/10PEG	246.0	283.0	261.0	240.0	210.0	248.00	26.95
PLA/[SiO ₂ -CaCO ₃](1:20)/10PEG	232.4	255.0	264.0	309.0	290.1	270.10	30.00
PLA/[SiO ₂ -CaCO ₃](1:10)/10PEG	375.0	305.0	318.0	290.0	290.0	315.60	35.20
PLA/10TbC	211.0	290.5	175.9	206.4	215.2	219.80	42.44
PLA/CaCO ₃ /10TbC	182.0	241.7	242.2	194.8	210.1	214.16	27.25
PLA/[SiO ₂ -CaCO ₃](1:30)/10TbC	46.4	56.4	58.0	87.1	32.6	56.10	20.07
PLA/[SiO ₂ -CaCO ₃](1:20)/10TbC	69.1	38.7	38.3	70.5	42.2	51.76	16.55
PLA/[SiO ₂ -CaCO ₃](1:10)/10TbC	38.7	45.5	50.6	57.2	34.4	45.28	9.11

Average impact strength of PLA nanocomposite in phase III

Type of nanocomposites	Measure 1	Measure 2	Measure 3	Measure 4	Measure 5	Impact strength (kJ/m ²)	S.D.
PLA	2.62	3.48	2.55	2.49	2.56	2.74	0.42
PLA/CaCO ₃	1.85	2.23	2.68	2.29	3.39	2.49	0.58
PLA/[SiO ₂ -CaCO ₃](1:30)	2.99	2.72	1.92	2.28	3.13	2.61	0.50
PLA/[SiO ₂ -CaCO ₃](1:20)	2.32	2.96	3.27	3.36	2.35	2.85	0.50
PLA/[SiO ₂ -CaCO ₃](1:10)	3.07	3.22	3.63	2.70	3.25	3.17	0.34
PLA/10PEG	4.34	3.09	4.59	4.18	2.82	3.80	0.79
PLA/CaCO ₃ /10PEG	3.34	2.38	2.23	3.62	2.25	2.76	0.66
PLA/[SiO ₂ -CaCO ₃](1:30)/10PEG	3.00	3.18	2.68	2.08	3.18	2.83	0.46
PLA/[SiO ₂ -CaCO ₃](1:20)/10PEG	3.12	3.15	3.36	3.03	2.83	3.10	0.20
PLA/[SiO ₂ -CaCO ₃](1:10)/10PEG	3.57	2.37	4.81	3.91	2.99	3.53	0.92
PLA/10TbC	3.31	3.89	3.73	3.05	4.04	3.61	0.41
PLA/CaCO ₃ /10TbC	2.85	2.90	2.85	2.97	3.65	3.05	0.34
PLA/[SiO ₂ -CaCO ₃](1:30)/10TbC	2.85	3.14	3.42	3.22	3.52	3.23	0.26
PLA/[SiO ₂ -CaCO ₃](1:20)/10TbC	3.33	3.54	3.77	3.62	3.10	3.47	0.26
PLA/[SiO ₂ -CaCO ₃](1:10)/10TbC	3.71	3.34	3.80	3.58	3.94	3.67	0.23

Average O₂ transmission of PLA nanocomposite sheets

Type of PLA nanocomposite sheet	Measure 1	Measure 2	Measure 3	Average O ₂ TR*	Average thickness**	Normalize***	S.D.
PLA	40.29	44.04	35.75	40.03	0.47	18.84	4.15
PLA/CaCO ₃	41.21	40.74	45.90	42.62	0.50	21.33	2.85
PLA/[SiO ₂ -CaCO ₃](1:30)	44.64	41.87	34.30	40.27	0.43	17.16	5.35
PLA/[SiO ₂ -CaCO ₃](1:20)	29.82	40.16	34.89	34.96	0.43	15.16	5.17
PLA/[SiO ₂ -CaCO ₃](1:10)	28.68	25.48	37.13	30.43	0.45	13.65	6.02
PLA/10PEG	50.85	55.15	59.68	55.23	0.35	19.57	4.42
PLA/CaCO ₃ /10PEG	58.89	55.78	62.05	58.91	0.35	20.69	3.14
PLA/[SiO ₂ -CaCO ₃](1:30)/10PEG	52.54	39.38	43.72	45.21	0.44	20.07	6.71
PLA/[SiO ₂ -CaCO ₃](1:20)/10PEG	43.65	47.40	50.29	47.11	0.38	17.76	3.33
PLA/[SiO ₂ -CaCO ₃](1:10)/10PEG	49.43	39.75	40.74	43.31	0.41	17.70	5.33
PLA/10TbC	54.38	50.79	43.14	49.44	0.46	22.85	5.74
PLA/CaCO ₃ /10TbC	55.82	47.74	51.41	51.66	0.46	23.82	4.05
PLA/[SiO ₂ -CaCO ₃](1:30)/10TbC	50.07	42.97	42.76	45.27	0.48	21.70	4.16
PLA/[SiO ₂ -CaCO ₃](1:20)/10TbC	38.49	45.94	34.15	39.53	0.50	19.59	5.96
PLA/[SiO ₂ -CaCO ₃](1:10)/10TbC	37.45	33.60	46.66	39.24	0.49	19.23	6.71

*O₂TR unit : cm³/m².day.bar

**Thickness unit : mm

***Normalized unit : cm³.mm/m².day.bar

Average CO₂ transmission of PLA nanocomposite sheets

Type of PLA nanocomposite sheet	Measure 1	Measure 2	Measure 3	Average CO ₂ TR [*]	Average thickness ^{**}	Normalize ^{***}	S.D.
PLA	73.7	61.3	70.8	68.60	0.47	32.21	6.49
PLA/CaCO ₃	72.2	65.7	79.9	72.60	0.48	34.82	7.11
PLA/[SiO ₂ -CaCO ₃](1:30)	68.2	72.4	60.1	66.90	0.45	29.78	6.25
PLA/[SiO ₂ -CaCO ₃](1:20)	56.8	65.4	65.6	62.60	0.47	29.58	5.02
PLA/[SiO ₂ -CaCO ₃](1:10)	60.7	65.5	55	60.40	0.47	28.24	5.26
PLA/10PEG	65.1	75.3	76.8	72.40	0.47	34.27	6.37
PLA/CaCO ₃ /10PEG	82.9	89.7	74	82.20	0.43	35.36	7.87
PLA/[SiO ₂ -CaCO ₃](1:30)/10PEG	80.4	71.3	83.5	78.40	0.44	34.73	6.34
PLA/[SiO ₂ -CaCO ₃](1:20)/10PEG	60.9	69.7	56.6	62.40	0.48	30.04	6.68
PLA/[SiO ₂ -CaCO ₃](1:10)/10PEG	68.5	57.8	52.2	59.50	0.48	28.43	8.28
PLA/10TbC	67.3	74.6	82.2	74.70	0.49	36.68	7.45
PLA/CaCO ₃ /10TbC	71.7	78.4	83	77.70	0.48	37.31	5.68
PLA/[SiO ₂ -CaCO ₃](1:30)/10TbC	70.5	78.9	71.4	73.60	0.50	36.68	4.61
PLA/[SiO ₂ -CaCO ₃](1:20)/10TbC	65.9	58.1	68.9	64.30	0.51	33.09	5.57
PLA/[SiO ₂ -CaCO ₃](1:10)/10TbC	68.2	62.8	54.4	61.80	0.51	31.47	6.95

*CO₂TR unit : cm³/m².day.bar

**Thickness unit : mm

***Normalized unit : cm³.mm/m².day.bar

Average water vapor transmission of PLA nanocomposite sheets

Type of PLA nanocomposite sheet	Measure 1	Measure 2	Measure 3	Average WVTR *	Average thickness **	Normalize ***	S.D.
PLA	25.4	20.1	28.6	24.70	0.45	11.18	4.29
PLA/CaCO ₃	22.9	28.6	24.4	25.30	0.46	11.70	2.95
PLA/[SiO ₂ -CaCO ₃](1:30)	19.6	23.4	26	23.00	0.43	9.85	3.22
PLA/[SiO ₂ -CaCO ₃](1:20)	18.6	25.4	19	21.00	0.46	9.57	3.82
PLA/[SiO ₂ -CaCO ₃](1:10)	23.7	16.5	17.1	19.10	0.49	9.45	3.99
PLA/10PEG	27.4	35.1	31.1	31.20	0.48	14.86	3.85
PLA/CaCO ₃ /10PEG	55.7	43.3	51.3	50.10	0.41	20.70	6.29
PLA/[SiO ₂ -CaCO ₃](1:30)/10PEG	50.1	54.2	40.6	48.30	0.43	20.58	6.98
PLA/[SiO ₂ -CaCO ₃](1:20)/10PEG	41.2	33.7	43.3	39.40	0.46	18.30	5.05
PLA/[SiO ₂ -CaCO ₃](1:10)/10PEG	32.4	37.8	42.6	37.60	0.46	17.33	5.10
PLA/10TbC	30	23.5	28.7	27.40	0.47	12.99	3.44
PLA/CaCO ₃ /10TbC	29.9	23.6	32.9	28.80	0.46	13.34	4.75
PLA/[SiO ₂ -CaCO ₃](1:30)/10TbC	20.5	25.8	20.6	22.30	0.48	10.74	3.03
PLA/[SiO ₂ -CaCO ₃](1:20)/10TbC	20.1	15.4	21.8	19.10	0.50	9.50	3.32
PLA/[SiO ₂ -CaCO ₃](1:10)/10TbC	19.7	15.7	14.4	16.60	0.49	8.17	2.76

*WVTR unit : cm³/m².day.bar

**Thickness unit : mm

***Normalized unit : cm³.mm/m².day.bar

APPENDIX B
PUBLICATION AND PRESENTATION

Paper Publication

1. Thermal-mechanical property and fracture behavior of plasticized PLA-CaCO₃ nanocomposite

The part of the dissertation as the topic of “Thermal-mechanical property and fracture behavior of plasticized PLA-CaCO₃ nanocomposite” was accepted to publish in peer-reviewed international journal (Plastics, Rubber and Composite: Macromolecular Engineering, U.K.) on 7 November 2011.

Your submission PRCME3017R1 Inbox x

Plastics, Rubber and Composites xwang5@bradford.ac.uk via editorialmanager.com 11/8/11 ☆ ↶ ↷
to me ▾

Ref: PRCME3017R1
Thermal-mechanical property and fracture behavior of plasticized PLA-CaCO₃ nanocomposite
Plastics, Rubber and Composites: Macromolecular Engineering

Dear Dr. Patanathabutr

Thank you for submitting a revised version of the above submission and your response to the comments made by the reviewers. I am pleased to confirm that the paper is accepted for publication in Plastics, Rubber and Composites: Macromolecular Engineering. It was accepted on 07 Nov 2011

We will contact you again only if problems arise with the text or figure files. Otherwise your paper will be passed to the Production Department.

You will shortly receive an email detailing log-in instructions for ManeyTrack - Maney Publishing's web-based production tracking system. Via ManeyTrack you will be able to view the production status of your article at any time, and also have the option to place orders for offprints, issue copies (if the journal has a print offering) and to make your article open access via Maney's MORE OpenChoice offering (see below).

You will receive PDF proofs by email in approximately three to four weeks' time. Please note that any corrections from this point on must be made when you receive your PDF proofs. Instructions for proof correction will be supplied within the email which contains the proofs.

The final version of your paper will be posted online in approximately seven to eight weeks from acceptance, providing you meet the timescales outlined in the email which contains your proofs. You can view your paper at <http://www.ingentaconnect.com/content/maney/prc/pre-prints>. Please note that you can cite your paper using the Digital Object Identifier (DOI).

For any production-related queries, please contact the Production Editor at prc@maney.co.uk.

MORE OpenChoice

Maney Publishing offers an open access option, that we call MORE OpenChoice. Authors may choose to participate by paying an article charge of \$2000/£1250 in return for which Maney will undertake to prepare and deposit a final version in PubMed Central or other nominated repositories. MORE OpenChoice papers are also publicly accessible via our online hosting platforms, IngentaConnect and/or Highwire, and are supplied in print to all subscribers. More detailed information on MORE OpenChoice can be found at www.maney.co.uk/moreopenchoice.

To participate in MORE OpenChoice, authors will be required to make payment via ManeyTrack, Maney Publishing's web-based production tracking system. Log-in details for ManeyTrack are supplied via email to the corresponding author once his/her paper has entered production.

For more detailed information regarding payment options please visit www.maney.co.uk/moreopenchoice/info.

Thank you for submitting your work to Plastics, Rubber and Composites: Macromolecular Engineering.

With kind regards

A G Gibson
Associate Editor
Plastics, Rubber and Composites: Macromolecular Engineering

Thermal–mechanical property and fracture behaviour of plasticised PLA–CaCO₃ nanocomposite

B. Nekhamanurak^{1,2}, P. Patanathabutr^{*1,2} and N. Hongsriphan^{1,2}

This study investigates the influence of two plasticisers, polyethylene glycol (PEG) and tributyl citrate (TbC), on the thermomechanical properties and fracture behaviour of nanosized calcium carbonate blended poly(lactic acid). Various compositions of nanocomposites were compounded and processed using co-rotating twin screw extrusion and compression moulding. DMA analysis shows that adding nano-CaCO₃ reduced the storage modulus (E') of the nanocomposite while the glass transition temperature (T_g) of the samples was not affected. Furthermore, plasticised poly(lactic acid) (PLA) showed an improvement in elongation at break in all samples, and the impact resistance of the nanocomposites was also improved by 1.6 times with the addition of 20 phr PEG plasticiser and by 1.4 times with the addition of 20 phr TbC plasticiser. Morphological study reveals that the fracture behaviour of PLA–CaCO₃ nanocomposites changed from brittle to ductile after plasticisers were incorporated.

Keywords: Poly(lactic acid), Nanocomposite, Plasticiser, Extrusion, Compression moulding, Thermomechanical analysis, Mechanical properties, Fracture surface

Introduction

Aliphatic polyesters such as poly(lactic acid) (PLA) nowadays play an important role in various applications due to their biodegradable and biocompatible characters.^{1–5} PLA, typically polymerised through the fermentation products of starch and sugar,⁴ offers a potential alternative to petrochemical based plastics in many applications such as biomedical applications and food packaging.^{1,6,7} PLA, however, is comparatively brittle and stiff at room temperature,^{4,8} so modification of PLA is needed for applications that require flexibility such as food packaging.

Adding fillers to plastics is usually done to improve their mechanical properties. Recently, there have been extensive efforts to improve polymeric materials' properties with nanosized inorganic fillers such as ZnO, SiO₂, clay, precipitated calcium carbonate surface modified with rare earth elements and noble metals.^{9,10} Properties of filler filled composites are closely related to the dispersion of particles in the polymer matrix. Since PLA is well known for its difficulty in crystallisation, adding CaCO₃ could have an impact on its properties as well as potential applications replacing petrochemical based plastics.^{11,12}

Moreover, previous researches have shown that addition of plasticisers such as polyethylene glycol (PEG), glucosomonesters, and partial fatty acid esters successfully improves the brittleness and widens PLA's applications.^{8,13} Thus, in the present contribution, the effect of two plasticisers, PEG and tributyl citrate (TbC), on thermomechanical properties and fracture behaviour of PLA–CaCO₃ nanocomposites was investigated.

Experimental

Materials

Poly(lactic acid) (Natureworks2002D, NatureWorks LLC, USA), Calcium carbonate (NPCC 101, Behn Meyer Chemical), Poly(ethylene glycol) (PEG, Mw ~400, Fluka), and Tributyl citrate (TbC, Mw ~360, Fluka) were used as received.

Preparation of plasticised PLA–CaCO₃ nanocomposites

Prior to compounding, PLA and CaCO₃ were dried overnight at 60°C in order to remove structural water. The EN MACH SHJ-25 co-rotating twin screw extruder was used to compound the nanocomposites (Table 1). PLA and CaCO₃ blends were prepared by weight percentage while PEG and TbC were added as parts per hundred (phr) into the blends. The barrel temperature profile adopted during blending ranged from 150°C in the feed zone to 170°C in metering zone at a fixed screw speed of 130 rev min⁻¹. The extruded materials were then compression moulded into standard tensile

¹Department of Materials Science and Engineering, Faculty of Engineering and Industrial Technology, Silpakorn University, Nakhon Pathom 73000, Thailand

²Center of Excellence for Petroleum, Petrochemicals, and Advanced Materials, Chulalongkorn University, Bangkok 10330, Thailand

*Corresponding author, email ppatanathabutr@gmail.com

and impact specimens using LabTech compression moulding with mould temperature of 170°C and mould pressure of 20 000 psi for 5 min.

Thermal analysis

The storage modulus (E') of the PLA, and PLA nanocomposites as a function of temperature was determined by dynamic mechanical analysis method using DMA, GABO EPLEXOR QC25. DMA spectra were taken in the tension mode at a frequency of 1 Hz, in a temperature range of 25–160°C at a heating rate of 2 K min⁻¹.

The melting and crystallisation behaviour of the nanocomposites were studied by a differential scanning calorimeter (DSC) (Mettler Toledo DSC822e) under nitrogen atmosphere. The temperature was raised from 20 to 180°C at a heating ramp of 10 K min⁻¹.

Mechanical analysis

Tensile tests were carried out according to ASTM D638 type V using a universal testing machine (LR50K, Lloyd Instruments, UK) under ambient conditions with cross-head speeds of 10 mm min⁻¹. Izod impact tests, according to ASTM D256, were done on notched impact specimens, by using an instrument impact tester (Radmana Model ITR2000).

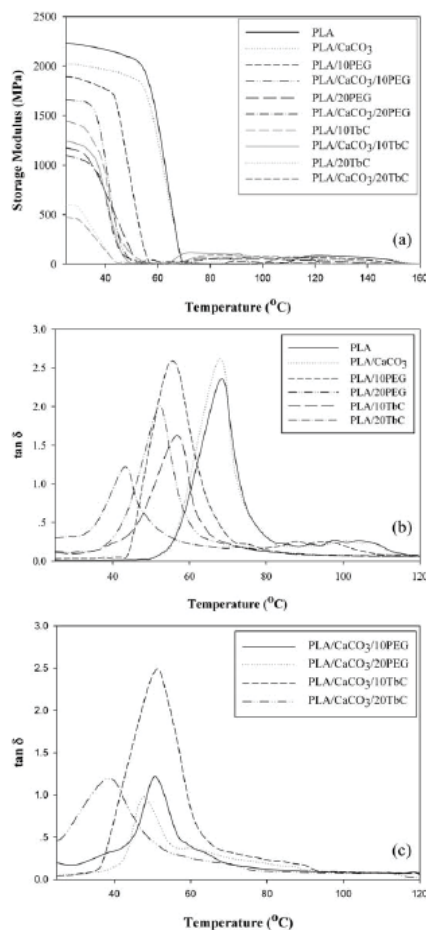
2 Morphological study

The morphology of nanocomposite was investigated by scanning electron microscopy (SEM). The fracture surfaces of samples were sputtered with platinum and then the morphology was observed in an SEM instrument (Hitachi Model S3400N).

Results and discussion

Thermal analysis

Figure 1 shows the dynamic mechanical analysis results of plasticised PLA-CaCO₃ nanocomposites over a temperature range of 25–160°C. From Fig. 1a, showing the E' of the nanocomposites as a function of temperature, it can be seen that the E' of samples was rather stable as the temperature increased from 25 to 50°C. Subsequently, the E' dropped rapidly at about the temperature designated as their T_g , and then increased slightly again at temperatures above T_g , because of the cold crystallisation of PLA matrix.^{14,15} Additionally, from Fig. 1a, the incorporation of CaCO₃ nanoparticles in the composites resulted in the reduction of the E' , but did not affect T_g of PLA. This was due to the lubricating effect of sizing agents from fatty acids used to treat the CaCO₃ surface in order to prevent it from agglomeration.¹⁶ Furthermore, the spherulitic structure

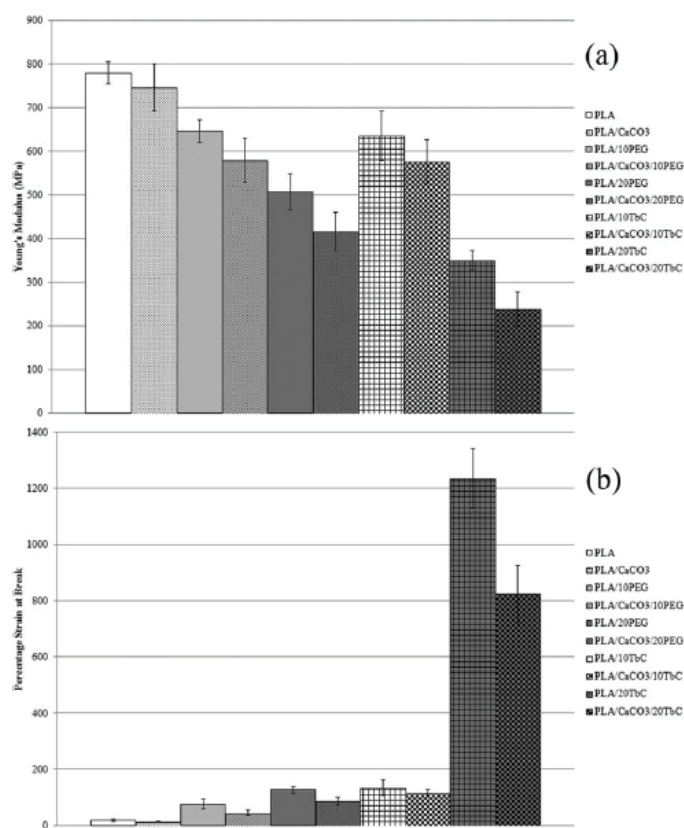


1 a storage modulus, and b, c tan δ as a function of temperature of PLA/CaCO₃/plasticisers nanocomposites

is destroyed because of the nucleating effect of the CaCO₃ nanoparticles. A reduction in the spherulite size and crystallinity decreases the modulus of polymer,

Table 1 Designations of materials and their compositions

Names	Designations	Compositions	Parts
PLA	PLA	PLA	100
PLA-CaCO ₃	PLA/CaCO ₃	PLA/CaCO ₃	95/5
10 phr PEG plasticised PLA	PLA/10PEG	PLA/PEG	100/10
10 phr PEG plasticised PLA-CaCO ₃	PLA/CaCO ₃ /10PEG	PLA/CaCO ₃ /PEG	95/5/9.5
20 phr PEG plasticised PLA	PLA/20PEG	PLA/PEG	100/20
20 phr PEG plasticised PLA-CaCO ₃	PLA/CaCO ₃ /20PEG	PLA/CaCO ₃ /PEG	95/5/19
10 phr TbC plasticised PLA	PLA/10TbC	PLA/TbC	100/10
10 phr TbC plasticised PLA-CaCO ₃	PLA/CaCO ₃ /10TbC	PLA/CaCO ₃ /TbC	95/5/9.5
20 phr TbC plasticised PLA	PLA/20TbC	PLA/TbC	100/20
20 phr TbC plasticised PLA-CaCO ₃	PLA/CaCO ₃ /20TbC	PLA/CaCO ₃ /TbC	95/5/19



2 Mechanical properties of PLA/CaCO₃/plasticisers nanocomposites: a Young's modulus and b percentage elongation at break of the samples

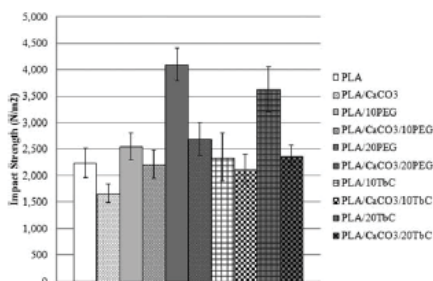
because large spherulites are believed to have a much higher load bearing capability.^{17,18}

Figure 1b and c shows $\tan \delta$ of the nanocomposites as a function of temperature. Clearly, both of these figures show the effect of plasticisers on the viscoelastic

properties of the PLA nanocomposites. When PEG or TbC was blended into PLA, the T_g of all samples dropped significantly in line with the amount of plasticisers added. This implies that the plasticiser enhances the mobility of PLA polymer chains at low

Table 2 DSC of PLA, PLA nanocomposite and plasticised PLA nanocomposites

Materials	First heat scan				Cool scan	Second heat scan			
	T_g	T_c	T_m			T_g	T_c	T_m	
			Peak 1	Peak 2				Peak 1	Peak 2
PLA	56-16	123-07	...	149-13	...	54-36	126-14	...	149-90
PLA/CaCO ₃	55-75	109-1	...	150-09	...	54-60	125-97	...	150-22
PLA/10PEG	43-34	83-79	136 (shoulder)	148-25	...	36-54	95-99	135-83	146-54
PLA/CaCO ₃ /10PEG	39-98	77-19	134 (shoulder)	146-29	81-63	28-61	83-66	131-65	145-52
PLA/20PEG	42-13	77-8	129-84	146-2	...	24-52	87-84	133-18	146-37
PLA/CaCO ₃ /20PEG	40-74	76-15	128 (shoulder)	145-99	80-42	23-13	...	128-99	143-68
PLA/10TbC	47-44	111-92	...	148-42	...	47-2	122-73	...	148-48
PLA/CaCO ₃ /10TbC	38-5	92-34 (shoulder)	136-2	148-28	...	36-53	101-83	138-49	147-93
PLA/20TbC	27-35	88-8	133 (shoulder)	145-57	...	27-13	102-48	138-29	145-59
PLA/CaCO ₃ /20TbC	25-5	77-51	130 (shoulder)	145-83	...	22-06	90-84	131-16	144-69

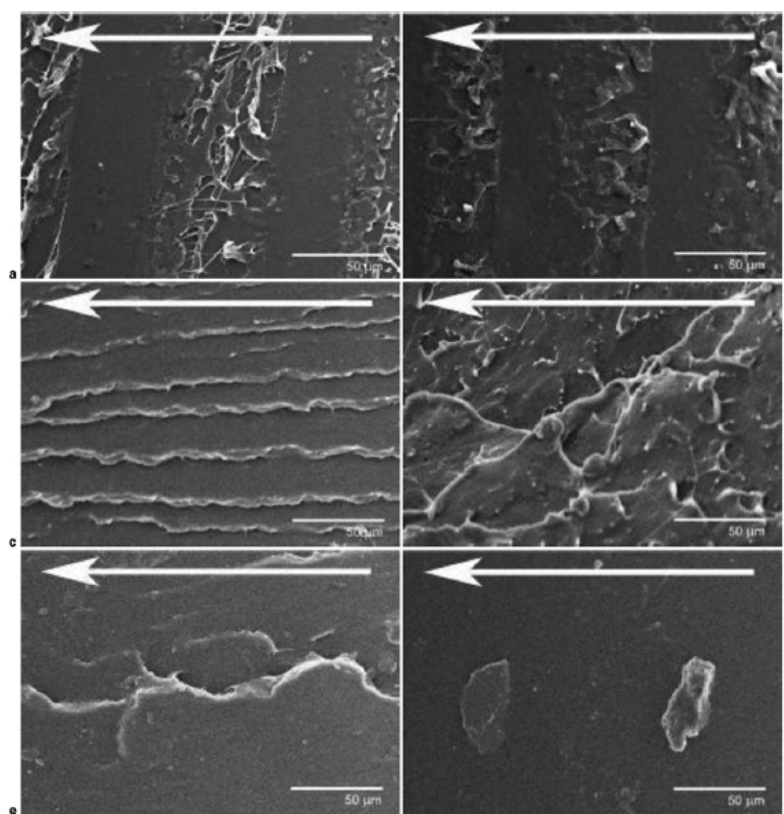


3 Dependence of impact strength on composition of prepared nanocomposites

temperature.^{13,15} Moreover, the incorporation of CaCO₃ nanoparticles and plasticisers tends to reduce T_g of PLA more than using plasticiser alone, indicating a synergistic plasticising effect between sizing agents and plasticiser.

DSC analysis was conducted to study effect of adding of CaCO₃ and PEG or TbC on composite thermal properties. The glass transition temperature (T_g), melting temperature (T_m), and crystallisation temperature (T_c) of the nanocomposites are summarised in Table 2. It is interesting to note that the T_c peak for PLA appeared during cooling only in PEG plasticised PLA-CaCO₃ nanocomposites. It is believed that the main reason for this occurrence was due to a very slow crystallisation rate of PLA during cooling.¹³ Furthermore, PLA crystallisation temperature decreases strongly with PEG addition. This indicates a higher mobility of PLA macromolecules. This enhancement of the PLA molecular mobility is claimed to be the major factor acting on the crystallisation kinetic of this polymer.¹⁹

In addition, it can be observed from Table 2 that the T_g of the nanocomposites shows the same trend as in the DMA results, where the T_g of PLA drops with an increasing amount of plasticisers. Moreover, increasing loading of plasticiser resulted in the shift of T_c to lower temperatures. This was due to better mobility of PLA molecules that were plasticised by PEG and TbC.



a PLA; b PLA/CaCO₃; c PLA/10PEG; d PLA/20PEG; e PLA/10TbC; f PLA/20TbC

4 Images (SEM) of impact fractured specimen of PLA/CaCO₃/plasticisers nanocomposites (White arrow indicates stress direction in impact test)

Comparing the effect of these plasticisers, it is found that the lowest T_g of the nanocomposite was obtained at the content of 20 phr of TbC.

Mechanical analysis

The mechanical properties of the nanocomposites were examined by tensile test according to the ASTM D638 standard. Figure 2 reveals the tensile properties of nanocomposites incorporating various contents and types of plasticisers. It shows that elastic modulus of PLA-CaCO₃ nanocomposites was slightly lower than those of neat PLA, similar to the reduction in storage modulus. Adding plasticisers further decreased the elastic modulus of PLA, and plasticising with TbC decreased elastic modulus of PLA dramatically. In the presence of CaCO₃, the decrease in percentage elongation at break of PLA demonstrates that fillers induce a definite decrease in elongation²⁰ because CaCO₃ acted as stress concentrator to promote crack initiation. After plasticising, percentage elongation at break of neat PLA and PLA composites were higher. Adding plasticisers increased percentage elongation at break by 40 times when compared to neat PLA and unplasticised PLA nanocomposites.

Figure 3 presents the notched impact strengths of the nanocomposites. From the results, it can be seen that CaCO₃ reduced the impact strength of PLA. This might be resulted by coarse morphologies of smaller particle sizes (<0.7 μm) lowering the toughening efficiency.²¹ On the other hand, the impact resistance of the samples was improved by 1.6 times with the addition of 20 phr PEG plasticiser and by 1.4 times with the addition of 20 phr TbC plasticiser.

Morphological study

Figure 4 is the SEM image showing that the fracture behaviour of PLA-CaCO₃ nanocomposites changed from brittle to ductile after plasticisers were incorporated. The fracture surface of neat PLA was smooth with local ductile breaking as craze and crack propagation occurred during the fast breaking. When CaCO₃ was added into the polymer matrix, it behaved as stress concentrators, promoting crack initiation and reducing local ductile breaking. When plasticisers were blended into PLA, nanocomposites were tougher and ductile failure was dominant. Stripes of local extension in the polymer matrix were present in the fracture surface of 10 phr plasticised PEG nanocomposite, and these stripes became more randomly distributed when PEG was 20 phr. Meanwhile, TbC plasticised PLA nanocomposites broke mainly in ductile failure, even when CaCO₃ nanoparticles were added.

Conclusions

In this study, plasticised PLA-CaCO₃ nanocomposites were prepared using twin screw extruder and compression moulding. The elongation of all samples was improved with increasing loadings of plasticisers. DMA and DSC results reveal that the incorporation of plasticisers can improve the thermal properties of PLA, particularly in reduction in T_c and T_m . Finally, morphological study reveals that the fracture behaviour of PLA-CaCO₃ nanocomposites changed from brittle to ductile after plasticisers were incorporated.

Acknowledgements

The authors would like to thank Department of Material Science and Engineering, Faculty of Engineering and Industrial Technology, Silpakorn University and the Center of Excellence for Petroleum, Petrochemicals and Advanced Materials for financial support.

References

1. F. P. L. Mantia and M. Morreale: *Composites Part A*, 2011, **42A**, 579–588.
2. D. Garlotta: *J. Polym. Environ.*, 2001, **9**, 63–84.
3. T. D. Lam, T. V. Hoang, D. T. Quang and J. S. Kim: *Mater. Sci. Eng., A*, 2009, **A501**, 87–93.
4. L.-T. Lim, R. Auras and M. Rubino: *Prog. Polym. Sci.*, 2008, **33**, 820–852.
5. S. S. Ray and M. Bousmina: *Prog. Mater. Sci.*, 2005, **50**, 962–1079.
6. B.-K. Chen, C.-H. Shen, S.-C. Chen and A. F. Chen: *Polymer*, 2010, **51**, 4667–4672.
7. V. Siracusa, P. Rocculi, S. Romani and M. D. Rosa: *Trends Food Sci Technol*, 2008, **19**, 634–643.
8. M.-A. Paul, M. Alexandre, P. Degée, C. Henrist, A. Rulmont and P. Dubois: *Polymer*, 2003, **44**, 443–450.
9. I. Pluta, M. Murariu, M. Alexandre, A. Galeski and P. Dubois: *Polym. Degrad. Stab.*, 2008, **93**, 925–931.
10. C. Thellen, C. Orroth, D. Froio, D. Ziegler, J. Lucciarini, R. Farrell, N. A. D'Souza and J. A. Ratto: *Polymer*, 2005, **46**, 11716–11727.
11. S. Miao: *Appl. Surf. Sci.*, 2003, **220**, 298–303.
12. K. Goma, M. Hund, M. Vucčak, F. Gröhn and G. Wegner: *Mater. Sci. Eng. A*, 2008, **477A**, 217–225.
13. H. Balakrishnan, A. Hassan, M. U. Wahit, A. A. Yussuf and S. B. A. Razak: *Mater. Des.*, 2010, **31**, 3289–3298.
14. T. Miyata and T. Masuko: *Polymer*, 1998, **39**, 5515–5521.
15. N. Ljungberg and B. Wessle: *Polymer*, 2003, **44**, 7679–7688.
16. S. Yan, J. Yin, J. Yang and X. Chen: *Mater. Lett.*, 2007, **61**, 2683–2686.
17. C.-M. Chan, J. Wu, J.-X. Li and Y.-K. Cheung: *Polymer*, 2002, **43**, 2981–2992.
18. J. L. Way, J. R. Atkinson and J. Nutting: *J. Mater. Sci.*, 1974, **9**, 293–299.
19. I. Pillin, N. Montrely and Y. Grohens: *Polymer*, 2006, **47**, 4676–4682.
20. Z. Bartczak, A. S. Argon, R. E. Cohen and M. Weinberg: *Polymer*, 1999, **40**, 2347–2365.
21. W. C. J. Zuidenduin, C. Westzaan, J. J. Hučtink and R. J. Gaymans: *Polymer*, 2003, **44**, 261–275.

2. Surface modified CaCO₃ nanoparticles with silica via sol-gel process using in poly(lactic acid) nanocomposite

The part of the dissertation as the topic of “Surface modified CaCO₃ nanoparticles with silica via sol-gel process using in poly(lactic acid) nanocomposite” was online published in peer-reviewed international journal (Advanced Materials Research Journal, vols. 488-489, pp. 520-524, 2012, Switzerland) on 15 March 2012.

From: ICKEM 2011 <ickem@vip.163.com>  [Hide](#)

Subject: K0058.ICKEM2012.Review Form [Inbox - Windowslive](#)

Date: November 10, 2554 BE 6:25:08 PM GMT+07:00

To: bawornkit@windowslive.com , pajaera p

2 Attachments, 377 KB Save ▾ Quick Look

Dear **Bawornkit Nekhamanurak, Pajaera Patanathabutr and Nattakarn Hongsriphan** ,

Paper ID : **K0058**
Paper Title : **Surface modified CaCO₃ Nanoparticles With Silica Via Sol-Gel Process Using In Poly(Lactic Acid) Nanocomposite**

Congratulations! The review processes for 2012 2nd International Conference on Key Engineering Materials (ICKEM 2012) has been completed. The conference received submissions from nearly 12 different countries and regions, which were reviewed by international experts, and about 100 papers have been selected for presentation and publication. Based on the recommendations of the reviewers and the Technical Program Committees, we are pleased to inform you that your paper identified above has been accepted for publication and oral presentation. You are cordially invited to present the paper orally at ICKEM2012 to be held on February 26-28, 2012, in Singapore.

The ICKEM 2012 is organized by International Association of Computer Science and Information Technology (IACSIT), and has been listed in the TTP Conference Search.

Advanced Materials Research Vols. 488-489 (2012) pp 520-524
Online available since 2012/Mar/15 at www.scientific.net
 © (2012) Trans Tech Publications, Switzerland
 doi:10.4028/www.scientific.net/AMR.488-489.520

Surface Modified CaCO₃ Nanoparticles with Silica via Sol-Gel Process using in Poly(lactic acid) Nanocomposite

Bawornkit Nekhamanurak^{1,2,a}, Pajaera Patanathabutr^{1,2,b}
 and Nattakarn Hongsriphan^{1,2,c}

¹ Department of Materials Science and Engineering, Faculty of Engineering and Industrial Technology, Silpakorn University, Nakhon Pathom, 73000, Thailand

² Center of Excellence for Petroleum, Petrochemicals, and Advanced Materials, Chulalongkorn University, Bangkok, 10330, Thailand

^a bawornkit@windowslive.com, ^b pajaera@su.ac.th, ^c nattakar@su.ac.th

Keywords: nanocomposite, poly(lactic acid), calcium carbonate nanoparticle, silica, sol-gel

Abstract. The goal of this work is to modify surface of calcium carbonate nanoparticles with silica (CaCO₃@SiO₂) via sol-gel process, and to investigate the influence of CaCO₃@SiO₂ on mechanical properties and fracture behavior of poly(lactic acid) nanocomposite. Modified CaCO₃@SiO₂ nanoparticles were prepared with different Si/Ca ratios. It is found that the Si:Ca wt% ratio was increased with respect to the Si:Ca mole ratio used in the reaction. Incorporating CaCO₃@SiO₂ of 5 wt% increased elastic modulus, %elongation at break and notched impact strength of PLA nanocomposites, which these properties of CaCO₃@SiO₂-PLA nanocomposite was increased with respect to increasing of SiO₂ content on the surface of CaCO₃ nano-particles. This implies that better compatibility between polymer matrix and filler was achieved after modification surface of CaCO₃ with SiO₂ layers.

Introduction

Poly(lactic acid) (PLA) is a linear aliphatic biodegradable thermoplastic polyester, produced from renewable resources typically polymerized through the fermentation products of starch and sugar [1]. PLA play an important role in various applications due to their biodegradable and biocompatible characters [1-5]. It offers a potential alternative to petrochemical plastics in many applications such as biomedical applications and food packaging [2, 6-7]. PLA, however, is comparatively brittle and stiff at room temperature [1, 8], so modification is needed for PLA in order to apply with flexible-desired applications such as food packaging.

Adding fillers into plastics are usually implemented not only confined to cost reduction, but also to control their physical and mechanical performance [5, 9-10]. Recently, there are widely improving of polymer properties using nano-size inorganic fillers such as ZnO, SiO₂, clay, precipitated calcium carbonate (PCC) surface modified with rare earth elements, and noble metals [11-12]. In consideration of various fillers, calcium carbonate (CaCO₃) is the famous material, widely used in various industries, due to its high amount of loading in plastics and low cost [13-14]. Since PLA is well known for its difficulty to crystalline, adding CaCO₃ could have an impact on its properties as well as potential applications replacing petrochemical based plastics [14-15].

In order to produce CaCO₃@SiO₂.nH₂O nanocomposite particles, CaCO₃ was use as a template nucleus and the surface of nucleus was encapsulated by a SiO₂.nH₂O nanolayer. Synthetic silica fixed on the surfaces of calcium carbonate particles has good properties such as a high specific surface area and high absorbability, benefits to form linkage at the interface of two materials (plastic and filler), connecting to improve mechanical properties of materials [16-17]. Therefore, this work aims to modify surface of calcium carbonate nano-particles with silica (CaCO₃@SiO₂) via sol-gel process, and to investigate the influence of CaCO₃@SiO₂ on mechanical properties and fracture behavior of poly(lactic acid) nanocomposite.

Experimental

Materials. Poly(lactic acid) (PLA, Natureworks®2002D, NatureWorks LLC, USA) and calcium carbonate (CaCO_3 , NPCC 101, Behn Meyer Chemical) were used as received.

In the preparation of SiO_2 coated CaCO_3 particles, tetraethylorthosilicate (TEOS, Fluka), ethanol and ammonium hydroxide (NH_4OH , 35% NH_3 , Mallinckrodt Chemical) were used.

Preparation of silica coated calcium carbonate composite particles. The $\text{CaCO}_3@ \text{SiO}_2$ particles were prepared by hydrolysis-condensation polymerization of TEOS on the surface of CaCO_3 particles. The CaCO_3 particles were dispersed into the mixture of TEOS, 200 ml ethanol and 300 ml distillation water. The mole ratios of TEOS to CaCO_3 were vary as 1:30, 1:20 and 1:10 then, 100 ml NH_4OH was added slowly, and the mixture was vigorously stirred at 40 °C for 6 h. After the reaction, the SiO_2 coated CaCO_3 particles ($\text{CaCO}_3@ \text{SiO}_2$) were filtrated and washed with ethanol followed by distillation water for several times to remove dissociative polysiloxane, unreacted monomer, and polysiloxane oligomers. The $\text{CaCO}_3@ \text{SiO}_2$ particles were then dried at 60°C in vacuum oven.

Particle characterization. Morphology of $\text{CaCO}_3@ \text{SiO}_2$ particles were investigated using transmission electron microscopy (TEM, Jeol model JEN-1230). The elemental content of $\text{CaCO}_3@ \text{SiO}_2$ particle was analyzed by X-ray fluorescence spectrometer (XRF, Phillips PW-2404).

Preparation of PLA nanocomposites. Prior to compounding, PLA, CaCO_3 and $\text{CaCO}_3@ \text{SiO}_2$ were dried overnight at 60 °C in order to remove residual moisture. EN MACH SHJ-25 co-rotating twin-screw extruder was used to compound the 5%wt content of CaCO_3 - and $\text{CaCO}_3@ \text{SiO}_2$ -PLA nanocomposites. The barrel temperature profile adopted during blending was ranged from 150°C in the feed zone to 170°C in metering zone at the fixed screw speed of 130 rpm. Then the extruded materials were compression molded into standard tensile and impact specimens using LabTech Compression Molding with mold temperature of 170°C and mold pressure of 20,000 psi for 5 min.

Mechanical analysis. Tensile test was carried out in according to ASTM D638 type V using a universal testing machine (INSTRON 5969) under ambient conditions with crosshead speeds of 10 mm/min. Nocthed Izod impact test, according to ASTM D256, was done on notched impact specimens, by using an instrument impact tester (Zwick model B5102.202 Izod Pendulum 4 J).

Morphological studied. Morphology of nanocomposite was investigated by scanning electron microscopy (SEM) using a Hitachi Model S3400N SEM instrument. Prior to testing, the fracture surfaces of samples were sputtered with platinum.

Results and discussion

Characterization of modified CaCO_3 nanoparticle

Fig. 1 shows TEM images of CaCO_3 and $\text{CaCO}_3@ \text{SiO}_2$ nanoparticles. It is seen that there were SiO_2 layers coated around the CaCO_3 nanoparticles causing the slightly increase in particle sizes, however, the particle size of $\text{CaCO}_3@ \text{SiO}_2$ particles were still in the range of nano-scale. Layers of synthesized SiO_2 were coated on the surface of CaCO_3 nanoparticles. However, some crystals of synthesized SiO_2 grew stacked to each other. The elemental content of $\text{CaCO}_3@ \text{SiO}_2$ was analyzed by XRF, which the Si:Ca wt% ratio was calculated and presented in Table 1. It is found that the Si:Ca wt% ratio was increased with respect to the Si:Ca mole ratio used in the reaction.

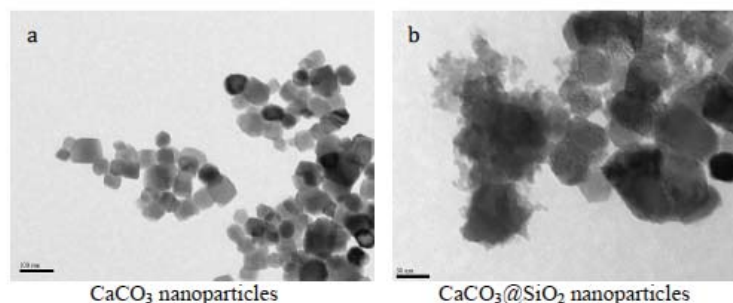


Fig.1. Morphologies of (a) CaCO_3 nanoparticles and (b) $\text{CaCO}_3@SiO_2$ nanoparticles.

Table 1. Comparison of Si/Ca ratio in $\text{CaCO}_3@SiO_2$ particles.

Particles (mole ratio)	Si/Ca (%wt), XRF
$\text{CaCO}_3@SiO_2$ (30:1)	2.17
$\text{CaCO}_3@SiO_2$ (20:1)	4.37
$\text{CaCO}_3@SiO_2$ (10:1)	8.71

Mechanical analysis

Fig. 2 shows the tensile properties of PLA- CaCO_3 and PLA- $\text{CaCO}_3@SiO_2$ nanocomposites. Compared with neat PLA, incorporating CaCO_3 nanoparticles of 5 wt% relatively did not improve elastic modulus of PLA nanocomposite. It indicates that CaCO_3 nanoparticles did not have good efficiency to reinforce nanocomposite as well as those used nanoclays. Lack of reinforcing ability of CaCO_3 nanoparticles would come from their cubic shape that did not good for load bearing compared to the platelets in nanoclays. Moreover, the fatty acid based sizing agents treated on CaCO_3 surface to prevent them from agglomeration would cause lubricating effect in the nanocomposites during the load bearing [18]. In the other hand, incorporating $\text{CaCO}_3@SiO_2$ at the same content did increase elastic modulus of PLA nanocomposites, and elastic modulus of PLA- $\text{CaCO}_3@SiO_2$ nanocomposite was increased in according to increasing of SiO_2 content on the surface of CaCO_3 nano-particles.

In this work, compatibility between PLA matrix and CaCO_3 nanoparticles was not modified by means of coupling agents. In the presence of nano-fillers, the decrease of %elongation at break of PLA composite demonstrates that the interfacial interaction between PLA matrix and CaCO_3 was so poor that fillers induced a definite decrease in elongation [19], because they acted as stress concentrator to promote crack initiation. Surprisingly, the increase of SiO_2 content on $\text{CaCO}_3@SiO_2$ retarded crack propagation to occur at higher % elongation at break. This implies that better compatibility between polymer matrix and filler was achieved. This might due to there was interaction between SiO_2 coated around the CaCO_3 and the hydroxyl groups at the chain ends in PLA matrix. This is also possibly the reason how the elastic modulus of $\text{CaCO}_3@SiO_2$ -PLA nanocomposite was improved.

Fig. 3 presents the notched impact strength of PLA- CaCO_3 and PLA- $\text{CaCO}_3@SiO_2$ nanocomposites. Similarly to tensile test, the presence of CaCO_3 nanoparticle became the stress concentration in the PLA matrix causing them to premature breakage. Adding $\text{CaCO}_3@SiO_2$ nanoparticles with Si/Ca ratio more than 2 wt% could improve impact strength of PLA composite to be higher than those of neat PLA. This means that modification the surface of CaCO_3 nanoparticles with small amount of SiO_2 via sol-gel process could provide better compatible with PLA matrix and CaCO_3 nanoparticle yielding more desired mechanical properties.

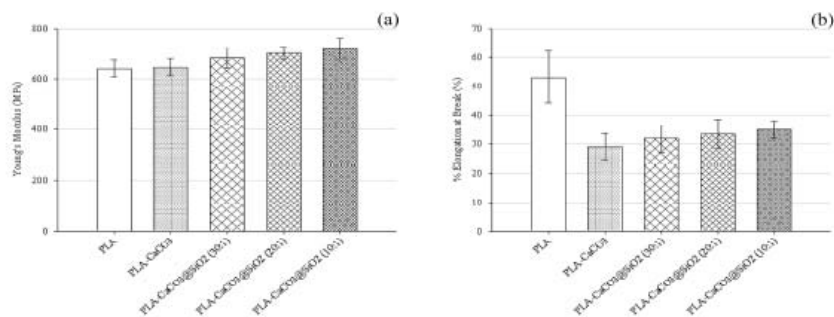


Fig. 2. Tensile properties of PLA nanocomposites: (a) Young's modulus and (b) %Elongation at break.

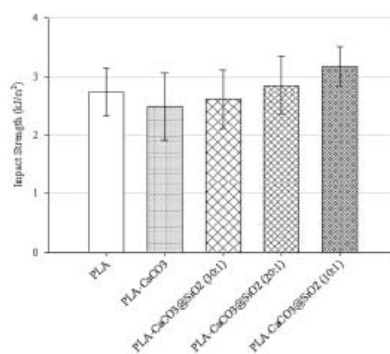


Fig. 3. Impact strength of PLA nanocomposites.

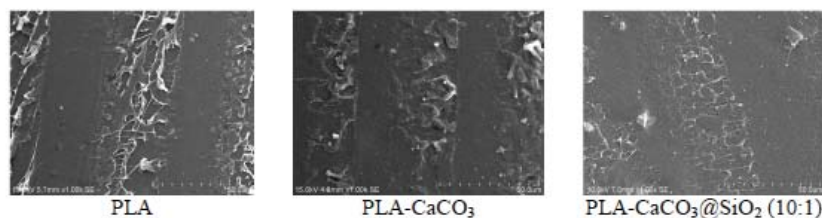


Fig.4. SEM micrographs of impact fracture surface of neat PLA and PLA nanocomposites.

Morphology of fracture surface

SEM micrographs in Fig. 4 reveal the fracture behavior of neat PLA, PLA-CaCO₃ and PLA-CaCO₃@SiO₂ nanocomposites. Fracture surface of neat PLA was smooth with local ductile breaking as craze and crack propagation occurred during the impact loading. When CaCO₃ was added into PLA matrix, they became stress concentrators promoting crack initiation, thus local ductile breaking diminished causing decrease in impact strength. Fracture surface of PLA-CaCO₃@SiO₂ nanocomposites looked smooth similarly to that of neat PLA. However, it presented finer local ductile breaking indicating crack initiation occurred at the CaCO₃ nanoparticles but crack propagation occurred with higher extension.

Conclusion

In this study, modified $\text{CaCO}_3@SiO_2$ nanoparticles were prepared with different Si/Ca ratios. SiO_2 layers coated around the $CaCO_3$ nanoparticles causing the slightly increase in particle sizes, however, the particle size of $CaCO_3@SiO_2$ particles were still in the range of nano-scale. It is found that the Si:Ca wt% ratio was increased with respect to the Si:Ca mole ratio used in the reaction. Compared to PLA- $CaCO_3$ nanocomposite, incorporating $CaCO_3@SiO_2$ at the same content increased elastic modulus, %elongation at break and notched impact strength of PLA nanocomposites, which these properties of PLA- $CaCO_3@SiO_2$ nanocomposite was increased with respect to increasing of SiO_2 content on the surface of $CaCO_3$ nano-particles. This implies that better compatibility between polymer matrix and filler was achieved after modification surface of $CaCO_3$ with SiO_2 .

References

- [1] L.-T. Lim, R. Auras and M. Rubino: Prog. Polym. Sci. Vol. 33 (2008), p. 820
- [2] F.P.L. Mantia and M. Morreale: Composites Part A Vol. 42 (2011), p. 579
- [3] D. Garlotta: J. Polym. Environ. Vol. 9 (2001), p. 63
- [4] T.D. Lam, T.V. Hoang, D.T. Quang and J.S. Kim: Mater. Sci. Eng., A Vol.51 (2009), p. 87
- [5] S.S. Ray and M. Bousmina: Prog. Mater. Sci. Vol. 50 (2005), p. 962
- [6] B.-K. Chen, C.-H. Shen, S.-C. Chen and A. F. Chen: Polymer Vol. 51 (2010), p. 4667
- [7] V. Siracusa, P. Rocculi, S. Romani and M.D. Rosa: Trends in Food Science & Technology Vol. 19 (2008), p. 634
- [8] M.-A. Paul, M. Alexandre, P. Degée, C. Henrist, A. Rulmont and P. Dubois: Polymer Vol. 44 (2003), p. 443
- [9] R. Dantungee and P. Supaphol: Polymer Testing Vol. 27 (2008), p. 951
- [10] A. Sorrentino, G. Gorrasi and V. Vittoria: Trends in Food Science & Technology Vol. 18 (2007), p. 84
- [11] I. Pluta, M. Murariu, M. Alexandre, A. Galeski and P. Dubois: Polym. Degrad. Stab. Vol. 93 (2008), p. 925
- [12] C. Thellen, C. Orroth, D. Froio, D. Ziegler, J. Lucciarini, R. Farrell, N.A. D'Souza and J.A. Ratto: Polymer Vol. 46 (2005), p. 11716
- [13] S. Zhang, X. Li: Powder Technology Vol. 141 (2004), p. 75
- [14] S. Miao: Appl. Surf. Sci. Vol. 220 (2003), p. 298
- [15] K. Gorna, M. Hund, M. Vučak, F. Gröhn and G. Wegner: Mater. Sci. Eng., A Vol. 477 (2008), p. 217
- [16] J. Chen, R. Liu, Y. Jimmy, Z. Shen, H. Zou and F. Guo, U.S. Patent No. 0170178 (2005)
- [17] K. Tanabe and K. Mitsuhashi, U.S. Patent No. 7060127 (2006)
- [18] S. Yan, J. Yin, J. Yang and X. Chen: Mater. Lett. Vol. 61 (2007), p. 2683
- [19] Z. Bartzczak, A.S. Argon, R.E. Cohen and M. Weinberg: Polymer Vol. 40 (1999), p. 2347

3. Mechanical Properties of Hydrophilicity Modified CaCO₃-Poly(Lactic Acid) Nanocomposite

The part of the dissertation as the topic of “Mechanical Properties of Hydrophilicity Modified CaCO₃-Poly(Lactic Acid) Nanocomposite” was online published in peer-reviewed international journal (International Journal of Applied Physics and Mathematics, Vol. 2, No. 2, March 2012, pp. 98-103, Singapore) on 24 March 2012.

	
International Journal of Applied Physics and Mathematics (IJAPM)	
CONTENTS	
Volume 2, Number 2, March 2012	
Exploring the Potential Use of Adhesion Strength for Coating Analysis.....	67
<i>Yunan Prawoto, Nazri Kamsah, and Zaini Ahmad</i>	
Study on the Engineering Property of Fiberglass-Polyester Paving Mat.....	73
<i>Yi Chaojue and Zhai Pengcheng</i>	
Design and Development of a Centrifugal Atomizer for Producing Zinc Metal Powder.....	77
<i>Phairote Sungkhaphaitoon, Thawatchai Plookphol, and Sirikul Wisutmethangoon</i>	
Flow Stress Characteristics of AZ31B Magnesium Alloy Sheet at Elevated Temperatures.....	83
<i>LI Wen-juan, ZHAO Guo-qun, MA Xin-wu, and GAO Jun</i>	
Structure and Crystallization of Borate-Based Glasses for Machinable Material Applications.....	89
<i>Pat Sooksaeen</i>	
Computer –Aided Design of Helical Cutting Tools.....	93
<i>Ngoc-Thiem Vu, Shinn-Liang Chang, Jackson Hu, and Tacker Wang</i>	
Mechanical Properties of Hydrophilicity Modified CaCO ₃ -Poly (Lactic Acid) Nanocomposite.....	98
<i>B. Nekhamanurak, P. Patanathabutr, and N. Hongsriphan</i>	
Integrating Geo-Electrical and Geotechnical Data for Soil Characterization.....	104
<i>Fahad Irfan Siddiqui and Syed Ba harom Azhar Bin Syed Osman</i>	
Three Synthetic Routes to a Commercial N3 Dye.....	107
<i>R. Jitchatt, Y. Thathong, and K. Wongkhan</i>	
Failure Strength of Thin-walled Cylindrical GFRP Composite Shell against Static Internal and External Pressure for various Volumetric Fiber Fraction.....	111
<i>S. Gohari, A. Golshan, M. Mostakhdemin, F. Mozafari, and A. Momenzadeh</i>	
Optimized Energy Based Design of Tunnel Lining with Macro Synthetic Fiber Composites.....	117
<i>Massoumeh Farjadmand and Mohammad Safi</i>	
Study of Flexible Polyurethane Foams Reinforced with Coir Fibres and Tyre Particles.....	123
<i>Chan Wen Shan, Maizlinda Izwana Idris, and Mohd Imran Ghazali</i>	
The Effect of Sample Geometry and Placement of Sample on Microwave Processing of Iron Ore.....	131
<i>K. Barani, SMJ. Koleini, B. Rezai, and A. Khodadadi</i>	
Fabrication and Nonlinear Refractive Index Measurement of Colloidal Silver Nanoparticles	135
<i>Adeleh Grammayeh Rad, Hamed Abbasi, and Keyhan Golyari</i>	

Mechanical Properties of Hydrophilicity Modified CaCO₃-Poly (Lactic Acid) Nanocomposite

B. Nekhamanurak, P. Patanathabutr, and N. Hongsriphan

Abstract—The goal of this work is to modify surface of calcium carbonate nanoparticles with silica (CaCO₃@SiO₂) via sol-gel process, and to investigate the influence of CaCO₃@SiO₂ on mechanical properties and fracture behavior of poly(lactic acid) nanocomposite. Modified CaCO₃@SiO₂ nanoparticles were prepared with different Si:Ca ratios. It is found that the Si:Ca wt% was increased with respect to the Si:Ca mole ratio used in the reaction. Incorporating CaCO₃@SiO₂ of 5 wt% increased elastic modulus, %elongation at break and notched impact strength of PLA nanocomposites. These properties of hydrophilic-modified CaCO₃-poly(lactic acid) nanocomposite was increased with respect to the increasing of SiO₂ content on the surface of CaCO₃ nanoparticles. This implies that better compatibility between PLA matrix and nano-fillers was achieved after modification surface of CaCO₃ with SiO₂ layers.

Index Terms—Nanocomposite, poly(lactic acid), calcium carbonate nanoparticle, silica, sol-gel process.

I. INTRODUCTION

Poly(lactic acid) (PLA) or polylactide is a linear aliphatic biodegradable thermoplastic polyester, produced from renewable resources typically polymerized through the fermentation products of starch and sugar [1]. PLA plays an important role in various applications due to their biodegradable and biocompatible characters [1]-[5]. It offers a potential alternative to petrochemical plastics in many applications such as biomedical applications, controlled release films for fertilizers and waste-composting food package because of its high strength and stiffness with their biodegradable and biocompatible characters [2], [6], [7]. PLA, however, is comparatively brittle and stiff at room temperature [1], [8], so modification is needed for PLA in order to apply with flexible-desired applications such as food packaging.

Adding fillers into plastics are usually implemented not only confined to cost reduction, but also to control their physical and mechanical performance such as gas barrier properties, thermal stability, strength, melt viscosity and biodegradation rate [1], [4], [5], [9], [10].

Manuscript received February 22, 2012; revised March 24, 2012. This work was supported in part by the Department of Materials Science and Engineering, Faculty of Engineering and Industrial Technology, Silpakorn University and the Center of Excellence for Petrochemicals and Materials Technology, Chulalongkorn University, Bangkok, 10330 Thailand

B. Nekhamanurak is with the Department of Materials Science and Engineering, Faculty of Engineering and Industrial Technology, Silpakorn University, Thailand (e-mail: bawornkit@windowslive.com).

P. Patanathabutr is with the Department of Materials Science and Engineering, Faculty of Engineering and Industrial Technology, Silpakorn University, Thailand (e-mail: pajaera@su.ac.th).

N. Hongsriphan is with the Department of Materials Science and Engineering, Faculty of Engineering and Industrial Technology, Silpakorn University, Thailand (e-mail: nattakar@su.ac.th).

Recently, there are widely improving of polymer properties using nano-size inorganic fillers such as ZnO, SiO₂, clay, precipitated calcium carbonate (PCC), and noble metals [11], [12]. Nano-reinforcements of biodegradable polymers have strong promises in designing eco-friendly green nanocomposites for several applications. A fairly new area of composites has emerged in which the reinforcing materials have the dimensions in nanometric scale. These composites are significant due to their nano-scale dispersion, even with very low level of nano-filler incorporation (<5 wt%) which results in high surface area [5]. Properties of filler-filled composites are closely related to the dispersion of the particles in polymer matrix.

In consideration of various fillers, calcium carbonate (CaCO₃) is the famous material, widely used in various industries, due to its high amount of loading in plastics and low cost [13], [14]. The reinforcing effect of CaCO₃ particles has been studied in polymer systems such as high density polyethylene (HDPE) [15], nylon [16], polypropylene (PP) [17], polyketone[18], acrylonitrile butadiene styrene (ABS) [19], and thermoplastic polyurethane (TPU) [20]. The mechanical properties were found to be significantly improved by the addition of fine CaCO₃ particles [15]-[20]. Large scale plastic deformation was found to be initiated by interfacial debonding and the subsequent relaxation of triaxial tensile stress [21]. Since PLA is well known for its difficulty to crystalline, adding CaCO₃ could have an impact on its properties as well as potential applications replacing petrochemical based plastics [14], [22].

In order to produce CaCO₃@SiO₂.nH₂O nanocomposite particles, CaCO₃ was used as a template nucleus and the surface of nucleus was encapsulated by a SiO₂.nH₂O nanolayer. Synthetic silica fixed on the surfaces of calcium carbonate particles has good properties such as a high specific surface area and high absorbability, benefits to form linkage at the interface of two materials (plastic and filler), connecting to improve mechanical properties of materials [23], [24].

Therefore, this work aims to modify surface of calcium carbonate nanoparticles with silica (CaCO₃@SiO₂) via sol-gel process, and to investigate the influence of CaCO₃@SiO₂ on mechanical properties and fracture behavior of poly(lactic acid) nanocomposite.

II. EXPERIMENTAL

A. Materials

Poly(lactic acid) (PLA, 2002D, NatureWorks LLC) and calcium carbonate (CaCO₃, NPCC 101, Behn Meyer Chemical) were dried overnight at 60 °C in order to remove structural water before they were brought into the compounding process.

In the preparation of $\text{CaCO}_3@/\text{SiO}_2$ particles via sol-gel process, tetraethylorthosilicate (TEOS, Fluka), ethanol and ammonium hydroxide (NH_4OH , 35% NH_3 , Mallinckrodt Chemical) were used.

B. Preparation of Silica Coated Calcium Carbonate Composite Particles

The Hydrophilic SiO_2 Surface Modified CaCO_3 ($\text{CaCO}_3@/\text{SiO}_2 \cdot n\text{H}_2\text{O}$) particles were prepared by hydrolysis-condensation polymerization of TEOS on the surface of CaCO_3 particles. The CaCO_3 particles were dispersed into the mixture of TEOS, 200 ml ethanol, and 300 ml distillation water. The mole ratios of TEOS to CaCO_3 were vary as 1:30, 1:20 and 1:10, then 100 ml NH_4OH was added slowly, and the mixture was vigorously stirred at 40 °C for 6 h. After the reaction, the $\text{CaCO}_3@/\text{SiO}_2$ particles were filtrated and washed with ethanol followed by distillation water for several times to remove dissociative polysiloxane, unreacted monomer, and polysiloxane oligomers. The $\text{CaCO}_3@/\text{SiO}_2$ particles were then dried at 60 °C in oven.

C. Particle Characterization

The characteristic of the $\text{CaCO}_3@/\text{SiO}_2$ particles was characterized by Fourier transform infrared (FT-IR, Bruker vector-22). The morphology of $\text{CaCO}_3@/\text{SiO}_2$ particles were investigated using transmission electron microscopy (TEM, Jeol model JEM-1230). The elemental content of $\text{CaCO}_3@/\text{SiO}_2$ particle was analyzed by X-ray fluorescence spectrometer (XRF, Phillips PW-2404).

D. Preparation of PLA Nanocomposites

Prior to compounding, PLA, CaCO_3 and $\text{CaCO}_3@/\text{SiO}_2$ were dried overnight at 60 °C in order to remove residual moisture. En Mach SHJ-25 co-rotating twin-screw extruder was used to compound the 5 wt% content of CaCO_3 and $\text{CaCO}_3@/\text{SiO}_2$ -PLA nanocomposites. The barrel temperature profile adopted during blending was ranged from 150 °C in the feed zone to 170 °C in metering zone at the fixed screw speed of 130 rpm. Then, the extruded materials were compression molded into standard tensile and impact specimens using LabTech Compression Molding machine with mold temperature of 170 °C and mold pressure of 20,000 psi for 5 min.

E. Mechanical Analysis

Tensile test was carried out in according to ASTM D638 type V using a universal testing machine (Instron 5969) under ambient conditions with crosshead speeds of 10 mm/min. Notched Izod impact test, according to ASTM D256, was done on notched impact specimens, by using an instrument impact tester (Zwick model B5102.202 Izod Pendulum 4 J).

In order to study the compatibility of PLA and fillers, glass transition temperature (T_g) and crystallization temperature (T_c) of PLA and PLA nanocomposites were studied by differential scanning calorimeter (DSC, Mettler Toledo DSC822e) under nitrogen atmosphere. The temperature was raised from -20 to 180 °C with the heating ramp of 10 °C/min.

F. Morphological Studied

Morphology of nanocomposite was investigated by scanning electron microscopy (SEM) using Hitachi Model S3400N instrument. Prior to testing, the fracture surfaces of

samples were sputtered with platinum.

III. RESULTS AND DISCUSSION

A. Characterization of Modified CaCO_3 Nanoparticle

Infrared spectra of CaCO_3 and $\text{CaCO}_3@/\text{SiO}_2$ were presented in Fig. 1. The FT-IR absorption peaks of CaCO_3 and $\text{CaCO}_3@/\text{SiO}_2$ displayed the absorption peak of crystal at about 875 cm^{-1} and 710 cm^{-1} . The absorption peak at 875 cm^{-1} indicated the CO_3^{2-} out-of-plane deformation mode of the aragonite while the absorption peak of 710 cm^{-1} showed the calcite formed [25]. It shows that the product was the mixture of calcite and aragonite. In addition there were interesting absorption peak at about 1,780 cm^{-1} , 2,950-2,850 cm^{-1} and the broad about 3,600-3,200 cm^{-1} . These peaks indicated C=O stretching in carboxylic acid, alkyl C-H stretching and O-H stretching, respectively. The absorption proved that all types of CaCO_3 were surface treated by some fatty acid for preventing the re-agglomeration of particles.

The hydrolysis of TEOS would be occurred in the presence of water and alkaline catalysts, and $\text{Si}(\text{OH})_4$ was formed as one of the of hydrolysates (scheme 1). The adding of NH_4OH was to promote the hydrolysis of TEOS. Then, $\text{Si}(\text{OH})_4$ molecule would polymerize with other $\text{Si}(\text{OH})_4$ or TEOS molecule (scheme 2 or scheme 3). The product of this step was the monomer or oligomers of polysiloxane. Finally, the monomers or oligomers of polysiloxane continue to polymerize and form a film of high relative molecular mass polysiloxane with a three-dimensional network structure (scheme 4). Because water and TEOS are immiscible, a mutual solvent such as ethanol is normally used as a homogenizing agent. Fine particles CaCO_3 can provide nucleation centers and decrease the kinetic barrier to nucleation of hydrophilic silica. Furthermore, the monomers or oligomers of polysiloxane along with $\text{Si}(\text{OH})_4$ molecules have very high activities, so they can be adsorbed to the surface of CaCO_3 rapidly. The polymerization of silica (scheme 4) occurs on the surface of the CaCO_3 particles and the silica film thus covers around the CaCO_3 particles tightly.

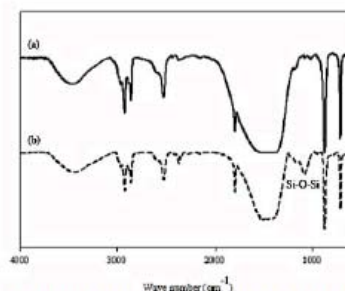
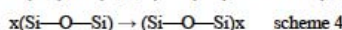
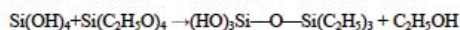
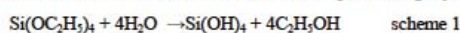


Fig. 1. FT-IR spectra of (a) CaCO_3 nanoparticle and (b) $\text{CaCO}_3@/\text{SiO}_2$ nanoparticle.

The infrared spectra of the particles from FT-IR characterization were analyzed in the range of 400 cm^{-1} to $4,000\text{ cm}^{-1}$ as shown in Fig. 1. It can be seen that the spectrum of blank CaCO_3 nanoparticles is quite the same as the spectrum of $\text{CaCO}_3@/\text{SiO}_2$ but there was transmitting bands at about $1,100\text{ cm}^{-1}$ of Si—O—Si asymmetric stretching [27] of $\text{CaCO}_3@/\text{SiO}_2$ nanoparticles. This revealed that the SiO_2 was occurred in the reaction proved the successful of the development of $\text{CaCO}_3@/\text{SiO}_2$ nanoparticles.

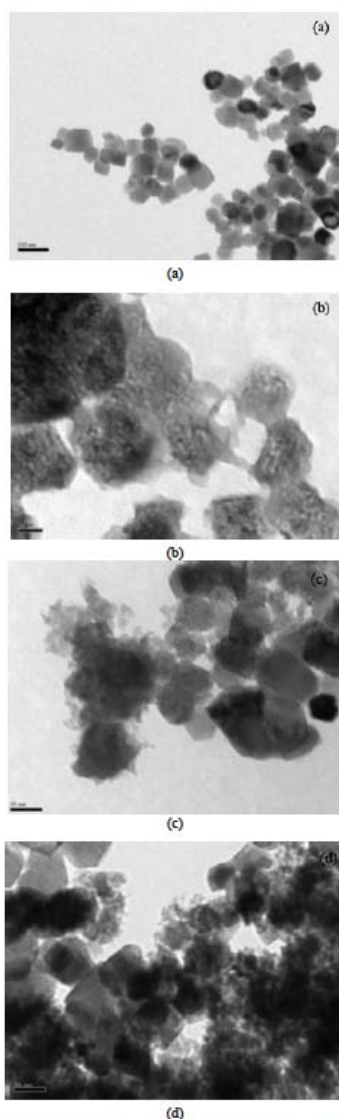


Fig. 2. Morphologies of (a) CaCO_3 nanoparticles and (b-c) $\text{CaCO}_3@/\text{SiO}_2$ nanoparticles (magnificent 200,000x).

In addition, morphologies of CaCO_3 nanoparticles and $\text{CaCO}_3@/\text{SiO}_2$ nanoparticles were shown as TEM images in Fig. 2. It can be seen that there were SiO_2 layers coated around the CaCO_3 nanoparticles causing the slightly increase in particle sizes, however, the particle size of $\text{CaCO}_3@/\text{SiO}_2$ particles were still in the range of nano-scale. Layers of synthesized SiO_2 were coated on the surface of CaCO_3 nanoparticles. However, some crystals of synthesized SiO_2 grew stacked to each other. The elemental content of $\text{CaCO}_3@/\text{SiO}_2$ as shown in Table I was analyzed by XRF, which the Si/Ca wt% was calculated and presented in Table II. It is found that the Si/Ca wt% in $\text{CaCO}_3@/\text{SiO}_2$ particles was increased with respect to the Si:Ca mole ratio used in the reaction.

TABLE I: THE ELEMENTAL ANALYSIS OF $\text{CaCO}_3@/\text{SiO}_2$ NANOPARTICLES

Element	Concentration (%wt)		
	$\text{CaCO}_3@/\text{SiO}_2$ (30:1)	$\text{CaCO}_3@/\text{SiO}_2$ (20:1)	$\text{CaCO}_3@/\text{SiO}_2$ (10:1)
O	58.72	53.83	50.83
Na	0.02	0.04	0.07
Mg	0.13	0.16	0.13
Al	0.04	0.05	0.07
Si	0.87	1.92	3.91
P	N/D	N/D	N/D
S	0.02	0.02	0.01
Cl	N/D	N/D	N/D
K	N/D	N/D	N/D
Ca	40.11	43.89	44.9
Fe	0.05	0.05	0.04
Sr	0.04	0.04	0.04
Total	100	100	100

TABLE II: COMPARISON OF Si/Ca ratio in $\text{CaCO}_3@/\text{SiO}_2$

Particles (mole ratio)	Si/Ca (%wt), XRF
$\text{CaCO}_3@/\text{SiO}_2$ (30:1)	2.17
$\text{CaCO}_3@/\text{SiO}_2$ (20:1)	4.37
$\text{CaCO}_3@/\text{SiO}_2$ (10:1)	8.71

B. Mechanical Analysis

Fig. 3 shows tensile properties of PLA- CaCO_3 and PLA- $\text{CaCO}_3@/\text{SiO}_2$ nanocomposites. Young's moduli of PLA and PLA nanocomposites are illustrated in Fig. 3(a). Compared with neat PLA, incorporating CaCO_3 nanoparticles of 5 wt% relatively did not improve elastic modulus of PLA nanocomposite. It indicates that CaCO_3 nanoparticles did not have good efficiency to reinforce nanocomposite as well as those added nanoclays. Lack of reinforcing ability of CaCO_3 nanoparticles would come from their cubic shape that did not good for load bearing compared to the platelets in nanoclays. Moreover, the fatty acid based sizing agents, treated on CaCO_3 surface to prevent them from agglomeration, would cause lubricating effect in the nanocomposites during the load bearing [27]. In the other

hand, incorporating $\text{CaCO}_3@SiO_2$ with the same content did increase elastic modulus of PLA nanocomposites, and elastic modulus of $\text{PLA-CaCO}_3@SiO_2$ nanocomposite increased with respect to increasing of SiO_2 content on the surface of CaCO_3 nanoparticles.

In this work, compatibility between PLA matrix and CaCO_3 nanoparticles was not modified by means of coupling agents. In the presence of nano-fillers, the decrease of %elongation at break of PLA nanocomposite in Fig. 3(b) demonstrates that the interfacial interaction between PLA matrix and CaCO_3 was so poor that fillers induced a definite decrease in elongation [15], because they acted as stress concentrator to promote crack initiation. Surprisingly, the increase of SiO_2 content on $\text{CaCO}_3@SiO_2$ retarded crack propagation to occur at higher % elongation at break. This implies that better compatibility between polymer matrix and filler was achieved. This was due to good interaction between SiO_2 coated around the CaCO_3 and the hydroxyl groups at the chain ends in PLA matrix. And, this is also possibly the reason how the elastic modulus of $\text{PLA-CaCO}_3@SiO_2$ nanocomposite was improved.

The compatibility of PLA and $\text{PLA-CaCO}_3@SiO_2$ was studied by means of thermal properties (T_g and T_c) from DSC test. Addition of CaCO_3 did not affect T_g of PLA in the same fashion of $\text{CaCO}_3@SiO_2$ did as seen in Table III. This confirms no interaction between CaCO_3 and PLA molecules. Meanwhile, more energy is required for PLA molecules to vibrate when they were surrounded with $\text{CaCO}_3@SiO_2$. It is observed that T_c of PLA and its nanocomposite appeared in the heating scan rather than in the cooling scan. T_c of PLA decreased with respect to SiO_2 contents on CaCO_3 surface. This implies the synergism between polymer matrix and filler on PLA crystallization [28]. Since the $\text{CaCO}_3@SiO_2$ particles were dispersed well in PLA matrix, the relatively higher hydrophilic SiO_2 coated layers acted like the nucleating sites for PLA molecules to crystalline so that the crystallization of PLA occurred at lower T_c than those CaCO_3 without SiO_2 coating.

TABLE III. T_g AND T_c OF $\text{PLA-CaCO}_3@SiO_2$ NANOCOMPOSITE

Particles (mole ratio)	T_g (°C)	T_c (°C)
PLA- CaCO_3	51.98	123.70
PLA- $\text{CaCO}_3@SiO_2$ (30:1)	52.22	123.53
PLA- $\text{CaCO}_3@SiO_2$ (20:1)	52.38	120.18
PLA- $\text{CaCO}_3@SiO_2$ (10:1)	52.34	117.43

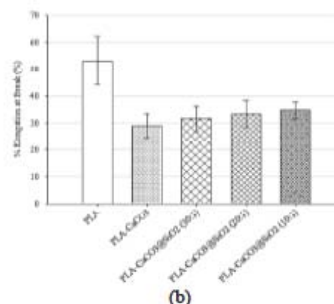
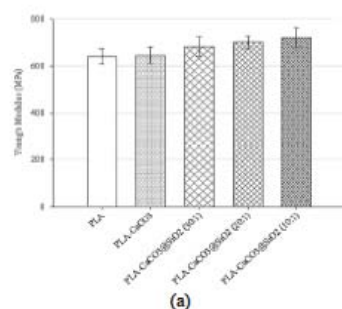


Fig. 3. Tensile properties of PLA nanocomposites: (a) Young's modulus and (b) %Elongation at break.

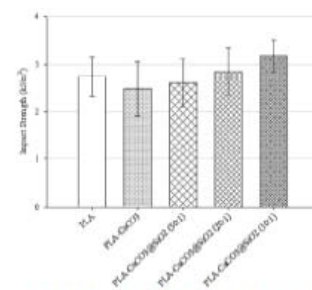


Fig. 4. Impact strength of PLA nanocomposites.

Fig. 4 presents the notched impact strength of PLA-CaCO_3 and $\text{PLA-CaCO}_3@SiO_2$ nanocomposites. Similarly to tensile test, the presence of CaCO_3 nanoparticles became the stress concentration in the PLA matrix causing them to premature breakage. Adding $\text{CaCO}_3@SiO_2$ nanoparticles showed the improvement in impact resistance of PLA. Impact strength of PLA was increased with the increasing content of SiO_2 on the surface of CaCO_3 particles. The incorporation of $\text{CaCO}_3@SiO_2$ nanoparticles with Si/Ca wt% in PLA more than 2 wt% could improve impact strength of PLA nanocomposite to be higher than those of neat PLA. This means that modification the surface of CaCO_3 nanoparticles with small amount of SiO_2 via sol-gel process could provide better compatible with PLA matrix and CaCO_3 nanoparticle yielding more desired mechanical properties.

C. Morphology of PLA Nanocomposite

SEM micrographs in Fig. 4 reveal the fracture behavior of neat PLA, PLA-CaCO_3 and $\text{PLA-CaCO}_3@SiO_2$ nanocomposites. Fracture surface of neat PLA was smooth with local ductile breaking as craze and crack propagation occurred during the impact loading. When CaCO_3 was added into PLA matrix, they became stress concentrators promoting crack initiation, thus local ductile breaking diminished causing decrease in impact strength. Fracture surface of $\text{PLA-CaCO}_3@SiO_2$ nanocomposites looked smooth similarly to that of neat PLA. However, it presented finer local ductile breaking indicating crack initiation occurred at the CaCO_3 nanoparticles but crack propagation occurred with higher extension.

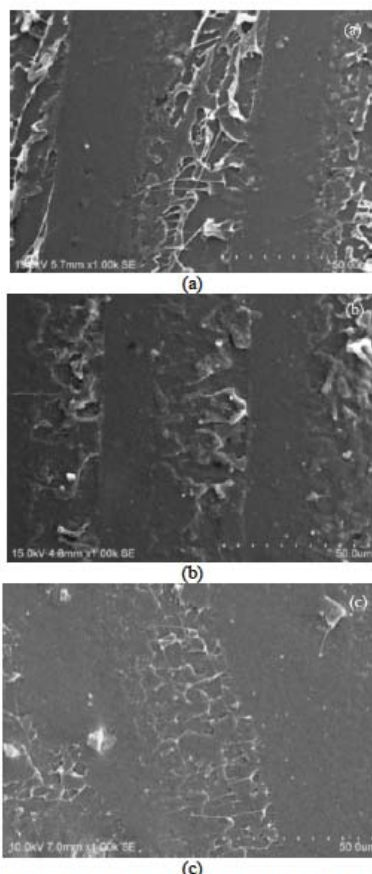


Fig. 4. SEM micrographs of impact fracture surface of neat PLA and PLA nanocomposites : (a) PLA, (b) PLA-CaCO₃, and (c) PLA-CaCO₃@SiO₂.

IV. CONCLUSION

In this study, modified CaCO₃@SiO₂ nanoparticles were prepared with different Si/Ca ratios. SiO₂ layers coated around the CaCO₃ nanoparticles causing the slightly increase in particle sizes, however, the particle size of CaCO₃@SiO₂ particles were still in the range of nano-scale. It is found that the Si/Ca wt% was increased with respect to the Si:Ca mole ratio used in the reaction. Compared to PLA-CaCO₃ nanocomposite, incorporating CaCO₃@SiO₂ at the same content increased elastic modulus, %elongation at break and notched impact strength of PLA nanocomposites, which these properties of PLA-CaCO₃@SiO₂ nanocomposite was increased with respect to the increasing of SiO₂ content on the surface of CaCO₃ nanoparticles. This implies that better compatibility between polymer matrix and filler was achieved after modification surface of CaCO₃ with SiO₂.

REFERENCES

- [1] L.-T. Lim, R. Auras, and M. Rubino, "Processing technologies for poly(lactic acid)," *Prog. Polym. Sci.*, Vol. 33, pp. 820-852, Aug. 2008.
- [2] F.P.L. Mantia and M. Morreale, "Green composites: A brief review," *Composites Part A* Vol. 42, pp. 579-588, Jun. 2011.
- [3] D. Carlotta, "A Literature Review of Poly(Lactic Acid)," *J. Polym. Environ.*, Vol. 9, pp. 63-84, Apr. 2001.
- [4] T.D. Lam, T.V. Hoang, D.T. Quang, and J.S. Kim, "Effect of nanosized and surface-modified precipitated calcium carbonate on properties of CaCO₃/polypropylene nanocomposites," *Mater. Sci. Eng., A*, Vol. 501, pp. 87-93, Feb. 2009.
- [5] S.S. Ray and M. Bousmina, "Biodegradable polymers and their layered silicate nanocomposites. In greening the 21st century materials world," *Prog. Mater. Sci.*, Vol. 50, pp. 962-1079 Nov. 2005.
- [6] B.-K. Chen, C.-H. Shen, S.-C. Chen and A. F. Chen, "Ductile PLA modified with methacryloyloxyalkylisocyanate improves mechanical properties," *Polymer*, Vol. 51, pp. 4667-4672, Oct. 2010.
- [7] V. Siracusa, P. Rocculi, S. Romani, and M.D. Rosa, "Biodegradable polymers for food packaging: a review," *Trends in Food Science & Technology*, Vol. 19, pp. 634-643, Dec. 2008.
- [8] M.-A. Paul, M. Alexandre, P. Degée, C. Henrist, A. Rulmont, and P. Dubois, "New nanocomposite materials based on plasticized poly(l-lactide) and organo-modified montmorillonites: thermal and morphological study," *Polymer*, Vol. 44, pp. 443-450, Jan. 2003.
- [9] R. Dangumgee and P. Supaphol, "Melt rheology and extrudate swell of titanium (IV) oxide nanoparticle-filled isotactic polypropylene. Effects of content and surface characteristics," *Polymer Testing*, Vol. 27, pp. 951-956, Dec. 2008.
- [10] A. Sorrentino, G. Gorraasi, and V. Vittoria, "Potential perspectives of bio-nanocomposites for food packaging applications," *Trends in Food Science & Technology*, Vol. 18, pp. 84-95, Feb. 2007.
- [11] I. Pluta, M. Murariu, M. Alexandre, A. Galeski, and P. Dubois, "Polylactide composites. The influence of ageing on the structure, thermal and viscoelastic properties of PLA/calcium sulfate composites," *Polym. Degrad. Stab.*, Vol. 93, pp. 925-931, May 2008.
- [12] C. Thellen, C. Orroth, D. Froio, D. Ziegler, J. Lucciarini, R. Farrell, N.A. D'Souza, and J.A. Ratto, "Influence of montmorillonite layered silicate on plasticized poly(l-lactide) blown films," *Polymer*, Vol. 46, pp. 11716-11727, Nov. 2005.
- [13] S. Zhang and X. Li, "Synthesis and characterization of CaCO₃@SiO₂ core-shell nanoparticles," *Powder Technology*, Vol. 141, pp. 75-79, Mar. 2004.
- [14] S. Miao, "Investigation on NIR, coating mechanism of PS-b-PAA coated calcium carbonate particulate," *Appl. Surf. Sci.*, Vol. 220, pp. 298-303, Dec. 2003.
- [15] Z. Bartzak, A.S. Argon, R.E. Cohen, and M. Weinberg, "Toughness mechanism in semi-crystalline polymer blends: II. High-density polyethylene toughened with calcium carbonate filler particles," *Polymer*, Vol. 40, pp. 2347-2365, Apr. 1999.
- [16] M.W.L. Wilbrink, A.S. Argon, R.E. Cohen, and M. Weinberg, "Toughenability of Nylon-6 with CaCO₃ filler particles: new findings and general principles," *Polymer*, Vol. 42, Dec. 2001. pp.10155-10180, Dec. 2001.
- [17] W.C.J. Zuiderduin, C. Westzaan, J. Huétink, and R.J. Gaymans, "Toughening of polypropylene with calcium carbonate particles," *Polymer*, Vol. 44, pp. 261-275, Jan. 2003.
- [18] W.C.J. Zuiderduin, J. Huétink, and R.J. Gaymans, "Rigid particle toughening of aliphatic polyketone," *Polymer*, Vol. 47, pp. 5880-5887, Jul. 2006.
- [19] L. Jiang, Y.C. Lam, K.C. Tam, T.H. Chua, G.W. Sim, and L.S. Ang, "Strengthening acrylonitrile-butadiene-styrene (ABS) with nano-sized and micron-sized calcium carbonate," *Polymer*, Vol. 46, pp. 243-252, Jan. 2005.
- [20] L. Jiang, Y.C. Lam, K.C. Tam, D.T. Li, and J. Zhang, "The influence of fatty acid coating on the rheological and mechanical properties of thermoplastic polyurethane (TPU)/nano-sized precipitated calcium carbonate (NPCC) composites," *Polymer Bulletin*, Vol. 57, pp. 575-586, May 2006.
- [21] L. Jiang, J. Zhang, and M.P. Wolcott, "Comparison of polylactide/nano-sized calcium carbonate and polylactide/montmorillonite composites: Reinforcing effects and toughening mechanisms," *Polymer*, Vol. 48, pp. 7632-7644, Dec. 2007.
- [22] K. Gorna, M. Hund, M. Vucak, F. Gröhn, and G. Wegner, "Amorphous calcium carbonate in form of spherical nanosized particles and its application as fillers for polymers," *Mater. Sci. Eng., A*, Vol. 477, pp. 217-225, Mar. 2008.
- [23] J. Chen, R. Liu, Y. Jimmy, Z. Shen, H. Zou, and F. Guo, "CaCO₃/SiO₂.nH₂O nanocomposite particles and SiO₂.nH₂O

- hollow-structures nanomaterials and synthesizing method," U.S. Patent 170 178, Aug. 4, 2005.
- [24] K. Tanabe and K. Mitsuhashi, "Silica-calcium carbonate composite particles," U.S. Patent 7 060 127 Jun. 13, 2006.
- [25] C.-L. Yao, C.-X. Qi, J.-M. Zhu, and W.-H. Xu, "Unusual morphology of calcium carbonate controlled by amino acids in agarose gel," *J. Chil. Chem. Soc.*, Vol. 55, pp. 270-273, Jun. 2010.
- [26] Z.-P. Cheng, Y. Yang, F.-S. Li, and Z. -H. Pan, "Synthesis and characterization of aluminum particles coated with uniform silica shell," *Trans. Nonferrous Met. Soc. China* Vol. 18, pp. 378-382, Apr. 2008.
- [27] S. Yan, J. Yin, J. Yang and X. Chen, "Structural characteristics and thermal properties of plasticized poly(l-lactide)-silica nanocomposites synthesized by sol-gel method," *Mater. Lett.*, Vol. 61, pp. 2683-2686, May 2007.
- [28] H.T. Lim, H. Liu, K. H. Ahn, S. J. Lee, and J. S. Hong, "Effect of added ionomer on morphology and properties of PP/organoclay nanocomposites," *Korean J. Chem. Eng.*, Vol. 27, pp. 705-715, 2010.



Baworakit Nekhmanurak was born in Ayutthaya, Thailand on September 1982. He received bachelor degree in Petrochemical and Polymeric Materials in 2005 and master degree in Polymer Science and Engineering in 2007 from Silpakorn University, Thailand. From 2008-2012, he has been a doctoral candidate in polymer science and engineering program of Silpakorn University, Thailand. He was a project manager of National Innovation Agency and a coordinator of Thai Bioplastics Industry Association. His principal researches have been in the field of polymer science and engineering. His interests include compounding, fabrication and characterization of biopolymer and biocomposites, and the recycling process of plastics.



Pajaera Patanathabutr was born in Bangkok, Thailand on March 1972. She is assistant professor at department of materials science and engineering, faculty of engineering and industrial technology, Silpakorn University, Thailand. Since her Ph.D. graduation from university of Cambridge, UK in 1999, she has involved in natural dyeing and biodegradable polymer researches. She is a member of polymer society (Thailand). Currently, she engaged in research centre for art and design materials, Silpakorn University to promote university-industrial co-operations in arts, crafts and fashions including ink-jet printing on fabric.



Nattakarn Hongsririphan was born in Sukhothai, Thailand on May 1972. She received the bachelor degree in Chemistry from Chiangmai University, Thailand in 1996, and the D.Eng. in Plastics Engineering from University of Massachusetts Lowell, USA in 2003. Since then, she is one of the faculty members in department of Materials Science and Engineering, Faculty of Engineering and Industrial Technology, Silpakorn University, Nakhon Pathom, Thailand. Her principal research interests have been in the fields of polymer composite and polymer processing. Her interests include properties modification of wood-plastic composite, packaging film fabrication and characterization, and biodegradable plastics.

Presentation at the conference with the proceeding

1. Thermal-mechanical property and fracture behavior of plasticized PLA-CaCO₃ nanocomposite

The part of the dissertation as the topic of “Thermal-mechanical property and fracture behavior of plasticized PLA-CaCO₃ nanocomposite” was accepted for oral presentation with proceeding in “A Joint Sheffield-Cambridge Conference Deformation and Fracture of Composites (DFC-11) & Structural Integrity and Multi-scale Modelling (SI-5)” at Queens’ College, Cambridge, U.K., on 14 April 2011.



14 th April 2011, Bowett Room, Queens' College			
S11: Composites Design			
Chairs: Mark Kortschot, University of Toronto & Jim Thomason, University of Strathclyde			
9.45 – 10.05	T41	Maria Kashtalayan, University of Aberdeen	Performance Of Sandwich Panels With Graded Core Under Distributed And Concentrated Loadings
10.05 – 10.25	T42	Christopher York, University of Aberdeen	Design Concepts For Laminated Fabrics With Thermal And/Or Mechanical Coupling Response
10.25 – 10.45	T43	Felicity Guild, Queen Mary, University of London	The Optimisation of Comeld™ Joints Between Composites and Metal
10.45 – 11.10		Coffee & Tea	
S12: Green Composites			
Chairs: Vadim Silberschmidt, Loughborough University & Eli Ghassemieh, The University of Sheffield			
11.10 – 11.45	K8	Mark Kortschot, University of Toronto, Canada	Keynote: Modeling the Work of Fracture for Wood Fibre Composites
11.45 – 12.05	T44	Jim Thomason, University of Strathclyde	Natural Fibre Reinforced Epoxy Composites: Determination Of Fibre Volume Fraction, Fibre Mechanical Properties And Fibre Cross-Section Variability
12.05 – 12.25	T45	Edgars Spāmiņš, University of Latvia	Interfacial Shear Strength Of Flax Fibers In a Vinyl Ester-Impregnated Yarn
12.25 – 12.45	T46	Pete Bailey, University of Sheffield	Morphology of Biodegradable Polymer-Polymer Nanocomposites
12.45 – 13.05	T47	Bawornkit Nekhamanurak, Silpakom University, Thailand	Thermal-Mechanical Property And Fracture Behavior Of Plasticized PLA-CaCO ₃ Nanocomposite
13.05 – 14.00		Lunch: Cripps Hall	
S13: SHM			
Chairs: Victor Giurgiutiu, University of South Carolina & Paul Robinson, Imperial College			
14.00 – 14.35	K9	Victor Giurgiutiu, University of South Carolina, USA	Keynote: Structural Health Monitoring of Composite Structures With Piezoelectric Wafer Active Sensors
14.35 – 14.55	T48	Maryna Menshykova, University of Aberdeen	Carbon Reinforced Composites In Well Monitoring
14.55 – 15.15	T49	Alkis Paipetis, University of Ioannina, Greece	Acoustic Structural Health Monitoring of Composite Materials
15.15 – 15.35	T50	Andrew Sanderson, University of Surrey	Use Of A Surface-Mounted Chirped Fibre Bragg Grating Sensor To Monitor Delamination Growth In a Double-Cantilever Beam Test
15.35 – 15.55	T51	Costas Soutis, The University of Sheffield	SHM Of Bonded Patch Repairs



Celebrating 20 Years of DFC
A Joint Sheffield-Cambridge Conference
Deformation and Fracture of Composites (DFC-11) &
Structural Integrity and Multi-scale Modelling (SI-5)
Queens' College, Cambridge, 12-15 April 2011

Queens' College: The Conference Venue



The Fitzpatrick Hall



The Old Hall



Conference URL: <http://www.sheffield.ac.uk/csic/conferencedetails.html>

Conference email: csic@sheffield.ac.uk

Conference Chairs: Costas Soutis and Alma Hodzic (Sheffield) & Peter Beaumont (Cambridge)

Technical Committee: Prof. L. Asp, Swerea, Sweden; Dr R. Butler, Bath; Prof. Tsu-Wei Chou, Delaware, USA; Prof. P.T. Curtis, DSTL-Farnborough; Dr E. Ghassemieh, Sheffield; Prof. A.G. Gibson, Newcastle; Prof I. Guz, Aberdeen; Dr S. A. Hayes, Sheffield; Prof. A. Kinloch, Imperial College; Prof. S. L. Ogin, Surrey; Prof. G. Papanicolaou, Patras; Prof. I.K. Partridge, Cranfield; Dr Y.D.S. Rajapakse, ONR, USA; Dr P. Robinson, Imperial College; Prof. K. Schulte, TU Hamburg; Prof V. Silberschmidt, Loughborough; Prof. R. Talreja, Texas A & M, USA; Prof. S. van der Zwaag, Delft, NL; Prof. P. M. Weaver, Bristol, and Prof. R. J. Young, Manchester.

DFC11/SI5 Conference Secretariat
 Composite Systems Innovation Centre
 The University of Sheffield

Tel: +44 (0) 114 222772
 Email: csic@sheffield.ac.uk
www.sheffield.ac.uk/csic

Thermal-Mechanical Property and Fracture Behavior of Plasticized PLA-CaCO₃ Nanocomposite

Bawornkit Nekhamanurak^{1,2}, Pajaera Patanathabut^{1,2,*} and Nattakam Hongsriphan^{1,2}

¹Department of Materials Science and Engineering, Faculty of Engineering and Industrial Technology, Silpakorn University, Nakhonpathom, 73000 Thailand

²Center of Excellence for Petroleum, Petrochemicals, and Advanced Materials, Chulalongkorn University, Bangkok, 10330 Thailand
E-mail address: pajaera@su.ac.th

Abstract

This research aims to investigate the influence plasticizers as polyethylene glycol (PEG) plasticizer and tributyl citrate (TbC) on the thermo-mechanical properties and fracture behavior of PLA-CaCO₃ nanocomposite. Various compositions of nanocomposites were compounded and fabricated by co-rotating twin-screw extrusion and compression molding, respectively. DMA result shows that adding nano-CaCO₃ reduced the storage modulus (E') of the nanocomposite while the glass transition temperature (T_g) of the samples was not affected. Furthermore, plasticized PLA showed an improvement in elongation at break in all samples, and the impact resistance of the nanocomposites was also improved the addition of PEG and TbC. In addition, Scanning Electron Microscopy (SEM) studies reveal that the fracture behavior of PLA-CaCO₃ nanocomposites changed from brittle to ductile after plasticizers were incorporated.

Keyword: Polylactic acid, Polyethylene glycol, Tributyl citrate, CaCO₃, Nanocomposite

Introduction

Poly(lactic acid) (PLA) is a linear aliphatic biodegradable thermoplastic polyester, produced from renewable resources. It is one of the interesting biopolymer candidates for future green composites in many applications such as electrical/electronic housings and automotive interior parts [1-3]. Unfortunately, its main drawbacks are brittleness and poor thermal stability [4,5]. In order to enhance its toughness, plasticizers need to be added in PLA during melt processing [6]. This research aims to study the influences of two plasticizers; polyethylene glycol (PEG) and tributyl citrate (TbC) on thermo-mechanical properties and fracture behavior of nano-particle calcium carbonate blended poly(lactic acid) (PLA-CaCO₃)

Experiment

The nanocomposites were melt blended by adding 5 wt% of 50 nm sized CaCO₃ particles into PLA by a co-rotating twin screw extruder. The plasticized nanocomposites were prepared by melt blending of two plasticizers; polyethylene glycol (PEG) and tributyl citrate (TbC) with contents of 0-20 phr. Then specimens were fabricated by compression moulding. Dynamic mechanical analysis (DMA) and differential scanning calorimetry (DSC) were used to investigate thermo-mechanical and thermal properties of neat and plasticized nanocomposites. Tensile tests were performed in accordance to ASTM D638 by using a universal testing machine. Young's modulus and %elongation at break were evaluated. Notch Izod impact test were performed by using an impact tester with a test speed of 3.4 m/s, and impact energy to break were calculated. The fracture surfaces of specimen after impact testing were sputtered with platinum and then observed by a scanning electron microscopy (SEM) instrument.

Results and discussion

DMA results showed that adding CaCO_3 nano-particles reduced storage modulus (E') but did not affect glass transition temperature (T_g) of PLA. This was due to lubricating effect of sizing agents (i.e. fatty acid) treated on CaCO_3 surface in order to prevent them from agglomeration. Figure 1 shows that E' of neat PLA and PLA- CaCO_3 nanocomposites drop sharply at T_g but slightly increased at above T_g due to cold crystallization. In addition, it found that neat PLA did not crystallize during the cooling scan ($10^\circ\text{C}/\text{min}$) in DSC test, but the cold crystallization was clearly present in the 2nd heating scan. Adding CaCO_3 nano-particles reduced the cold crystallization temperature (T_c) of PLA implying that crystallization of PLA molecules occurred easier when nano-particles were present because of nucleating effect.

When plasticizers were blended into PLA and PLA- CaCO_3 nanocomposites, glass transition temperatures were dropped clearly with respect to amount of plasticizers. This plasticizing effect was observed in both DMA and DSC tests. Moreover, plasticizers reduced the cold crystallization temperature (T_c) of PLA to occur at lower temperature in DSC test. This was due to better mobility of PLA molecules to form crystals after PLA was plasticized by PEG and TbC. Nevertheless, plasticized PLA nanocomposites became more flexible than unplasticized ones as evidenced from decreasing of E' with respect to plasticizer contents.

From tensile test, it found that elastic modulus of PLA- CaCO_3 nanocomposites was slightly lower than those of neat PLA, similarly to reducing of storage modulus. Adding plasticizers further decreased elastic modulus of PLA, and plasticizing with TbC decreased elastic modulus of PLA dramatically. In the presence of CaCO_3 , %elongation at break of PLA was decreased because CaCO_3 acted as stress concentrator to promote crack initiation. After plasticizing, %elongation at break of neat PLA and PLA composites were higher. Adding plasticizers increased elongation at break by 40 times when compared to neat PLA and unplasticized PLA nanocomposites. Impact resistance of nanocomposites were improved by 1.6 times with adding 20 phr PEG plasticizers and by 1.4 times with adding 20 phr TbC plasticizers.

SEM micrographs in figure 2 show that the fracture behavior of PLA- CaCO_3 nanocomposites changed from brittle to ductile after plasticizers were incorporated. Fracture surface of neat PLA was smooth with local ductile breaking as craze and crack propagation occurred during the fast breaking. When CaCO_3 was added into polymer matrix, they behaved as stress concentrators promoting crack initiation, and thus local ductile breaking diminished. When plasticizers were blended into PLA, nanocomposites were tougher and broken in favor of ductile failure. Stripes of locally extension in polymer matrix were presented in fracture surface of 10 phr PEG-plasticized nanocomposite, and these stripes became more randomly distributed when PEG was 20 phr. Meanwhile, TbC-plasticized PLA nanocomposites were broken mainly in ductile, even CaCO_3 nano-particles were added.

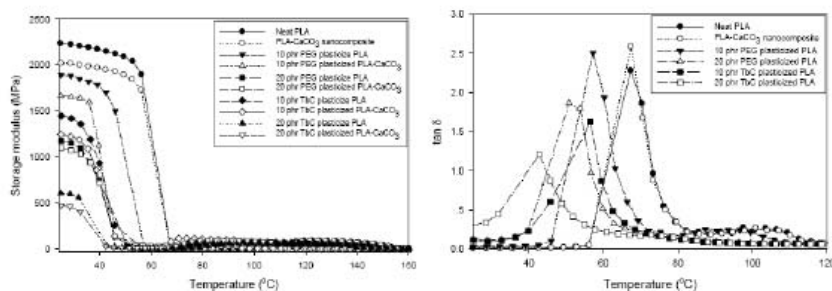


Figure 1. Storage modulus and $\tan \delta$ of neat PLA, PLA- CaCO_3 nanocomposites and plasticized PLA- CaCO_3 nanocomposites.

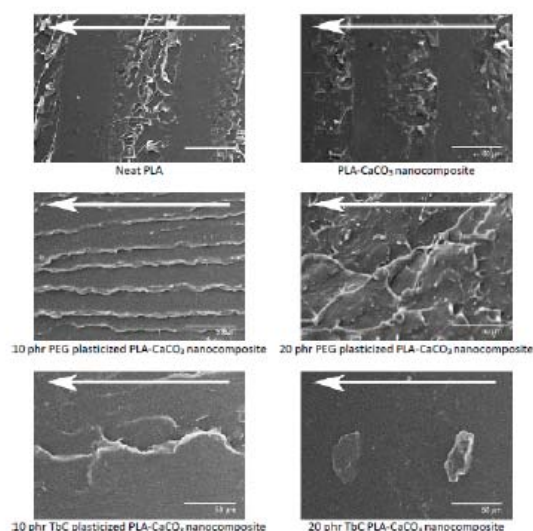


Figure 2. SEM micrographs of impact fractured specimen of neat PLA, PLA-CaCO₃ nanocomposites, and plasticized nanocomposites. The white arrow indicates stress direction in the impact test.

Conclusions

Plasticized PLA-CaCO₃ nanocomposites were prepared using twin-screw extruder and compression molding. The elongation of all samples was improved with increasing loadings of plasticizers. DMA and DSC results reveal that the incorporation of plasticizers can improve the thermal properties of PLA, particularly in reductions in T_c and T_m . Finally, Scanning Electron Microscope studies reveal that the fracture behavior of PLA-CaCO₃ nanocomposites changed from brittle to ductile after plasticizers were incorporated.

Acknowledgements

Authors would like to thank Department of Material Science and Engineering, Faculty of Engineering and Industrial Technology, Silpakorn University and the Center of Excellence for Petroleum, Petrochemicals and Advanced Materials for the financial support.

References

- [1] F.P.L. Mantia and M. Morreale: *Composites Part A*, 2011, 42, 579-588.
- [2] D. Garlotta: *J. Polym. Environ.*, 2001, 9, 63-84.
- [3] T.D. Lam, T.V. Hoang, D.T. Quang and J.S. Kim: *Mater. Sci. Eng., A*, 2009, 501, 87-93.
- [4] L.-T. Lim, R. Auras and M. Rubino: *Prog. Polym. Sci.*, 2008, 33, 820-852.
- [5] M.-A. Paul, M. Alexandre, P. Degée, C. Henrist, A. Rulmont and P. Dubois: *Polymer*, 2003, 44, 443-450.
- [6] H. Balakrishnan, A. Hassan, M.U. Wahit, A.A. Yussuf and S.B.A. Razak: *Materials & Design*, 2010, 31, 3289-3298.

2. The influence of size and loading of calcium carbonate on melt flow index and thermal properties of polylactic acid extrusion sheet

The part of the dissertation as the topic of "The influence of size and loading of calcium carbonate on melt flow index and thermal properties of polylactic acid extrusion sheet" was accepted for poster presentation with proceeding in "35th Congress on Science and Technology of Thailand" at The Tide Resort (Bangsaen Beach), Chonburi, Thailand, on 15 - 17 October 2009.

THE INFLUENCE OF SIZE AND LOADING OF CALCIUM CARBONATE ON MELT FLOW INDEX AND THERMAL PROPERTIES OF POLYLACTIC ACID EXTRUSION SHEET

Bawonkit Nekhammarak^{1,2}, Pajara Patanathabutr^{1,2,*} and Nattakorn Hongpraphan^{1,2}

¹Department of Materials Science and Engineering, Faculty of Engineering and Industrial Technology, Silpakorn University, Nakhonpathom, 73000 Thailand

²Center of Excellence for Petroleum, Petrochemicals, and Advance Materials, Thailand

E-mail address: pajara@su.ac.th

Abstract: The objectives of the research are to prepare PLA-calcium carbonate sheet by twin-screw extruder and investigate the effect of particle size and calcium carbonate loading on melt flow index and thermal properties of micro and nano-size calcium carbonate-PLA extrusion sheet. The thermal properties and polymer melt properties including glass transition temperature, melting temperature, crystallization temperature, and melt flow index were examined as a function of filler particle size and filler loading. The results on the melt flow index show that the viscosity of PLA after processing is lower than PLA before processing. The increasing of CaCO₃ loading makes the decreasing of viscosity of the blend of PLA-calcium carbonate. The nano-size CaCO₃ has more effect than micro-size CaCO₃. The DSC results show that adding of micro and nano-size CaCO₃ has effects on the glass transition temperature, melting temperature and crystallization temperature of the PLA-calcium carbonate extrusion sheet.

Keywords: Polylactic acid, PLA, nano CaCO₃, extrusion sheet, melt properties

Introduction: PLA, one of renewable bioplastics, offers a potential alternative to petrochemical plastics in many applications because of its high strength and stiffness. Adding fillers into plastics is usually implemented to improve their mechanical properties[1-4]. Recently, there are widely attempts to improve polymeric materials' properties with nano-size inorganic fillers such as ZnO, SiO₂, clay, precipitated calcium carbonate (PCC) surface modified with rare earth elements, and noble metals. Properties of filler-filled composites are closely related to the dispersion of the particles in polymer matrix. Since PLA is well known for its difficulty to crystalline, adding CaCO₃ could have an impact on its properties as well as potential applications replacing petrochemical plastics. Thus, this research has investigated effect of CaCO₃ particle size and particle loading on thermal property of PLA-calcium carbonate composites.

Methodology: All materials in this research were used as received. PLA (extrusion sheet grade, 3002D) was supplied by NatureWorks LLC, USA. There are three groups of CaCO₃ used in the research, CaCO₃ micro-particle (IQC, Quality Mineral Co., Ltd., Thailand), and two grades of CaCO₃ nano-particles by precipitation method (NPCC 101, Behm Meyer Chemical Co., Ltd., Thailand; CNANO P-23, BRS Intertrade Co., Ltd., Thailand). Prior experiment, morphology and initial particle size of CaCO₃ particles were analyzed by Scanning Electron Microscopy and size analysis technique. The average single particle size of micro-size CaCO₃ was 1.60 μm and its agglomerate size was about 50 μm. Both grades of nano-size CaCO₃ had the average single particle size of about 50 nm, and the agglomerate size of NPCC 101 and CNANO P-23 were 0.28 μm and 1.04 μm, respectively. Their code names in the experiment were Micro-CaCO₃, 1740, Nano-CaCO₃, 1041, and Nano-CaCO₃, 280, respectively. Before blending with CaCO₃, neat PLA was characterized by a melt flow index and a Differential Scanning Calorimeter.



The extruder temperature profile was in the range of 150°C in the feeding zone down to 170 °C in the die and the screw speed was 130 rpm. Neat PLA was also processed under the same condition to be the reference. The amount of each CaCO₃ in PLA composites were varied in the range of 0-20% wt.

Results, Discussion and Conclusion: The melt flow index (170°C/2.16 kg) values of neat PLA before and after processing are 2.50 and 4.07 g/10 min, respectively. The viscosity of neat PLA after processing decreased significantly compared with neat PLA before processing. This is due to either largely alignment of polymer chains during casting sheets or decrease of its molecular weight by heating and shearing. When incorporating PLA with CaCO₃, the nano-size CaCO₃ has profound effect on melt viscosity more than the micro-size CaCO₃ did.

In Figure 1, the melt flow index indicates that viscosity of PLA composite decreased with respect to CaCO₃ loading. Decrease of viscosity when adding micro- or nano-size CaCO₃ in PLA would attribute from characteristics of CaCO₃ particles in the polymer matrix. As seen in SEM images later, the single particle of CaCO₃ and their particle agglomeration is sphere-like which would lubricate PLA polymeric chains during flow.

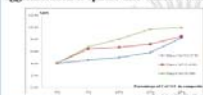


Figure 1 The melt flow index of pure PLA after extrusion process and those of micro and nano-size CaCO₃ PLA composite sheet at 5, 10 and 20 %wt of CaCO₃



Figure 2 The melt flow index variation with filler loading fraction of micro and nano-size PLA-CaCO₃ composite sheet at 170°C and 2.16 kg test load condition for MFI.

The Figure 2 shows the relation of $1/\log \eta_{0.01}$ and $1/\Phi$ where $\eta_{0.01}$ is $MF(T,0)/MF(T, \Phi)$ and Φ is mass fraction of filler[5]. It clearly shows that micro and nano-size CaCO₃ influences composite viscosity in different degree. Nano-size CaCO₃ lowers composite viscosity than micro-size ones, since smaller size of sphere-like particle (or agglomerated particles) can lubricate the movement of polymer chain better during flow. It is also found that filler loading of micro-size CaCO₃ affects composite viscosity more pronouncedly than those of nano-size particles. Higher loading of micro-size filler would create self-lubrication during flow.

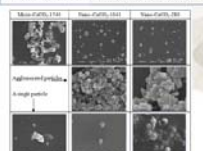


Figure 3 The SEM micrographs of CaCO₃ shows sphere-like particles, agglomerated particles and a single particle

Comparing between nano-size particles, it is found that Nano-CaCO₃-280 lowered composite viscosity than Nano-CaCO₃-1041. The best explanation would come from different agglomeration size of CaCO₃ nano-particle as seen in SEM micrographs. Particle size of single particle in both commercial Nano-CaCO₃ is about 50 nanometers. Particle size analysis reveals that the agglomerated CaCO₃ particle of Nano-CaCO₃-280 (279.5 nm) is much smaller than Nano-CaCO₃-1041 (1041 nm). As seen in Figure 1, low filler loading of Nano-CaCO₃-280 has the same composite viscosity as Nano-CaCO₃-1041. When filler loading is higher, Nano-CaCO₃-1041 composite viscosity becomes higher than Nano-CaCO₃-280 composite. This is due to higher agglomeration of filler particle occurs with higher filler loading, and the agglomerated particle size of Nano-CaCO₃-1041 is larger than Nano-CaCO₃-280 significantly.

Table 1 Characteristic thermal properties of PLA-CaCO₃ extrusion sheet

CaCO ₃ (wt %)	Filler ratio (%)	First heat scan						Second heat scan	
		T _g	T _m	T _c	T _g	T _m	ΔH _c	peak 1	peak 2
0	54.38	-	151.77	58.01	108.15	24.47	146.77	153.77	
5	54.41	-	151.10	54.99	111.33	26.23	147.69	154.11	
10	52.57	-	151.10	56.75	112.83	24.77	148.19	154.78	
15	51.85	-	151.19	56.78	113.85	24.59	148.36	154.65	
20	51.31	-	150.19	55.94	112.66	23.53	147.82	154.01	
5	55.32	-	150.53	56.83	108.41	26.34	146.94	153.95	
10	54.82	-	150.61	58.39	109.19	26.44	147.71	154.21	
15	54.19	-	150.38	56.06	109.95	24.60	147.11	153.62	
20	54.81	-	151.12	57.26	112.36	24.46	147.86	153.80	
5	55.45	-	151.38	56.95	108.02	26.29	146.87	153.80	
10	55.77	-	151.36	56.82	108.02	26.29	146.87	153.80	
15	53.10	-	151.04	58.09	105.38	25.03	146.28	154.03	
20	52.54	-	152.95	56.25	105.32	26.65	146.28	154.28	

The DSC technique was used to study effect of adding micro and nano-size CaCO₃ on composite thermal properties. Glass transition temperature, melting temperature, and crystallization temperature of the PLA-calcium carbonate extrusion sheet are presented in Table 1. There is one T_g but no T_c in all first heat scan. Meanwhile, there are one T_g and two T_m in all second heat scan. In this research, blend of PLA-CaCO₃ was calculated by nip rolls after extruded from die to cast sheets. Quenching of PLA-CaCO₃ extrusion sheet causes no T_c is detected in the first heat scan. Drawing of the extrusion sheet causes stress induced crystallization[6], so there is one broad T_m about 151°C in all composite sheets.

In the second heat scan, T_c is detected in all types and all loading of CaCO₃ in PLA because of reorientation of polymer chain to form crystalline. There are two separated T_m because PLA can be found in the four form of crystalline upon the condition of processing and the tendency to crystalline upon purity of the purity of PLA polymer [6-8]. In general, commercial PLA contains D-form as impurity, so in this case the two melting peak are built from one imperfect crystalline showed as lower T_m and another form of crystalline that is stronger showed as higher T_m. These crystalline was explained based on melt-recrystallization model, that small and imperfect crystals changed successively into more stable crystals through the melting and recrystallization. The crystallization temperature of the PLA increased when it was blended with Micro-CaCO₃-1740 and Nano-CaCO₃-1041, and decreased when it was blended with Nano-CaCO₃-280. The increase of crystalline temperature implies that adding of these particles reduce the ability of PLA to crystalline. C.M. Chan *et al.* (*refer to Khaw et al.*) showed that the incorporation of CaCO₃ with a particle size of 6 micrometer reduced the crystallization of half-time significantly[9]. The decrease of crystallization temperature indicates an enhanced crystallization ability of PLA in the presence of nanofillers, which might behave as nucleating agents. The effect come from the agglomerated size of CaCO₃ particle. From the size analysis, the agglomerated size of Micro-CaCO₃-1740, Nano-CaCO₃-1041 and Nano-CaCO₃-280 are 1740, 1041 and 279.5 nm, respectively. The agglomerated size of Nano-CaCO₃-280 has smallest size as nanofiller, so it eased PLA to crystallize. At the same filler loading (5% and 20%) NPCC showed stronger nucleating effect by giving a lower cold crystallization temperature (T_c) and higher enthalpy of crystallization (ΔH_c). This could be due to larger surface areas and volume ratios of the NPCC agglomerated particulates which give rise to more nucleating sites.

In conclusion, the PLA was modified by three different sizes of CaCO₃ particles. The increasing of amount of CaCO₃ makes the decreasing of viscosity of the blend of PLA-calcium carbonate. The nano-size CaCO₃ has more effect on melt and thermal properties than micro-size CaCO₃. The agglomerate size of Nano-CaCO₃-280 which has smallest size as nanofiller, eased PLA to crystallize. This could be due to larger surface area and volume ratio of the Nano-CaCO₃-280.

References:

- S. S. Ray and M. Roumina. *Progress in Materials Science* 2005;50:962-1079
- L. T. Lim, R. Auras and M. Rubino. *Process in polymer science* 2008;33:820-832
- T.D. Lam, T.V. Hoang, D.T. Quang and J.S. Kim. *Materials Science and Engineering A*, Accepted date: 22 September 2008
- A. Sorrentino, G. Gorrao and V. Vittoria. *Trends in Food Science & Technology* 2007;18:84-95
- A. V. Shetty. *Rheology of Filled Polymer Systems*. Dordrecht: Kluwer Academic Publishers; 1999
- X. Ou and M. Cakmak. *Polymer* 2008;49:3344-3352
- T. L. Jung, J. Zhang and M. P. Wolcott. *Polymer* 2007;48:7612-7644
- G. S. Gu, Y.F. Yang, S.M. Fan and Z.F. Cai. *Polymer Technology* 2005;153:153-158
- C.M. Chan, J. Wu, J.X. Li and Y.K. Cheung. *Polymer* 2002;43:2981-2992

Acknowledgment:

This research is partially supported on analysis cost by the National Metal and Material Technology Center (MTEC), Thailand.



Abstracts

THE 35th CONGRESS
on SCIENCE and TECHNOLOGY
of THAILAND (STT 35)

การประชุมวิชาการวิทยาศาสตร์และเทคโนโลยีแห่งประเทศไทย
ครั้งที่ 35 (วทท 35)

วิทยาศาสตร์และเทคโนโลยีเพื่ออนาคตที่ดีขึ้น
SCIENCE AND TECHNOLOGY FOR A BETTER FUTURE

*To Celebrate the 35th Anniversary of Faculty of Science, Burapha University
To Celebrate the 30th Anniversary of Ministry of Science and Technology*

October 15 - 17, 2009

Venue : The Tide Resort (Bangsaen Beach), Chonburi, Thailand.

15-17 ตุลาคม 2552 ณ เดอะ ไทด์ รีสอร์ท (หาดบางแสน) จังหวัดชลบุรี

WWW.STT35.SCISOC.OR.TH

E_E0020 NATURAL DYE-ALUMINUM-SILICATE POLYMER COMPOSITE FOR pH INDICATORSivaphan Rattanapatiphan^{1,2} and Pajaera Patanathabutr^{1,2*}¹Department of Material Science and Engineering, Faculty of Engineering and Industrial Technology, Silpakorn University, Nakorn Pathom, 73000, Thailand;²Center of Excellence for Petroleum, Petrochemicals and Advanced Materials, Chulalongkorn University, Bangkok, 10330, Thailand. E-Mail: pajaera@su.ac.th

Abstract: Natural dye extracted from Sappan wood (*Caesalpinia sappan* L.) has a characteristic chromophore and auxochrome which are shade-sensitive to acid and alkaline environment. The aim of this research is to prepare polyvinyl alcohol (PVA)-natural dye-aluminum-silicate (Al_2O_3 - SiO_2) composites by sol-gel technique, following by film casting method in aqueous solution. The aluminum-silicate powder was characterized by FTIR and X-ray diffraction (XRD) and the distribution of the powder in film was investigated by scanning electron microscopy (SEM). The composites showed visual change in color shade of film in acid and alkaline condition which can be applied as pH indicator in food packaging.

E_E0021 PREPARATION OF TITANIUM METAL INJECTION MOULDING FEEDSTOCK USING A PEG/PMMA BINDERNuthita Chuankrerkkul¹, Wen Xu², Muhammad Hussain Ismail², Alfred Sidambe² and Iain Todd²¹Metallurgy and Materials Science Research Institute, Chulalongkorn University,

Soi Chula 12, Phayathai Road, Bangkok 10330, Thailand

²Department of Engineering Materials, University of Sheffield, Mappin Street, Sheffield, United Kingdom

Abstract: Titanium and its alloys are well-known for their unique properties such as relatively low density, excellent corrosion resistance, high strength and biocompatible. They are widely used in aerospace or biomedical applications. Metal injection moulding (MIM) is a cost effective process for a fabrication of small, complex-shaped components for high performance applications. In this work, a binder system, composed of polyethylene glycol (PEG) and polymethyl methacrylate (PMMA), was developed for the preparation of feedstock of titanium for MIM. The processing parameters and the rheological behaviour have been investigated. Feedstocks, containing 69 vol% of powder, can be successfully prepared and extruded with a small plunger-typed injection moulding machine. They exhibited pseudoplastic behaviour over the range of shear rates tested. The preliminary study showed that the PEG/PMMA binder system can be employed in the preparation of the feedstock for MIM.

E_E0022 THE INFLUENCE OF SIZE AND LOADING OF CALCIUM CARBONATE ON MELT FLOW INDEX AND THERMAL PROPERTIES OF POLYLACTIC ACID EXTRUSION SHEETBawornkit Nekhamanurak^{1,2}, Pajaera Patanathabutr^{1,2,*} and Nattakarn Hongsrirphan^{1,2}¹Department of Materials Science and Engineering, Faculty of Engineering and Industrial Technology, Silpakorn University, Nakhonpathom, 73000 Thailand²Center of Excellence for Petroleum, Petrochemicals, and Advance Materials, Thailand

E-mail address: pajaera@su.ac.th

Abstract: The objectives of the research are to prepare PLA-calcium carbonate sheet by twin-screw extruder and investigate the effect of particle size and calcium carbonate loading on melt flow index and thermal properties of micro and nano-size calcium carbonate-PLA extrusion sheet. The thermal properties and polymer melt properties including glass transition temperature, melting temperature, crystallisation temperature, and melt flow index were examined as a function of filler particle size and filler loading. The results on the melt flow index show that the viscosity of PLA after processing is lower than PLA before processing. The increasing of $CaCO_3$ loading makes the decreasing of viscosity of the blend of PLA-calcium carbonate. The nano-size $CaCO_3$ has more effect than micro-size $CaCO_3$. The DSC results show that adding of micro and nano-size $CaCO_3$ has effects on the glass transition temperature, melting temperature and crystallisation temperature of the PLA-calcium carbonate extrusion sheet.

E_E0023 ANALYSIS OF POZZOLANIC ACTIVITY OF RICE HUSK ASH BY IMPEDANCE SPECTROSCOPYSirirat Janjaturaphan¹, Supaporn Wansom¹, Waraporn Pinyo¹, Sakprayut Sinthupinyo²¹National Metal and Materials Technology Center (MTEC), National Science and Technology Development Agency (NSTDA), 114 Thailand Science Park, Paholyothin Rd., Klong 1, Klongluang, Pathumthani 12120, Thailand²SCI Research and Innovation Co., Ltd., 51 Moo 8, Tubkwang, Kaeng Khoi, Saraburi 18260, Thailand

E-mail: siriratj@mtec.or.th

อิทธิพลของขนาดและปริมาณแคลเซียมคาร์บอเนตที่มีต่อค่าดัชนีการไหลและสมบัติทางความร้อนของแผ่นพอลิแลคติกแอซิดชนิดอครีต

THE INFLUENCE OF SIZE AND LOADING OF CALCIUM CARBONATE ON MELT FLOW INDEX AND THERMAL PROPERTIES OF POLYLACTIC ACID EXTRUSION SHEET

บวรกิตต์ เนกมานุรักษ์^{1,2}, ปาเจรา พัฒนถาบุตร^{1,2,*} และ นัทฏกาญจน์ หงส์ศรีพันธ์^{1,2}

Bawornkit Nekhamanurak^{1,2}, Pajaera Patanathabutr^{1,2,*} and Nattakam Hongsriphan^{1,2}

¹Department of Materials Science and Engineering, Faculty of Engineering and Industrial Technology, Silpakom University, Nakhonpathom, 73000 Thailand

²Center of Excellence for Petroleum, Petrochemicals, and Advance Materials, Thailand
E-mail address: pajaera@su.ac.th

บทคัดย่อ:

วัตถุประสงค์ของงานวิจัยนี้คือการขึ้นรูปแผ่นพอลิแลคติกแอซิดผสมแคลเซียมคาร์บอเนตโดยใช้เครื่องอครีตเกลียวหนอนคู่

และศึกษาผลกระทบของขนาดอนุภาคและปริมาณการเติมแคลเซียมคาร์บอเนตต่อค่าดัชนีการไหลและสมบัติทางความร้อนของแผ่นพอลิแลคติกแอซิดชนิด

อครีตที่มีการเติมอนุภาคแคลเซียมคาร์บอเนตขนาดนาโนและไมโคร

โดยทำการศึกษาอิทธิพลของขนาดและปริมาณของสารตัวเติมที่มีผลต่อสมบัติทางความร้อนและสมบัติของพอลิเมอร์หลอมเหลว ประกอบด้วยอุณหภูมิการเปลี่ยนสถานะคล้ายแก้ว อุณหภูมิหลอมเหลว

อุณหภูมิการเกิดผลึก และ

ค่าดัชนีการไหล

โดยจากผลการทดลองพบว่าความหนืดของพอลิแลคติกแอซิดหลังจากผ่านการอครีตจะมีค่าน้อยกว่าก่อนการอครีต

ซึ่งการเติมอนุภาคแคลเซียมคาร์บอเนตในปริมาณที่มากขึ้นจะส่งผลให้ความหนืดของพอลิแลคติกแอซิดผสมแคลเซียมคาร์บอเนตมีค่าลดลง โดยแคลเซียมคาร์บอเนต

ที่มีอนุภาคขนาดนาโนจะส่งผลต่อการพฤติกรรมเปลี่ยนแปลงค่าความหนืดมากกว่าขนาดไมโคร

ในผลการทดลองส่วนของ DSC

พบว่าการเติมแคลเซียมคาร์บอเนตขนาดไมโครและนาโนส่งผลต่ออุณหภูมิการเปลี่ยนสถานะคล้ายแก้ว อุณหภูมิหลอมเหลว และอุณหภูมิการเกิดผลึกของแผ่น

พอลิแลคติกแอซิดผสมแคลเซียมคาร์บอเนต

Abstract: The objectives of the research are to prepare PLA-calcium carbonate sheet by twin-screw extruder and investigate the effect of particle size and calcium carbonate loading on melt flow index and thermal properties of micro and nano-size calcium carbonate-PLA extrusion sheet. The thermal properties and polymer melt properties including glass transition temperature, melting temperature, crystallisation temperature, and melt flow index were examined as a function of filler particle size and filler loading. The results on the melt flow index show that the viscosity of PLA after processing is

lower than PLA before processing. The increasing of CaCO₃ loading makes the decreasing of viscosity of the blend of PLA-calcium carbonate. The nano-size CaCO₃ has more effect than micro-size CaCO₃. The DSC results show that adding of micro and nano-size CaCO₃ has effects on the glass transition temperature, melting temperature and crystallisation temperature of the PLA-calcium carbonate extrusion sheet.

Introduction: PLA, one of renewable bioplastics, offers a potential alternative to petrochemical plastics in many applications because of its high strength and stiffness. Adding fillers into plastics is usually implemented to improve their mechanical properties[1-4]. Recently, there are widely attempts to improve polymeric materials' properties with nano-size inorganic fillers such as ZnO, SiO₂, clay, precipitated calcium carbonate (PCC) surface modified with rare earth elements, and noble metals. Properties of filler-filled composites are closely related to the dispersion of the particles in polymer matrix. Since PLA is well known for its difficulty to crystalline, adding CaCO₃ could have an impact on its properties as well as potential applications replacing petrochemical plastics. Thus, this research has investigated effect of CaCO₃ particle size and particle loading on thermal property of PLA-calcium carbonate composites.

Methodology: All materials in this research were used as received. PLA (extrusion sheet grade, 2002D) was supplied by NatureWorks LLC, USA. There are three groups of CaCO₃ used in the research; CaCO₃ micro-particle (1QC, Quality Mineral Co., Ltd., Thailand), and two grades of CaCO₃ nano-particles by precipitation method (NPCC 101, Behn Meyer Chemical Co., Ltd., USA Thailand; CNANO P-23, BRS Intertrade Co., Ltd., Thailand). Prior experiment, morphology and initial particle size of CaCO₃ particles were analyzed by Scanning Electron Microscopy and size analysis technique. The average single particle size of micro-size CaCO₃ was 1.60 μm and its agglomerate size was 1.74 μm. Both grades of nano-size CaCO₃ had the average single particle size of about 50 nm, and the agglomerate size of NPCC 101 and CNANO P-23 were 0.28 μm and 1.04 μm, respectively. Their code names in the experiment were then Micro-CaCO₃-1740, Nano-CaCO₃-1041, and Nano-CaCO₃-280, respectively. Before blending with CaCO₃, neat PLA was characterized by a melt flow indexer and a Differential Scanning Calorimeter. PLA and CaCO₃ was blended in a co-rotating twin screw extruder and extruded throughout a T-slit die and drawn by nip rolls at speed of 15 Hz to cast flat sheet. The extruder temperature profile was in the range of 150°C in the feeding zone down to 170 °C in the die and the screw speed was 130 rpm. Neat PLA was also processed under the same condition to be the reference. The amount of each CaCO₃ in PLA composites were varied in the range of 0-20% wt. The PLA-CaCO₃ composite were then characterized by a melt flow indexer and a Differential Scanning Calorimeter to investigate the effect of particle size and particle loading.

Results, Discussion and Conclusion: The melt flow index (170°C/2.16 kg) values of neat PLA before and after processing are 2.50 and 4.07 g/10 min, respectively. The viscosity of neat PLA after processing decreased significantly compared with neat PLA before processing. This is due to either largely alignment of polymer chains during casting sheets or decrease of its molecular weight by heating and shearing. When incorporating PLA with CaCO₃, the nano-size CaCO₃ has profound effect on melt viscosity more than the micro-size CaCO₃ did. As shown in Figure 1, the melt flow index indicates that viscosity of PLA composite decreased with respect to CaCO₃

loading. Decrease of viscosity when adding micro- or nano-size CaCO_3 in PLA would attribute from characteristics of CaCO_3 particles in the polymer matrix. As seen in SEM images later, the single particle of CaCO_3 and their particle agglomeration is sphere-like which would lubricate PLA polymeric chains during flow.

The Figure 2 shows the relation of $1/\log a_{\text{MFI}}$ and $1/\Phi$ where a_{MFI} is $\text{MFI}(T,0)/\text{MFI}(T, \Phi)$ and Φ is mass fraction of filler[5]. It clearly shows that micro and nano-size CaCO_3 influences composite viscosity in different degree. Nano-size CaCO_3 lowers composite viscosity than micro-size ones, since smaller size of sphere-like particle (or agglomerated particles) can lubricate the movement of polymer chain better during flow. It is also found that filler loading of micro-size CaCO_3 affects composite viscosity more pronouncedly than those of nano-size particles. Higher loading of micro-size filler would create self-lubrication during flow.

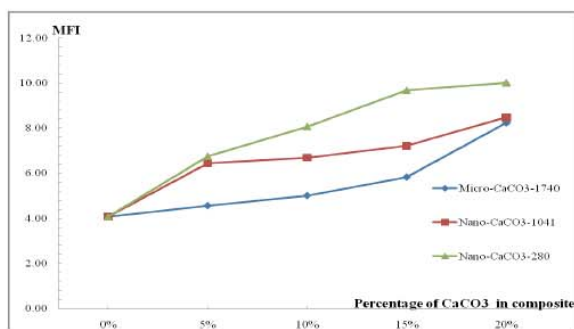


Figure 1 The melt flow index of pure PLA after extrusion process and those of micro and nano-size CaCO_3 -PLA composite sheet at 5, 10 and 20 %wt of CaCO_3 .

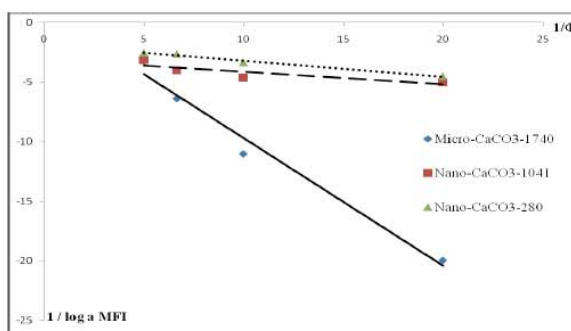


Figure 2 The melt flow index variation with filler loading fraction of micro and nano-size PLA- CaCO_3 composite sheet at 170°C and 2.16 kg test load condition for MFI.

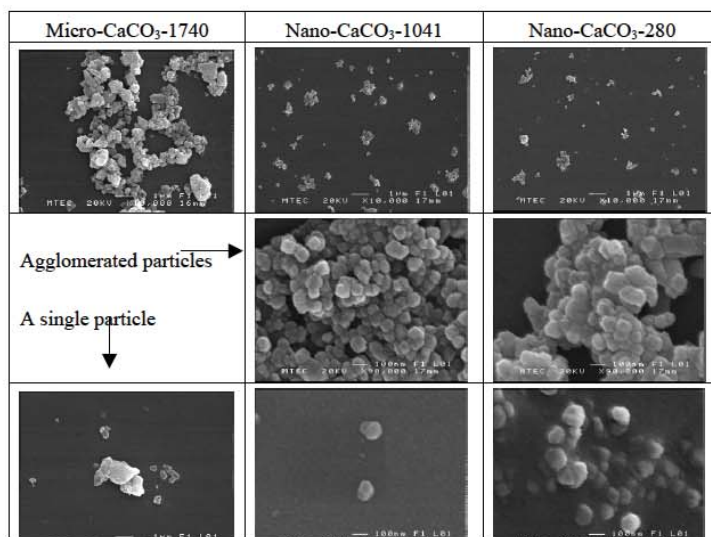


Figure 3 The SEM micrographs of CaCO₃ shows sphere-like particles, agglomerated particles and a single particle.

Comparing between nano-size particles, it is found that Nano-CaCO₃-280 lowered composite viscosity than Nano-CaCO₃-1041. The best explanation would come from different agglomeration size of CaCO₃ nano-particle as seen in SEM micrographs. Particle size of single particle in both commercial Nano-CaCO₃ is about 50 nanometers. Particle size analysis reveals that the agglomerated CaCO₃ particle of Nano-CaCO₃-280 (279.5 nm) is much smaller than Nano-CaCO₃-1041 (1041 nm). As seen in Figure 1, low filler loading of Nano-CaCO₃-280 has the same composite viscosity as Nano-CaCO₃-1041. When filler loading is higher, Nano-CaCO₃-1041 composite viscosity becomes higher than Nano-CaCO₃-280 composite. This is due to higher agglomeration of filler particle occurs with higher filler loading, and the agglomerated particle size of Nano-CaCO₃-1041 is larger than Nano-CaCO₃-280 significantly.

The DSC technique was used to study effect of adding micro and nano-size CaCO₃ on composite thermal properties. Glass transition temperature, melting temperature, and crystallisation temperature of the PLA-calcium carbonate extrusion sheet are presented in Table 1. There is one T_m but no T_c in all first heat scan. Meanwhile, there are one T_c and two T_m in all second heat scan. In this research, blend of PLA-CaCO₃ was calendared by nip rolls after extruded from die to cast sheets. Quenching of PLA-CaCO₃ extrusion sheet causes no T_c is detected in the first heat scan. Drawing of the extrusion sheet causes stress induced crystallisation[6], so there is one broad T_m about 151°C in all composite sheets.

Table 1 Characteristic thermal properties of PLA-CaCO₃ extrusion sheet.

CaCO ₃	Filler ratio (%)	First heat scan			Second heat scan				
		T _g	T _c	T _m	T _g	T _c	ΔH _c	T _m	
								peak 1	peak 2
Micro-CaCO ₃ -1740	0	54.38	-	151.27	58.01	108.15	24.47	146.77	153.77
	5	53.41	-	151.10	54.59	111.33	26.22	147.69	154.11
	10	52.57	-	151.10	56.75	112.83	24.77	148.19	154.76
	15	51.95	-	151.19	56.78	113.92	24.59	148.36	154.61
	20	51.31	-	150.19	55.94	112.66	23.33	147.85	154.03
Nano-CaCO ₃ -1041	5	55.22	-	150.53	56.82	108.41	26.74	146.94	153.95
	10	54.82	-	150.61	58.39	109.19	26.44	147.71	154.21
	15	54.19	-	150.28	56.06	109.92	24.90	147.11	153.62
	20	54.85	-	151.12	57.26	112.36	24.46	147.96	153.80
Nano-CaCO ₃ -280	5	53.45	-	151.38	56.95	108.02	30.39	146.97	153.80
	10	53.77	-	151.23	56.06	107.42	27.96	146.95	154.54
	15	53.10	-	151.04	58.09	105.58	25.03	146.28	154.03
	20	52.54	-	152.95	56.25	105.32	26.65	146.28	154.28

In the second heat scan, T_c is detected in all types and all loading of CaCO₃ in PLA because of reorientation of polymer chain to form crystalline. There are two separated T_m because PLA can be found in four forms of crystalline upon the condition of processing and the tendency to crystalline upon purity of the purity of PLA polymer [6-8]. In general, commercial PLA contains D-form as impurity, so in this case the two melting peaks are built from one imperfect crystalline showed as lower T_m and another form of crystalline that is stronger showed as higher T_m. These crystallines were explained based on melt-recrystalline model, that small and imperfect crystals changed successively into more stable crystals through the melting and recrystallization. The crystallization temperature of the PLA increased when it was blended with Micro-CaCO₃-1740 and Nano-CaCO₃-1041, and decreased when it was blended with Nano-CaCO₃-280. The increase of crystalline temperature implies that adding of these particles reduce the ability of PLA to crystalline. *C.M. Chan et al. (refer to Khare et al.)* showed that the incorporation of CaCO₃ with a particle size of 6 micrometer reduced the

crystallisation of half-time significantly[9]. The decrease of crystallization temperature indicates an enhanced crystallization ability of PLA in the presence of nanofillers, which might behave as nucleating agents. The effect come from the agglomerated size of CaCO_3 particle. From the size analysis, the agglomerated size of Micro- CaCO_3 -1740, Nano- CaCO_3 -1041 and Nano- CaCO_3 -280 are 1740, 1041 and 279.5 nm, respectively. The agglomerated size of Nano- CaCO_3 -280 has smallest size as nanofiller, so it eased PLA to crystallize. At the same filler loading (5% and 20%) NPCC showed stronger nucleating effect by giving a lower cold crystallization temperature (T_c) and higher enthalpy of crystallization (ΔH_c). This could be due to larger surface areas and volume ratios of the NPCC agglomerated particulates which give rise to more nucleating sites.

In conclusion, the PLA was modified by three different sizes of CaCO_3 particles. The increasing of amount of CaCO_3 makes the decreasing of viscosity of the blend of PLA- calcium carbonate. The nano-size CaCO_3 has more effect on melt and thermal properties than micro-size CaCO_3 . The agglomerate size of Nano- CaCO_3 -280 which has smallest size as nanofiller, eased PLA to crystallize. This could be due to larger surface area and volume ratio of the Nano- CaCO_3 -280.

References:

1. S. S. Ray and M. Bousmina. Biodegradable polymers and their layered silicate nanocomposites: In greening the 21st century materials world. Progress in Materials Science 2005;50:962–1079.
2. L.-T. Lim, R. Auras and M. Rubino. Processing technologies for poly(lactic acid). Process in polymer science 2008;33:820-852.
3. T.D. Lam, T.V. Hoang, D.T. Quang and J.S. Kim. Effect of nano-sized and surface-modified precipitated calcium carbonate on properties of CaCO_3 /polypropylene nanocomposites. Materials Science and Engineering A; Accepted date 22 September 2008.
4. A.Sorrentino, G. Gorrasi and V. Vittoria. Potential perspectives of bio-nanocomposites for food packaging applications. Trends in Food Science & Technology 2007;18:84-95.
5. A.V. Shenoy. Rheology of Filled Polymer Systems. Dordrecht: Kluwer Academic Publishers; 1999.
6. X. Ou and M. Cakmak. Influence of biaxial stretching mode on the crystalline texture in polylactic acid films. Polymer 2008;49:5344-5352.
7. L. Jiang, J. Zhang and M.P. Wolcott. Comparison of polylactide/nano-sized calcium carbonate and polylactide/montmorillonite composites: Reinforcing effects and toughening mechanisms. Polymer 2007;48:7632-7644.
8. G.S. Gai, Y.F. Yang, S.M. Fan and Z.F. Cai. Preparation and properties of composite mineral powders. Powder Technology 2005;153:153–158.
9. C.M. Chan, J. Wu, J.X. Li and Y.K. Cheung. Polypropylene/calcium carbonate nanocomposites. Polymer 2002;43:2981-2992.

Keywords: Polylactic acid, PLA, nano CaCO_3 , extrusion sheet, melt properties

Acknowledgments: This research is partially supported on analysis cost by the National Metal and Material Technology Center (MTEC), Thailand.

Biography

Name : Mr. Bawornkit
Last name : Nekhamanurak
Date of Birth : September 11, 1982
Nationality : Thai
Address : 3 Moo 3, Tambon Banpom,
 Phra Nakhon Si Ayutthaya,
 Phra Nakhon Si Ayutthaya 13000, Thailand
E-mail : bawornkit@windowslive.com



Academic Achievements

- | | |
|-----------------------|--|
| 2008 – present | Ph.D. candidate in Polymer Science and Engineering program (International program), Silpakorn University
<u>Dissertation Title</u> : Effect of surface-modified calcium carbonate nano-particles on properties of biocomposites |
| 2007 | Master of Engineering Degree in Polymer Science and Engineering, Silpakorn University
<u>Thesis Title</u> : The design of the HIPS and ABS separation system used in froth floatation technique |
| 2005 | Bachelor of Engineering Degree in Petrochemical and Polymeric Materials, Silpakorn University
<u>Thesis Title</u> : The development of a small semi-closed cycle gas turbine engine burning biomass |

Experiences

- | | |
|--------------------|---|
| 2004 | Internship, Thai Bridgestone Co., Ltd. |
| 2005 - 2007 | Teaching Assistant, Department of Materials Science and Engineering, Silpakorn University |
| 2007 - 2008 | Project Manager, National Innovation Agency, Ministry of Science and Technology |
| 2007 - 2008 | Coordinator, Thai Bioplastics Industry Association |
| 2008 - 2011 | Teaching Assistant (Senior supervisor), Department of Materials Science and Engineering, Silpakorn University |